

## 2. SITE 398

### Shipboard Scientific Party<sup>1</sup>

#### SITE DATA

**Date Occupied:**

Hole 398: 1937, 13 April 1976

**Date Departed:**

Hole 398: 0600, 9 May 1976

**Time on Hole:**

Hole 398: 25 days, 10 hours, 23 minutes

**Position:**

40°57.6 'N, 10°43.1 'W

**Water Depth (sea level):**

3910 corrected meters, echo sounding

**Water Depth (rig floor):**

3920 corrected meters, echo sounding

**Bottom Felt at:**

3900 meters, drill pipe

**Penetration:**

Hole 398: 126.5 meters  
Hole 398A: 210.5 meters  
Hole 398B: 239.0 meters  
Hole 398C: 79.0 meters  
Hole 398D: 1740.0 meters

**Number of Cores:**

Hole 398: 4  
Hole 398A: 2  
Hole 398B: 1  
Hole 398C: 1  
Hole 398D: 138

**Total Length of Cored Section:**

Hole 398: 35.0 meters  
Hole 398A: 19.0 meters  
Hole 398B: 9.5 meters  
Hole 398C: 0 meters  
Hole 398D: 1298.0 meters

**Total Core Recovered:**

Hole 398: 22.08 meters  
Hole 398A: 17.24 meters  
Hole 398B: 8.26 meters  
Hole 398C: 0.75 meters  
Hole 398D: 936.6 meters

**Percentage Recovery:**

Hole 398: 63.1 per cent  
Hole 398A: 90.7 per cent  
Hole 398B: 86.9 per cent  
Hole 398C: —  
Hole 398D: 72.2 per cent

**Oldest Sediment Cored:**

Depth sub-bottom: 1740 meters  
Nature: Limestone  
Age: Early Cretaceous (Hauterivian)  
Measured velocity: 3.5 km/s  
Basement: Probably penetrated

**Principal Results:** Site 398 is located on the southern apron of Vigo Seamount, 160 km off the western coast of the Iberian Peninsula. A thick Cenozoic section was encountered above an even thicker Cretaceous series.

Drilling terminated in Hauterivian pelagic limestones belonging to the acoustical basement clearly of sedimentary origin.

Stratigraphic gaps, induced by the erosion of ocean bottom currents and/or condensed zones produced by very slow deposition, were detected in the upper to middle Miocene, lower Oligocene, lower Eocene, between the Campanian/ Santonian and the Cenomanian, and between lower Albian and upper Aptian sediments.

Five major lithologic units are differentiated. Unit 1 is a marly nannofossil ooze to siliceous marly chalk that is dated Pleistocene to early Oligocene (0 to 594 m sub-bottom). Rhythmic bedding is conspicuous, indicating both dilution and dissolution cycles. Unit 2 is a siliceous marly chalk to mudstone, dated as Eocene to early Paleocene (594 to 774 m). Unit 2 is characterized by abundant zeolite levels rich in magnesium silicates, moderately low carbonate contents, and numerous thin sand and silt layers reflecting deposition of reworked deep-sea sediments by both downslope turbidity currents and traction transporting benthic boundary currents. Unit 3 is a calcareous mudstone, alternating with a marly chalk and grading downward to a red barren mudstone, dated as early (reworked) Paleocene to Campanian (774 to 945 m), containing fine-grained quartz, mica, and some gypsum and, in part, deposited near or below the CCD. Unit 4, deposited during the Cenomanian to early Barremian (945 to 1668 m), containing fine-grained quartz, mica, and some gypsum and, in part, deposited near or below the CCD. Unit 4 is a dark, laminated and only occasionally bioturbated mudstone to claystone, grading down into terrigenous shales with abundant carbonaceous material derived from land plants and thin lenses (and concretions of authigenic siderite). Unit 4 extends downward into thin turbiditic

<sup>1</sup> William B. F. Ryan, (Co-Chief Scientist), Lamont-Doherty Geological Observatory, Palisades, New York; Jean-Claude Sibuet (Co-Chief Scientist), CNEXO, Brest, France; Michael A. Arthur, Princeton University, Princeton, New Jersey (now at: Scripps Institution of Oceanography, La Jolla, California); Boris G. Lopatin, Research Institute of the Geology of the Arctic, Leningrad, USSR; David G. Moore, Scripps Institution of Oceanography, La Jolla, California; Andrés Maldonado, Instituto "Jaime Almera," Barcelona, Spain; Jean-Pierre Rehault, Université de Paris VI, Villefranche-sur-Mer, France; Silvia Iaccarino, University of Parma, Parma, Italy; Jacques Sigal, Institut Français de Pétrole, Rueil-Malmaison, France; Gerald E. Morgan, University of Leeds, Leeds, United Kingdom; Gretchen Blechschmidt, University of Washington, Seattle, Washington; Carol A. Williams, Lamont-Doherty Geological Observatory, Palisades, New York; David Johnson, Exxon Production Research Company, Houston, Texas; Ross O. Barnes, Walla Walla College, Anacortes, Washington; and Daniel Habib, Queens College of the City University of New York, Flushing, New York.

sandstones, siltstones, and calcareous mud-flow debris with associated mud-chip conglomerates containing clasts of pelagic limestone dated as Berriasian to late Tithonian. Several of the calcareous breccias contain fragments of a granulite-facies bedrock. Unit 5 is basically composed of fine-grained nannofossil limestone that is Hauterivian (1668 to 1740 m), interbedded with some varved brown mudstone rich in amorphous sapropelic matter.

Although turbidites are a common lithofacies component of the post-Cenomanian stratigraphic section, they are volumetrically most significant in the Paleocene and Oligocene intervals. Many turbidites consist of redeposited pelagic biogenic components.

Beginning in the Hauterivian, water depths were already well below the neritic zone and sedimentation was primarily of pelagic biogenic ooze. The site subsequently subsided below the level of carbonate dissolution during the late Barremian and remained in this environment until the late Albian, while receiving an important terrigenous input from coastal deltas.

A downward excursion of the dissolution level is inferred for the late Albian and Cenomanian interval containing more carbonate-rich marls and chalks which may have experienced some downslope mass movement. Strong dissolution effects reappear immediately above the erosional unconformity underlying the Campanian/Santonian. Moderate carbonate preservation is detected in the Maestrichtian and the site remained generally above the CCD in the Cenozoic, although for much of the Paleocene and Eocene it was situated well below the lysocline.

Measurements of remanent magnetization permit the detection of numerous changes in the earth's magnetic polarity during the Cenozoic and Late Cretaceous. However, the entire pre-Campanian is of a single polarity, part of which may represent the long Cretaceous normal polarity epoch and part of which may be an overprint on earlier sediments which had at one time experienced reversals of the earth's magnetic field. A downhole measurement indicates low temperatures. No volumetrically significant hydrocarbon gases were detected from apparently thermally immature sediments.

## BACKGROUND AND OBJECTIVES

### Introduction

Galicia Bank had the topographic appearance of a detached and isolated fragment of the Iberian Peninsula cut off from the mainland of Europe by a rather deep (~3000 m) trough. The location of Site 398 is within the axis of this trough approximately 160 km from the present-day coast of Portugal and immediately to the south of a major prominence known as Vigo Seamount (Figure 1).

The JOIDES Passive Margin Advisory Panel considered the Galicia region as belonging to the continental margin province of the eastern North Atlantic. The attractiveness of the Galicia region for deep drilling in IPOD Phase I focused on the general absence of major offshore deltas (ancient and modern) along the western coast of Portugal, and hence, the likelihood of encountering a thinner blanket of Mesozoic and Cenozoic clastic sediments (Montadert et al., 1974) than exists on segments of the northwest African margin.

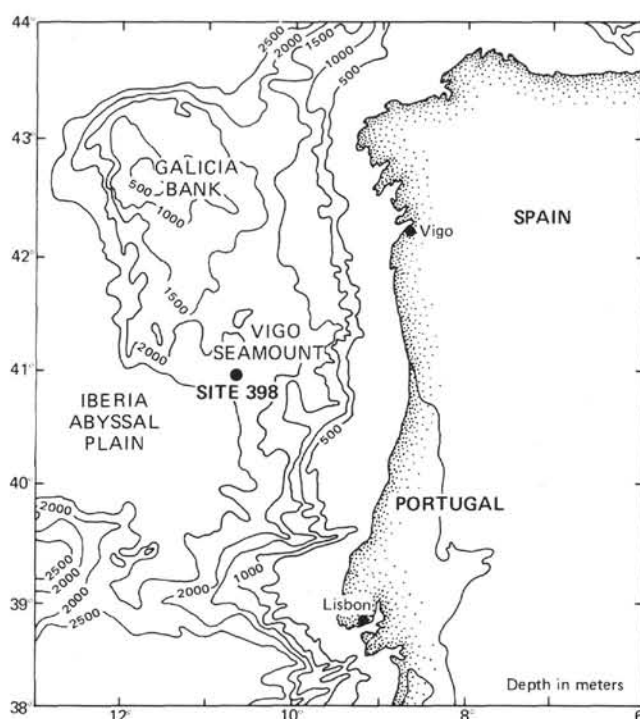


Figure 1. Site 398 location map, showing Galicia Bank area bathymetry from Laughton et al. (1975).

From the earliest planning stage of IPOD Phase I, the location of Site 398 showed promise of permitting penetration with existing drilling technology into ancient marine sediments deposited on and transgressive across a continental edge during the rupture of southern Europe from North America.

The existence in the Galicia region of limestones formerly deposited in a shallow, sunlit epicontinental seaway has been confirmed by several dredge-hauls containing upper Jurassic calcarenites near the summits and around the marginal escarpments of both Galicia Bank proper and Vigo and Vasco da Gama seamounts (Black et al., 1964; Dupeuble et al., 1976; Rehault and Mauffret, this volume; Groupe Galice, this volume). The sialic nature of the underlying bedrock of these prominences is similarly demonstrated by the sampling of feldspathic gneisses, granodiorites, and micaschists presently at bathymetric levels below the limestones.

Prior to continental fragmentation (Figure 2), this epicontinental seaway covered parts of western Iberia (e.g., the Lusitanian Basin), the Grand Banks (e.g., the Carson, Jeanne d'Arc, Horseshoe, and Whale basins), and northern Europe (e.g., Celtic and North Sea basins, Paris and Aquitanian basins). Along the Portuguese margin and beneath the Grand Banks, the oldest marine sediments are transgressive above evaporites (localized in certain depocenters) of the Lower Jurassic (pre-Pliensbachian) and upper Triassic (Oertel, 1956; Ramirez de Pozo, 1971; Hallam, 1971; Williams, 1972; Sherwin, 1973; Jansa and Wade, 1975; Gradstein et al., 1975).

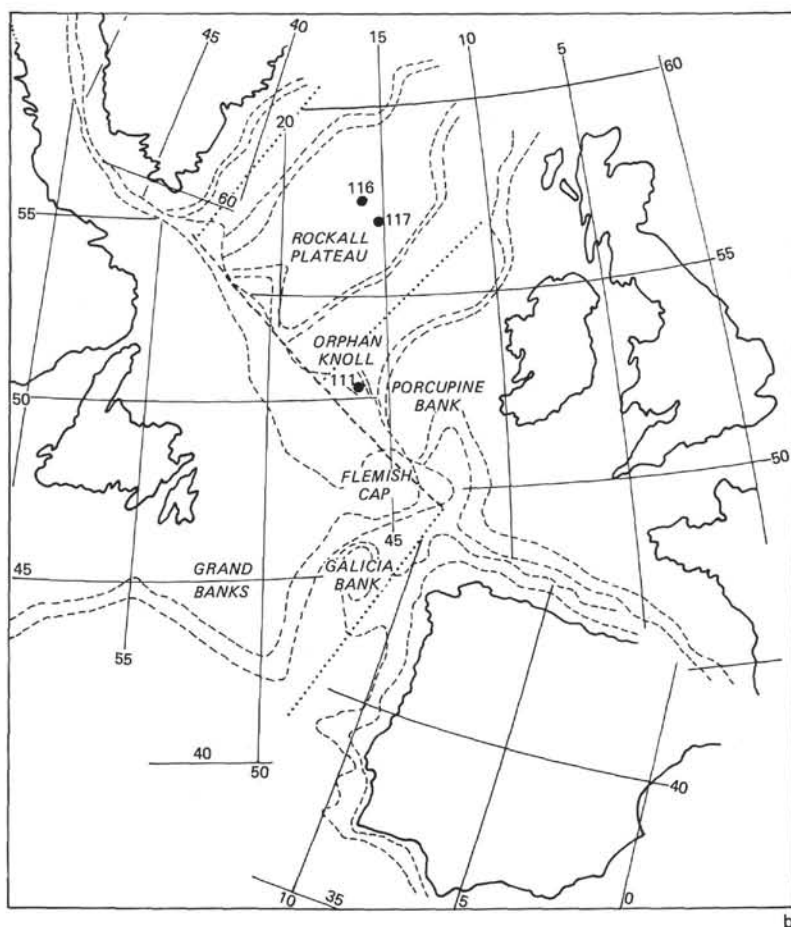
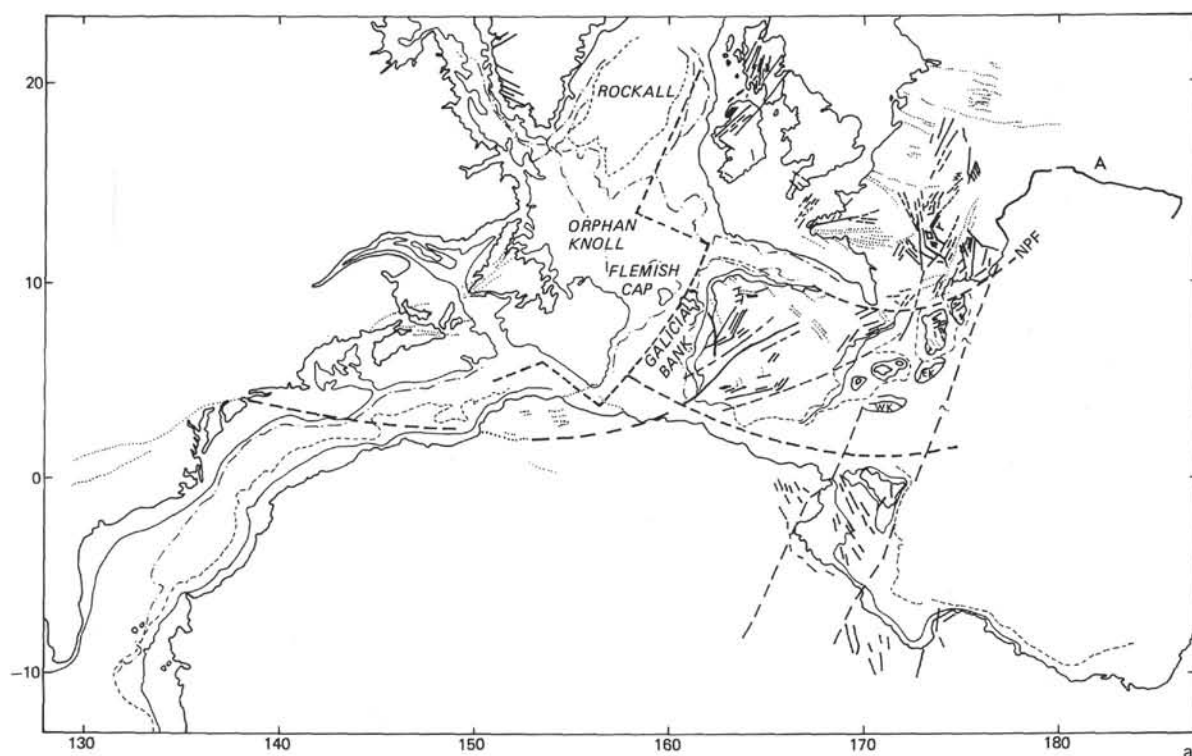


Figure 2. Examples of a relatively "tight-fit reconstruction." (a) Late Hercynian, from Le Pichon et al., 1977 and a relative "loose-fit reconstruction." (b) Late Jurassic, from Laughton et al., 1975, of the plates defining the western and eastern paleoboundaries of the North Atlantic Ocean.

## Uncertainty as to the Age of the Opening of the North Atlantic

There is a general consensus that both the timing and geometry of the breakup and the initial separation of Iberia away from North America and from the rest of Europe are not completely understood (e.g., see Wilson, 1975). However, several lines of evidence suggest that this event took place somewhere between the Permian and the Late Cretaceous. The various sources of information include:

- 1) Paleomagnetic polar wandering curves from sites in northern Spain for the timespan of the Permian to the Late Cretaceous, which point out a rotation of Iberia relative to Europe since the Kimmeridgian.

- 2) Core samples from the subsurface of the Cantabria Seamount at DSDP Site 119, which demonstrate that Upper Cretaceous (Maestrichtian) strata extend continuously across the Bay of Biscay and post-date the major component of the rotation of Iberia (Laughton and Berggren, 1972).

- 3) Marine magnetic anomalies seaward of Galicia which reveal the presence of a considerable width (>220 km) of the Atlantic sea floor between the present coastline and anomaly lineations originally identified as Anomaly 31 (Williams and McKenzie, 1971; Pitman and Talwani, 1972; Williams, 1975) and later as Anomaly 34 (according to the latest revision of Cande and Kristoffersen, 1977). Anomaly 34 corresponds to the top of the long Cretaceous interval of normal magnetic polarity. In the Gubbio section of Italy, Anomaly 34 can be correlated to the top of the *Globotruncana concavata carinata* Zone of the upper Santonian (Alvarez et al., 1977).

- 4) An extensive angular unconformity observed beneath the entire Grand Banks of North America, and in both the Lusitanian and Aquitanian basins of Europe; this unconformity separates folded and truncated Jurassic and lowermost Cretaceous sediments below from more-or-less flat-lying Albian strata above (Amoco Canada Petroleum Company, Ltd., and Imperial Oil, Ltd., 1973; Gradstein et al., 1975; Jansa and Wade, 1975; Daradel and Rosset, 1971; Winnock, 1971; Rey, 1972).

- 5) An angular discordance consisting of flat-lying Albian to Cenomanian limestones above tilted and folded Middle Jurassic continental sandstones at DSDP Site 111 on Orphan Knoll (Laughton, Berggren, et al., 1972; Ruffman and van Hinte, 1973).

- 6) The occurrence of specific mineral assemblages in deltaic sands in southern England the subsurface of the Celtic and North seas, belonging to the so-called Wealden facies. These assemblages are interpreted as having been derived in part from a westerly source of metamorphic and crystalline terraces in either northern Iberia (Allen, 1972) or possibly in North America (personal communication of V. Pujalte, 1974, cited in Wilson, 1975). Although the Wealden deposits are mostly terrestrial, they are dated as Early Cretaceous

and are probably no older than latest Jurassic (i.e., "Purbeck" facies).

## Uncertainty as to the Geometry of the Initial Continental Fragmentation

Among the many attempts to reconstruct the pre-drift fit of Europe and North America (Bullard et al., 1965; Pitman and Talwani, 1972; Laughton, 1972; Roberts, 1974; Wilson, 1975; Jansa and Wade, 1975; van der Linden, 1975; Le Pichon et al., 1977), there are those which can be considered as "tight" or "loose" assemblies. The "tight-fitting" reconstruction assumes the closure of Rockall Trough plus either independent movements for Flemish Cap and Galicia Bank or their complete elimination. The "loose-fitting" reconstruction allows significant gaps in the areas of the present-day Tagus Basin and the East Newfoundland Basin. Figure 2 illustrates examples of "tight" and "relatively loose" reconstructions.

The relevance of Site 398 to the reconstruction ambiguity was never made clear during the advisory panel deliberations. In the "tight-fit" approach, this site is situated fairly close to the axis of an extensional zone where some emplacement of oceanic crust might have occurred. Although sampling of such crust in the trough between Galicia Bank and the mainland was desirable, the targeting of a single hole to reach this objective would have required sub-bottom penetrations far in excess of 2 km.

As a compromise, Site 398 was positioned in a small local depression on the flank of a prominence within the trough; in certain respects, this site is analogous to Site 111 on Orphan Knoll except that it is not directly on the crest of a prominence. Perhaps more important for the determination of the tightness of the pre-drift reconstruction is the facies and stratigraphic position of the lowermost conformable sedimentary unit overlying the acoustic basement. According to the "loose-fit" concept, the region of Site 398 should possess a crust which was already in existence prior to the Late Triassic and Early Jurassic rifting of Africa from North America; additionally, this region should have had sedimentary covers at least as old as those in depressed basins within the Grand Banks, possibly even Paleozoic sediments equivalent to the Canadian Windsor Formation (Carboniferous) or the Meguma Formation (Ordovician).

Since the deepest conformable sedimentary unit which can be recognized on the acoustic profiles extends as far south as Gorringe Bank (i.e., the Azores-Gibraltar plate boundary) and as far west as the magnetic quiet zone seaward of Galicia Bank proper (unpublished L-DGO reflection profiles of R/V *Vema* and R/V *Robert D. Conrad*), the discovery of pre-Jurassic age for any part of this crust would provide very strong support for the "looser-fit" reconstructions. In the same context, the recovery of any sediments or rocks belonging to the Early Jurassic evaporite and salt deposits of Nova Scotia (Argo Formation) or Morocco (Doukala Formation) would in-

dicates a much broader northward penetration of the "pre-drift" seaway than that presently preserved in the seaward "truncated" coastal Lusitanian Basin of Iberia and the poorly explored Carson half-graben of the easternmost Grand Banks.

### SCIENTIFIC OBJECTIVES FOR SITE 398

The target selected to the south of Vigo seemed to have possibly the least amount of total geologic section missing. Four principal acoustic formations or units are identifiable on the seismic records obtained during the site surveys of IFP-CNEXO (Montadert et al., 1974; Passive Margin Advisory Panel Site Prospectus; Groupe Galice, this volume). The deepest unit (4) is detected only south and east of Galicia Bank, although it is separated from Unit 3 by a prominent reflecting horizon (Orange) which can be traced westward of Galicia for some tens of kilometers, where it lies directly above a topographically irregular and diffracting basement unit.

Acoustic Unit 1 is faintly stratified to transparent. Its upper surface is often sculptured by relatively recent erosional events allowing outcropping or shallow subcropping of internal horizons. Acoustic Unit 1 drapes underlying relief and is separated unconformably from Unit 2 by a reflecting horizon (Green) which exhibits both depositional and erosional bed forms (drifts and channels).

Acoustic Unit 2 is highly stratified. It contains some internal reflecting horizons such as Reflector Blue, which truncate and bevel underlying sedimentary layers. In the Vigo region, acoustic Unit 2 has the most variable thickness. Surprisingly, this unit is sometimes thicker on topographic highs than in lows. It is generally thinnest in the transition zones. Near its base, one finds a prominent reflector (Red) which has certain reflectivity and reverberation characteristics similar to Horizon A of the western North Atlantic.

Acoustic Unit 3 is transparent and internally homogeneous. Its top at Site 398 corresponds to Reflector Yellow and its base to Reflector Orange. This unit is invariably thickest in depressions and thin to absent on elevations. It is never seen to crop out and is absent altogether on the steep marginal escarpments of Vigo Seamount. Its upper surface is often correlated as evidenced by diffraction patterns (Profile GP-19, see Figure 3) and megaundulations (Profile *Charcot* 6). The uppermost part of transparent Unit 3 is tentatively traced as far seaward as Anomaly 34 of Cande and Kristoffersen (1977).

Acoustic Unit 4 is generally obscure except on digitally processed records. It appears to be the deepest sedimentary cover directly overlying acoustic basement. Like acoustic Unit 3, Unit 4 is only expressed in topographic depressions such as half grabens. It cannot be followed westward of Galicia Bank in the abyssal plain, and as yet is detected only in the region between Galicia and the mainland of Iberia.

The upper surface of acoustic Unit 4 is locally smooth and generally nondiffractive. In the half grabens, it sometimes shows some evidence of minor disturbance

by faulting with vertical throws of less than a few tens of meters. Although not very tectonically deformed, it is the only formation which in the immediate drill site area shows clear indications of significant post-depositional alteration either by tilting, folding, faulting, or intrusion. Acoustic Unit 4 lies above a basement which occasionally is internally reflective and which is offset by large (i.e., several tens to hundreds of meters relative movement) down-to-basin faults which produced tilted half grabens opening towards the axis of the Galicia Trough. At Site 398, the surface of the acoustic basement is about 1800 meters below the sea floor. Its great depth was the principal reason for the deployment of a re-entry cone.

### Mesozoic Objectives

The sequence of sedimentation events for the Mesozoic along the northwestern continental margin of Spain and Portugal is only poorly known, mostly from dredge hauls and inference from seismic correlations. Knowledge of the sedimentary history of this region is important (1) for the interpretation of timing of the early opening and the post-opening subsidence history of the North Atlantic Ocean; and (2) for interpretation and documentation of paleoceanographic events at this mid-latitude location related both to climatic change and to patterns of ocean basin evolution.

The important objectives of Mesozoic age at Site 398 are enumerated here and briefly discussed below:

- 1) To core and date acoustic basement.
- 2) Age determination and paleoenvironment of oldest sediments overlying acoustic basement and monitoring of paleodepths of succeeding lithologies to obtain estimates of subsidence rates and a subsidence history for the continental margin after rifting.
- 3) Age and paleoenvironment of Early Cretaceous black shales.
- 4) Determine possible circulation events in the North Atlantic related to the opening of major seaways in early Campanian (Rockall-Europe) and Maestrichtian (Greenland-Canada). These openings perhaps allowed high latitude, cool bottom waters to funnel for the first time into the North Atlantic through the Iberian-Newfoundland opening.
- 5) Examining evidence for major climatic events (e.g., mid-Barremian, Cenomanian, late Maestrichtian) and possible associated hiatuses, using biostratigraphic and isotopic tools.
- 6) Study of the Maestrichtian-Danian transition in light of current theories on calcite compensation depth excursions, major extinctions, and climatic change.

Various pre-drift reconstructions of continental blocks in the North Atlantic establish Site 398 on the Vigo Seamount as crucial for the determination of the timing and pattern of breakup in the North Atlantic north of the Newfoundland fracture zone (Figure 2). South of the Newfoundland fracture zone, it appears that the North Atlantic had already begun opening by the Early Jurassic. North of this transform fault boundary, however, sea-floor spreading was apparently de-

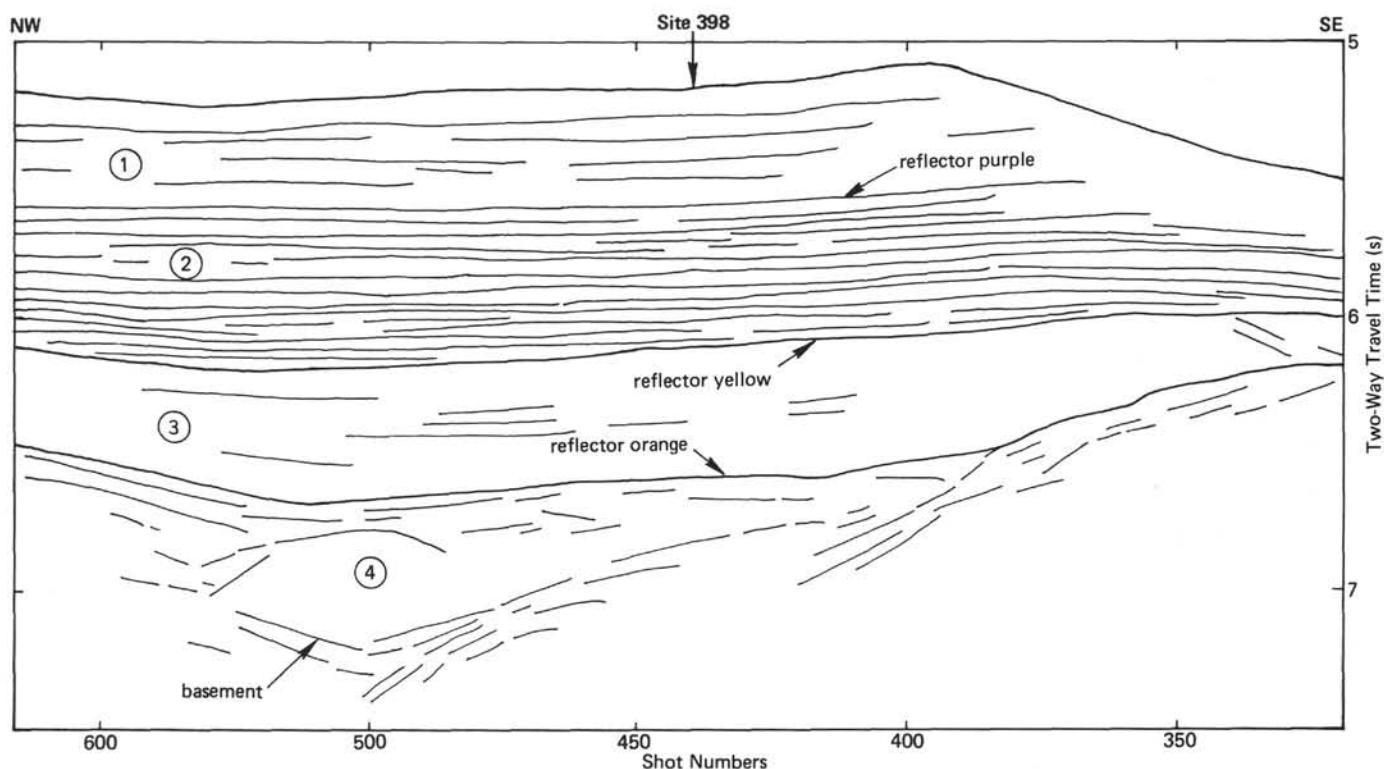


Figure 3. Interpretation of processed profile GP-19 (IFP-CNEXO-CEPM) at Site 398. Numbers indicate litho-stratigraphic units discussed in text.

layed until later. By drilling, it is possible to determine an age of generation for the first known oceanic basement in this region through the stratigraphic dating of the seismic reflector below acoustic Unit 3. This is a reasonable estimate of the time of separation of Grand Banks-Newfoundland from the Iberian Peninsula.

A further problem of interest is that of the subsidence history of continental margins. In this situation, the Galicia Bank-Vigo Seamount block may have separated from the main Iberian crustal block. It would be useful to determine the behavior of such small blocks consisting of crust of continental affinities after they have experienced thermal uplift during the early rifting phase and during their collapse below sea level. This subsidence history could be partially documented by study of the sequence of sedimentary facies and by evolution of benthic faunal communities, mainly that of foraminifers. Hopefully, a subsidence curve could be generated and compared with predicted rates from geophysical considerations.

A further objective of at least regional importance is that of detailed coring of acoustic Unit 3 (maximum of about 550 m thick). This generally seismically transparent layer is the typical expression of Lower to Middle Cretaceous black hemipelagic muds or shales. In the Galicia Bank region, this acoustic layer exhibits pronounced thickness variations related to the underlying basement topography, as previously mentioned.

Black shales (Aptian-Albian) occur on most of the North Atlantic sea floor (Lower Cretaceous) south of the Newfoundland fracture zone. Black shales (high

organic carbon content, pyritic, usually laminated with absence of benthic faunas) have been detected as old as Hauterivian, with some as young as Santonian. The Aptian-Albian period seems to be a time of exceptionally widespread deposition of "black shales." Many of these deposits, especially those in the North Atlantic, seem to be indicative of anoxic environments on the sea floor. The cause of such an episode of euxinic conditions is thought to be a combination of climatic influence on oceanic circulation rates and oxygen regeneration to bottom and intermediate waters, with local circulation restrictions imposed by young, narrow, and possibly silled ocean basins. The Aptian-Albian "stagnation event" is globally exhibited but is very intense and of somewhat longer duration in the North Atlantic than elsewhere.

In the Atlantic north of the Newfoundland fracture zone, black, organic-rich Lower Cretaceous deposits presently are known only from eastern Greenland (Donovan, 1961) and northern Spain (Flysch Negro). Wealden deltaic deposits of Early to Middle Cretaceous age are known from many of the margins bordering this part of the Atlantic. Site 398 is therefore of importance in establishing whether the North Atlantic oceanwide stagnation extended farther north than presently known and may answer questions about the causes of this event. The causes may be related to restriction of bottom circulation or to intensification and expansion of the oxygen-minimum zone due to extremely warm, equable climates and reduced oceanic convection rates, or to some combination of the two extremes. The

absence of black shales at this site could imply that this region may have been a conduit for oxygenated bottom water flowing south into the North Atlantic or perhaps only that euxinic conditions were restricted in extent to deeper and older within the North Atlantic.

Also of interest is the subsequent history of circulation changes in the North Atlantic due to dispersal of continental blocks such as the separation of Rockall Bank from the European block or Greenland from Canada. The first fragmentation may have occurred during the early Campanian (anomaly 34), the latter during the Maestrichtian (anomaly 32-31). If, during this interval, there was a constricted oceanic passage between the Grand Banks and Galicia, relatively older Boreal bottom waters would have been funneled through gaps between the more northern rifted margins, and might possibly have plunged through the Galicia-Grand Banks and Galicia Iberia openings. The expression of this bottom-water activity may be found in the form of a Late Cretaceous hiatus, with intensified circulation producing bottom scour, by the piling up of large amounts of drifted sediment at the exit point to the larger southern North Atlantic basin (Tagus area) when current velocities drop off and/or by intensified dissolution due to colder undersaturated waters analogous to the modern Antarctic bottom waters. Sedimentary structures, sedimentation rates, and provenance of detritus are important in documenting this possibility.

Such current may have, however, been diverted through the open Bay of Biscay-Pyrenees Trough into the Tethys Ocean and, therefore, may not have been manifested here.

Although the recovery of a good calcareous Cretaceous section deposited above the lysocline is unlikely, it would allow isotopic and paleontological studies of the Middle and Late Cretaceous climatic history of a middle latitude, Northern Hemisphere site, which has not been previously accomplished because most sites were either too shallow or too deep to recover good, continuous pelagic sequences. It is imperative to date these Mesozoic climatic events in the North Atlantic, especially the possible Cenomanian and late Maestrichtian to Paleocene cooling episodes.

Occurrences of hiatuses within the section could also aid in interpretation of climatic and circulation events. Hiatuses are prevalent during certain intervals (Cenomanian, Campanian, late Maestrichtian) in the western Atlantic. It will be necessary to determine presence or absence of hiatuses in the eastern Atlantic for an understanding of the processes involved in the formation of these disconformities.

Investigation of events occurring at the Cretaceous/Tertiary boundary is also of current interest. Recent hypotheses (e.g., Worsley, 1974) suggest a pronounced upward CCD excursion into the photic zone at this time. Several DSDP sites have recovered calcareous sections across the Cretaceous/Tertiary boundary, which seem to eliminate the preceding hypothesis. A continuous fossil-bearing section allows isotopic, geochemical, and paleontological studies to elucidate the picture of

climatic changes in ocean chemistry, as well as the enigmatic evolution and extinction of various faunal groups at this time.

### Cenozoic Objectives

The most important Cenozoic accomplishment would be the recovery of a complete Paleocene and Eocene sequence permitting us to see if the abrupt cooling of ocean bottom water about 40 m.y.B.P. seen in the Tasman Sea and South Atlantic Ocean was also expressed north of the equator. Of additional high priority is the documentation of siliceous productivity in Eocene to early Miocene time relative to a global east-west circulation between Africa and Europe.

The Neogene section was expected to reveal the extent of higher latitude climatic deterioration following the first extensive development of glaciation in the Southern Hemisphere in the Miocene and the abrupt cooling of the Labrador and Greenland seas in the Pliocene. Attention was given to the recovery of a transition from the Miocene to the Pliocene which might reveal a response of Atlantic climate to the late Miocene Mediterranean salinity crisis.

### Other Objectives

On Leg 47B, we tested and evaluated a new downhole *in-situ* pore-water sampler and the systematic use of a downhole temperature recorder.

The shipboard program of organic geochemistry focused on the detection, monitoring, and analyses of entrained hydrocarbon gases in the sediments penetrated, with emphasis on evaluation of the "*in-situ* young diagenesis" model developed on Leg 47A. An important test to this model was the synclinal setting of Site 398 and its bearing on the relative role played by migration of gases generated elsewhere by thermal and chemical processes, and the role of biologically produced heavier hydrocarbons up to and including pentane.

Deep penetration allows first-time recovery of organic-rich sediments which have experienced a direct thermal regime sufficient for the maturation of liquid hydrocarbons (a process generally considered to require 50°C or greater temperatures over periods of tens to a hundred million years). The location of black organic shales at this depth is a DSDP first.

A shipboard spinner magnetometer was utilized routinely to determine polarity of remanent magnetism in the recovered sediment sequence and, hence, afforded a new opportunity for a higher-resolution physical stratigraphy.

## OPERATIONS

### Site Approach

Site 398 was approached during the evening of 13 April on a heading of 211° (Figure 4). A satellite fix was calculated for a position at 1850 hours, which confirmed that the dead-reckoning track was along the right longitude. Additional longitude control was also pro-



TABLE 1  
Coring Summary, Site 398

Core	Date (April 1976)	Time	Depth From Drill Floor (m)	Depth Below Sea Floor (m)	Length Cored (m)	Length Recovered (m)	Recovery (%)
<b>Hole 398</b>							
1	14	1200	391.5-3925.0	15.5-25.0	9.5	0.01	0
2	14	1325	3925.0-3934.5	25.0-34.5	9.5	7.73	81
3	14	1530	3934.5-3944.0	34.5-44.0	9.5	7.49	79
4	14	1845	4020.0-4026.5	120.0-126.5	6.5	6.85	105
Total					35.0	22.08	63
<b>Hole 398A</b>							
1	16	0320	4072.5-4082.0	172.5-182.0	9.5	8.61	91
2	16	1220	4101.0-4110.5	201.0-210.5	9.5	8.63	91
Total					19.0	17.24	91
<b>Hole 398B</b>							
1	17	2245	4129.5-4139.0	229.5-239.0	9.5	8.26	87
<b>Hole 398C</b>							
1	20	0250	3900.0-3979.0	0.0-79.0	0.0	0.75	—
<b>Hole 398D</b>							
1	20	0510	3900.0-3909.5	0.0- 9.5	9.5	0.00	0
2	20	1100	4171.0-4180.5	271.0-280.5	9.5	3.49	37
3	20	1535	4218.5-4228.0	318.5-328.0	9.5	9.72	102
4	20	1815	4266.0-4275.5	366.0-375.5	9.5	9.15	96
5	20	2255	4294.4-4304.0	394.5-404.0	9.5	8.39	88
6	21	0135	4313.5-4323.0	413.5-423.0	9.5	9.71	102
7	21	0355	4332.5-4342.0	432.5-442.0	9.5	9.62	101
8	21	0610	4351.5-4361.0	451.5-461.0	9.5	8.16	86
9	21	0835	4370.5-4380.0	470.5-480.0	9.5	9.62	101
10	21	1040	4389.5-4399.0	489.5-499.0	9.5	0.01	0
11	21	1300	4399.0-4408.5	499.0-508.5	9.5	0.00	0
12	21	1700	4408.5-4418.0	508.5-518.0	9.5	7.51	79
13	21	1945	4427.5-4437.0	527.5-537.0	9.5	9.63	101
14	22	0245	4437.0-4446.5	537.0-546.5	9.5	0.96	10
15	22	0530	4446.5-4456.0	546.5-556.0	9.5	8.55	90
16	22	0835	4456.0-4465.5	556.0-565.5	9.5	1.05	11
17	22	1100	4465.5-4475.0	565.5-575.0	9.5	0.50	5
18	22	1305	4475.0-4484.5	575.0-584.5	9.5	0.10	1
19	22	1815	4484.5-4494.0	584.5-594.0	9.5	8.73	92
20	22	2000	4494.0-4503.5	594.0-603.5	9.5	9.09	96
21	22	2135	4503.5-4513.0	603.5-613.0	9.5	5.57	59
22	22	2320	4513.0-4522.5	613.0-622.5	9.5	7.52	79
23	23	0145	4522.5-4532.0	622.5-632.0	9.5	5.52	58
24	23	0350	4532.0-4541.5	632.0-641.5	9.5	9.02	95
25	23	0640	4541.5-4551.0	641.5-651.0	9.5	1.55	16
26	23	0900	4551.0-4560.5	651.0-660.5	9.5	9.66	102
27	23	1100	4560.5-4570.0	660.5-670.0	9.5	7.56	80
28	23	1300	4570.0-4579.5	670.0-679.5	9.5	8.14	86
29	23	1445	4579.5-4589.0	679.5-689.0	9.5	9.48	100
30	23	1630	4589.0-4598.5	689.0-698.5	9.5	7.45	78
31	23	1900	4598.5-4608.0	698.5-708.0	9.5	5.72	60
32	23	2055	4608.0-4617.5	708.0-717.5	9.5	8.15	86
33	23	2315	4617.5-4627.0	717.5-727.0	9.5	8.47	89
34	24	0155	4627.0-4636.5	727.0-736.5	9.5	9.68	102
35	24	0425	4636.5-4646.0	736.5-746.0	9.5	9.63	101
36	24	0635	4646.0-4655.5	746.0-755.5	9.5	9.65	102
37	24	0840	4655.5-4665.0	755.5-765.0	9.5	6.50	68
38	24	1050	4665.0-4674.5	765.0-774.5	9.5	7.04	74
39	24	1405	4674.5-4684.0	774.5-784.0	9.5	6.00	63
40	24	1750	4684.0-4693.5	784.0-793.5	9.5	9.58	101
41	24	2145	4693.5-4703.0	793.5-803.0	9.5	9.56	101
42	25	0100	4703.0-4712.5	803.0-812.5	9.5	3.84	40
43	25	0400	4712.5-4722.0	812.5-822.0	9.5	7.88	83
44	25	0750	4722.0-4731.5	822.0-831.5	9.5	9.52	100
45	25	1020	4731.5-4741.0	831.5-841.0	9.5	9.00	95
46	25	1330	4741.0-4750.5	841.0-850.5	9.5	5.86	62
47	25	1530	4750.5-4760.0	850.5-860.0	9.5	7.13	75
48	25	1845	4760.0-4769.5	860.0-869.5	9.5	9.62	101
49	25	2200	4769.5-4779.0	869.5-879.0	9.5	0.60	6
50	25	2345	4779.0-4788.5	879.0-888.5	9.5	9.58	101
51	26	0150	4788.5-4798.0	888.5-898.0	9.5	4.33	46
52	26	0415	4798.0-4807.5	898.0-907.5	9.5	6.30	66
53	26	0635	4807.5-4817.0	907.5-917.0	9.5	9.27	98
54	26	0915	4817.0-4826.5	917.0-926.5	9.5	3.32	35
55	26	1135	4826.5-4836.0	926.5-936.0	9.5	2.15	23
56	26	1430	4845.5-4855.0	945.5-955.0	9.5	9.21	9
57	26	1730	4855.0-4864.5	955.0-964.5	9.5	7.17	75
58	27	0315	4864.5-4874.0	964.5-974.0	9.5	2.68	28
59	28	0035	4874.0-4883.5	974.0-983.5	9.5	9.73	102
60	28	0315	4883.5-4893.0	983.5-993.0	9.5	4.65	49
61	28	0530	4893.0-4902.5	993.0-1002.5	9.5	2.15	23
62	28	0745	4902.5-4912.0	1002.5-1012.0	9.5	9.21	97
63	28	1000	4912.0-4921.5	1012.0-1021.5	9.5	8.35	88
64	28	1215	4921.5-4931.0	1021.5-1031.0	9.5	0.00	0
65	28	1410	4931.0-4940.5	1031.0-1040.5	9.5	9.23	97
66	28	1615	4940.5-4950.0	1040.5-1050.0	9.5	2.26	24
67	28	1805	4950.0-4959.5	1050.0-1059.5	9.5	5.25	55
68	28	2015	4959.5-4969.0	1059.5-1069.0	9.5	6.85	72
69	28	2220	4969.0-4978.5	1069.0-1078.5	9.5	7.01	74
70	29	0030	4978.5-4988.0	1078.5-1088.0	9.5	4.05	43
71	29	0250	4988.0-4997.5	1088.0-1097.5	9.5	5.45	57
72	29	0610	5007.0-5016.5	1107.0-1116.5	9.5	9.70	102
73	29	0835	5016.5-5026.0	1116.5-1126.0	9.5	8.44	89
74	29	1045	5026.0-5035.5	1126.0-1135.5	9.5	7.87	83
75	29	1335	5035.5-5045.0	1135.5-1145.0	9.5	6.24	66
76	29	1620	5045.0-5054.5	1145.0-1154.5	9.5	4.00	42
77	29	1950	5064.0-5073.5	1164.0-1173.5	9.5	9.60	101

TABLE 1 – Continued

Core	Date (April 1976)	Time	Depth From Drill Floor (m)	Depth Below Sea Floor (m)	Length Cored (m)	Length Recovered (m)	Recovery (%)
78	30	0050	5073.5-5083.0	1173.5-1183.0	9.5	9.58	101
79	30	0250	5083.0-5092.5	1183.0-1192.5	9.5	6.36	67
80	30	0450	5092.5-5102.0	1192.5-1202.0	9.5	5.54	58
81	30	0630	5102.0-5111.5	1202.0-1211.5	9.5	5.85	62
82	30	0900	5111.5-5121.0	1211.5-1221.0	9.5	8.77	92
83	30	1045	5121.0-5130.5	1221.0-1230.5	9.5	0.10	1
84	30	1515	5130.5-5140.0	1230.5-1240.0	9.5	9.70	102
85	30	1715	5140.0-5149.5	1240.0-1249.5	9.5	5.60	59
86	30	1910	5149.5-5159.0	1249.5-1259.0	9.5	7.50	79
87	30	2105	5159.0-5168.5	1259.0-1268.5	9.5	8.06	85
88	30	2305	5168.5-5178.0	1268.5-1278.0	9.5	9.70	102
(May 1976)							
89	1	0100	5178.0-5187.5	1278.0-1287.5	9.5	7.96	84
90	1	0250	5187.5-5197.0	1287.5-1297.0	9.5	7.51	79
91	1	0435	5197.0-5206.5	1297.0-1306.5	9.5	6.44	68
92	1	0645	5206.5-5216.0	1306.5-1316.0	9.5	9.27	98
93	1	1915	5216.0-5225.5	1316.0-1325.5	9.5	8.90	94
94	3	0040	5225.5-5227.5	1325.5-1327.5	2.0	2.00	100
95	3	0255	5227.5-5235.0	1327.5-1335.0	7.5	8.84	118
96	3	0500	5235.0-5244.5	1335.0-1344.5	9.5	7.50	79
97	3	0655	5244.5-5254.0	1344.5-1354.0	9.5	8.08	85
98	3	0945	5254.0-5263.5	1354.0-1363.5	9.5	2.10	22
99	3	1600	5263.5-5273.0	1363.5-1373.0	9.5	9.70	102
100	3	1911	5273.0-5282.5	1373.0-1382.5	9.5	8.16	86
101	3	2140	5282.5-5292.0	1382.5-1392.0	9.5	8.91	95
102	3	2350	5292.0-5301.5	1392.0-1401.5	9.5	9.16	96
103	4	0200	5301.5-5311.0	1401.5-1411.0	9.5	8.87	93
104	4	0415	5311.0-5320.5	1411.0-1420.5	9.5	5.07	53
105	4	0630	5320.5-5330.0	1420.5-1430.0	9.5	4.50	47
106	4	0840	5330.0-5339.5	1430.0-1439.5	9.5	8.55	90
107	4	1055	5339.5-5349.0	1439.5-1449.0	9.5	7.05	74
108	4	1425	5349.0-5358.5	1449.0-1458.5	9.5	9.44	99
109	4	1645	5358.5-5368.0	1458.5-1468.0	9.5	5.45	57
110	4	1950	5368.0-5377.5	1468.0-1477.5	9.5	0.20	2
111	4	2350	5377.5-5387.0	1477.5-1487.0	9.5	7.45	78
112	5	0205	5387.0-5396.5	1487.0-1496.5	9.5	7.65	81
113	5	0410	5396.5-5406.0	1496.5-1506.0	9.5	9.13	96
114	5	0555	5406.0-5415.5	1506.0-1515.5	9.5	7.53	83
115	5	0830	5415.5-5425.0	1515.5-1525.0	9.5	4.50	47
116	5	1200	5425.0-5434.5	1525.0-1534.5	9.5	3.92	41
117	5	1430	5434.5-5444.0	1534.5-1544.0	9.5	9.58	101
118	5	1700	5444.0-5453.5	1544.0-1553.5	9.5	8.30	87
119	5	1920	5453.5-5463.0	1553.5-1563.0	9.5	8.17	86
120	5	2140	5463.0-5472.5	1563.0-1572.5	9.5	9.13	96
121	6	0035	5472.5-5482.0	1572.5-1582.0	9.5	9.30	98
122	6	0335	5482.0-5491.5	1582.0-1591.5	9.5	9.57	101
123	6	0545	5491.5-5501.0	1591.5-1601.0	9.5	6.85	72
124	6	0810	5501.0-5510.5	1601.0-1610.5	9.5	7.57	80
125	6	1125	5510.5-5520.0	1610.5-1620.0	9.5	8.98	95
126	6	1420	5520.0-5529.5	1620.0-1629.5	9.5	8.11	85
127	6	1705	5529.5-5539.0	1629.5-1639.0	9.5	9.56	101
128	7	0130	5539.0-5548.5	1639.0-1648.5	9.5	7.38	78
129	7	0445	5548.5-5558.0	1648.5-1658.0	9.5	9.64	101
130	7	0745	5558.0-5567.5	1658.0-1667.5	9.5	8.53	90
131	7	1050	5567.5-5577.0	1667.5-1677.0	9.5	0.70	7
132	7	1615	5577.0-5586.5	1677.0-1686.5	9.5	5.29	56
133	7	1915	5586.5-5596.0	1686.5-1696.0	9.5	7.22	76
134	7	2210	5596.0-5605.5	1696.0-1705.5	9.5	5.00	53
135	8	0120	5605.5-5615.0	1705.5-1715.0	9.5	6.80	72
136	8	0440	5615.0-5624.5	1715.0-1724.5	9.5	4.57	48
137	8	0820	5624.5-5634.0	1724.5-1734.0	9.5	6.76	71
138	8	1545	5634.0-5640.0	1734.0-1740.0	6.0	6.05	101
Total					1298.0	936.6	72

the drill bit had plugged itself after Core 398D-10 at 489 meters sub-bottom (see Table 1). Two attempts with the core-breaker and small-diameter core-shoe were necessary to free the bit orifice.

The bit again plugged at 584 meters after the cutting of Core 398D-18. Core 398D-25 required an extra wire-line run because of a sheared pin in the overshot.

At 622 meters, a straight-hole test was made with the inclinometer giving a reading of less than one-half degree off vertical. Another test at 802 meters gave a one degree inclination.

At 1300 hours on 25 April, the vertical reference gyro in the dynamic positioning system failed, leading to an excursion away from the hole of an unknown magnitude.

The first bit change took place after the cutting of Core 398D-58 at a depth of 974 meters with a little over 50 hours of rotation time. A new bit of the same type (Smith F93ck, long insert 10-in. diameter, four-cone) was made up and successfully re-entered the cone at 1900 hours on 27 April.

A third straight-hole test at 1012 meters showed two degrees off vertical.

Additional problems with plugged bits re-occurred twice, once while cutting Core 398D-77 and again with Core 398D-83. The bits were unplugged both times by pumping-down the small-diameter core-shoe. A fourth straight-hole test at 1212 meters gave a reading of three and three-quarters degrees off vertical. The most serious mishap occurred on the morning of 1 May when the core barrel for Core 398D-93 was retrieved from the pipe with the core-catcher sleeve, catchers, plastic liner, and entire core missing and somewhere down the drillstring. An attempt at fishing with a pronged spear was unsuccessful and indicated the liner to be stuck in the pipe five joints above the bottom hole assembly. The entire string had to be tripped to the surface, the bit replaced, and a second re-entry attempted.

Upon tripping-out of the hole, the liner and core material were recovered practically intact. A second new drill bit was prepared and re-entry commenced at 0425 hours on 2 May. However, only seconds after the EDO scanning tool was turned on, it lost electrical power. When the tool was retrieved, it was discovered that the sonar transducer and extender-shoe were broken off and missing. A core barrel was immediately pumped-down to assure that the bottom hole assembly flapper valve, and bit orifice were clear of these mechanical parts and that the scanner had dropped from the drillstring onto the sea floor. A new re-entry scanning tool was utilized; at 1557 hours, a second successful re-entry was completed after scanning for only five minutes.

By the early morning of 3 May we were back to coring operations at a sub-bottom depth of 1325.5 meters. Shortly afterward, the bit became plugged during the cutting of Core 398D-98. Two trips with the small-diameter core-shoe were required to free the orifice of shale and mudstone fragments. Core 398D-110 was discovered to be tightly wedged in the bottomhole assembly and the first attempt to retrieve it sheared a pin in the overshot and caused an extra wire-line trip.

A fifth straight-hole test at 1411 meters gave an indication of greater than six degrees and a following run at 1430 meters confirmed this to be seven degrees off vertical.

Plugged bits became a constantly re-occurring hazard. Considerable time was lost with each wire-line run to free them. Some attempts required up to four trips with either the small-diameter extended shoe or the core-breaker, or some alternating combination of the two. Additional plugged bits developed during the cutting of Cores 115, 120, 127, 131, and 134 in Hole 398D.

A seventh straight-hole test at 1696 meters strengthened our suspicions that the drillstring was deviating seriously from the vertical. Bedding planes in the cores were consistently greater than 12 degrees and the formation being penetrated also had an independent dip on the seismic profile. A reading of 23 degrees on the straight-hole run may be somewhat excessive, but is not out of the realm of the possible.

At 0600 hours on 8 May, winds gusting to greater than 35 knots required the shifting of an engine from one of the stern thrusters to one of the propulsion shafts to assist the single engine there. Positioning was achieved with manual steering on the helm. Two excursions from the hole were encountered.

The new lithologies of pelagic limestones discovered in Cores 398D-136 and 398D-137 indicated that the major objective of penetrating into acoustic Formation 4 was clearly successful and that "pre-drift" strata had been encountered. Hence, the Operations Manager, Captain, and Drilling Supervisor were informed; at 1000 hours on 8 May a decision was made to terminate the cutting of Core 398D-138 at 1740 meters sub-bottom and "head for the barn."

The original beacon signal became inaudible and a second beacon was quickly dispatched to allow staying over the hole. The second beacon failed and the remaining time in the hole was spent positioning intermittently with weak signals from the first beacon.

Winds were now gusting to 40 mph. The core barrel for Core 398D-138 was recovered after filling the hole with weighted mud, prior to the cement plug. The lowermost two sections were totally occupied with downhole cuttings while the upper two sections contained the now-precious limestone.

After the string was lifted above the mudline, a final test of the pore-water sampler was accomplished.

The vessel became underway for Brest, France, at 0600 hours on 9 May on only four of the six propulsion engines in gale force winds, endeavoring to make an ETA prior to 0200 hours on Thursday 13 May, when she would be required in drydock for major repairs to the thrusters and two electrical generators.

## LITHOSTRATIGRAPHY

### Cenozoic Deposits

#### Introduction

Two main units subdivided into five sub-units are recognized for the Cenozoic of Site 398 (see Site Summary Chart 1 in rear pocket, this volume). This subdivi-

sion is based on subtle but recognizable criteria described below. Lithologic changes downhole are generally gradual but noticeable and are characterized by an overall trend towards decreasing carbonate content resulting in a transition from Pleistocene-Pliocene nannofossil ooze and marly nannofossil ooze and chalk to nearly barren Eocene and Paleocene red to brown mudstones and claystones. Superimposed on this trend are brief fluctuations in carbonate content (e.g., middle Oligocene, lower Eocene, lower Paleocene), an input of biogenic silica mainly in the form of sponge spicules and radiolarian tests (lower Miocene, middle to upper Oligocene, middle to upper Eocene), and the occurrence of slumped intervals (Oligocene and Eocene), sand and silt layers representing "distal" (*sensu* Bouma and Hollister, 1973) turbidites and possibly current-winnowed lag deposits (lower Miocene through Paleocene), and thinly laminated marly chalks and mudstones of possible bottom-current origin (Eocene to lower Miocene).

Lithologic Unit 1 consists of three sub-units (1A, 1B, 1C) and extends from 0 to 594 meters sub-bottom depth. It is composed predominantly of bioturbated calcareous biogenic oozes and chalks that are white, greenish gray, and light olive-gray (lower Oligocene through Pleistocene). Sub-unit 1A (0 to 326 m) is a cyclically interbedded nannofossil ooze and marly nannofossil ooze; Sub-unit 1B (326 to 424 m) is a rhythmically interbedded nannofossil chalk and marly nannofossil chalk; Sub-unit 1C (424 to 594 m) is a siliceous marly nannofossil chalk with rhythmically interbedded thin sand-silt layers and slump deposits. Lithologic Unit 2 (594 to 774 m) consists of greenish gray to pale yellow-brown siliceous marly chalk to mudstone, laminated and rhythmically interbedded with thin sand or silt layers. Lithologic Unit 2 (upper Paleocene to lower Oligocene) also includes slumps, debris flow deposits and mud-flow deposits. Sub-unit 3A (774 to 880 m) is a red to brown marly chalk with a few thin silt laminae. The upper part of this unit comprises lower Paleocene sediments. The changes from one lithologic unit to the next are generally transitional and boundaries are placed approximately at the point of greatest contrast. Continuous coring began at 527.5 m, so that recovery of the earlier, more homogeneous-appearing sediment is not as complete, especially from 0 to 400 m (see Site Summary Chart 1 in rear pocket, this volume). Reference can be made to this chart for summary of the various aspects of the lithologic variations at Site 398.

#### Lithologic Units

##### *Unit 1: Cores 398-1 to 398D-19 (0 to 594 m sub-bottom); Lower Oligocene to Pleistocene*

Marly nannofossil ooze, nannofossil ooze, marly nannofossil chalk, and calcareous terrigenous mud are the dominant lithologies with siliceous marly chalk present near the base. Cyclic to rhythmic bedding (discussed below) is visible throughout (see also Maldonado, this volume). Predominant colors are (5Y5/2) light olive-

gray (N8 to N9) light gray to white, (5GY8/1) light greenish gray and some yellowish tinges as well as (5B7/1) light bluish gray. Some lamination is visible throughout; bioturbation and mottling is moderate to intense, but variable. Carbonate contents (see Site Summary Chart 1 in rear pocket, this volume) range from 5 to 80 per cent, with a general decline to lower values downhole, but also with lows of 10 to 25 per cent in the nannofossil mud-marly nannofossil ooze rhythms of the upper Pleistocene. Organic carbon contents reach a maximum of 0.6 weight per cent in the uppermost (Pleistocene) sediments (Core 398-2), but decline to low background levels of 0.1 weight per cent or less below Core 398A-1 (~180 m sub-bottom). Unit 1 is subdivided into three sub-units as discussed below.

##### *Sub-Unit 1A: Cores 398-1 to 398D-3 (0 to 326 m sub-bottom); Upper Miocene to Pleistocene*

This unit is characterized by predominantly light colored marly nannofossil ooze (5Y5/2-5Y7/2, N8 to N9, some 5GY8/1 and 5B7/1 which are light olive-gray and yellow-gray, white, light gray, and light greenish to bluish gray). Carbonate contents are highest in this sub-unit, but extremely variable, averaging about 60 per cent. Siliceous fossils, with the exception of trace amounts of sponge spicules, are absent and the primary biogenic components are calcareous nannofossils with a small percentage of foraminifers. Pyrite contents average from 0 to 5 per cent and clay minerals, quartz, mica, and dolomite along with more minor glauconite and heavy minerals are the main terrigenous components. Illite, montmorillonite, kaolinite, and minor chlorite (in order of abundance) are the clay minerals present (see Site Summary Chart 1 in rear pocket, this volume). Trace amounts of isotropic euhedral light green crystals have been identified as volcanic glass.

Alternations (cycles) of marly nannofossil ooze and light colored nannofossil ooze characterize this sub-unit throughout (Figure 5; see also Maldonado, this volume). Laminations of various colors occur within these interbedded lithologies (0.3 to 10 cm thick) and the transition from less calcareous to more calcareous alternations is generally gradational, but contacts between different cycles may be sharp. These cycles (from 1.7 to 10 m thick) are especially apparent through the Pleistocene, where short-term carbonate variations seem most pronounced. They are similar to features attributed to Pleistocene climatic cycles with either increased terrigenous dilution or increased carbonate dissolution or both within the darker colored marly intervals: each cycle may represent from 50,000 to 250,000 years. Similar cycles are found within the Paleogene of this site (Figure 6). The sedimentation rate of these marly nannofossil oozes and nannofossil oozes range from about 30 to 50 m/m.y.

The significance of finer laminations found in some intervals (e.g., Core 398-3 or Core 398-4) is not clear, although some may possibly be attributed to the activity of bottom currents, since black pyritic placers and foraminiferal laminae are occasionally seen, and also incomplete turbiditic sequences (base cut-out). Sediment

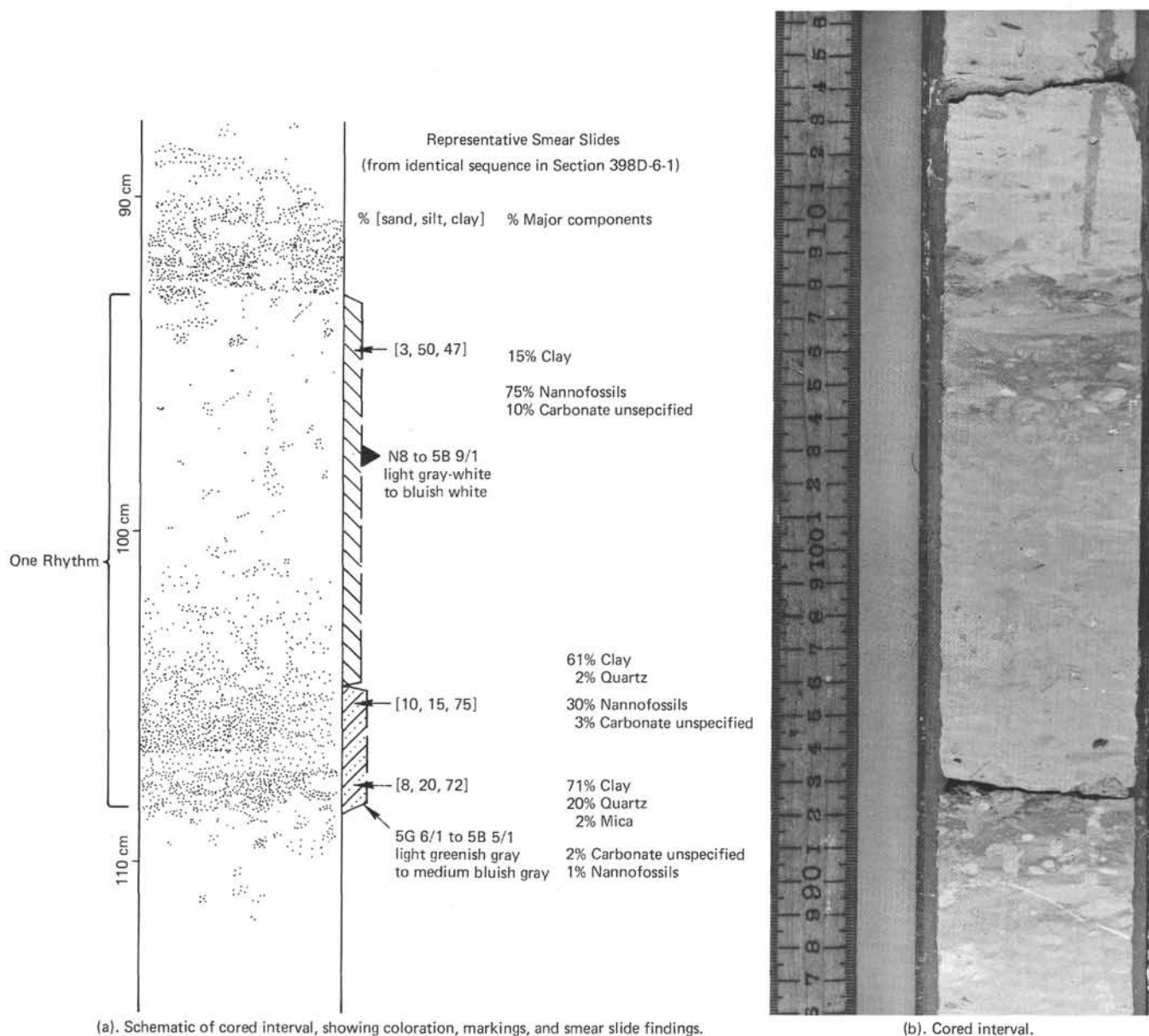


Figure 5. Rhythmic bedding type 1, lower Miocene to Pleistocene sediments from Section 398D-6-3.

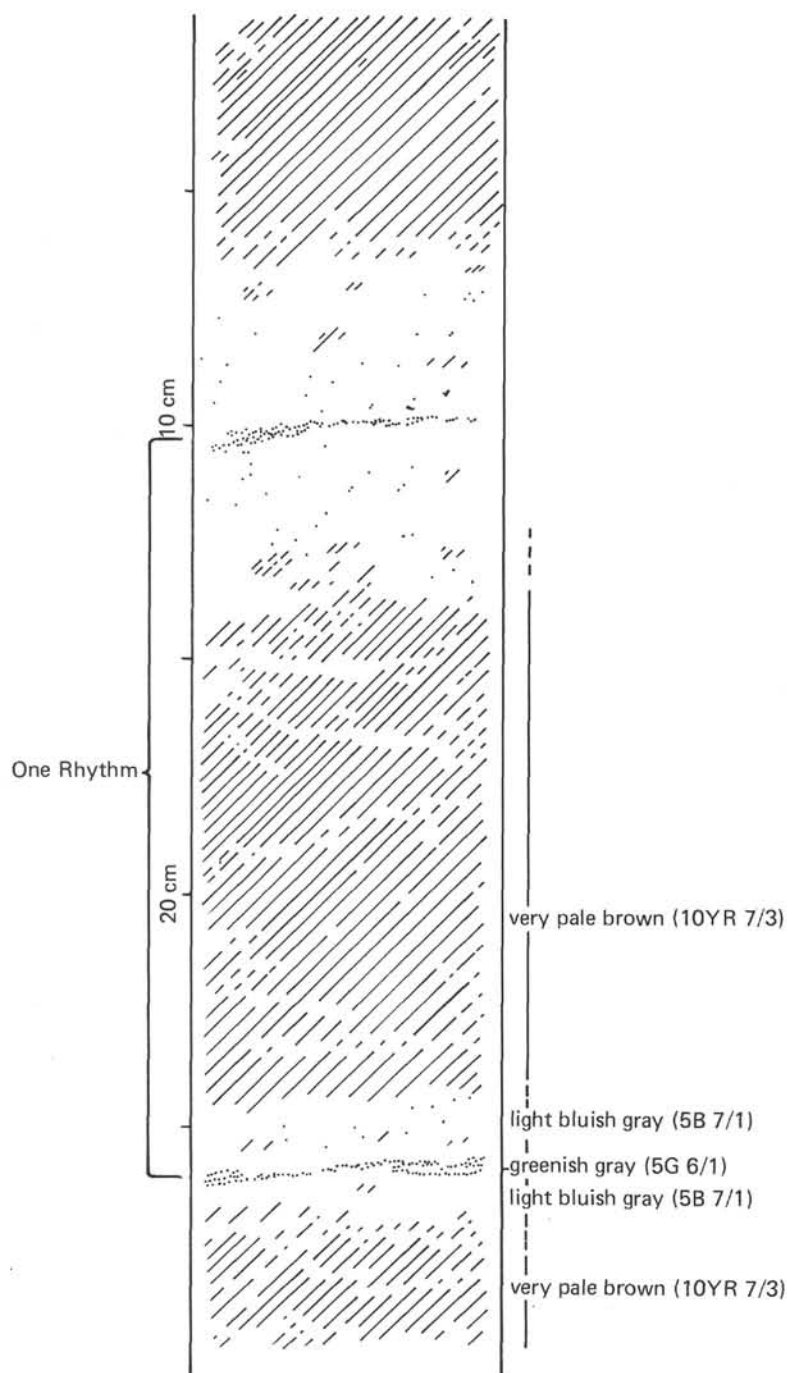
ranges from homogeneous and massive to faintly laminated. Organic-rich mottles (with associated pyrite) are found through most of Sub-unit 1A. Recognized burrowing organisms are *Mycellia* and *Chondrites*. A few intervals have no apparent burrow mottling; others are intensely bioturbated. Composite and halo burrows (e.g., Core 398D-2) are also seen. Burrows generally are most visible near lithologic contacts or as black sulfidic specks and smears.

**Sub-Unit 1B: From End of Core 398D-3 Through 398D-6 (326 to 424 m); Middle to Upper Miocene**

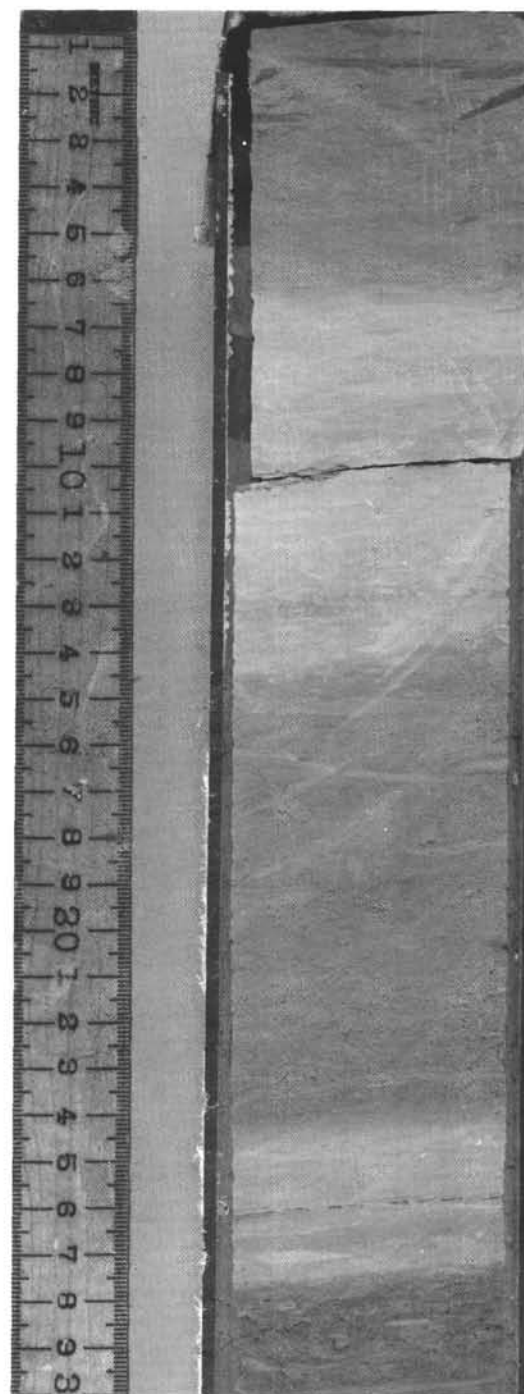
This sub-unit is similar to 1A, but is better lithified into a marly nannofossil chalk and occasionally nannofossil chalk of light blue, white, and gray to olive-

green-gray (5B7/1-9/1 to 5G6/1 and N7 to N8), as shown in Figure 5.

The core surface is usually homogeneous and burrow-mottled, but some laminations occur (dark gray to bright green). These laminations are always associated with the top and, occasionally, the bottom of darker colored intervals. The laminations are not cut by burrows (laminations often pass through burrows), and sometimes surround darker organic-rich burrow fillings. They are interpreted as having a diagenetic origin, possibly due to migration of reduced iron species away from intervals of higher initial organic content and consequent bacterial activity. Good examples can be found in Cores 398D-4 and 398D-5. These laminations were also seen in parts of Sub-unit 1A.



(a) Schematic of cored interval, indicating coloration and markings



(b) Cored interval

Figure 6. *Rhythmic bedding type 2, Paleogene sediments from Section 398D-33-4.*

The clay mineralogy of Sub-unit 1B is similar to that of Sub-unit 1A, with a slight decrease in kaolinite and an increase in montmorillonite. A brief hiatus occurs during the middle Miocene, but is not marked by a pronounced lithologic change.

Evidence of burrowing activity is similar to that in Sub-unit 1A, except that *Zoophycos spreite* often can be recognized and mottling is generally moderate to intense.

***Sub-Unit 1C: Cores 398D-7 Through 398D-19 (424 to 594 m); Lower Oligocene Through Lower Miocene***

This sub-unit is distinguished from the others on the basis of a decrease in  $\text{CaCO}_3$  content, the sudden occurrence of a biogenic siliceous component (sponge spicules, radiolarians), and an increased quartz-mica fraction. Interlayered thin sandstones and siltstones occur at the top of this unit and continue downward

through the remainder of the Cenozoic section. Sedimentation rates are much lower in this sub-unit, typically less than 10 m/m.y.

The transition from Sub-unit 1B to Sub-unit 1C is gradational from Core 398D-5 to Core 398D-7; however, the most marked change occurs between Cores 398D-6 and 398D-7 (see Site Summary Chart 1 in rear pocket, this volume). Siliceous fossils comprise up to 30 per cent of the siliceous marly nannofossil chalks of this sub-unit (Cores 398D-7, 398D-8, 398D-9), averaging 10 to 15 per cent but dominant in the sand fraction. However, certain marly nannofossil chalk intervals are not rich in these remains (Cores 398D-12 and 398D-15 to 398D-18). Colors are typically (5B9/1-7/1) light bluish white to gray 5GY7/1, 6/1 medium greenish gray, 5Y6/1 light olive-gray, and 5Y6/4 dusky yellow at the base of the sub-unit. Carbonate content generally remains between 13 and 70 per cent averaging 45 per cent, while organic carbon is uniformly low at less than 0.1 per cent.

Quartz, mica, clay minerals, minor feldspar, glauconite, and some heavy minerals (primarily tourmaline, ore minerals, and zircon) comprise the terrigenous fraction of the sediment with clay minerals generally the most abundant. These consist of montmorillonite, illite, kaolinite, and chlorite. Montmorillonite increases downhole while kaolinite decreases and chlorite is replaced by interlayered chlorite-vermiculite. There are no distinctive minerals noted in smear slides which are provenance diagnostic. Dolomite, pyrite, and traces of volcanic glass were commonly noted in smear slides along with up to 30 per cent of unidentifiable carbonate material, probably badly dissolved foraminiferal fragments and broken, cemented nannofossil-micrite-clay mineral aggregates.

The entire sub-unit is characterized by rhythmic sedimentation, somewhat different from the previous sub-units. Beginning with Core 398D-5 and especially Core 398D-7, thin silt layers and occasional sandy laminae punctuate the section at from 10- to 50-cm intervals (from 2.5 to 9.5 beds per m). These thin siltstones and sandstones, usually less than 1-cm but as much as 5-cm thick, are carbonate-rich, containing a higher proportion of foraminifers, unidentifiable carbonate fragments, and nannofossils than the fine-grained sediment above or below. Quartz and mica are also important constituents. Enrichment of glauconite and pyrite in thin laminae also occurs. The silt and sand layers generally have an erosional base and exhibit thin parallel, microcross, or ripple lamination, grain-size gradation (upward fining), discontinuous lenticular laminae to flaser structure, or are rarely completely massive and ungraded. Some thicker sandstones (up to 5 cm) show multilayer accretion with several erosional surfaces and thin gradational sequences. These layers may be due to bottom traction currents, i.e., geostrophic flow in the benthic boundary layer.

These sandstone-siltstone intercalations define a rhythmic sedimentation. In lithologic Sub-unit 1C, each rhythm begins with such a layer. A typical sequence is as

follows (see Figures 7 and 8, also Site Summary Chart 1 in rear pocket, this volume):

a) Thin 3-mm to 5-cm turbiditic silt or sand layer, occasionally graded or laminated with sharp basal contact, possibly scoured. The color is generally (5G4/1 to 6/1) dark to light; greenish gray. It may be burrowed, especially in the upper part.

b) Associated with the turbiditic layer is the finer grain-size "tail" which is a (5G6/1 to 5GY4/2) light greenish gray to olive-gray marly nannofossil chalk to nannofossil chalk interval. It may be somewhat silty and burrowed and has a sharp or gradational contact with the underlying sand-silt interval.

c) Interval b (described above) grades upward into a lighter colored, usually (5B7/1-9/1 to 5Y6/4) light bluish gray or white to dusky yellow marly nannofossil chalk, usually siliceous. Carbonate content is generally the same or higher in intervals b or a.

d) Above interval c, just below the next overlying sand or silt layer is another darker colored interval (5-cm thick), similar to b but usually with lesser carbonate content. The coloration may be diagenetic, influenced by the overlying, rapidly sedimented, more organic and carbonate-rich interval (see discussion of diagenesis).

Such rhythms range from 10 to 50 cm in thickness, but may exceptionally reach as much as 1 meter thick. The period of the rhythmicity and possible origins are discussed in more detail by Maldonado (this volume). These rhythms do not always begin with a recognizable silt or sand layer (e.g., Core 398D-9) especially in the upper part of the unit.

In addition to the rhythmic silt-sand and cyclic marly chalk or mudstone pairs, several other sedimentary types with distinctive structures are seen in a few cores. Thinly wavy laminated marly chalks and mudstones with rapid, sharp color changes occur in Cores 398D-8, 398D-12, and 398D-15. These intervals range in thickness from about 20 cm (Core 398D-12) to over 5 meters (Core 398D-15). Thin parallel laminations, wavy lamination (approaching flaser structure), sharp, erosional truncation of underlying laminated units, and lack of visible bioturbation (possibly stretched or sheared during slumping to produce apparent lamination) are characteristic of these occurrences (see Figure 9). Color alternations are somewhat rhythmic as well with repetition of (5Y6/1) light olive-gray and (5B9/1) light bluish white (398D-8) siliceous marly nannofossil chalk and siliceous marly foraminiferal nannofossil chalk and (5Y7/2) light gray, (5Y8/1) yellowish gray, (5Y6/3) pale olive, (5B7/1) light bluish gray, and (5G6/1) greenish gray in 1 mm to 3 cm laminae, with rapid alternations from one color to the next (Core 398D-15).

Core 398D-15 displays an interesting development of laminated varicolored marly chalks, large slump folds (Figure 10), microfaults (Figure 11), and the youngest pebbly mudstones. These lithotypes are more typical of lithologic Unit 2 and occur only once in Sub-unit 1C, in the mid-Oligocene. Slump masses from 20 cm to 90 cm thick occur in five distinct intervals of somewhat dif-

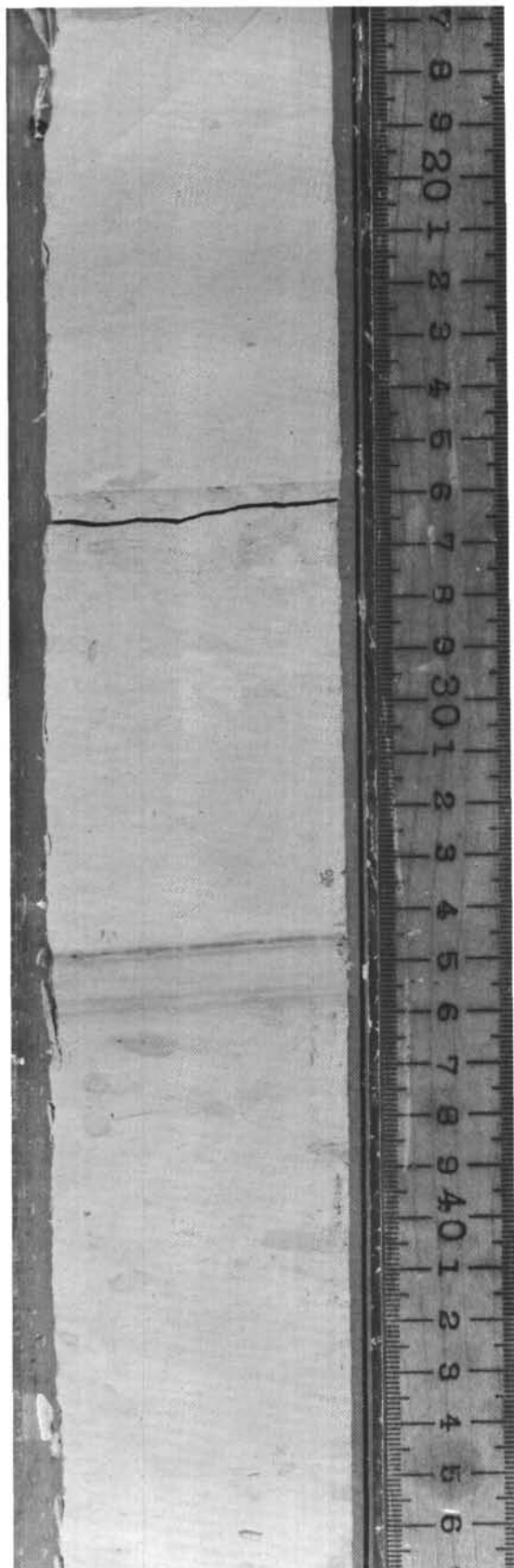


Figure 7. Faint lamination (diagenetic) and sharp contacts in Pleistocene burrowed marly nannofossil ooze (Sample 398D-4-4, 17-47 cm).



Figure 8. Typical, thin, partly graded and laminated sands and silty sands (burrowed) which exhibit a marked rhythmicity in Sub-unit 1C. (Sample 398D-12-2, 11-37 cm).

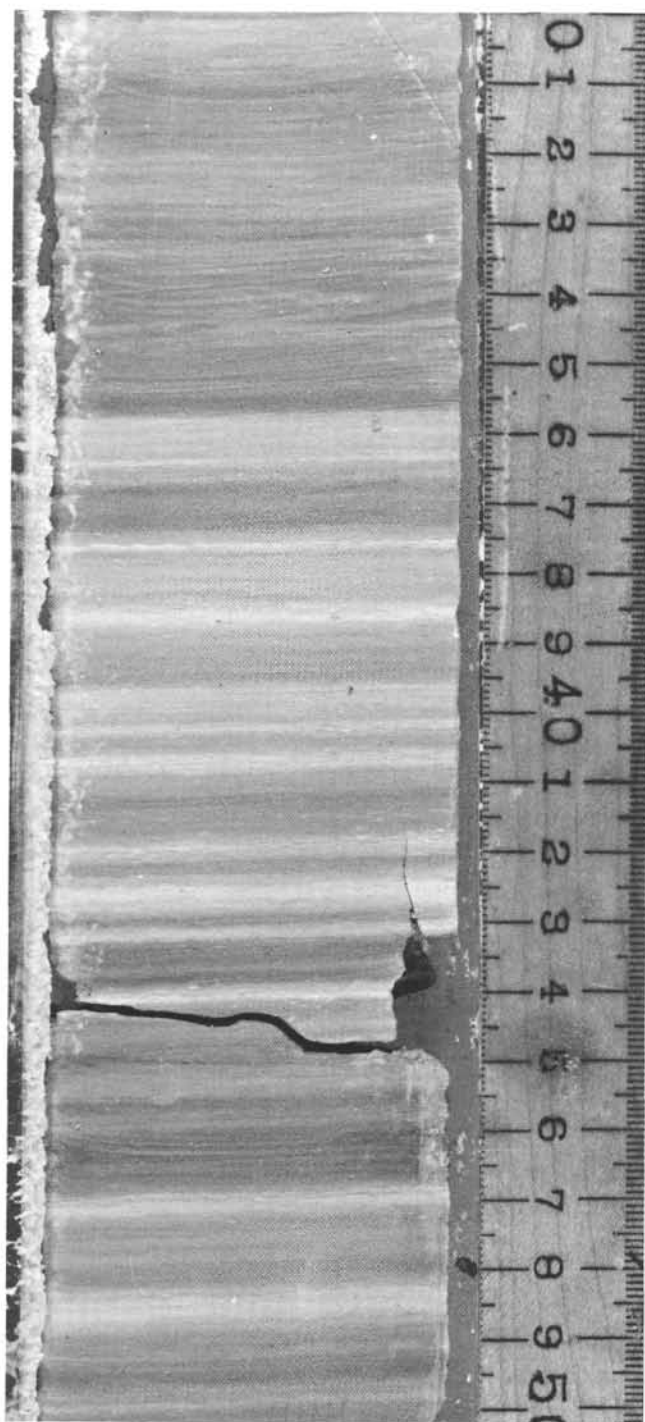


Figure 9. Thin lamination of rapidly alternating colors; note zones of small burrow mottles which have apparently been stretched to produce lamination (Sample 398D-15-4, 30-50 cm); also, note very fine extensional microfaulted zones as at 37.5 cm.

ferent lithology. Thin lamination in several of the units shows isoclinal, recumbent, and monoclinical folds. A faint axial plane cleavage may be seen cutting the laminae. Burrowing is generally absent except for a few *Chondrites* in the upper parts. A thinner slumped and

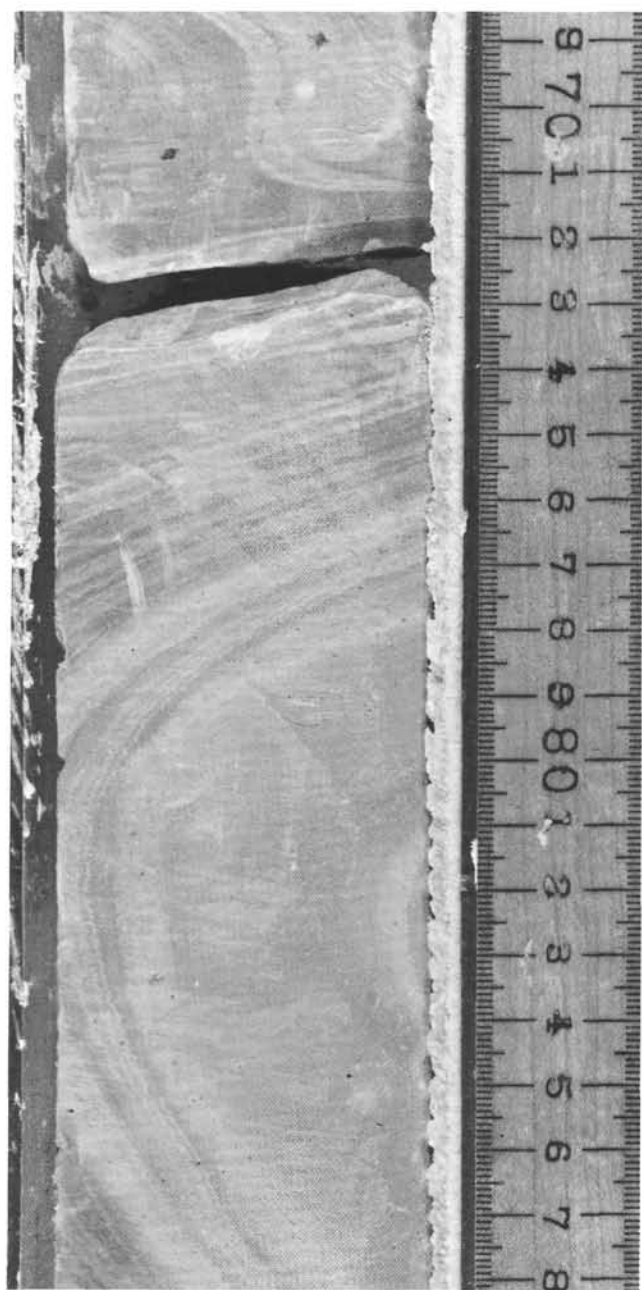


Figure 10. Axial nose of slump-folded siliceous marly nannofossil chalk of the Oligocene (Sample 398D-15-1, 68-88 cm).

formerly partly fluidized interval consists of a contorted pebbly mudstone with subangular quartz and white subrounded granules of hard calcite. One uncontorted interval also contains a layer of calcite granules. Numerous microfaults, apparently tensional fractures with up to 3 to 5 mm of offset of laminae, occur in parts of the laminated sequence and are interpreted as having been stretched and sheared during slumping and sliding. These faults are low angle, oblique to bedding surfaces, and have lengths on the scale of centimeters. They are closely spaced, as little as 1 or 2 mm apart. Faulting ap-

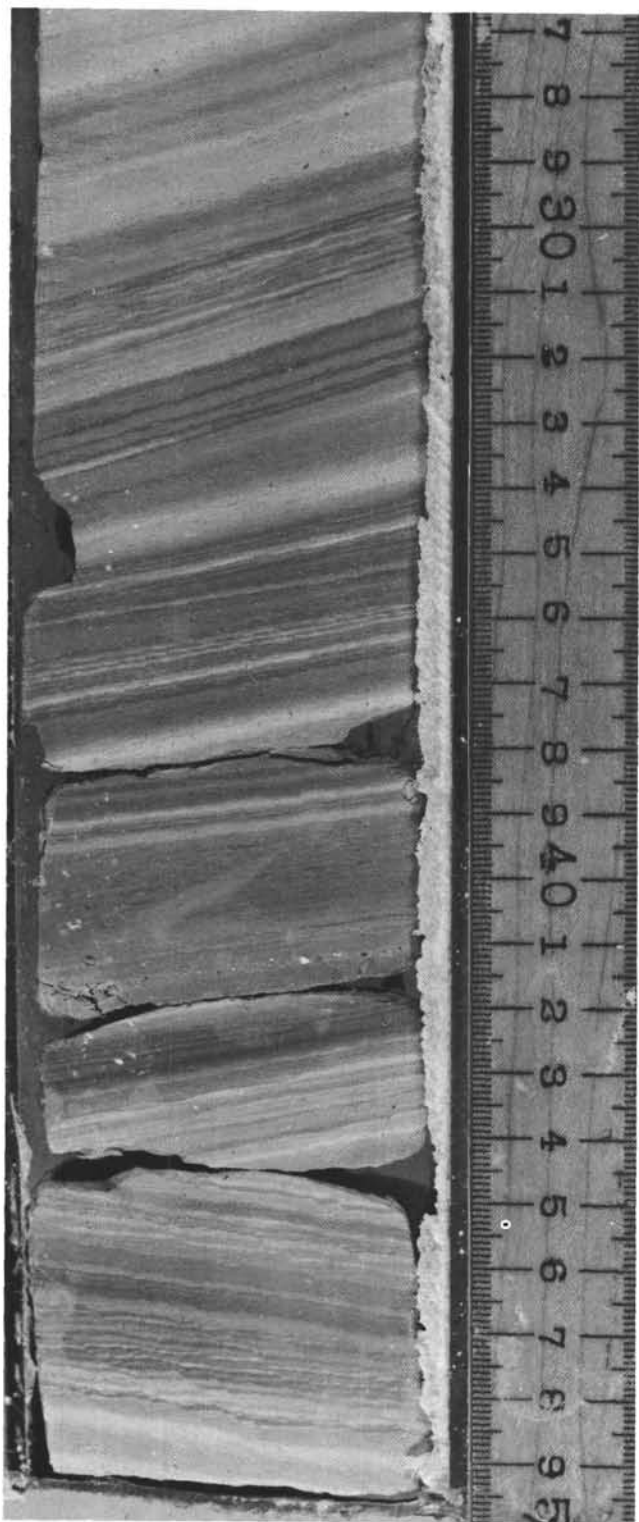


Figure 11. Stretched and microfaulted laminae in slump deposit of the Oligocene (Sample 398D-15-2, 27-50 cm).

pears to have been brittle and syn-depositional or early post-depositional (rapid tensional stress application?) in sediments that were water-charged and thixotropic (Figure 11).

The majority of Sub-unit 1C is intensely bioturbated with common *Zoophycos*, *Mycellia*, *Chondrites*, and possibly *Helminthoides*(?) as well as numerous unrecognizable mottles, many of which have gray to greenish gray halos. Composite burrows are rare. Burrowing seems most intense in upper, lighter parts of rhythms (c), especially at the contact with (b) as described above.

**Unit 2: Cores 398D-19 Through 398D-38 (594 to 774 m sub-bottom); Mid-Paleocene to Lower Oligocene**

This lithologically more complex unit comprises siliceous marly nannofossil chalk and mudstones with thin, intercalated sands and silts, rhythmically bedded along with more frequent slumped intervals and sequences of laminated to cross-laminated mudstone and marly chalk (possibly bottom-current produced accumulations or redeposited intervals). Thin pebbly mudstone beds also occur. Colors of sands, silts, and adjacent mudstones range from 5GY4/2 to 5G6/1-7/2 olive-gray to greenish gray while marly chalks, and mudstones comprising the bulk of the sequence are 5Y6/4 to 10YR7/3 and 10YR4/4, dusky yellow to pale brown and moderate brown. Even with this variety of sedimentation, the rates of accumulation average about 5 to 10 m/m.y.

The upper boundary with lithologic Sub-unit 1C is defined at a sharp decrease in  $\text{CaCO}_3$  content and concomitant increase in the siliceous biogenic component (radiolarians and sponge spicules) to 20 or 30 per cent. Carbonate contents are < 70 per cent, dropping nearly to zero in certain portions of the section. They average about 25 per cent. Organic carbon content is uniformly low at < 0.1 per cent. Quartz and mica are important components, and dolomite is a persistent mineral species seen in smear slides up to 5 to 7 per cent. In addition, beginning with Core 398D-19, acicular needles of the zeolite clinoptilolite frequently occur, at times up to 10 per cent as recognized in smear slides. Abundant attapulgite and sepiolite occur in Cores 398D-32 to 398D-34. Clay minerals, in order of abundance, are montmorillonite, illite, kaolinite, and minor chlorite, with traces of chlorite-vermiculite and attapulgite throughout.

Again, lithologic Unit 2 is characterized by rhythmic sedimentation throughout, with the typical intercalation of sandstone or siltstone, followed by grayish-colored marly chalk, then yellow to yellow-brown or brown marly chalk or mudstone stained grayish near the bottom of the next sandstone or siltstone. These rhythms average 20 to 25 cm thick over much of lithologic Unit 2, but increase in thickness downwards, especially from Cores 398D-31 to 398D-38 where they average about 50 cm thick and range up to 1 meter or more. Sandstones and siltstones (predominantly silts) again rarely exceed 5 cm in thickness and are generally < 1 to 2 cm; grading, parallel lamination and cross-lamination are common structures. Erosional basal contacts are ubiquitous. Evidence of bioturbation of sands is slight, usually only in the upper parts of each layer. Sand-filled burrows occasionally occur within fine-grained intervals which

have no obvious sand source. This suggests that some thin sands may be completely bioturbated and dispersed. Otherwise, bioturbation seems effective throughout but may not always be visible, especially in more homogeneous brown mudstones. The most intense bioturbation seems to occur in the upper muddy part of the rhythms. Identified burrows include mainly *Zoophycos*, some *Helminthoides*, *Chondrites*, and more rarely composite burrows and halo burrows.

Laminated intervals of marly chalk and mudstone also occur within lithologic Unit 2 (e.g., Cores 398D-24, 398D-26, 398D-34, 398D-36); these intervals (see Figure 12) are usually siliceous, exhibit thin parallel lamination, cross-lamination, erosion (cut-and-fill), clay-flake breccias, flame structures, and shearing, stretching, and overturning of burrows in underlying sediment. Laminated sections, however, are usually unburrowed. These sedimentary structures are evidence of a type of rapid, current-related deposition (possibly by redeposition from the flanks of Vigo Seamount) which scours, erodes, and redeposits fine-grained sediment. Underlying, water-charged, plastic sediment is sheared in the process, if not eroded, causing stretching and overturning of burrows (Core 398D-24) and is possibly the cause of numerous low-angle, small displacement microfaults which cut the laminae in certain portions of individual units. The faults appear to be syndepositional as they do not propagate in a vertical direction for more than 5 cm.

Larger scale "faults" covering up to 50 cm of section (Cores 398D-24, 398D-34, 398D-36, 398D-37) may also be seen (Figure 13). These faults, inclined at angles up to 60° from the horizontal, have sinuous traces and both normal and reversed senses of offset up to 3 cm. None are seen to terminate within the cores. Some dewatering may have occurred along these planes, as sediment is often smeared upward in the 1 to 5 mm wide traces, some of which show no displacement. The faults do not appear to be confined to any particular type of sediment.

Slumps also occur (Cores 398D-28, 398D-29, 398D-35) usually in masses less than 1 meter thick in marly chalk or mudstone. Contorted, isoclinal beds are typical. These may be due to downslope movements induced by current shear imposed on thixotropic mud bottoms or induced by tectonic movements.

A few conglomeratic intervals (Cores 398D-27, 398D-33, 398D-34, 398D-35) contain pebbles and granules of white to yellow, sparry, rounded, vuggy limestone fragments, possibly of shallow water origin (Figure 14). Calcareous algae were identified in one such pebble from Core 398D-34. The largest clasts reach 5 to 6 cm in diameter, but granules to 1 cm pebbles are more typical. Claystone pebbles are a mutually occurring type in a few beds.

**Sub-Unit 3A: Cores 398D-39 to 398D-50 (774 to 880 m sub-bottom); Campanian to Mid-Paleocene**

This sub-unit represents a change from siliceous mudstones at the bottom of lithologic Unit 2 to red-brown marly nannofossil chalks with rhythmically interbedded sandstones or siltstones. Sub-unit 3A has a

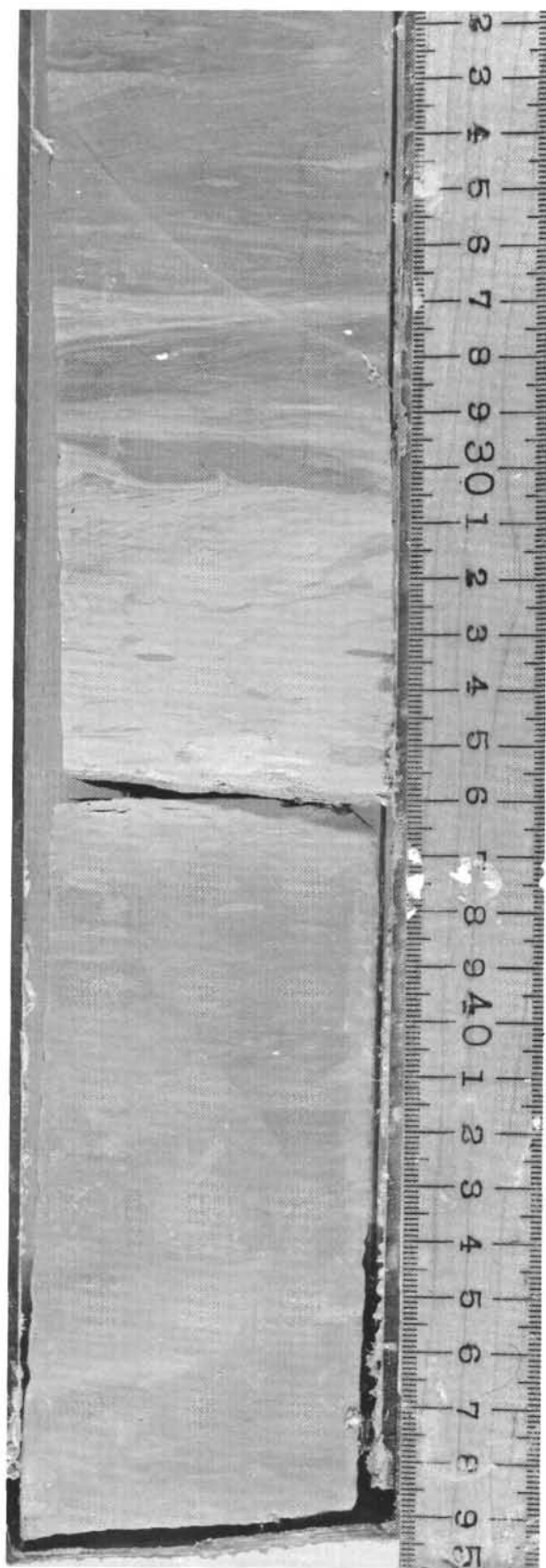


Figure 12. Thin parallel lamination, cross-lamination, and faulting in Eocene marly chalk and mudstone (Sample 398D-24-4, 22-50 cm).

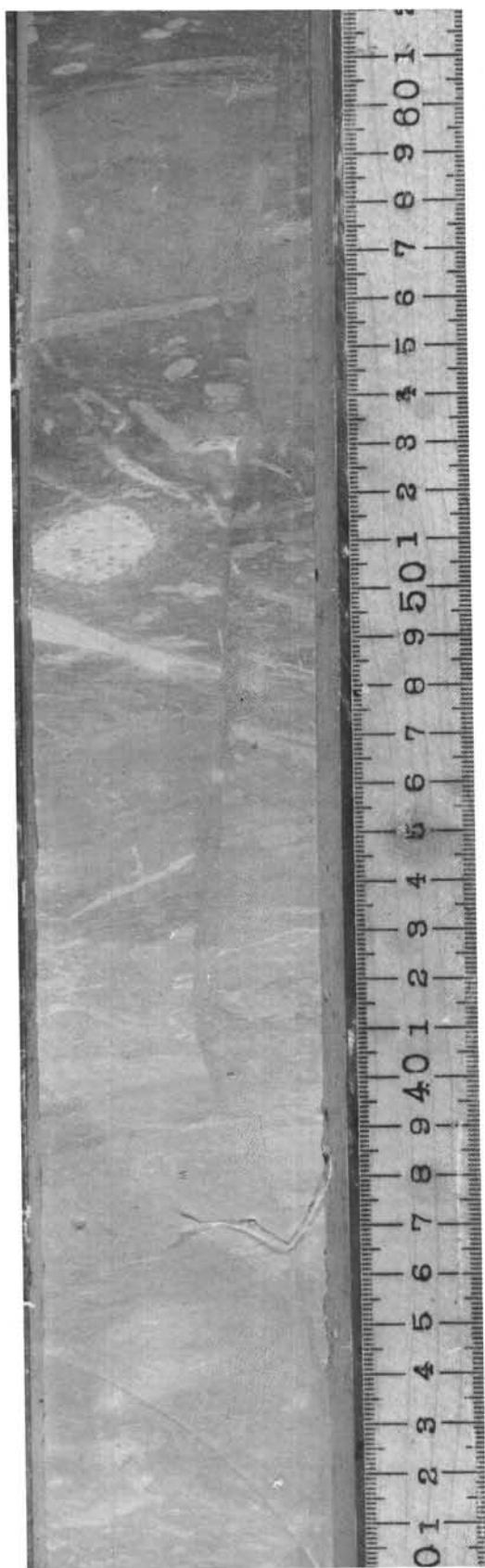


Figure 13. High-angle normal fault in bioturbated mudstone (Sample 398D-24-1, 30-62 cm).

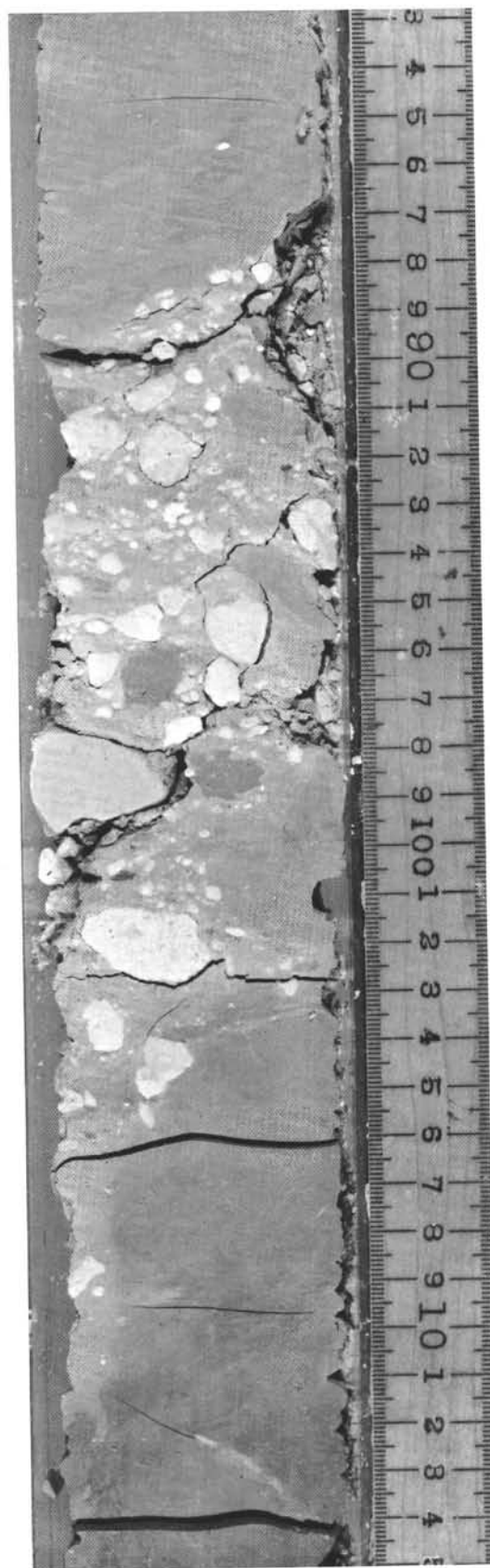


Figure 14. Large white calcite granules along with mud clasts in slumped marlstone (probably a debris flow unit) of the Eocene (Sample 398D-27-3, 83-115 cm).

distinctly higher  $\text{CaCO}_3$  content than either Unit 2 or Sub-unit 3B (which comprises barren red mudstones and claystones). Sedimentation rates average less than 5 m/m.y.

Organic carbon content is low, less than 0.1 weight per cent, while  $\text{CaCO}_3$  contents vary between 5 and 75 per cent, average about 40 per cent, and decrease down-section. Colors include 5GY5/2-10GY5/2 dusky grayish green marly foraminiferal nannofossil chalk associated with 5Y8/1 and 7/2 white to light gray silt or sand laminae, and 10R5/4 to 5YR/6 moderate yellowish brown to reddish yellow variegated marly nannofossil chalks and nannofossil mudstones.

Quartz, clay minerals, mica, nannofossils, foraminifers, and dolomite are persistent smear-slide components. The sporadic occurrence of feldspars has been identified by X-ray diffraction studies; zeolites also occur. Sands and silts contain large amounts of quartz and foraminifers as well as identifiable carbonate fragments. The clay mineral assemblage shows distinct trends towards decreasing montmorillonite and increasing illite downhole. Chlorite and kaolinite are common and their relative proportions are uniform throughout the unit; large amounts of attapulgite occur at the Cretaceous/Tertiary boundary.

Rhythmic bedding, as before, is typical of this unit; however, the average thickness of each rhythm is greater, about 50 cm or more to 1 meter in the lower part. The development of this rhythm is identical to preceding units.

The Cretaceous/Tertiary boundary occurs in Core 398D-41. Variegated, laminated, slumped and folded, unburrowed nannofossil mudstone occurs in Cores 398D-41 to 398D-43. There seems to be no marked lithologic change from upper Maestrichtian to lowermost Paleocene.

Many of the mudstones of lithologic Sub-unit 3A readily expand upon contact with fresh water and drying, which is possibly due to pressure unloading. This can also be noted in lithologic Unit 2.

#### Interpretation of the Cenozoic Sequence

##### Diagenesis

There are a number of interesting diagenetic problems to be investigated within the section cored. Unlike Holes 397 and 397A, on the northwestern African continental margin, Holes 398A, 398B and 398D demonstrate that biogenic productivity during the late Cenozoic was appreciably lower north of the Gibraltar Straits than to the south. Organic carbon contents are minimal except within the Pleistocene. Green to gray and light blue colors prevail within the Pliocene to Pleistocene intervals, but below this, an oxidized-appearing brown to red predominates, especially within the lower sedimentation rate sequences in the Eocene and Paleocene. There is a general relationship between gray colors, somewhat higher organic carbon contents (up to 0.6 wt. per cent) and higher sedimentation rates. Within the Pliocene-Pleistocene interval, numerous black to gray

laminae, specs, and mottles occur which are concentrations of iron sulfides, often framboidal. Pyrite was noted infrequently through the rest of the section in smear slides. Bacterial sulfate reduction did not lead to the exhaustion of  $\text{SO}_4^{--}$  in pore waters of Cenozoic sediment (Barnes et al., this volume).

Another feature of note is the green-gray to gray or dusky yellow-green "coloration" associated with the base of rhythmic beds as defined here, especially where thin sandstones or siltstones occur. This coloration extends from 1 to 10 cm both above and below these beds (Figure 15), usually slightly thicker above than below. One possible interpretation is that this darker gray coloration (it occurs in association with intervals of nannofossil chalk, marly chalk, and mudstone which is lighter white or red to brown) represents allochthonous fine-grained sediment associated with the current laminated sand-silt layers, hence its darker less-oxidized appearance when compared to the sediment interpreted as autochthonous "pelagic" or "hemipelagic." However, since this coloration in many cases extends both above and below the sands-silts and these coarser grained sediments have erosional contacts with the underlying sediments, it seems that this coloration may be diagenetic in origin, at least for the interval below the sand-silt beds. The sand-silt layers, which are more calcareous than the surrounding sediment, initially may have been more organic-rich and certainly more rapidly deposited. Bacterial activity related to the higher organic content may have led to development of reducing conditions in the interstitial waters associated with the silts, which created diffusion gradients of reduced iron and sulfide into overlying and underlying more-oxidized, relatively slow-deposited intervals. This could then have led to adsorption of reduced iron on clays, pyrite formation, or at least could have inhibited formation of oxidized iron species which might impart a reddish or yellowish coloration. There is some relation between thickness of sand-silt beds and distance of diffusion coloration, especially when coarser beds are closely spaced. Also, burrows in the upper part of these grayish intervals are not filled with sediment of the color of that above (red or brown, etc.), but are uniformly stained gray as is the rest of the interval. In addition, no gray coloration is mixed upward. This suggests a post-depositional, post-burrowing origin for the color.

In addition to the coloration, carbonate preservation seems better in the gray colored sediment just above the sand-silt layers for several centimeters than in overlying fine-grained sediment. In a few examinations using closely spaced total carbonate data and smear slides, a progressive decrease in  $\text{CaCO}_3$  content was noted from the sand or silt to the upper part of a rhythm. In contrast, the gray colored sediment just below the sand or silt contains generally less  $\text{CaCO}_3$  than similar-appearing material above the silt, and is slightly poorer in  $\text{CaCO}_3$  content than the more oxidized-appearing sediment below. There are at least two possible ways to account for this phenomena.

1) Higher carbonate contents in fine-grained sediment above the silts represent the fine "tail" of the

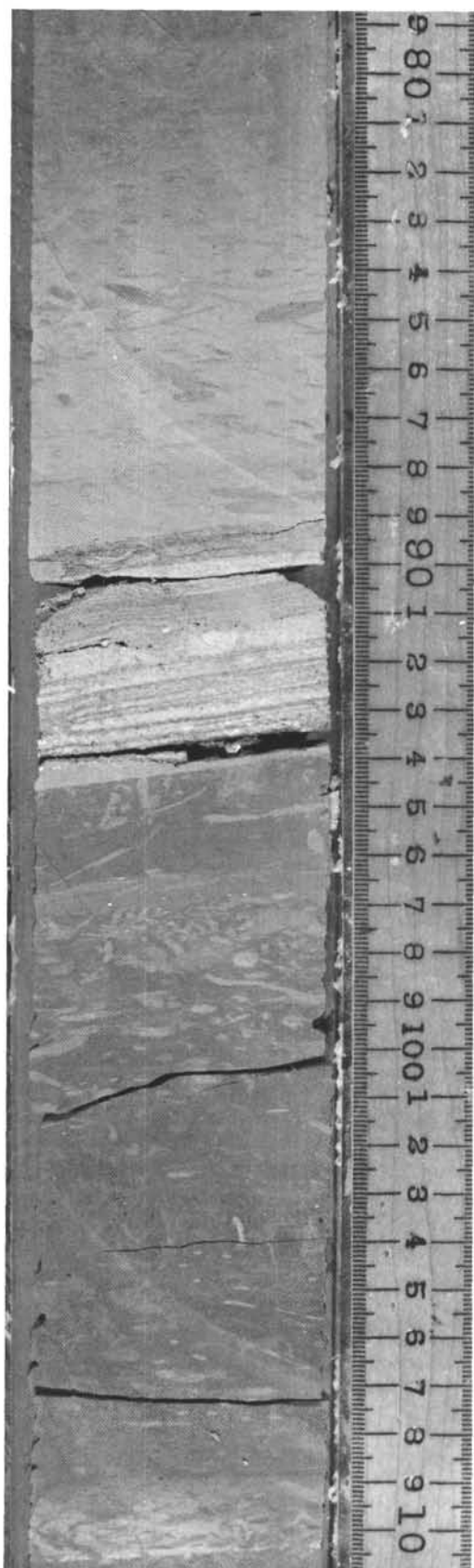


Figure 15. Laminated sand layer with darker coloration extending downward (below base) about 1.5 cm (Sample 398D-24-6, 79-111 cm).

event causing sedimentation of the silts or sands, while lower  $\text{CaCO}_3$  in all other sediment is due to equilibrium with carbonate undersaturated bottom waters perhaps near or below the foraminiferal lysocline under conditions of slow pelagic sedimentation. This does not account for the coloration of sediment below sand.

2) Carbonate preservation is enhanced in the vicinity of the sand-silt layers because pore waters become more quickly saturated in the presence of a large source of soluble calcareous components (foraminifers and possible high Mg-calcite and aragonitic debris from shallower depths). Thus, diffusion of  $\text{CaCO}_3$  upward from the calcareous silt-sand layers buffers the interstitial waters in finer grained, slowly sedimented material above, preserving more of the calcareous components settling to the sea floor. Above a certain limit, usually less than 5 to 10 cm or so, this buffering action becomes ineffective and the calcareous components are not well preserved. This buffering effect apparently does not operate below the sand layer, even though the previously discussed gray "diagenetic" coloration extends downward at least several centimeters. However, the sparseness of carbonate below the sand layer may be because solution already has removed most of the carbonate before sedimentation of the sand or silt layer.

Also associated with the silt-sand layers and related gray intervals (especially in the upper 400 m of this section) are several dark green to gray fine parallel laminations (e.g., Figure 8). These are sometimes but not always at the transitional zone between the more carbonate-poor deposits and the overlying carbonate-rich deposits (cf. Section 398D-4-5) and at the tops of the fine turbidite tails. The laminations have a color identical to the halos around gray mottles. These laminations occur singly or in groups of up to five or six and are  $< 1.0$  mm thick. The color and association suggest a diagenetic origin, as a liesegang-type banding, possibly consisting of reduced iron species diffusing outward from zones of higher initial organic contents in which some sulfate reduction has taken place. These bands or laminae pass through burrow mottles and surround certain burrows, further supporting interpretation of their being of an early diagenetic origin. Gray burrow halos are typically associated structures.

No limestones were encountered in the Cenozoic section, but the ooze-chalk transition occurs at about 320 meters sub-bottom. This correlates with a distinct reflector on seismic profiles crossing the site. Interstitial water chemistry also reflects this diagenetic transition (see "Geochemistry"); below 320 meters,  $\text{Sr}^{++}$  values increase, alkalinity decreases rapidly, and  $\text{Ca}^{++}$  increases. Pronounced dissolution of calcareous microfossils occurs throughout the Cenozoic section; however, there are periods of better preservation, especially during the Pliocene-Pleistocene. In intervals containing siliceous microfossils, little or no diagenetic change other than dissolution was noted. Although siliceous microfossils are present, cherts do not occur during Eocene time (Horizon A) as they do in many other North Atlantic drill sites (e.g., von Rad and Röscher, 1972). This may be due to the relatively low accumula-

tion rates of siliceous components as well as the very low thermal gradients within the sediment column at Site 398.

Magnesium-bearing silicates (montmorillonite, attapulgite, sepiolite) are present in parts of the Paleocene and Eocene. Sepiolite and attapulgite occur as fragile needles which were probably not transported, but grew within the sediment. There is no obvious genetic relationship between biogenic siliceous remains and the occurrence of sepiolite as there apparently is between biogenic silica and clinoptilolite (e.g., Core 398D-19). The origin of the high magnesium contents necessary to promote growth of these neoformed silicates in this interval is puzzling. There is no evidence of residual high  $Mg^{++}$  in pore waters as might be expected. Chamley et al. (this volume) have suggested a link to regional climate, but the origin of these silicates, especially sepiolite, still remains a question.

#### *Turbidite-Bottom Current Sedimentation*

One of the major problems in interpretation of the Cenozoic deposits is the transport mechanism and provenance of silt and sand layers within the Paleocene to lower Miocene. These thin intercalated beds define the base of a persistent rhythm which seems to vary in thickness proportional to the sedimentation rate. The interpretive debate centers on whether these thin beds represent episodic pulsations of bottom currents (e.g., deep geostrophic currents) producing winnowed traction layers, or whether the thin beds are periodic turbidity-current deposits.

Some evidence of bottom current-produced features is visible on the surface of the split core sections. Laminated chalks, marly chalks, and mudstones occur from upper Paleocene to lower Miocene, although intermittently. These intervals, ranging from 5 cm to several meters thick (e.g., Cores 398D-8 and 398D-15) are characterized by a suite of sedimentary structures implying active current erosion, transport, and deposition. These include truncated sets of thin laminae (color variations), microcross-lamination and ripple lamination, flame structures, smeared and stretched burrow mottles (see Figure 16), flaser lamination, and low-angle repetitive microfaults (Figures 9 to 11). In addition, some winnowed sand or silt placers commonly consisting of foraminifers and pyrite and small mud-chip layers occur within certain intervals. Microfaults and overturned beds are pervasive at some levels (e.g., Core 398D-15, see Figures 10 through 12). We interpret these features (common in many intervals) as current-shear induced structures. As strong currents sweep the bottom, they impose a shear stress on the water-charged ooze. This causes tensional stretching within the upper several centimeters of the sediment column, and small low-angle normal faults develop. These faults lie at angles commonly  $30^\circ$  to the horizontal and show brittle deformation, implying rapid stress application because the sediments are semifluidized. The shear planes may be as closely spaced as several millimeters and can impart a pseudoflaser-type structure to the sediment (Figure 17).

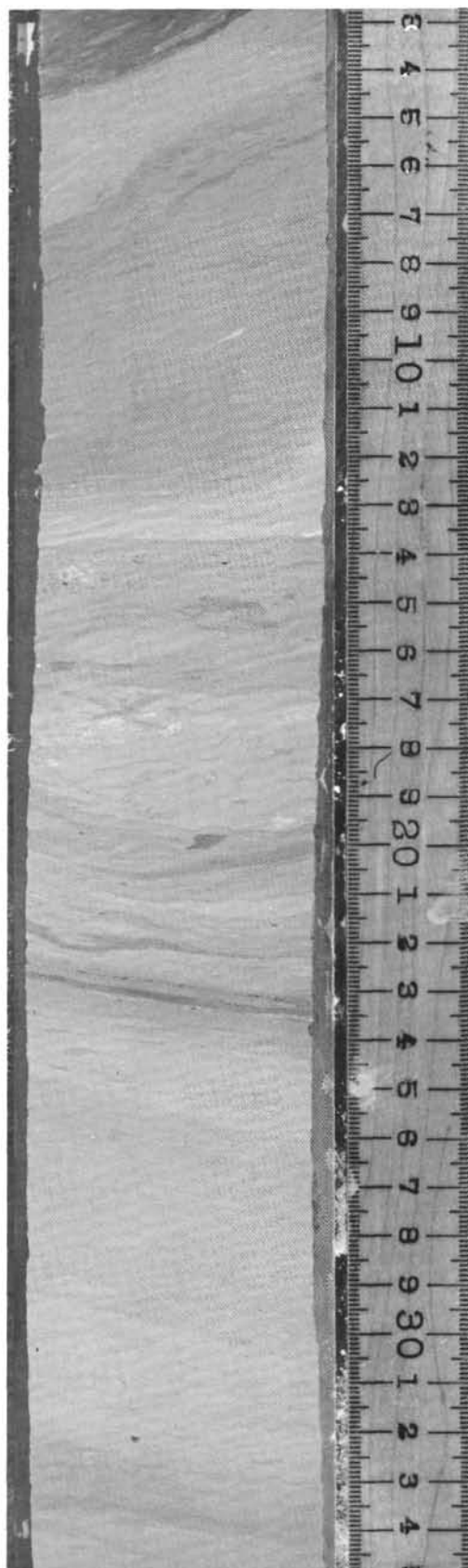


Figure 16. Slumped, folded, and sheared marly nannofossil chalk; note small mud clasts and sandy intervals near center (Sample 398D-34-5, 3-35 cm).

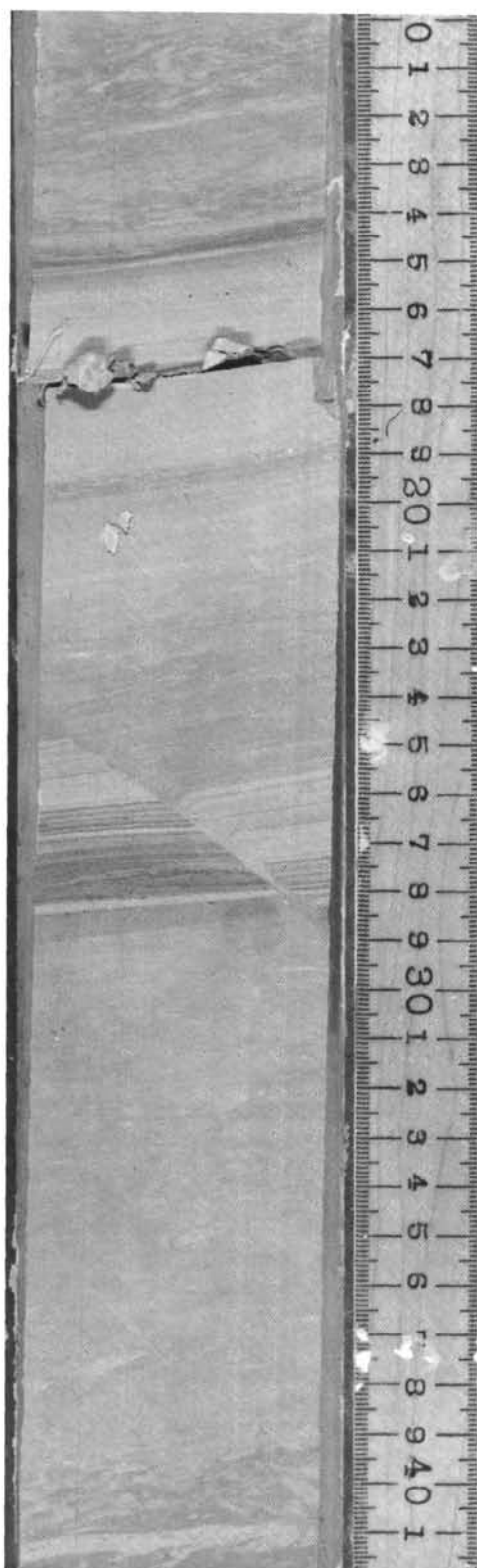


Figure 17. Sheared marl (stretched lamination) overlain by faulted, laminated silt bed. Note brittle deformation during plastic state (upturning of laminae along fault plane). Fault appears to have normal sense of offset in core, but is actually a reverse fault offsetting a dipping layer; also note sense of disturbance of laminae (Sample 398D-36-5, 10-42 cm).

Further evidence for plastic deformation comes from extremely stretched and flattened burrow traces (Figures 9 and 16). In Core 398D-24, several sets of burrows in an underlying layer are truncated and overturned in the apparent direction of current transport and overlain by laminated mud. The bottom currents could have originated from a passing density flow or gravity-driven redeposition of sediment from upslope.

Sand-silt layers are most enigmatic in origin. Most have erosional basal contacts with underlying sediment and range in thickness between 1 mm and 5 cm; silts predominate. Slightly graded bedding is present in some beds. Many are laminated; some show current-ripple features, microcross-lamination, irregular laminae to flaser structure; and some are massive. Grain sizes are generally finer than fine-grained to medium-grained sand. Most are poorly sorted with 20 to 30 per cent clay, but a few are well sorted. Primary mineralogical constituents are foraminifers, quartz, mica, glauconite, sponge spicules, pyrite, and minor heavy minerals, with zeolites in certain intervals. These sands and silts are rhythmically deposited; the distance between layers seems to increase with an increase in sedimentation rate.

The composition of the sand and silt gives no specific clue as to provenance. None of the components are diagnostic of a particular source area and could easily be winnowed remains of nearby hemipelagic muds, although quartz and mica may have been derived from schistose rocks of the Precambrian or Variscan basement which has been dredged on nearby Vigo Seamount (Dupeuble et al., 1976) and crops out extensively on the northwestern Iberian Peninsula. Sedimentary structures are not always characteristic enough of turbidites to act as a definite indicator for this mode of deposition. In addition, although scouring at the base and cannibalism of subadjacent strata commonly occur, sharp contacts can be seen in many cases in sediment up to 2 cm below the base of the silts. This lends the appearance of a complete reverse grading to normal grading sequence from clay to silt or sand to clay (e.g., Section 398D-8-3). To our knowledge, this cycle from fine to coarse to fine is not characteristic of turbidites. One possible explanation is that bottom currents are periodically intensified, causing slight scour and transport of fine-grained detritus, gradually increasing in strength with the competence to transport a traction layer of winnowed sand and silt constituents, then losing strength to produce a gradation to normal pelagic sedimentation. Upon occasion, when the acme of the current is great enough to erode the substratum, the basal coarsening upward sequence is removed. However, there is little doubt that many of these sand-silt layers originated as turbidity current flows (see Maldonado, this volume).

Vigo Seamount (Figure 1) may have provided a local source for many constituents seen in smear slides. Evidence from dredge hauls (Dupeuble et al., 1976) shows that rocks of different ages are exposed on its flanks, including Precambrian to Variscan(?) metamorphic rocks and Jurassic neritic carbonate rocks. The sands and silts and other redeposited sediment may simply be part of a narrow wedge of sediment developed around

and derived from this submarine high (see Maldonado, this volume; Rehault and Mauffret, this volume). In fact, the timing of the slump units and other redeposited sediment in Sub-unit 1C and Unit 2 (pre-Early Miocene; mainly Eocene-Oligocene) corresponds to a period of compressional tectonics along the southern margin of the Bay of Biscay (northern Spain) which may have been active as early as the Late Cretaceous. The gravity flows and evidence for redeposition of sediment seen at Site 398 may be related to slight readjustments of crustal blocks along pre-existing faults in response to the compressional movements farther to the north (see also Group Galice; Rehault and Mauffret; both this volume).

### *Rhythmic and Cyclic Bedding*

Repetitious alternating beds of several sediment types is a prevalent feature throughout the Cenozoic section in Holes 398, 398A, 398B, and 398D. From the middle Miocene through the Pleistocene, the deposits are characterized by cyclic alternations of marly nannofossil mud-nannofossil chalk as shown in Figures 5 and 6. The base of each cycle is usually sharp but can be gradational, especially where bioturbation has been intense. Colors are darker (5G6/1-5B7/1, 5Y7/2; light greenish gray, bluish gray, olive-yellow gray) at the base in the relatively carbonate-poor sediment, becoming lighter at the top of the cycle (N8, N9, 5B9/1; very light gray, white, bluish white) in more carbonate-rich nannofossil oozes and chalks.

These cycles may be a response to climatic oscillations typical of the Pleistocene, but thought by some workers to have also occurred earlier in the Cenozoic (Savin et al., 1975; Schlanger and Douglas, 1974; Arthur and Fischer, 1977; Dean et al., 1978). The difference in carbonate content between the two interbedded lithologies may be due either to carbonate dissolution pulses, episodes of higher terrigenous influx and dilution of carbonate skeletal materials, or a combination of both mechanisms. There is no suggestion that one lithology was deposited more rapidly than another because burrowing is effective and of equal intensity in both. The darker, more marly intervals are generally thinner, however, than the carbonate-rich beds. This does not necessarily imply a shorter interval of deposition for marly basal beds, unless they originate by terrigenous dilution.

Sediments older than middle Miocene contain the rhythmically bedded sand or silt-chalk to mudstone type already discussed (Figures 5 and 6). The origin and sedimentary processes developing the rhythmic and cyclic sedimentation are discussed by Maldonado (this volume).

### **Summary and Sedimentary Evolution for the Cenozoic**

Based on the preceding discussions and preliminary conclusions, we can make the following statements about the paleogeography, paleoenvironment, and sedimentary evolution during the Cenozoic.

1) Upper Santonian, nearly barren, red mudstones and claystones give way to calcareous mudstones and

marly chalks in the Maestrichtian, recording an apparent increase in productivity and/or a decrease in carbonate solution (depression of CCD).

2) Calcium-carbonate values remained uniformly low through the remainder of the Cretaceous to Eocene, with a slight increase in sediments deposited during the early Eocene. However, apparent sedimentation rates were higher from late Paleocene through early Eocene, following low rates in the early Paleocene and preceding lower rates in the late Eocene through early Oligocene.

3) From the late Paleocene through early Miocene, siliceous productivity shows a significant increase, mainly in the form of sponge spicules and radiolarian tests. This apparent siliceous productivity increase may be partly a function of carbonate dissolution and concentration of tests in the bottom sediments because there is a correlation of biogenic silica with low  $\text{CaCO}_3$ , and because calcareous biogenic assemblages show poorest preservation in this interval (Maldonado; Iaccarino and Salvatorini; Iaccarino and Premoli-Silva; all, this volume). Values of up to 25 per cent of siliceous biogenic material were recorded in smear slides and coarse fractions; radiolarians nor sponge spicules nor zeolites were noted in sediments younger than early Miocene or older than earliest Paleocene (except for occurrences in the Lower Cretaceous).

4) Evidence for intermittent bottom-current activity frequently occurs in sediments from at least Paleocene through the Pleistocene. The development of laminated and cross-laminated chalk and mudstone facies is not continuous and is most intense during the Oligocene through early Pliocene.

5) Periodic slumping, mud flows (rare), and occurrence of pebbly mudstone deposits during the early to mid-Eocene and again briefly in the mid-Oligocene suggest the presence of a slight paleoslope and/or a local high in the vicinity of the drill site and perhaps a local carbonate bank for pebbles and granules of white recrystallized, vuggy limestone (e.g., Vigo Seamount). Many of these redeposited intervals may have been in response to slight compressive tectonic movements during the Eocene-Oligocene. Some slumps, at least, may have been induced by strong bottom currents shearing water-charged oozes and inducing flowage, or by carbonate dissolution at the base of seamounts (e.g., Berger and Johnson, 1976). In general, slump units are thin (<1 m) and non-conglomeratic, do not have sharp erosional basal contacts, and are of similar sediment type to definite "autochthonous" facies. However, the state of preservation of the faunal assemblages is better than *in-situ* sediments. The rather good preservation of the original bedding features suggests a short distance transport for the displaced units, although the preservation of the faunal assemblages call for the source at shallower depth.

6) Thin sand and silt layers occur throughout the entire Cenozoic, but are best developed in the Paleocene through early Miocene interval. The source and origin of the rhythmically deposited layers is attributed mostly to mass gravity processes (turbidity current, debris flow, mud flow), although bottom-current activity may have

been of local importance. Individual constituents are generally not diagnostic of any particular source terrain. It is conceivable that Vigo Seamount could have shed much of the material recovered in the Site 398 cores, including quartz and mica (e.g., similar to constituents of dredged basement metamorphic rocks on Vigo Seamount; Dupeuble et al., 1976), calcite granules and diagenetically altered limestone fragments (Jurassic(?) neritic carbonates), and sponge spicules and foraminifers from shallower bottoms on the flanks or top of Vigo Seamount, thus accounting for better preservation of calcareous constituents. The Vigo provenance is attractive because there may have been a depositional trough between Site 398 and the Iberian mainland throughout the Cenozoic (Figure 1), and no major submarine canyons exist between the site and a possible shelf source directly east at the present edge of the Iberian continent. The silts and sands, though numerous, are thin (average ~1 cm) and volumetrically minor. A second alternative, however, is that the silt and sand were derived from the Iberian shelf margin and that the trough now present between Site 398 and the mainland is a more contemporary feature, resulting from continued Recent erosion by bottom currents. Seismic line GP13 shows the abrupt truncation of reflectors of at least Miocene through Recent age at the eastern margin of this trough. This may explain the lack of sand and silt layers in the Miocene to Recent portion of the section at Site 398. If the trough was originated by bottom-current erosion during the post-Oligocene, very little sand and silt of continental provenance could arrive at Site 398 after that time. Groupe Galice (this volume) has also suggested the prominent role of submarine currents near to and south of the Vigo Seamount area.

Some of the silt layers are attributed to episodic or pulsating bottom-current activity which winnows the coarse-fraction from the hemipelagic sediments and redistributes the material over the bottom. Both interpretations are important from a process approach because they suggest an intermittent influx of detritus from a submarine high, and less likely from more distal margin sources, and the continuous but rhythmic sweeping and winnowing of sediment by bottom currents on the eastern side of an ocean basin. In either case, net sedimentation occurred, and large-scale erosion by bottom currents seems not to have been important enough to develop major hiatuses, although minor stratigraphic discontinuities are observed in the middle Eocene and middle to upper Miocene intervals.

7) From the early Miocene through Pleistocene, sedimentation rates increased significantly, even considering compaction. Carbonate contents are also higher, and the sand-silt layers are rare or absent. Sedimentation is pronouncedly cyclic from the middle Miocene upward, and consists of alternating marly chalk-chalk beds of up to 1 meter thick. These may be the expression of climatic cycles with either pulses of carbonate dissolution, terrigenous clay dilution, or both.

Figure 18 shows a hypothetical subsidence curve for the drill site, allowing for an Aptian age (ca. 110

m.y.B.P.) for initiation of thermal decay and subsidence, and corrected for application of sedimentary load of about 1600 meters (see Sibuet and Ryan, this volume). A published North Atlantic CCD curve (van Andel, 1975) and an extension to Cretaceous times (from Tucholke, Vogt, et al., 1978) shows that generally the site should have been above the CCD. However, if the subsidence curve is approximately correct during Campanian-Maestrichtian and later Paleocene times when early barren mudstones were deposited at Site 398, it appears that the CCD may actually have been up to 1000 or 1500 meters shallower at the continental margin in the northern North Atlantic than in the basins (according to the published curve). Also, according to the published CCD curve and the projected subsidence curve, Site 398 should have been below CCD in the mid-Miocene. However, expected strong signs of dissolution of foraminiferal and nannofossil assemblages were not seen in lower Miocene to Pleistocene sediments. This absence of marked dissolution suggests that one or both of the curves may be incorrect for a continental margin situation.

Sedimentation at the site appears to have been influenced by climatic and circulation changes during the Cenozoic. Intensification of deep circulation with bottom-current winnowing and scour ensued from the late Paleocene to the Pleistocene, with probably the most intense period during the mid-Eocene to early Pleistocene. This, at least, may be related to climatic deterioration during this period and/or to the opening of the Labrador Sea. Although some bottom-current activity can be inferred for Miocene through Pleistocene times, the greatest overprint of climatic deterioration and variation during this time appears to be the cyclic carbonate-rich/carbonate-poor depositional regime. There is, of course, evidence from seismic profiles that important erosion by bottom currents has occurred in the region at least during the Pleistocene and Recent.

The period of siliceous productivity from late Paleocene to early Miocene time over Site 398 may have been influenced by climatic circulation factors as well. Cherts are widespread in the North Atlantic during mid to late Eocene time, and abundant siliceous fossils are found at many sites in sediment deposited during the late Oligocene. These deposits at Site 398 could reflect a substantially more fertile Atlantic due to the influx of older, nutrient-rich bottom waters from the Tethys and the Pacific. Nonetheless, productivity does not seem to have been as high as at other DSDP North Atlantic sites. Upon closure of the Tethyan Ocean and climatic deterioration during the Miocene, different patterns of deep-water production probably occurred. This possibly began the establishment of the present-day outflow of deep water from the North Atlantic, thereby reducing surface-water fertility and siliceous productivity, and favoring preservation of carbonate (e.g., see Berger, 1970).

Site 398 appears to have been insulated throughout the Cenozoic from major coarse-grained sediment input direct from the Iberian continental shelf edge. No turbi-

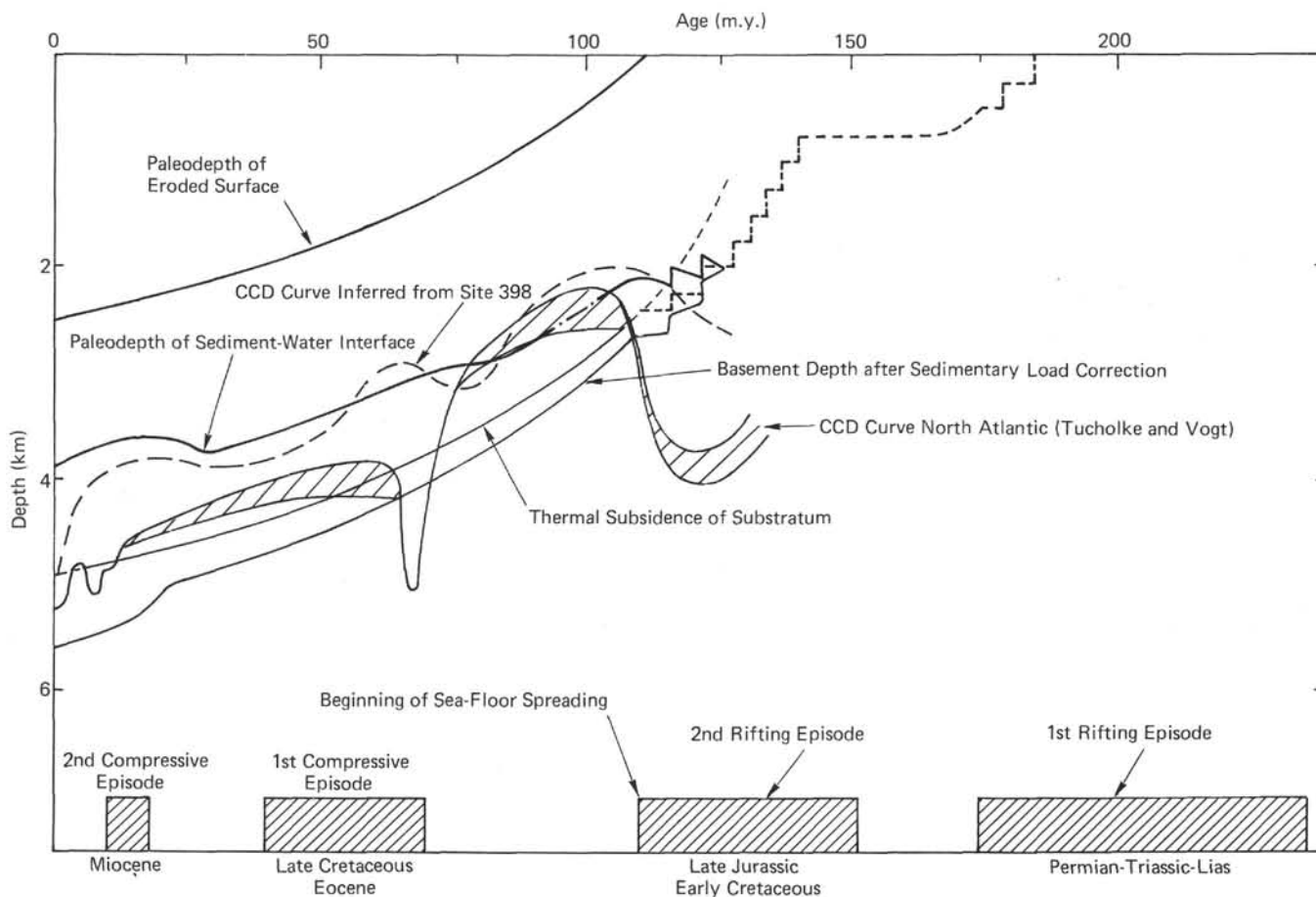


Figure 18. Theoretical subsidence curves for basement at Site 398 with corrections for sediment loading, assuming initiation of rifting in Hauterivian time (see Sibuet and Ryan, this volume).

rites or slump masses were found to contain a marked amount of terrigenous components necessitating a proximal continental source. Although quartz and mica were significant, mineral constituents in sands, silts, and even in finer grained sediment, they could have easily been derived from a local high such as Vigo Seamount or reworked from fine deposits rapidly accumulated on the upper slope. Conglomerates contained lithified, altered calcareous clasts which may have had a shoal water origin but are not age-diagnostic; these could be derived from a capping of Jurassic or Lower Cretaceous neritic carbonates on Vigo Seamount or Galicia Bank. Sedimentation of high background levels of clay-sized, non-calcareous fines may have been accomplished by turbid-layer transport or by deposition from sediment-laden currents sweeping the margin. Shelf-edge spillover processes may account for significant amounts of fine-grained detrital material found at Site 398.

## Mesozoic Deposits

### Introduction

Three major lithologic units can be recognized within the Mesozoic section (Hauterivian through Maestrichtian) cored at Site 398. Lithologic Unit 3 (774 to 945 m sub-bottom) is probably Campanian (possibly Santon-

ian) through Danian in age and consists primarily of red to yellow-brown marly nannofossil chalks, calcareous mudstone, and quartzose claystone ranging from fossiliferous to barren. Two sub-units have been defined primarily on the basis of carbonate content: Sub-unit 3A (774 to 880 m) is lighter colored and calcareous, while Sub-unit 3B (880 to 947 m) consists entirely of red, slightly calcareous mudstone to barren claystone. A few, thin intercalated silts occur within Unit 3. Lithologic Unit 4 (945 to 1667 m sub-bottom) has a more complex and variable lithology, and is composed of black, dark gray, and olive-green gray, relatively organic-rich mudstones, generally poor in calcium carbonate. Unit 4 has been separated into three sub-units based on pronounced lithologic variations within the dark mudstone theme. Lithologic Sub-unit 4A (945 to 1183 m) is composed of mostly black to dark gray mudstone to calcareous mudstone: laminated, massive, and occasionally burrowed. Sub-unit 4B (1183 to 1401 m) consists predominantly of dark gray to black, massive to laminated mudstones and claystones, but with persistent to abundant sideritic laminae, lenses, beds, aggregates (some porous structures filling the remains of molluskan shell fragments), molluskan shell debris, and ammonite remains. Sub-unit 4C (1401 to 1667 m) is composed of dark mudstones and claystones with a

number of intercalated debris flow and mudflow units consisting of rounded pebbles and cobbles of limestone bearing calpionellids of Tithonian age and marly limestone in a dark matrix. Also present are turbiditic sequences consisting of fine-grained, quartz-rich, calcareous sandstones and siltstones, and some interbedded, graded, light colored, shale chip conglomerates or sandstones. Lithologic Unit 5 (1667 to 1740 m) is composed of intercalated light bluish white nannofossil radiolarian limestones and very thinly laminated dark brown-black to gray mudstones which are gradational into one another. Some thin, laminated quartz-siltstones or sandstones also occur.

Each lithologic unit is gradational to the next with the exception of Sub-units 3B and 4A whose mutual boundary, as defined, is sharp. Calcium carbonate contents are generally low throughout the column, excepting lithologic Unit 5. Dissolution of calcareous microfossils seems to have been prevalent through the entire Cretaceous section cored here. Organic carbon values, after an initial high value of 7.1 weight per cent (shipboard), average 0.6 weight per cent for most of the Cretaceous interval below the Campanian/Cenomanian hiatus (or condensed section; see Sigal, this volume). Values are less than 0.1 weight per cent above the hiatus. However, several Aptian to Barremian sediment intervals possess higher values ranging to 3.1 weight per cent. In general, there is a correlation between higher organic carbon values and low carbonate within the dark mudstones. The sediment chart (see rear pocket, this volume) summarizes the major lithologic, carbonate, organic carbon, and mineralogic trends through the Cretaceous. Lithologic units are described in more detail below; discussion and interpretation follow.

#### Lithologic Units

**Unit 3: Core 398D-38 Through Sample 398D-56-2, 75 cm (774 to 945 m sub-bottom); Mid-Cenomanian Through Danian**

**Sub-Unit 3A: Cores 398D-38 Through 398D-50 (774 to 880 m); Campanian to Paleocene**

**Sub-Unit 3B: Core 398D-50 Through Section 398D-56-2 (880 to 947 m); Upper Santonian(?) to Mid-Cenomanian**

Unit 3 consists of brown to yellowish-brown, dark reddish brown, red and reddish gray (7.5YR5/4-4/4, 10YR5/4, 5YR4/4, 4/2, 2.5YR3/4, 5YR4/8) unfossiliferous mudstone and claystone, predominantly massive, homogeneous and apparently unburrowed (or wholly homogenized by burrowing). Rhythmic intercalation of thin (<1 cm thick) silt and sand laminae at 10-cm to 1-meter intervals is characteristic as in the previous unit. A bluish gray (5B7/1) stain is associated with claystones for <2 cm above and below each rhythmic coarser grained layer. One 13-cm-thick conglomerate consisting of poorly sorted angular, subrounded, and rounded white micritic limestone pebbles and granules occurs in Core 398D-50.

Quartz plus mica generally total over 30 per cent (smear slides) in association with the very low carbonate (1 to 3 per cent; seldom > 20 per cent) contents in this sub-unit. Clay minerals are the most prominent constituent in smear slides with some siderite, occasional feldspar, heavy minerals (including some possible "micro-nodules," especially in the lower part of Sub-unit 3B). Zeolites (clinoptilolite) are present; illite and montmorillonite are the dominant clay minerals, with subordinate kaolinite and chlorite also becoming very important (up to 40 per cent) near the contact with Sub-unit 4A. Minor amounts of gypsum (e.g., Cores 398D-52 to 398D-56) have also been recorded. Few siliceous microfossils were noted.

**Unit 4: Cores 398D-56 Through 398D-130 (945 to 1667 m sub-bottom); Barremian Through Cenomanian**

This unit consists of dark, relatively organic-rich and carbonate-poor shale and mudstone. Bioturbation is common but not prevalent, and is absent especially in darker, laminated intervals. Three sub-units are defined below based on lithological variations within the dark, organic shale interval.

**Sub-Unit 4A: Cores 398D-56 to 398D-79 (945 to 1183 m sub-bottom); Albian-Cenomanian**

The upper contact with Sub-unit 3B is sharply marked in Section 398D-56-2 at the beginning of intercalations of reddish brown (5YR4) and grayish green (10GY5/2 to 5YG, Y5/2, 5G5/1) zeolitic claystone. Just below this contact begin grayish green (10GY5/2 to 5GY5/2) marly nannofossil chalk to mudstone and calcareous mudstone, and dark gray to grayish black (N2 to N3) claystone (some laminated and unbioturbated) and a few thin radiolarian sands. Some thin quartzose sandstone beds occur in the upper part of the core as well as a dark graded, mudchip sandstone without erosional base (also in Core 398D-59). A value of 7.1 weight per cent organic carbon (shipboard analysis) was obtained from the first black sapropelic interval. There is minor lithologic evidence for a hiatus between Sub-units 3B and 4A as zeolites suddenly become abundant, indicating a possible condensed interval. A monotonous interbedded sequence of black to dark gray claystone or mudstone and greenish gray, olive-green, or bluish-gray (5GY6/1-4/1, 5GY3/2, and 5B7/1) marly nannofossil chalk, mudstone, and claystone begins below this level. The sediment becomes less calcareous (from 30 per cent, declining to as low as 0 per cent CaCO<sub>3</sub>) and slightly more organic carbon-rich downward (0.4 to 0.75 weight per cent C). Most of the very dark gray to nearly black mudstones are homogeneous to laminated and nonbioturbated; they are usually 20 to 40 cm thick, but may be thinner. Contacts between dark mudstones and burrowed, greenish gray mudstones and marly chalks are usually gradational, some interlamination occurs. *Chondrites* and *Zoophycos* are the recognizable burrowing organisms, but numerous organic-filled, flattened mottles also occur.

Clay minerals are the prominent constituents in smear slides with subordinate quartz, mica, and heavy

minerals. Attapulgite (higher content in Cores 398D-78 to 398D-68 than in Cores 398D-67 to 398D-60) also becomes an important mineral phase in the upper part of Sub-unit 4A. Clay minerals (Chamley et al., this volume) consists mostly of montmorillonite and illite with smaller amounts of kaolinite and chlorite. Siderite is very common, especially as laminations (yellow-gray) in the lower portion of the unit. Zeolites (clinoptilolite) occur in two major spikes in Cores 398D-56, 398D-57, 398D-62, and 398D-63. They do not seem to be associated with recognizable volcanic detritus. Pyrite is ubiquitous, occasionally composing up to 10 per cent of the darker claystones. Larger pyrite nodules were also noted in several cores. A 9-cm-thick nodule or bed, identified as barite, occurs in Core 398D-69. Near it, other small, lenticular laminae or masses of pinacoidal crystals occur. Radiolarian tests are also present in Sub-unit 4A, becoming abundant below Core 398D-59.

***Sub-Unit 4B: Cores 398D-79 Through 398D-102 (1183 to 1401 m sub-bottom); Lower to Middle Albian***

This sub-unit is similar in its background lithology to Sub-unit 4A and is more representative of the "black shale" facies. Very dark gray to black (N1 to N4), laminated (wavy to parallel, usually N2 to N4 or 5Y4/1), massive (usually darker N1 to N2), and occasionally slightly bioturbated claystones are interbedded with (5GY2/1 to 4/1) dark greenish gray to greenish gray (5G6/1) and yellow olive-green (5GY4/2) burrowed mudstone. Transitions between these types are gradational and often interlaminated. Burrows have dark fillings and are commonly pyritized. The main difference between Sub-units 4A and 4B is the greater prominence of siderite as laminae, thin stringers, lenses, beds, and vuggy aggregates in Sub-unit 4B, although siderite laminations were common to the lower part of Sub-unit 4A. The yellow-gray siderite exhibits a number of textural variations from detrital-appearing laminae composed of individual grains to indurated, cemented lenses with sharp outer boundaries and some with fuzzy, cloud-like transitions to dark claystone matrix.

Some siderite beds were found in association with calcareous nannofossils and may represent diagenetic alteration of nannofossil-rich beds. A few siderite layers are burrowed. A curious development of vuggy or porous, sometimes laminated mound-like siderite aggregates occurs in Cores 398D-89 to 398D-102 with a few noted in Cores 398D-78 to 398D-84. These lenses or aggregates (usually <2 cm thick) are difficult to interpret, but are suggestive of a structure growing on a smooth bottom, as laminations mound-up over the top and interfinger with or feather-out in surrounding dark gray claystone. In Cores 398D-95 to 398D-97, a few similar structures are found accumulating on substrates of a single curved mollusk-shell fragment. The porous spongy texture and evidence of some horizontal wavy lamination, originally determined aboard ship suggests an algal origin. Thin-section examination shows a composite "peloidal" texture which makes the determination of the origin of these features uncertain.

Molluskan shell fragments (1 to 3 cm long) occur, beginning in Core 398D-73 and continuing downward through the remainder of the sub-unit. In addition, nearly complete but crushed ammonites can be noted relatively frequently in Cores 398D-87 to 398D-100. It is puzzling that where ammonites and mollusk shell fragments occur in association with siderite, planktonic foraminifers are absent and nannofossils are rare. Radiolarians, however, are abundant in this interval. This is most likely an artifact of preservation (see Sigal, this volume).

Calcium carbonate contents (by BOMB method) are very low, falling below 10 per cent after Core 398D-76. Organic carbon contents are generally between 0.5 and 1.0 weight per cent until below Core 398D-88, where values suddenly increase to up to 3.1 weight per cent (shipboard analysis) in association with the cored interval containing the puzzling siderite structures. Wood fragments and spores are found in association with the higher organic carbon values (see Habib, this volume).

Dark gray to olive-gray and black mudstone and claystone becomes the predominant lithologic type below about Core 398D-88; the greenish gray, burrowed intercalations are less abundant and thinner. Siderite remains an important facet of the lithology. Lamination within the claystones is perhaps more common and bioturbation is more rare.

Other lithologies within lithologic Sub-unit 4B are rare but do occur. In Cores 398D-76 and 398D-85 through 398D-87, a few 10- to 20-cm mudstone intervals have sharp basal contacts and are faintly graded. These may be mud turbidites. Occasional thin sandstone layers with slight grain-size gradation upward occur in Cores 398D-75 and 398D-77; these have erosional basal contacts. Sand content also increases at the base of this unit in Core 398D-101. In Core 398D-76, a 13-cm-thick mudchip conglomerated with 1 to 3 mm granules of mudstone, calcite, and dolomite in a dark gray claystone matrix is present; in Core 398D-78, a truncated slump unit of laminated claystone occurs. A few faults of probable syndepositional origin have also been noted (e.g., Core 398D-95). In Core 398D-97, several fragments of probably shallow-water limestone (ooids, coralline fragments, white porous micritic limestone, pisolites, and mollusk fragments) occur in a gravel-cobble conglomerate.

Clay minerals, quartz, mica, siderite, and zeolites are the most common constituents noted with a predominance of clay minerals consisting again of illite, montmorillonite, and more minor chlorite and kaolinite. Pyrite is again ubiquitous and radiolarians are common.

***Sub-Unit 4C: Cores 398D-102 Through 398D-130 (1410 to 1667 m sub-bottom); Barremian Through Upper Aptian***

This lithologically complex sub-unit is composed of dark mudstone, claystone, and calcareous claystone ranging from black to dark gray to olive-green-gray with various interbedded mud and limestone pebble debris flows and mud-supported conglomerates (con-

taining Tithonian clasts), turbiditic mudstones, and thin to thick turbiditic sandstones and siltstones. The mud-supported conglomerates (debris flow units) occur in several intervals, notably Cores 104 to 106, 112, 115, 117, 124, 125, and 128 of Hole 389D. Thin (<1 cm) to thicker (10 cm) turbidites which occur as fine-grained quartzose, calcareous sandstones and siltstones, and which are occasionally amalgamated into up to 40 cm sets, characterize Sub-unit 4C. These sands are fewer in number and thinner at the top of the section, becoming more prominent downward, especially from Cores 398D-117 to 398D-131. Graded multicolored mudchip sands also occur in some of the cores studied. Siderite becomes less important, especially in lower Sub-unit 4C.

Carbonate contents are generally low, remaining below 5 per cent in Cores 398D-111 through 398D-121. In the intervals both preceding and following these cores, carbonate content may reach above 50 per cent, probably due to the mass transport of a large amount of more calcareous material to the site in slumps and debris flows, and as turbidites. However, towards the base of Sub-unit 4C, carbonate content increases in burrowed, pelagic, marly limestone beds in the transition to Unit 5. In Sub-unit 4C, planktonic foraminifers are nearly absent, a few probably being reworked through turbiditic transport to the site (see Sigal, this volume). Radiolarians are abundant to common throughout. Many of these are transported by turbidity currents as evidenced by smear-slide examination of turbidite units. Organic carbon values begin at the top of Sub-unit 4C at values of 0.2 to 0.6 weight per cent and increase rapidly below Core 398D-117 to values up to 2.25 weight per cent. Wood fragments (well preserved, often coalified) and spores increase in abundance at this point as well. This increase is attributed to transport by turbiditic influx possibly related to deltaic progradation (see also Habib, this volume) or build-out of a deep-sea fan complex (de Graciansky and Chenet, this volume). The quartz (angular grains) and mica components identified in smear slides increase slightly downward in Sub-unit 4C. The co-occurrence of mica and plant debris is notable. Pyrite is obvious in most samples. The clay mineral suite is basically the same as in Sub-units 4A and 4B with some slight variation.

Slump units and debris flow deposits occur prominently in some intervals. Individual units can exceed 1.5 meters in thickness. Most are matrix supported, containing angular to subrounded clasts of light colored limestones (appearing to have been indurated at time of redeposition and contain Tithonian calpionellids) and light colored mudstone and marly limestone flattened to plastically-deformed and indented by other pebbles. Clast sizes range from granules and sand-sized chips (>6 cm in diameter). A few pebbles of oolitic(?) limestone and some black shale clasts were also noted. The source for these flows seems to have been relatively nearby in comparison to the more distal source for the turbidite sands, possibly from upslope in a more carbonate-rich environment. Indications from nannofossils contained within clasts give approximate coeval

or slightly older ages (as old as Valanginian and some Tithonian) for the conglomeratic pebbles within strata of probably Aptian age. Dewatering veins (e.g. Cores 398D-104 to 398D-106) are found in underlying sediments, probably as a result of rapid loading by slumps and debris flows. Pelagic sediments below are also commonly sheared and folded with associated small-offset faults. Calcareous, light greenish gray graded mudchip sands occur both in association with the top of conglomeratic units or separately and are seen intermittently throughout Sub-unit 4C. The mudchips appear to be of approximately the same composition as the conglomeratic pebbles and may be derived from the same source (color 5GY6/1). They are possibly turbidites which represent the distal extension of debris flow units which came to rest nearer to the source upslope from the site.

Greenish gray to light gray (N6) sandstones and siltstones (usually <10 cm thick) which are especially important in the lower part of the sub-unit, are commonly composed of very fine-grained to coarse-grained silt, and exhibit parallel, wavy, and cross-laminations. Many show convoluted bedding at the top. These appear to be the upper portions of Bouma sequences; Bouma units a, b, and c are rarely found. Grading is not often present. In the lower part of Sub-unit 4C, sequences of these sands may be amalgamated into thicker units of up to 60 cm. The same applies to slightly graded, dark mudstone beds with sharp basal contacts interpreted as mud turbidites. These sands and muds are presently thought to represent a distal deltaic environment (prodelta or distal submarine fan) with common crevasse splay or natural levee deposits (see de Graciansky and Chenet, this volume). No definite channel sands were found. The sands contain primarily quartz, mica, radiolarians, wood fragments, and some foraminifers. Some gypsum was found in claystones within Sub-unit 4C, sometimes in thin laminated beds.

*Unit 5: Cores 398D-131 Through 398D-138 (1667 to 1740 m sub-bottom); Upper Hauterivian to Lower Barremian*

The transition from debris flows, abundant turbiditic sandstones, and dark gray to gray-green claystones and calcareous mudstones to bluish white to white (5B9/1 to N9) nannofossil limestone interbedded with thinly laminated medium dark to dark gray (N3, N4) brownish black and olive-gray (5Y4/1) mudstone marks the top of Unit 5. Thin turbiditic sandstones and siltstones become progressively less important and are nearly absent in some cores. A few light colored mudchip graded sandstones occur.

Carbonate contents increase to between 50 and 75 per cent. Nannofossil preservation is improved, but planktonic foraminifers are still very rare to absent; radiolarians are rare to frequent. Organic carbon content ranges from highs of 2.6 weight per cent to a low of 0.4 weight per cent; the former value is from the dark, thinly laminated calcareous mudstones, the latter is from nannofossil limestones.

Nannofossil limestones are transitional with the dark laminated calcareous mudstones as they are interlaminated both at upper and lower contacts. The limestones are usually intensely burrowed, and burrows are often pyritized. Pyrite concretions and blebs also occur. Dark green "diagenetic laminae," nearly identical to those noted in the Cenozoic sequence, are notable in light colored limestones. Again, these are likely related to diffusion of reduced iron species away from the more organic-rich mudstones into relatively more highly oxidized limestone.

The thinly laminated calcareous mudstones contain approximately 50 laminations per centimeter; these light-dark alternations are composed of clay to silt-sized lenticular grains and plant debris aligned in layers. Basal contacts are gradational, never sharp, and no upward fining is seen. These are probably not current-deposited or distal turbidites because of their uniform lamination and gradation into overlying and underlying sediment. They are relatively more organic carbon-rich than the limestones and may represent periodic bottom-water stagnation episodes due to oxygen-minimum layer fluctuations or basinwide stagnation. However, some of these units do show evidence of redeposition and may have originated by amalgamation of numerous thin (1 cm) mud turbidite layers.

Fine-grained sandstones or siltstones within Unit 5 are usually <1 cm thick, have parallel to wavy lamination, convolute lamination or ripple cross-lamination, and are light green-gray (5G6/1). They are generally quartz-rich and calcareous. Thin, graded mudclast sandstones (e.g. Cores 398D-133, 398D-136) also occur. These contain light tan sand-sized chips of limestone and marly limestone. Clay minerals consist of montmorillonite, illite, and chlorite. Quartz and feldspar are common mineral grains.

### Interpretation of the Mesozoic Sequence

#### Introduction

The evolution of sedimentation at Site 398 on the flanks of Vigo Seamount presents a number of intriguing problems in interpretation and possible solutions to questions of a tectonic and paleoceanographic nature. Important points to be considered in light of sedimentological evidence are the time of initiation of rifting and possible thermal updoming and subsequent spreading and subsidence related to opening of the North Atlantic Ocean north of the New Foundland fracture zone. Also of interest is the origin of the "black" shale episode typical of the Early Cretaceous, and especially Aptian-Albian.

#### Tectonic and Sedimentary Evolution

Several major episodes can be outlined in the evolution of the sedimentary sequence at Site 398, as discussed below.

**Hauterivian pelagic Phase 1:** This phase is represented by lithostratigraphic Unit 5 which consists of bluish white nannofossil limestones interbedded with laminated, dark colored mudstones. Though not fully

penetrated, this formation may continue downward to overlie a subsided basement of Precambrian(?) metamorphic rocks, possibly capped by Jurassic neritic clastics or carbonates.

It is envisioned that Unit 5 lithologies were deposited on a slowly subsiding sea-floor of moderate depth in a predominantly pelagic setting above the CCD. Calcareous nannofossils with moderate to good preservation are a major constituent of the bioturbated limestones, but planktonic foraminifers are nearly absent; the lack of abundant planktonic foraminifers may also be due to the dearth of species and numbers at this early stage in their evolution. No aragonitic fauna were found, which indicates at least some solution of carbonate. Rippled laminae, plus cut and fill structures of fine sand-sized pelagic limestones, perhaps indicate periodic bottom-current action or turbidites. Some redeposition is indicated by the presence of Berriasian nannofossils in a Hauterivian matrix (Blechschildt, this volume). Periodic basinwide stagnation episodes or downward excursions of an intensified oxygen-minimum layer are evidenced by finely varved, dark, unburrowed, organic carbon-rich calcareous mudstones which are gradationally interbedded with the burrowed limestones. Benthic faunas were apparently present only during better oxidized intervals at the time of the deposition of the light limestones. Periodic stagnation could be related to climatic influence or possibly to the restricted, predominantly shallow depths of the subsiding seaway during the Early Cretaceous. Overall sedimentation rates during this interval were about 10 m/m.y., typical of many pelagic settings. Deposition of these sediments followed an early phase of rifting and subsidence in this region (Triassic-Liassic) which led to the formation of relatively shallow, flat sea floor in the North Atlantic. The sediment of Unit 5 probably represents the top of acoustic basement which was faulted and began subsiding during the second phase of rifting (Late Jurassic-Early Cretaceous; see Sibuet and Ryan, this volume). Sediment of Unit 4 filled the grabens between rifted blocks.

**Barremian through Aptian subsidence and clastic influx, Phase 2:** This period, primarily during the deposition of lithostratigraphic Sub-unit 4C is represented by dark gray to olive-green-gray material identified as follows: (1) bioturbated mudstones; (2) repetitive amalgamated turbiditic mudstones; (3) thinly laminated and cross-bedded fine-grained sandstones and siltstones representing distal turbidites (upper parts of Bouma sequences; possibly crevasse-splay and inter-channel, natural levee deposits in a prodelta or deep-sea fan environment); and (4) periodic debris flows or mud flows and slumps containing more carbonate-rich pebbles in a dark mollusk-bearing matrix, probably from a local source (Tithonian-Berriasian aged micritic limestone pebbles with calpionellids; e.g., Bourbon, this volume). Basically, Sub-unit 4C represents a fining upwards distal(?) deltaic or submarine fan sequence, beginning with rapid influx of sand-silt at the base, and gradually waning during the late Aptian. A total of about 270 meters of such deposits is present with

inferred sedimentation rates of up to 100 m/m.y. This change in sedimentation type from that of lithostratigraphic Unit 5 was very rapid. This depositional transition was accompanied by an increased influx of plant debris (e.g., Habib, this volume), quartz, illite, kaolinite, and feldspar (Chamley et al., this volume); Site Summary, Chart 1, rear pocket of this volume), and decreasing  $\text{CaCO}_3$ .

The fine-grained sands contain primarily quartz and mica, some radiolarians and a few transported benthic and planktonic foraminifers. There is nothing diagnostic of source terrain; however, it is inferred as being geographically remote, possibly from Wealden deltas to the west (Newfoundland-Labrador) or from material shed from the uplifted and eroded metamorphic terrain of the northwestern Iberian Peninsula. It is less likely that the material, including a large amount of clay, was derived directly from the contiguous western Iberian margin farther south, because neritic carbonate shelves are more typical there during the Early Cretaceous (Wilson, 1975). In addition, local sources (except for calcareous debris flows) are unlikely because of the volume of detritus to be derived as evidenced by the gross thickness and widespread distribution of the lower part of acoustic Unit 3 and acoustic Unit 4 over the Galicia region (Groupe Galice, this volume).

Slump masses and debris flows which occur intermittently throughout lithostratigraphic Sub-unit 4C (Phase 2) and, especially near the top, contain pebbles of lighter color and more carbonate-rich than the predominant dark gray to green-gray "pelagic" or autochthonous sediment of Sub-unit 4C. These clasts contain nannofossils, belemnites, and calpionellids, but no fauna indicative of original environment or precise depth of deposition. Because of the contrast in carbonate content and in the better oxidized appearance between clasts, matrix, and the autochthonous sediment of Site 398 during this time, it is inferred that these were reworked from upslope in a better oxidized environment (or away from the influx of clay and organic matter fed in by the delta source) where conditions of enhanced carbonate preservation prevailed. The size and condition of the clasts (many were obviously soft and plastic at time of transport; sizes up to 10 cm) suggest a proximal source. In addition, a few better indurated, white, oolitic, or peloidal limestone clasts were found. Preliminary determination of the age of the nannofossil and calpionellid limestone clasts allows the possibility that these are from slightly older strata deposited at higher topographic levels and have slumped down to the site, possibly from Vigo Seamount. The locus of occurrence of these slump and debris flow events within Sub-unit 4C probably indicates initiation of some tectonic movements within the Galicia region and the presence of significant topographic relief along scarps. The sea floor in this region probably underwent subsidence below the CCD during deposition of Sub-unit 4C. Older tilted and deformed surfaces are visible on seismic records (e.g., Groupe Galice, this volume). Block faulting probably occurred during the Barremian-early Aptian interval, and significant topographic relief could

have been effected, making fault scarps or oversteepened slopes susceptible to gravity-induced downslope mass transport. This could provide clasts of sediment of the same age as the mass movement event as well as those of an older age exposed on fault scarps. The thinner, graded mudchip-limestone fragment sands may also be of this source, because they have no obvious association with the turbiditic quartzose sands and contain fragments similar to those of the conglomeratic units. Upon sedimentation of the mass movement deposits, underlying muds are often sheared and folded; rapid loading and lateral shearing of up to 2-meter debris flow units apparently causes synsedimentary normal faulting and the formation of sinuous dewatering conduits in underlying sediment.

Although turbidite sands, muds and debris flows are prevalent during the time interval represented by lower Sub-unit 4C (ca. Core 398D-120), sedimentation rates obtained from biostratigraphy are relatively low at about 50 m/m.y. Although sedimentation rates after this time appear to increase to over 100 m/m.y., a decline in the influence of the sand and silt transport to the site is noted. One interesting correlation may be noted: between Cores 398D-118 and 398D-134, within the range of the more important sand contribution, palynofacies indicate long-distance transport of an assemblage of spores and pollen, along with large (>40 mm) wood fragments. The assemblage, usually found closest inshore, is considered to be most rapidly sedimented upon arrival to the oceans from river transport. Either rapid long-distance transport by turbidity currents to the site, or perhaps more local river sources, is responsible for this terrestrial source assemblage. The high wood-spore assemblage (Habib, this volume) occurs during the interval of highest organic carbon values (up to 2.75 per cent) in the dark gray muds; prevalent, sand-silt sedimentation is interpreted as being in a distal deltaic or submarine fan environment. After Core 398D-118, the palynofacies indicates a more easily transported floating assemblage (Bisaccates) which could be carried by marine currents; organic carbon values decline to lower values (0.5 per cent). This may represent the decline of pronounced deltaic terrigenous influence in the upper part of Sub-unit 4C and the end of Phase 2, the sediment of which fills depressions in the sea floor between rifted blocks. The seismic character suggests that deposition was concurrent with some rotation and subsidence of crustal blocks during rifting.

**Albian "black shale" deposition, Phase 3:** The transition from Phase 2 to 3 is somewhat gradual. Sideritic beds, laminae, and lenses become more prominent upward in the Sub-unit 4C transition to Sub-unit 4B, which is the beginning of interpreted Phase 3. Sedimentation during Phase 3 is less variable than in Phase 2. A number of enigmatic problems do exist, however. The occurrence of yellow tan, vuggy, occasionally laminated, mound-like accretionary siderite deposits, and siderite lenses and laminae supplies interesting information on diagenetic processes (Arthur, this volume). Interstitial water sulfate concentrations must have been substantially lowered by bacterial sulfate reduction and

consequent metal sulfide precipitation. Reduced iron species and high carbonate alkalinity probably led to siderite precipitation (e.g., Berner, 1971). Vuggy siderite mounds appear to grow on individual substrates of concave-upward mollusk shells in Core 398D-96. Thin-section study of one such mound shows a peloidal structure. Siderite is most typical of fresh-water organic carbon-rich facies, but has been noted in deep basinal organic-rich deposits (DSDP Legs 11, 43) and continental slope organic carbon-rich sediments (e.g., DSDP Leg 47A). Another intriguing diagenetic aspect concerns preservation of calcareous fossils. Ammonites are well preserved but flattened in Cores 398D-99 to 398D-88 and molluscan fragments occur up to Core 398D-72. These originally aragonitic remains are paradoxically preserved in sediments in which planktonic foraminifers are completely absent and calcareous nannofossils rare. If ammonites were not present, the absence of planktonic foraminifers could easily be attributed to dissolution at or below CCD (see Sigal, this volume), which would allow the interpretation that the sea floor was already at depths of several thousand meters. One would expect aragonitic ammonite remains to be more highly soluble than foraminiferal tests. However, the possibility remains that the smaller surface area to volume ratio, larger size, and possible protective organic coatings allow preservation of ammonites over foraminifers and nannofossils in combination with high sedimentation rates (in excess of 100 m/m.y.) and rapid burial.

A few gypsiferous muds and laminae occur occasionally within Sub-unit 4B, along with the abundant and varied yellow-tan siderite. The gypsum may be wind-blown to the site from deflation of possible nearby coastal sabkas or may have originated by erosion of older evaporites exposed in fault scarps (possibly Triassic-Liassic). It is also possible that some of the gypsum formed subsequent to the opening of the cores. The growth of gypsum crystals on surfaces and in interstices of cores of the "black shales" is a common phenomena. It is probably related to oxidation of unstable sulfides and residual pore water sulfide which produces abundant dissolved sulfate. This, on draping of surfaces and pores, combines with dissolved  $\text{Ca}^{++}$  to precipitate gypsum. At this time we cannot distinguish between these types in the cores. It is doubtful that they are of primary origin.

A few minor debris mud flows and sands and slumps also occur within Sub-unit 4B between Cores 398D-75 and 398D-78, attesting to the existence of sea-floor topography and unstable scarps or slopes. The increase in carbonate content and the occurrence of light green calcareous beds in the upper Albian (Cores 398D-87, 398D-78) is probably a result of redeposition from slopes above the CCD. Reworked foraminifers are common, and the site is inferred to have been mostly below CCD at this time, although a lowering of the CCD could be indicated. Attapulgite also is suddenly prominent in

Core 398D-79. Its occurrence has been interpreted as related to detrital influx (Chamley et al., this volume).

Sedimentation Sub-units 4B and 4A leveled much of the sea floor relief originally present (Groupe Galice, this volume).

**Late Albian through Maestrichtian pelagic sedimentation, Phase 4:** Deposition of dark gray to black shales which were prevalent since the Barremian, continued through the Albian and into the early Cenomanian. Lighter colored green-gray, burrowed mudstones are more prominent, however, attesting to frequent oxygenation of waters impinging on the sea floor. Organic carbon contents are unusually and consistently low for black shales, generally  $> 0.75$  weight per cent. It is possible that high organic carbon contents and anoxic or near anoxic conditions in the water column during the Barremian through Aptian at this site were due primarily to gross inputs of terrestrial organic matter to a restricted northern North Atlantic Ocean by highly developed delta systems (e.g., Habib, this volume; see Arthur, this volume, for further discussion). Rhythmic transitions from relatively oxidized and burrowed gray to green claystones to dark gray to black unburrowed claystones may represent periodic intensification of oxygen deficits in deep waters of the depositional basin. Bottom-burrowing faunas seem to return relatively rapidly after the onset of oxidizing conditions. Sedimentation rates apparently decreased during the late Albian to Cenomanian to 15.5 m/m.y. Many of the light colored marly chalks or calcareous mudstones may be redeposited.

Whereas much of the organic matter in black Barremian-Albian mudstones was terrigenous plant debris and woody fragments and spores (Habib; Deroo et al.; both, this volume), several thin Cenomanian black mudstones are characterized by high amounts of marine phytoplanktic organic matter. The relationship of these sudden, rich influxes of marine organic material and abundant radiolarian tests suggests an increase in local sea-surface fertility and consequent productivity. The organic-rich layers and associated sediment in Core 398D-56 show signs of having been redeposited and may represent material originally deposited in oxygen-depleted mid-water regions, and then moved downslope (see Arthur, this volume).

The end of "black" shale deposition occurred in the mid(?) Cenomanian with a transition to barren red shales. A hiatus may be present between Santonian or Campanian and Cenomanian strata, but the barren claystones allow both a condensed section and/or hiatus (Sigal, this volume). Evidence of angular unconformities in seismic profiles between sediments of Sub-units 3B and 4A suggests that erosion or non-deposition of sediment occurred. Zeolites (clinoptilolite) are concentrated (reaching as high as 40 per cent of the total sediment) within the transition to red claystones; quartzose silts become common just above. The apparent end of black shale deposition and the possible hiatus may be related

to the onset of enhanced bottom-water circulation due to Campanian separation of Rockall Bank from Europe allowing relatively colder, oxygenated bottom waters originating on the Faeroe-Shetland shelf to circulate through the Iberia-Newfoundland seaway at this time.

Within the Maestrichtian, carbonate contents increase and faunal preservation improves. This probably represents a lowering of the CCD. A brief latest Maestrichtian hiatus may be present and is possibly due to increased circulation related to a climatic change. A slumped interval occurs just below the Cretaceous/Tertiary boundary (Figure 19). Rhythmic sand-silt intercalations also commence in the Campanian.

## X-Ray Mineralogy Methodology

### Cretaceous Samples

#### *Bulk Mineralogy*

The rock samples were dried at 70 °C and crushed to approximately 40  $\mu\text{m}$ . The method used to give semi-quantitative determinations mainly consists of estimating the absorption coefficient of each sample and then comparing its diagram with patterns of external standards. The diffractometer used was a Philips 1130 and operating conditions were as follows: nickel-filtered copper  $k\alpha$  radiation at 40 kv, 20 mA; back monochromator, scanning speed  $2^\circ 2\theta$  per minute.

#### *Clay Mineralogy*

The samples are mixed with distilled water for 10 hours, and then are decarbonated in 10N HCl. The excess acid is removed by successive centrifuging. The  $<2\ \mu\text{m}$  fraction is collected by decantation using Stokes law, and then oriented aggregates are sedimented on glass slides. A Philips X-ray diffractometer with copper Ni-filtered radiation is used to run three scans as follows: (a) from  $2^\circ$  to  $22^\circ\ 2\theta$  ( $8^\circ/\text{min}$ ) on natural sample; (b) from  $2^\circ$  to  $22^\circ\ 2\theta$  ( $8^\circ/\text{min}$ ) on glycolated sample; and (c) from  $24^\circ$  to  $26^\circ\ 2\theta$  ( $2^\circ/\text{min}$ ) on natural sample.

Quantitative determinations are carried out using peak heights above the background; the amount of each mineral is considered to be directly proportional to the peak height. The  $10\ \text{\AA}$  peak (natural sample) is used for illite and the  $18\ \text{\AA}$  peak (glycolated sample) for smectite. The amount of irregular mixed-layer (illite-smectite) is estimated by the difference of diagram traces between "natural" and "glycol" samples, between  $11\ \text{\AA}$  and  $13\ \text{\AA}$ . The  $7\ \text{\AA}$  peak gives the total kaolinite + chlorite, the ratio of these two minerals being deduced from the peak heights ratios at  $3.58\ \text{\AA}$  and  $3.54\ \text{\AA}$ , respectively. The total of percentages is summed to 100.

### Tertiary Samples

#### *Bulk Mineralogy*

Dried and pulverized samples of total sediments were analyzed according to the powder diagrams method using an internal standard (corindon). By comparison with synthetic reference samples this method permits



Figure 19. Slumped and folded interval just below Cretaceous/Tertiary boundary (Sample 398D-41-2, 45-77 cm).

semiquantitative estimates of quartz, calcite, dolomite, and feldspars (alkali and plagioclase). The diffractometer used is a Philips 1310 and operating conditions were as follows: nickel-filtered copper  $K\alpha$  radiation at 40 kv, 20 mA; automatic sample changer; step-scanning device and monitoring system of the goniometer.

### Clay Mineralogy

Total sediments were dispersed in pure water using mechanical agitation. Samples with high content of carbonates were first treated with 10N HCl.

After two or three washings in pure water,  $<2\ \mu\text{m}$  subfractions were separated by gravity settling. After centrifugation of the  $<2\ \mu\text{m}$  portion of suspensions, the thick paste obtained was spread across two slides with a standard laboratory spatula. The amount of clay per  $\text{cm}^2$  was controlled by the amount transferred to the slide. The slide was saturated first with ethylene glycol before analysis. A second slide was scanned untreated and then heated at  $550^\circ\text{C}$  for 1 hour before the second analysis.

The diffractometer used is a CGR Theta 60 and operating conditions were as follows: Cu  $K\alpha$  radiation (very thin focus  $0.1 \times 5\ \text{mm}$ ) selected with a Guinier monochromator: 40 kv, 10 mA; scanning speed:  $0.5^\circ\ \theta$  per minute.

Identification of minerals has been made from typical reactions of known minerals to classical treatment (Brown, 1961; Thorez, 1975).

Semiquantitative estimates of the different minerals have been made from diagrams of the glycolated slides. Height of 001 peaks have been used to determine the percentage of smectite ( $17\ \text{\AA}$ ), illite ( $10\ \text{\AA}$ ), and kaolinite + chlorite ( $7.1\ \text{\AA}$ ), a distinction between chlorite and kaolinite being made on the basis of the difference between 002 reflection of kaolinite and 004 of chlorite.

### Zeolite Analysis, Hole 398D<sup>2</sup>

Systematic study of Hole 398D zeolites is based on diffractometric data on powders  $<50\ \mu\text{m}$ . No characteristic peaks have been obtained on the  $<2\ \mu\text{m}$  fraction on oriented preparations. Sixteen samples were chosen for study based on the shipboard description.

The zeolitic mineral observed evokes essentially 5 diffraction peaks, as follows: (a)  $9.0\ \text{\AA}$ : sharp and predominant—100 per cent; (b)  $7.93\ \text{\AA}$ : sharp; maximum 25 per cent of a (above); (c)  $3.97\ \text{\AA}$ : always clear; approximately 50 per cent of a (above); (d)  $2.97\ \text{\AA}$ : broad; and (e)  $2.795\ \text{\AA}$ : little peak but clear.

The better-peak diffractograms were obtained on Aptian sediments in Sample 398D-118-2, 72-74 cm. The numerous peaks present permit the identification of a mineral of the clinoptilolite-heulandite family. This mineral is similar to zeolites extracted from the Turonian chalk of the Paris Basin and identified as clinoptilolite.

The zeolite from the Cenomanian (Cores 398D-39 to 398D-63) seems characterized by a  $7.93\ \text{\AA}$  peak clearly higher than in the Aptian levels (Cores 398D-113 to 398D-119).

### PHYSICAL PROPERTIES

Physical properties, unlike most sea-floor parameters, may be measured both on drilled samples and offshore by marine geophysical techniques. Through their correlation with regional geophysical measurements (seismic reflection, seismic refraction, gravity, magnetics), they have the potential to become a useful means by which to laterally extend the detailed knowledge gained from a drill site. Drilling, particularly in the deep ocean, is an expensive operation which generally results in the placement of drill holes that are widely spaced from one another. This provides the potential for geophysical correlation to be made between distal drill holes, thus broadening our knowledge of the geographic extent of the sea floor.

Having said this, one imagines an ideal world where parameters can be positively traced across the ocean floor. Site 398 demonstrated this imaginary model's impracticality when the anticipated stratigraphy and velocities failed to appear in the drilled column. Our techniques for the interpretation of remotely gathered geophysical parameters are not perfected and more control data from drill sites are required.

The parameters measured during Leg 47B at Site 398 were compressional wave velocities, made at a minimum of once per core, though frequently on alternate sections of each core. The measurements were made predominantly parallel, but also perpendicular to the bedding. Vane shear measurements were undertaken on the less consolidated sediments, but the deepest measurement was at 273 meters because of compaction.

Two independent techniques were used to evaluate wet-bulk density and porosity: the Gamma-Ray Porosity Evaluator (GRAPE), and weighing and immersion methods. The GRAPE was used in scanning mode down to Core 398D-27, by which time more indurated clays were being encountered and increased drill-fluid pressure tended to cause a ridged exterior to the core. This caused variations in core diameter greater than even the limited accuracy ( $\pm 12$  per cent) of GRAPE scans. At this point, GRAPE scanning ceased and two samples per core were subjected to 2-minute GRAPE analysis. Velocity, porosity, and density (both methods) and water content values are plotted against depth in Figure 20 and also compared with calcium carbonate content, grain density, and core-cutting time.

Interpretation of the physical properties data (in terms of the lithologies encountered in the cores) is attempted in the following paragraphs.

### Sonic Velocities

Velocity measurements were made on samples, normally within two hours of bringing the core aboard ship. Repeatability tests show the Hamilton Frame

<sup>2</sup> From G. S. Odin, Université Pierre et Marie Curie, Paris, France.

apparatus to be accurate to within 2 per cent. The values for each sample measured are plotted against depth (Figure 20), the wide scatter of velocities observed in some cores being largely a reflection of the contrasting lithologies encountered.

From the velocity-depth profile, different velocity groups were subdivided visually and the individual values within each group averaged. It is these mean values which are depicted in the velocity profile (Figure 21) and circled in Figure 20. A subjective choice was sometimes necessary to draw the velocity group boundary; in these instances, guidance was taken from lithologic and other physical or geochemical features of the core.

The major use for velocity measurements on DSDP material is their correlation with the seismic reflection profile (for fuller discussion, see "Correlation of Reflection Profiles with Drilling Results"). There are fundamental problems in making correlations between velocity measurements on samples and seismic reflectors. During sample handling, for example, the ambient temperature onboard raises the temperature of the drilled material from its *in-situ*  $\sim 2^\circ$  to approximately  $18^\circ\text{C}$ ; the sample is also no longer in a saturated environment, which causes significant water loss (especially in highly porous samples).

An unknown factor is the effect of a lack of confining pressure on the sample. This contributes largely to the discrepancy between *in-situ* and sample measurements on unconsolidated samples. The degree to which this factor is relevant in indurated samples is difficult to estimate.

Various practical problems also were encountered at Site 398. First, there were a large number of changes in microlithofacies within cores. Beds of frequently  $< 1$  cm thickness made representative sampling difficult. In some cases, for example, Cores 398D-102 and 398D-103, parts of the core were too soft, shattered, or disturbed by drilling to be sampled representatively, and the average velocities obtained do not represent the true mean velocity.

Another fundamental problem is that with  $< 100$  per cent core recovery, there is no way of knowing the exact original depth of a particular sample. Hole 398D fortunately provided 72.2 per cent overall recovery. This is well within the accuracy to which the correlations have been made with the seismic reflection profile.

Three significant observations can be made on the velocity profiles:

- a) Velocities are considerably lower than those calculated from seismic reflection arrivals along the site survey lines.
- b) Velocity increments are very gradual.
- c) Velocities do not invariably increase with depth.

It is normally assumed that velocity measurements on samples at normal pressure will show lower than true values. As a consequence of this assumption, two concessions have been made in drawing the velocity-depth profile (Figure 21). First, 10 per cent of the value has been added to the upper 373 meters which are quite unconsolidated; this increases the observed value of

1.69 to 1.82 km/s. Similarly, samples from 373 to 550 meters have 8 per cent added, increasing the observed 1.77 up to 1.91 km/s. The second concession is that while it is recognized that the sediments are anisotropic with velocities parallel to the bedding usually being slightly higher than those perpendicular to the bedding (Figure 22), and while the seismic profile is concerned with vertical velocities, i.e., perpendicular to the bedding, the higher horizontal values have been used to construct the velocity-depth profile.

### Acoustic Anisotropy

Anisotropy is not an unusual phenomenon in sediments; it is also observed in igneous and metamorphic rocks. Figure 22 shows that Site 398 generally showed a consistent predominance of higher horizontal velocities than vertical, with an anisotropy of approximately 15 per cent for the mixed lithologies with velocities up to 2.9 km/s, increasing to approximately 25 per cent for the velocities  $> 3.0$  km/s (all limestones). The anisotropy observed at Site 398 may well be related to the horizontal microbedding seen throughout most of the core and associated with mineral alignment and/or cementation. The latter could certainly explain the higher velocities parallel to the bedding if the sample happened to contain slightly better-cemented microlayers. Much of the Site 398 sediment column showed evidence of burrowing which, depending upon the burrow infill, could also affect anisotropy.

Gealy (1971) observed an anisotropy reversal where samples with velocities  $< 2.0$  km/s showed higher vertical than horizontal velocities, while samples whose velocity was  $> 2.0$  conversely had a lower vertical than horizontal velocity. The velocity range of samples from Site 398 is 1.64 to 3.68 km/s; very few of the samples demonstrate the anisotropy reversal above 2.0 km/s (Figure 22). Only two samples with velocities  $< 2.0$  km/s (ooze-marl) showed higher vertical velocities and five samples (1 clay, 1 marl, 1 sand, and 2 shale) with velocities  $> 2.0$  km/s showing higher vertical velocities.

### Comparison Between GRAPE and Gravimetric Density and Porosity Measurements

Figure 20 shows the general comparison between these two methods. Where both were conducted on the same sample, the porosity measurements are compared in Figure 23. Considering the large variations in lithology and physical properties between different beds within each core, the two methods show tolerable agreement, although it is difficult to compare plots when one curve contains more data points than the other. In Figure 23, the GRAPE measurements have more data points and show greater variability than the gravimetric results, although the gravimetric densities appear to average the fluctuations measured by the GRAPE method. Samples were intentionally taken from the dominant lithology for gravimetric weighing.

Since the porosity calculations utilize the densities derived from the same GRAPE measurements, a comparison of densities from the two methods shows a

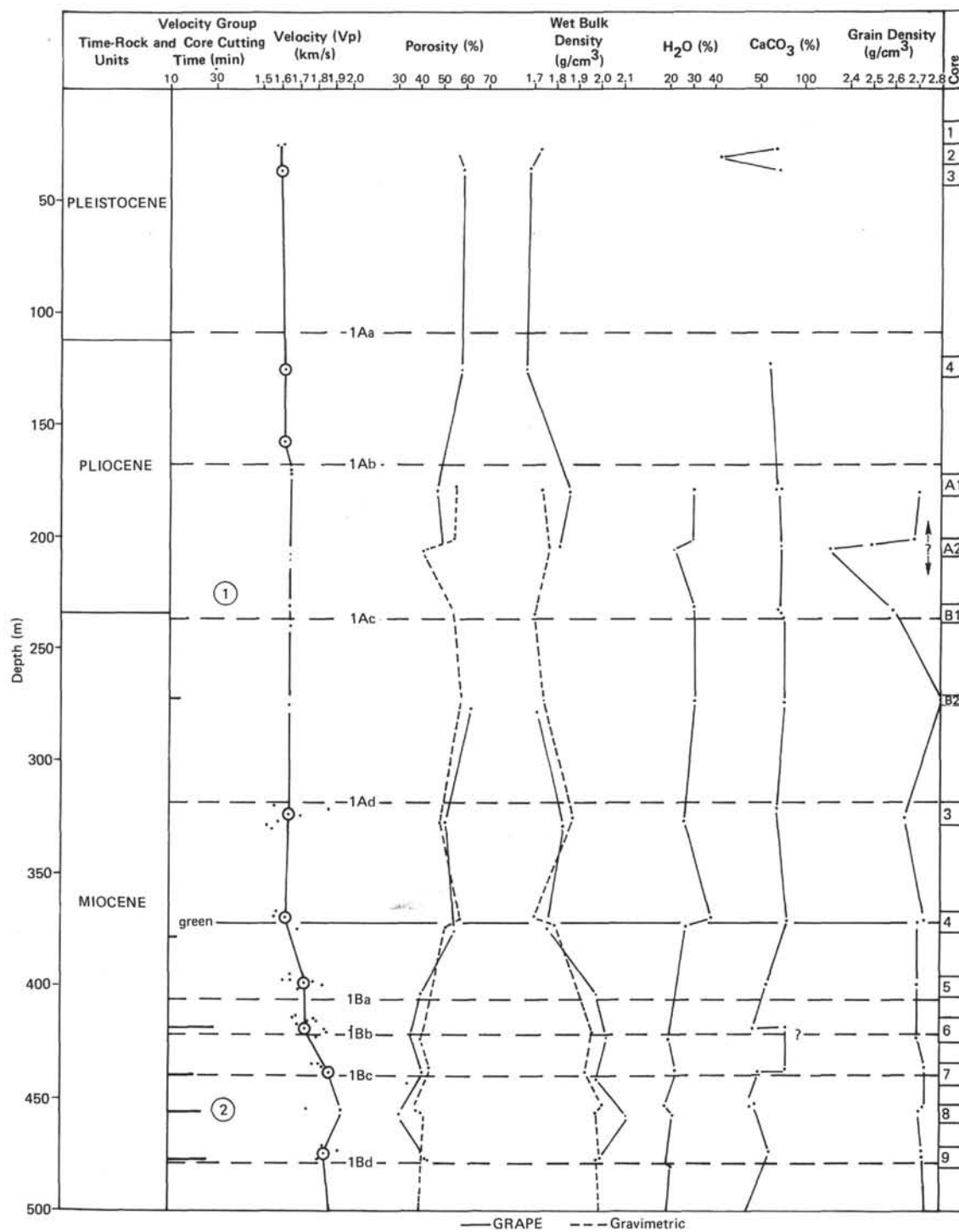


Figure 20. Plots against depth of sonic velocity, per cent porosity, wet bulk density, per cent water content, per cent CaCO<sub>3</sub> grain density, and core-cutting time. Individual velocity readings are shown by dots with the average for each core circled. Dashed lines to a second average, e.g., in Core 398D-118, include values from minority high velocity facies (usually thin sandstone layers). The water content is from gravimetric analyses and the calcium carbonate content from analyses at DSDP. Grain density is calculated from 2-minute GRAPE porosity and density values, is not precise, and should be used as a rough guide only. The major departures shown in this curve (notably, Cores 13, 56, 103, and 120 of Hole 398D) are usually accompanied by a decrease in porosity and water content, and may be related to compaction phenomena. The velocity groups and reflectors identified from the physical properties analyses are labeled and marked by horizontal lines.

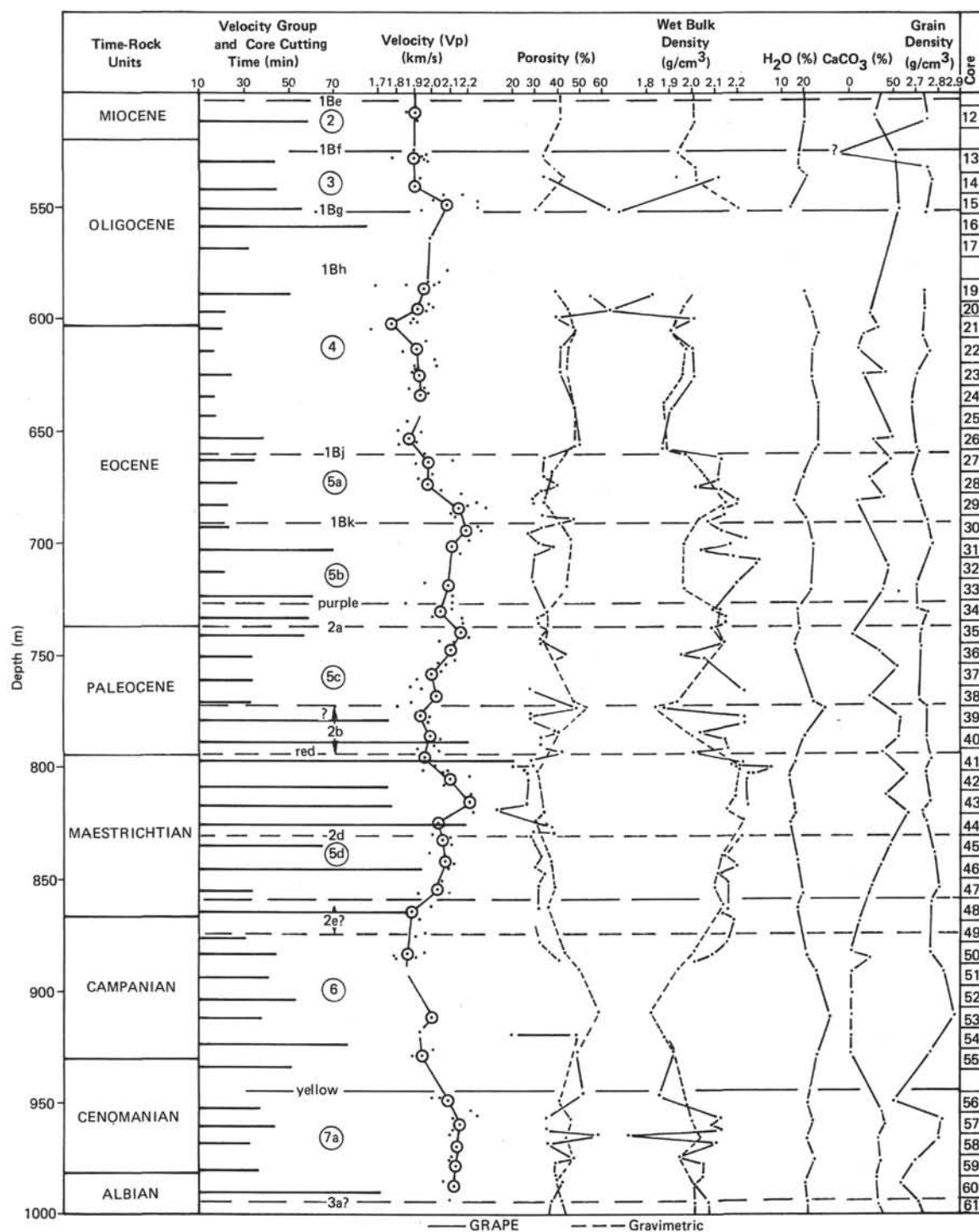


Figure 20. (Continued).

similar relationship to that of the compared porosity values.

Overall, there is a trend of increasing density from 1.70 g/cm<sup>3</sup> at the top of the hole, to 2.4 g/cm<sup>3</sup> at the bottom. The density increased gradually through the upper section of nannofossil oozes to 1.8 g/cm<sup>3</sup> at approximately 379 meters (Reflector Green). From the

onset of lithification at about this point, there is a large variation within each lithologic unit. The entire drilled column contained minor intercalations of sandstones, siderite, microconglomerates, etc. These provide a large scatter of density, porosity, water content, and velocity values within each few tens of centimeters of core. Despite this large scatter, the occurrence of a possible

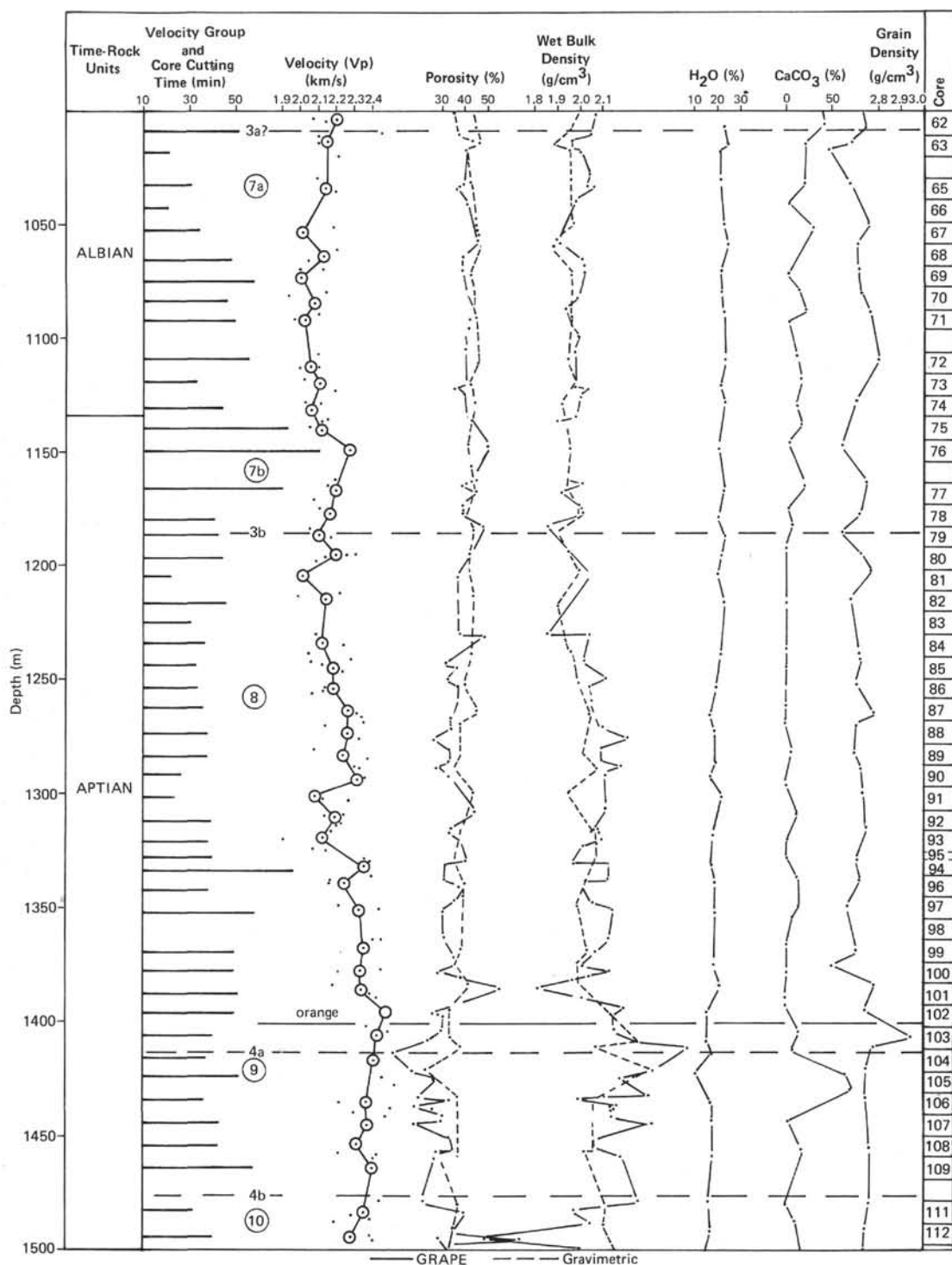


Figure 20. (Continued).

seismic reflector can be detected by a change in both amplitude and wavelength of the variations in these physical properties.

#### Water Content and Porosity

The water content is derived from the gravimetric weighings made prior to and after the sample is dried.

Throughout the core there is a general trend from a water content of 35 per cent and porosity of 60 per cent at the top of the core, to just below 10 per cent water content and 15 per cent porosity near 1740 meters sub-bottom. The largest fluctuations are seen across the softer clay layers, e.g., the red clays in Cores 398D-34 to 398D-39 (approximately 750 m), where the water con-

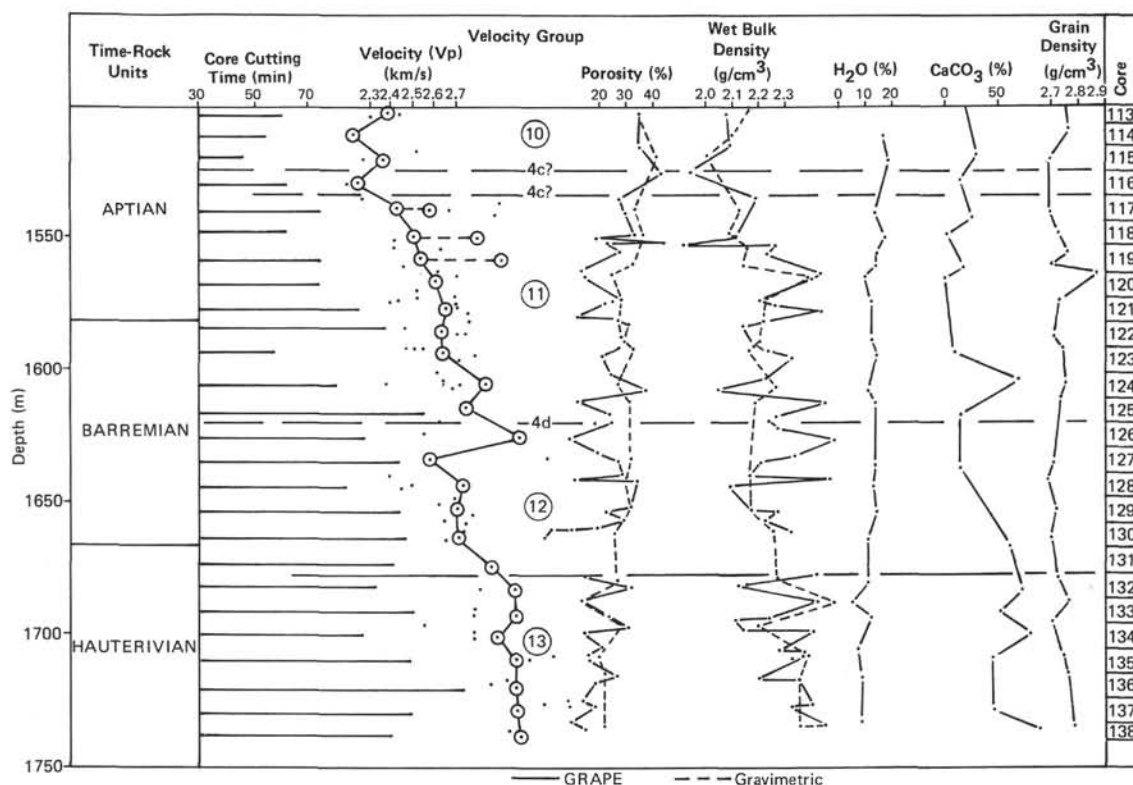


Figure 20. (Continued).

tent increased from 20 to 29 per cent and porosity from 33 to 46 per cent. Throughout the black shales (sedimentary Sub-units 4A, 4B, and 4C), the water content remains reasonably stable near 20 per cent. Below Core 398D-128 (164.5 m) pelagic limestones begin to predominate. These are indurated and well cemented, giving velocities frequently in excess of 3.0 km/s and their occurrence marks the decline in water content to below 10 per cent and porosities to approximately 10 per cent. Some idea of the degree of compaction of the upper layers may be gained from the water content curve. This indicates an approximate maximum of 25 per cent decline in water content with depth. Using a grain density of 2.75 g/cm<sup>3</sup>, this implies an increase in density of approximately 0.7 g/cm<sup>3</sup> between the top and bottom of Site 398, which is in agreement with the oozes at the top and the limestones at the bottom of the drilled interval and implies that this transformation is largely the result of simple compaction.

#### Acoustic Impedance

Acoustic impedance is the product of the compressional wave velocity and density in g/cm<sup>3</sup>. Since higher velocity and density are co-related, the impedance curve tends to enhance the contrasts within the core. From Figures 24 and 20, the reflecting horizons can be seen to correlate well with the changes in impedance. The two major departures (in velocity groups 11 and 12) are each due to a single measurement on well-cemented sandstones, both non-representative of their cores.

#### Drilling Rate

The drilling rate is monitored on the rig floor and can be useful in giving some indication of the *in-situ* properties of the core. For instance, certain clays (even at great depths) are very disturbed by the drilling process and it is difficult to know their original *in-situ* state. Comparison of the drilling time may allow some analogies to be made with other cores. Care must be taken, however, to ensure the meaningfulness of the drilling time records, since increase in pump pressure, which accelerates penetration, or stoppage of drilling for any reason are not indicated in these records. The scrutinized drill time is plotted alongside the physical properties data in Figure 20.

### GEOCHEMISTRY

#### Interstitial Water Chemistry

Eighteen sediment samples were squeezed aboard ship to extract interstitial waters; the waters were then analyzed for pH, alkalinity, chlorinity, salinity, Ca<sup>++</sup>, and Mg<sup>++</sup> contents (Table 2). The methods outlined by Gieskes (1974) were used in preparation and analysis of pore waters. Sample results are plotted in Figure 25. Sampling extended only to a sub-bottom depth of 1019 meters. One *in-situ* pore-water sample was obtained for comparison using the *in-situ* water sample for the first time in DSDP operations (see Barnes et al., this volume).

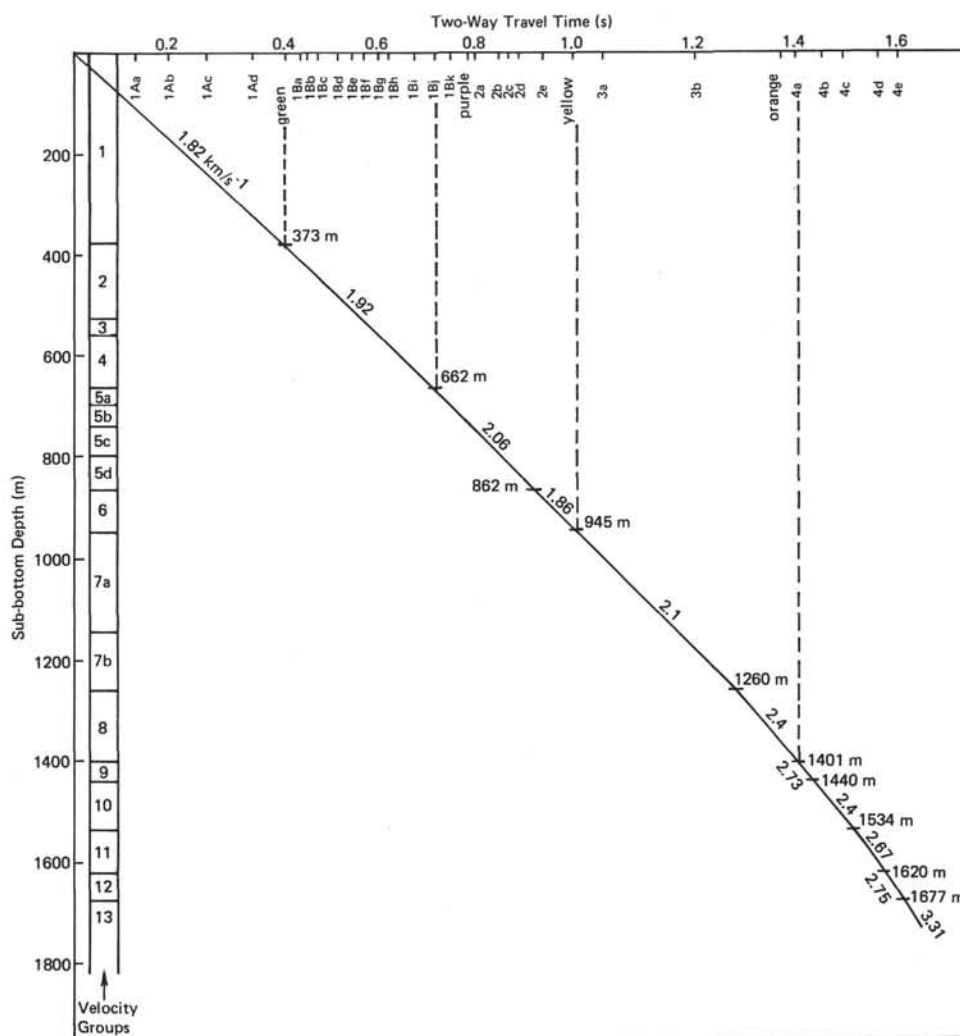


Figure 21. Velocity/depth profile demonstrating the average values within identified velocity groups (with the exception of the two upper groups which have augmented values by 10 and 8%, respectively). The 2-way travel time of reflectors observed on seismic profile GP-19 are marked on the x-axis with correlations to the velocity profile where these have been identified.

Alkalinity generally decreases downhole, but drops most rapidly in the upper 300 meters of the hole within nanofossil ooze and marly nanofossil ooze. The rate of decrease slows abruptly near the ooze-chalk transition to 320 meters sub-bottom.  $\text{Ca}^{++}$  contents in pore waters remain low and constant in the upper 300 meters of the hole, but increase rapidly at the ooze-chalk transition. The good correspondence of  $\text{Ca}^{++}$  and alkalinity changes with diagenetic changes noted in cores demonstrates that pore-water chemistry is often a good indicator of diagenetic conditions.  $\text{Sr}^{++}$  values in interstitial waters (Barnes et al., this volume) also increase in the upper 500 meters of the hole, possibly indicating the increasing extent of dissolution-cementation reactions within the nanofossil ooze and chalk section.  $\text{Mg}^{++}$  is progressively depleted downhole; the  $\text{Mg}^{++}$  curve roughly mirrors the  $\text{Ca}^{++}$  curve, but there is not a one-to-one correspondence. The decrease of  $\text{Mg}^{++}$  downhole in many DSDP sites commonly has been attributed

to either the formation of small amounts of dolomite (e.g., Manheim, 1976) or to exchange reactions in montmorillonites which might take up  $\text{Mg}^{++}$  in exchange for iron during sulfate reduction reactions in the sediment column (e.g., Drever, 1971; Manheim and Sayles, 1974). The latter process is probably not very extensive in the Cenozoic section at Site 398 as shown by the sulfate curve in Barnes et al. (this volume).

The *in-situ* water sample taken at 110 meters sub-bottom in Hole 398 shows very well the effect of squeezing and warming of samples and release of pressure on alkalinity measurements. The alkalinity value is nearly 3 meq/kg higher than that in a nearby squeezed sample (Section 398-4-3, 107.5 m sub-bottom). Other analyses compare more favorably between the *in-situ* sample and squeezed samples (see Barnes et al., this volume, for details).

There is some indication of a significant decrease in chlorinity (and salinity) within the Cretaceous part of

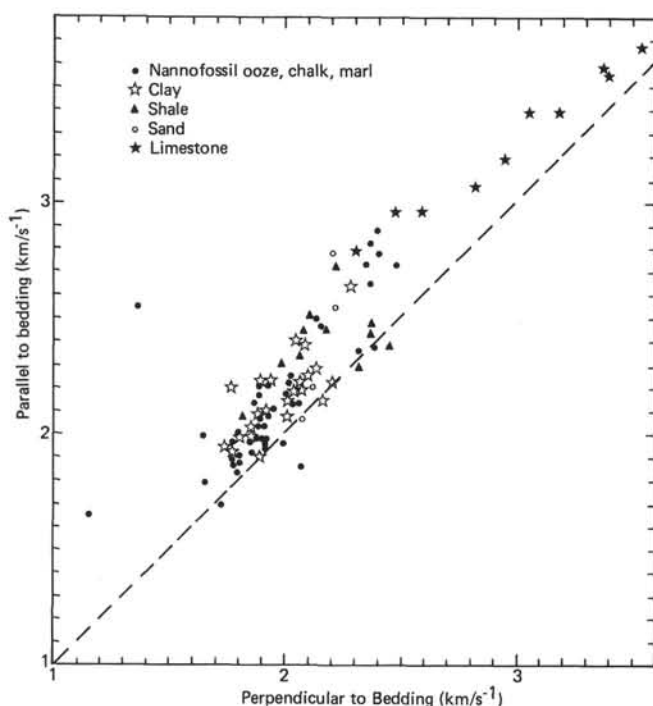


Figure 22. Acoustic anisotropy, with measurements made both parallel and perpendicular to the bedding on samples of varied lithology. The classification of lithologies is as determined onboard. No clear distinction is shown here between nannofossil ooze, chalk, and marl.

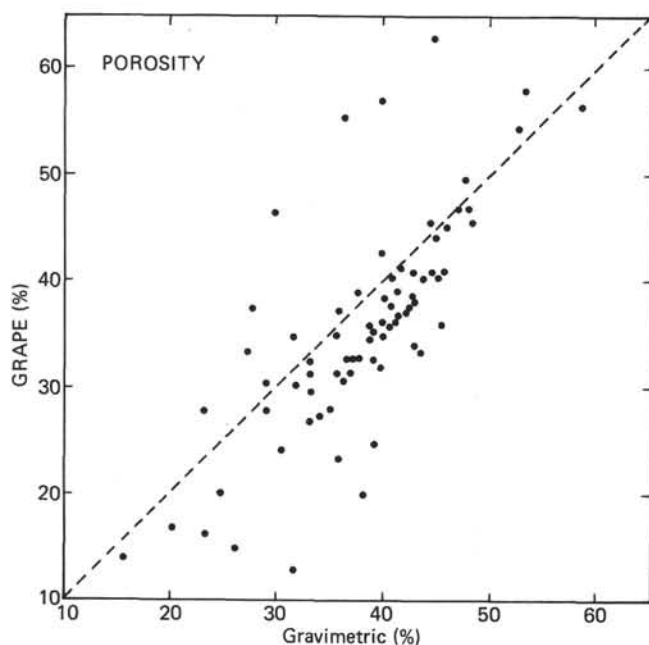


Figure 23. Comparison between porosity measurements using 2-minute GRAPE and onboard gravimetric techniques. The GRAPE values appear to be ~10% lower than the gravimetric values for porosities up to ~47% and up to 25% higher for porosities >47%.

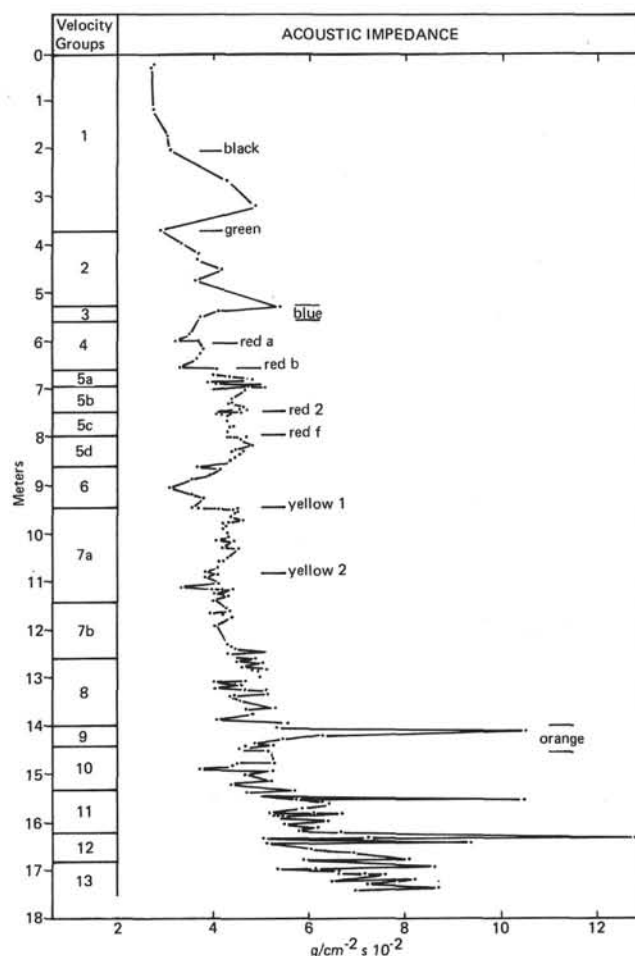


Figure 24. Acoustic impedance versus depth profile. The wet bulk densities from 2-minute GRAPE measurements were used to calculate the impedance, their variability may account for much of the scatter. The correlations with identified seismic reflectors and velocity groups are also marked. The two major excursions in velocity groups 11 and 12 are each due to a single measurement on well-cemented sandstones (i.e., non-dominant lithotypes).

the section (Cores 398D-54 and 398D-63) with the lowest value recorded in the last sample taken within the upper part of the "black shales" (lithologic Sub-unit 4A). The decreasing chlorinity in this part of the hole may indicate fresher waters at depth in the dark mudstone unit associated with a pronounced "deltaic" or deep-sea fan influence. Unfortunately, increasing lithification prevented further sampling which might have shown a further decrease in chlorinity-salinity down-hole.

#### Carbon-Carbonate

Carbonate carbon in Site 398 sediments was determined in 150 samples by the standard "carbonate bomb" method aboard ship. These analyses are plotted in the Site Summary Chart 1 (in rear pocket, this

TABLE 2  
Shipboard Interstitial Water Analyses, Site 398

Sample (Interval in cm)	Sub-Bottom Depth (m)	pH	Alkalinity (meq/kg)	Salinity (‰)	Ca <sup>++</sup> (mmoles/l)	Mg <sup>++</sup> (mmoles/l)	CL <sup>-</sup> (‰)
IAPSO		7.70	2.42	34.9	10.55	64.54	19.375
Surface sea water		8.10	2.39	35.5	10.67	66.63	19.8
2-4, 144-150	25-34.5	7.41	7.55	34.4	7.07	55.53	19.7
4-3, 144-150	120-126.5	7.46	8.10	33.6	4.95	58.06	19.5
1A-4, 144-150	172.5-182	7.42	6.70	33.6	6.53	58.27	19.4
2A-5, 144-150	201-210.5	7.43	5.69	34.1	9.27	56.76	19.7
1B-3, 144-150	239.5-249	7.42	6.23	34.1	7.29	58.47	19.7
2D-1, 144-150	271-280.5	7.60	3.91	34.1	4.96	59.01	19.6
3D-5, 140-150	318.5-328	7.50	3.88	33.6	11.83	57.97	19.6
4D-5, 140-150	366-375.5	7.12	4.60	34.9	14.77	57.16	19.5
5D-3, 120-130	394.5-404	7.18	5.38	34.6	17.43	54.78	19.8
8D-4, 140-150	451.5-461	7.15	4.62	35.2	20.44	54.24	19.7
12D-4, 140-150	508.5-518	7.20	3.73	35.2	25.65	51.91	19.8
23D-2, 106-116	622.5-632	6.98	6.06*	35.2	27.07	57.22	19.8
32D-4, 140-150	708-717.5	7.08	2.46	35.5	27.07	55.02	19.8
41D-4, 140-150	793.5-803	—	3.1*	34.9	26.48	54.10	19.6
54D-1, 140-150	917-926.5	—	4.0*	33.2	30.33	54.92	18.8
63D-5, 140-150	1012-1021.5	7.62	2.33	32.2	32.72	45.94	18.4

volume), along with LECO determinations from the DSDP shore-based studies. There is a pattern of highs and lows with peak carbonate values occurring within the Hauterivian-Barremian, upper Maestrichtian-lower Paleocene, and upper Oligocene to Quaternary (Pliocene high) parts of the section. Carbonate is nearly absent throughout much of the Cretaceous interval. The possible causes of these patterns are discussed in the "Lithostratigraphy" and "Biostratigraphy" sections of this Site Report, and in more detail by Maldonado, de Graciansky and Chenet, and Sigal (all, this volume).

#### Total Organic Carbon

Approximately 60 organic carbon values were obtained aboard ship (Table 3). These measurements were made on the insoluble residue from carbonate bomb determinations of selected samples using the Hewlett-Packard 185B CHN analyzer and have been corrected for the carbonate content of each sample. These measurements supplement analyses made subsequently by the DSDP shore-based studies using a LECO 70-second carbon analyzer. All measurements are plotted in the Site Summary Chart 1 (see rear pocket, this volume). In Cretaceous sediments (lithologic Units 4 and 5), shipboard organic carbon values tend to be higher than the average of DSDP shore-based values or those of other investigators because many samples were selected onboard ship specifically for their presumed high organic carbon content (primarily by color and/or sapropelic appearance). A maximum value of 7.1 weight per cent organic carbon was determined for one of the uppermost black clay layers in Core 398D-56 (mid-Cenomanian). Organic carbon content is generally below 0.3 weight per cent throughout the Cenozoic and Upper Cretaceous. Values for Lower and Middle Cretaceous range from 0.1 to 3.0 weight per cent (with one value of 7.1 weight per cent, as discussed above), averaging about 0.5 weight per cent. Except for the mid-

Cenomanian organic carbon high, a general correlation exists between periods of high clastic terrigenous influx, high proportion of land-plant material in organic matter, and maxima in organic carbon percentages (e.g., the Hauterivian to lower Aptian and the upper Albian). This aspect of the "black shale" problem is further discussed in other parts of this volume (e.g., Habib; Arthur; de Graciansky and Chenet; all, this volume).

#### Origin and Thermal Maturity of Organic Matter in Early Cretaceous Sediment

Although many portions of the "black shales" at Site 398 contain what is commonly thought to be sufficient organic matter to generate hydrocarbons (i.e., 1.0 to 1.5 weight per cent), the general consensus is that the thermal maturation level of this organic matter is low. In addition, most of the organic matter has a low hydrogen index (i.e., low pyrolysis-fluorescence index) and, therefore, probably a very low potential for petroleum generation. A number of workers using different techniques have established the predominantly terrestrial plant and reworked (second cycle) nature of the organic matter in the Lower Cretaceous section of Site 398, with the exception of certain upper Albian-Cenomanian levels (e.g., Habib; Deroo et al.; Doerenkamp and Robert; Kendrick et al.; all, this volume). Doerenkamp and Robert (this volume) and Kendrick et al. (this volume), using vitrinite reflectance data, have demonstrated the relatively low thermal alteration index of most of the terrigenous plant and relatively minor amounts of amorphous marine organic matter (reflectance generally <0.5). These conclusions are supported by the organic geochemistry studies of Kerogen by Deroo et al. (this volume) and Johnson et al. (this volume). The lack of significant thermal alteration at first seems surprising when the depth of burial is considered (up to 1.7 km) and considering that much of the organic-rich sediment was deposited on a rapidly subsiding rifted margin (ini-

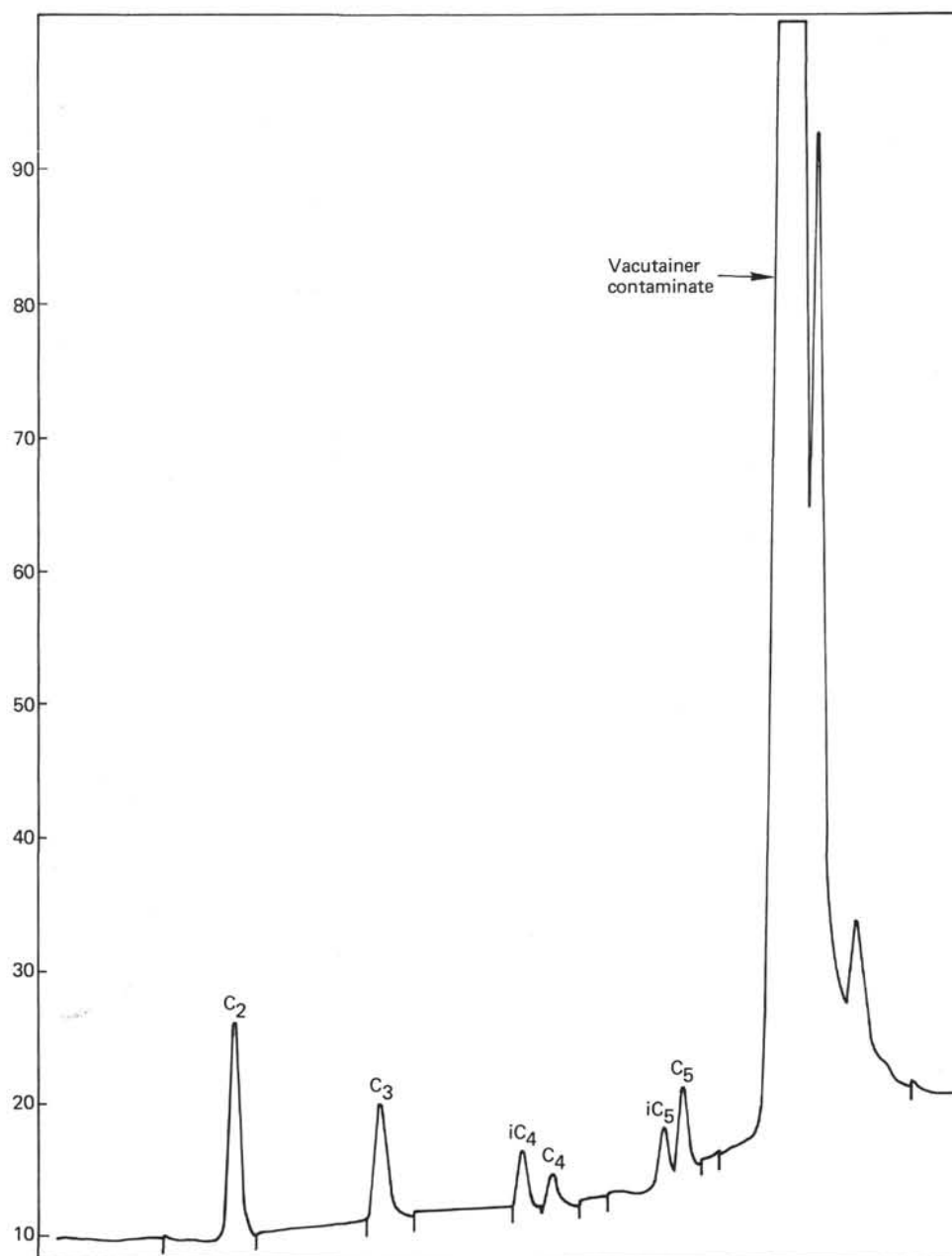


Figure 25. Chromatogram of sample from Section 398D-32-1, interstitial water chemistry analyses.

tiation of sea-floor spreading in Aptian time). However, preliminary downhole temperature measurements suggest an anomalously low thermal gradient, and Sibuet and Ryan (this volume) and de Charpal et al. (1978) have suggested a model of ductile stretching and opening of the northern North Atlantic which apparently requires no thermal bulging (e.g., Kinsman, 1975) or initial high heat flow. Thus, in light of these data, it is perhaps not so difficult to explain the low levels of thermal maturity.

Kendrick et al. (this volume), with supporting evidence from Deroo et al. (this volume), have also suggested that the petroleum-generating potential of most of the Lower Cretaceous organic carbon-rich interval is

very low. Their pyrolysis-fluorescence analysis (a measure of "effective carbon" or  $C_{eff}$ ) lead to ratios of  $C_{eff}/C_{org}$  of 0.02 or 0.03 on the average in the black shales. This is much lower than the value of  $C_{eff}/C_{org} = 0.27$  which is felt to be the minimum ratio necessary for a potential source rock.

#### Safety Monitoring

The potential safety hazard of gas or liquid hydrocarbon accumulations to the Deep Sea Drilling Project makes it necessary to take many precautions. A combination of several hydrocarbon detection instruments were used on Leg 47B to try to identify the presence of hydrocarbon gases and/or stains. These instruments are

TABLE 3  
Shipboard Results for Site 398  
Carbon/Carbonate Analyses

Hole-Core-Section	Sample Depth (m)	Organic Carbon (%)	CaCO <sub>3</sub> (%)
398-2-2	26.71	0.4	24
398-2-3	29.13	0.2	67
398-2-3	29.49	0.6	13
398-3-1	35.05	0.4	33
398-3-5	41.59	0.5	54
398-4-2	122.19	0.4	59
398A-1-1	173.14	0.2	64
398A-2-2	203.05	0.2	68
398D-2-1	271.96	0.0	47
398D-3-2	320.11	0.0	65
398D-4-4	371.31	0.0	77
398D-5-5	400.61	0.0	56
398D-6-4	418.19	0.0	74
398D-7-2	435.41	0.0	69
398D-7-3	435.84	0.0	37
398D-8-3	455.20	0.0	68
398D-9-2	472.94	0.0	58
398D-12-2	510.81	0.0	34
398D-13-4	532.21	0.0	47
398D-14-1	537.34	0.0	60
398D-15-1	546.72	0.1	40
398D-15-3	550.48	0.0	65
398D-20-5	600.19	0.1	8
398D-21-3	606.96	0.0	4
398D-21-3	607.03	0.0	24
398D-22-5	619.89	0.0	14
398D-23-2	624.09	0.0	26
398D-23-2	624.41	0.0	10
398D-24-3	636.24	0.0	21
398D-25-1	641.97	0.0	10
398D-26-4	656.11	0.1	28
398D-28-2	671.92	0.0	26
398D-29-3	683.08	0.0	38
398D-30-2	691.36	0.0	45
398D-31-3	701.89	0.1	23
398D-31-3	701.93	0.0	22
398D-32-3	711.99	0.0	48
398D-33-2	719.25	0.0	62
398D-34-2	729.19	0.0	3
398D-35-4	742.41	0.0	5
398D-36-3	749.93	0.1	33
398D-37-1	756.65	0.0	7
398D-38-2	767.34	0.0	7
398D-39-2	776.72	0.0	46
398D-40-4	789.41	0.0	61
398D-41-1	794.15	0.1	34
398D-43-1	813.28	0.0	52
398D-43-4	817.76	0.0	63
398D-44-2	824.47	0.0	68
398D-45-6	840.19	0.0	41
398D-46-2	843.54	0.1	30
398D-46-2	843.66	0.1	35
398D-46-2	843.71	0.1	25
398D-47-1	851.27	0.0	30
398D-48-2	861.89	0.0	22
398D-50-3	883.13	0.0	<2
398D-51-2	891.35	0.0	2
398D-52-2	900.84	0.1	5
398D-53-3	911.09	0.0	3
398D-54-2	919.49	0.0	3
398D-55-1	927.13	0.0	4
398D-56-2	947.26	7.1	<2
398D-56-2	947.67	0.1	<2
398D-56-3	949.65	0.2	<2
398D-57-2	956.74	0.5	31
398D-57-5	961.98	0.3	31

TABLE 3 – Continued

Hole-Core-Section	Sample Depth (m)	Organic Carbon (%)	CaCO <sub>3</sub> (%)
398D-58-1	965.17	0.0	32
398D-59-2	975.91	0.0	25
398D-60-1	984.58	0.4	31
398D-61-1	994.03	0.0	26
398D-62-4	1007.46	0.0	32
398D-63-3	1015.59	0.5	23
398D-65-2	1033.09	0.0	21
398D-66-1	1041.27	0.7	3
398D-67-2	1052.63	0.0	29
398D-68-4	1064.29	0.8	<3
398D-69-3	1073.12	0.8	3
398D-70-1	1079.58	0.0	10
398D-70-2	1080.66	0.0	13
398D-71-1	1089.08	0.0	23
398D-71-4	1093.19	0.5	5
398D-72-2	1109.04	0.0	14
398D-73-3	1119.87	0.2	20
398D-74-3	1129.62	0.0	19
398D-75-2	1137.47	0.8	6
398D-76-1	1145.86	0.7	<2
398D-77-2	1166.01	0.0	24
398D-77-2	1166.84	0.0	5
398D-78-2	1175.95	0.0	5
398D-79-1	1183.05	0.6	7
398D-80-2	1194.21	0.0	3
398D-81-3	1206.26	0.0	3
398D-82-3	1215.54	0.6	<2
398D-84-5	1237.70	0.5	<2
398D-85-2	1242.30	0.0	5
398D-86-2	1251.36	0.1	47
398D-87-1	1259.29	0.0	<2
398D-88-3	1272.38	0.0	6
398D-89-4	1283.42	0.8	<2
398D-90-2	1290.04	0.0	<2
398D-91-4	1302.52	0.0	<2
398D-92-3	1310.33	2.7	<2
398D-93-2	1317.98	0.0	3
398D-94-1	1325.90	0.0	9
398D-95-6	1335.07	1.2	<2
398D-96-1	1335.30	0.0	9
398D-97-5	1350.96	3.0	3
398D-98-1	1354.81	0.0	<2
398D-99-2	1365.65	1.8	<2
398D-100-2	1375.41	0.0	<2
398D-101-6	1390.77	1.9	<2
398D-102-1	1392.96	0.0	<2
398D-104-1	1412.17	0.0	29
398D-104-2	1413.01	0.2	28
398D-105-2	1423.06	0.0	84
398D-106-2	1432.45	0.0	31
398D-107-1	1440.70	0.4	29
398D-108-2	1451.59	0.0	24
398D-109-2	1460.65	0.3	21
398D-111-2	1479.15	0.0	<2
398D-111-3	1481.85	0.5	<2
398D-112-1	1487.99	0.0	<2
398D-113-2	1498.86	0.5	2
398D-114-4	1511.54	0.0	<2
398D-115-2	1517.84	0.0	<2
398D-116-1	1525.69	0.6	<2
398D-117-3	1538.52	0.0	<2
398D-118-2	1546.36	1.3	6
398D-119-2	1555.46	0.0	<2
398D-120-3	1567.15	2.7	5
398D-121-1	1572.67	0.0	7
398D-121-2	1574.31	2.2	16
398D-122-4	1586.76	0.0	28
398D-122-4	1586.78	0.0	33

TABLE 3 - Continued

Hole-Core-Section	Sample Depth (m)	Organic Carbon (%)	CaCO <sub>3</sub> (%)
398D-122-4	1587.33	0.0	25
398D-123-3	1595.35	1.2	52
398D-124-4	1605.81	2.0	35
398D-126-1	1621.15	1.3	60
398D-127-2	1631.43	0.0	19
398D-128-1	1639.18	2.6	11
398D-128-3	1642.66	0.0	39
398D-129-3	1652.19	0.0	6
398D-130-3	1661.37	2.6	10
398D-132-3	1680.91	1.6	55
398D-133-2	1688.71	0.0	81
398D-134-1	1696.78	2.3	43
398D-135-3	1709.70	0.0	74
398D-136-2	1716.53	0.0	64
398D-137-3	1728.63	0.4	33
398D-138-2	1736.67	0.0	45

the IMCO Fluoroscope, Turner Fluorometer, Exploration Logging Gas Chromatograph, and the Hewlett-Packard Gas Chromatograph.

### Fluorescence Analysis

Approximately 50 samples were observed for possible hydrocarbon stains. The results were all negative. The cores were first cut into sections and halved for sampling. At this point, a visual observation was made for any obvious sign of hydrocarbon stain or solid. The halved section was then subjected to inspection under fluorescent light. If the results of any visual inspection were in question, a pyrolysis-fluorescence analysis was made to confirm or deny the possible presence of a hydrocarbon stain.

### C<sub>1</sub> to C<sub>5</sub> Hydrocarbon Analysis

C<sub>1</sub> to C<sub>5</sub> analyses were run on 84 samples with negative results using routine procedures.

C<sub>2</sub> to C<sub>5</sub> hydrocarbons were detected in trace quantities in samples analyzed in the shale interval spanning 1164 to 1306 meters in Hole 398D. The methane content of the samples was below the detection limit of the Exploration Logging Gas Chromatograph.

An attempt was made to quantify the small amounts of C<sub>2</sub> to C<sub>5</sub>, without success. In fact, the method of sampling seems to be the determining factor in the case of analyzing trace quantity gases. There is no question that C<sub>1</sub> to C<sub>5</sub> components were present in the above-mentioned black shale interval, but these data should not be used for anything other than a visual guide to indicate the presence of C<sub>1</sub> to C<sub>5</sub> hydrocarbons. The above-described combination of analyses must be relied upon as indicator of what lies ahead of the bit.

### Sampling Technique

Sampling is perhaps the single most important element of instrumental analysis. This is especially true with gas sampling. The gas sampling technique used on-board ship on Leg 47B needs to be improved. The present technique calls for a sample to be taken in a void

within the core or between the core and the core liner. It has been observed that as the liner is removed from the core barrel, water is constantly being voided from the liner. The water escaping the liner is being replaced by surface air. The net effect is sample mixing which dilutes the gas content of that particular core gas sample. This effect is very important when dealing with low-level gas content samples, as on Leg 47B. Another factor which affects the ability to analyze C<sub>1</sub> to C<sub>5</sub> hydrocarbons is their solubility in water. It should be noted that as the core is being retrieved, the gases present are further dissolved in water (depending on their solubility). Due to the difficulty in analyzing methane, perhaps more emphasis should be taken to consider the heavier components, i.e., C<sub>3</sub>, C<sub>4</sub>, and C<sub>5</sub>. The ratios of the heavy components may prove to be more meaningful, especially when dealing with low-level gas content areas. This is not to say that the analysis of methane should be discontinued.

## BIOSTRATIGRAPHY

### Cenozoic

#### Cenozoic Foraminifers

The principal biostratigraphic subdivisions (Figure 26) for the Cenozoic are outlined below. More detailed discussion of assemblages, degree of preservation, and paleoenvironmental interpretations appear in Iaccarino and Salvatori (this volume) and in Iaccarino and Premoli-Silva (this volume).

#### Cretaceous/Paleocene Boundary

The Cretaceous/Paleocene boundary occurs on the top of Section 398D-41-2 and is well documented by a rich small-sized globigerinid and heterohelcid assemblage assignable to the lowermost Paleocene (*Globigerina eugubina* Zone).

#### Paleocene

Upwards to Section 398D-35-5, all the Paleocene zones have been identified, although the paleontological record at some intervals (Cores 398D-38, 398D-36) is interrupted due to dissolution effects.

Extending upwards from the Cretaceous/Paleocene boundary, one encounters first the *Globorotalia pseudobulloides* Zone in Core 398D-41 (sometimes mixed with or alternating with an assemblage characteristic of the *Globigerina eugubina* Zone); followed in Sample 398D-41-1, 123-125 cm by the *Globorotalia trinidadensis* Zone; in Sample 398D-40-2, 43-45 cm by the *Globorotalia uncinata* Zone; and in Sample 398D-39-4, 115-117 cm by the *Globorotalia angulata* Zone (which can be identified as high as Sample 398D-39-4, 65-71 cm).

The interval from Samples 398D-39-3, 131-133 cm to 398D-37, CC (in which *Globorotalia pseudomenardii* appears) is referred to the *Globorotalia pusilla pusilla* Zone. However, most of Core 398D-38 is barren of foraminifers. The *Globorotalia pseudomenardii* Zone can be documented only from Samples 398D-37, CC to 398D-37-1, 117-119 cm. The assemblage identified in

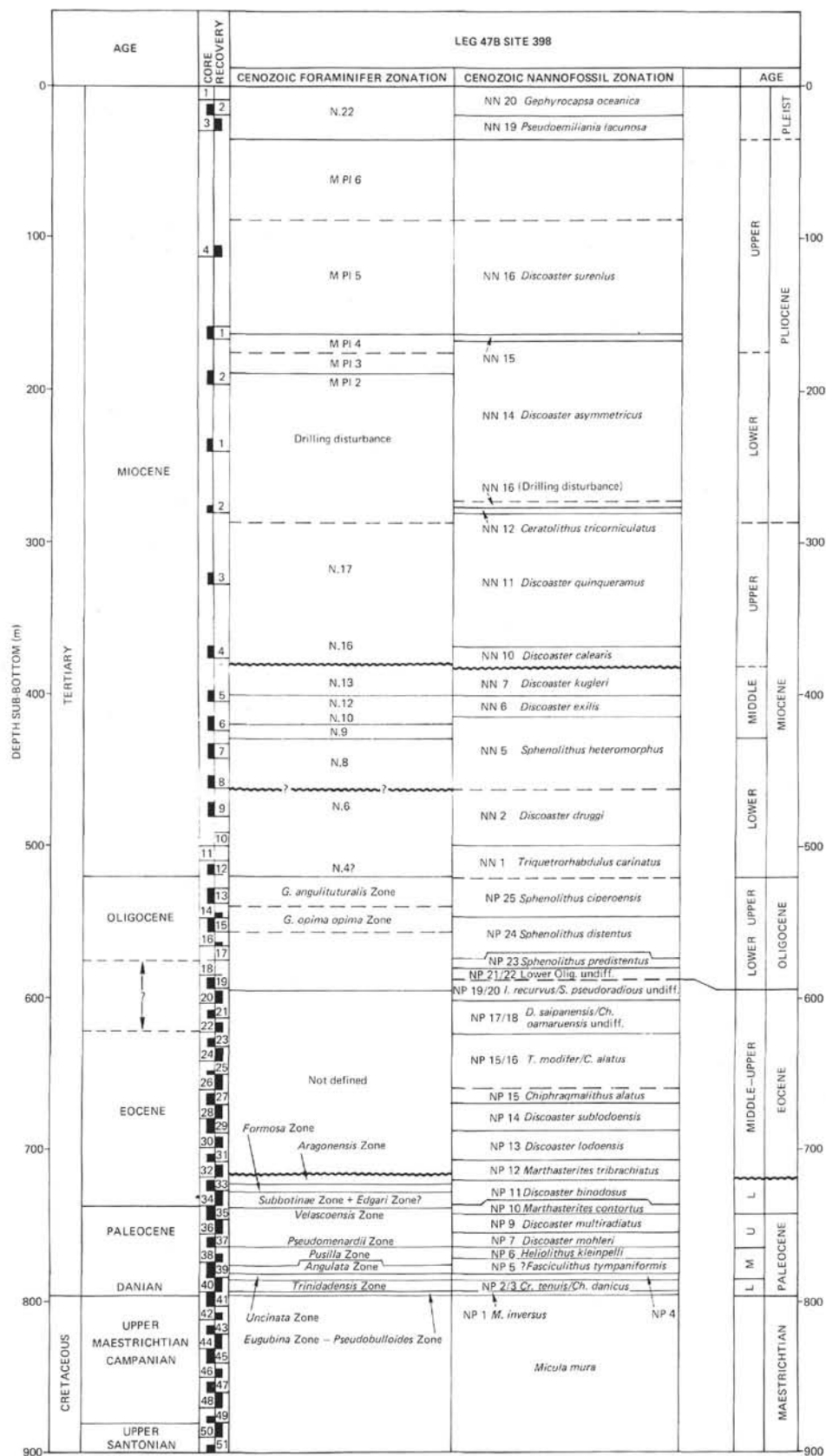


Figure 26. Cenozoic biostratigraphic summary, Site 398.

Core 398D-35 can be attributed to the topmost part of the *Globorotalia velascoensis* Zone because of the co-occurrence of the zonal marker, along with *G. subbotinae*, *G. marginodentata*, and *G. edgari*. The lower part of this zone has not been recorded because Core 398D-36 is mostly barren of planktonic foraminifers.

### Eocene

From Section 398D-35-5 to Core 398D-20, the foraminiferal assemblage is indicative of the Eocene. Reworking is sometimes considerable; often foraminifers from older formations are associated with the Eocene assemblages. In regards to the lower Eocene, the *Globorotalia edgari* Zone seems to be lacking or represented by a very short interval. In fact, in Sample 398D-35-1, 81-83 cm, *G. lensiformis* is already present. This taxon is considered to appear in the younger portion of the *Globorotalia subbotinae* Zone. There is either a small hiatus spanning the *G. edgari* Zone and the lower part of the *G. subbotinae* Zone corresponding to the lowermost Eocene, or a very slow sedimentation rate for this interval is indicated. The *Globorotalia subbotinae* Zone (occurring from Samples 398D-35-2, 81-91 cm to 398D-34-2, 26-28 cm) is followed in continuity by the *Globorotalia formosa formosa* Zone (Samples 398D-34-1, 143-145 cm to 398D-33-3, 81-83 cm) and by the lower part of the *Globorotalia aragonensis* Zone, representing the middle of the lower Eocene.

An important change in the planktonic foraminiferal assemblage occurs between Cores 398D-33 and 398D-32. There is no evidence of the upper part of *G. aragonensis* Zone, as well as the overlying *pentacamerata* zone.

The first occurrence in the topmost part of Core 398D-32 of the *Globigerinathea* zonal marker of the second zone of the middle Eocene suggests a gap in sedimentation spanning the upper part of the lower Eocene. Starting from Core 398D-32 up to Core 398D-20, planktonic foraminiferal faunas are primarily composed of *Globigerina senni*, *G. bullbrooki*, *G. spinuloinflata*, and *G. spinulosa* in different abundances from sample to sample. Their preservation varies from very highly dissolved to moderately preserved. In this long interval, besides *Globigerinathea*, few and scattered occurrences of significant taxa are recognizable: *cryptomphala* (Sample 398D-26-1, 64-66 cm), *lehneri* and *Hantkenina* spp. (Sample 398D-24-2, 93-95 cm), *cerroazulensis* s.l. (Sample 398D-23-1, 23-25 cm), and *Globigerinita* spp. (Sample 398D-22-2, 120-122 cm). Most of the above-mentioned assemblages are displaced and a zonal subdivision cannot be applied. The most common planktonic foraminiferal assemblages recovered in this interval are middle Eocene; however, some taxa (*Globigerinita*, *cryptomphala*, and *cerroazulensis* s.l.) have a longer vertical range and are generally frequent in the upper Eocene. Moreover, not all the faunas characteristic of the middle Eocene have been recorded and representative upper Eocene faunas are not documented. On the other hand, one cannot rule out that the sedimentary sequence from Cores 398D-32 to 398D-20

(about 123 m thick) could represent the middle and upper Eocene.

### Oligocene

The Eocene/Oligocene boundary cannot be recognized and poor preservation makes a biostratigraphic subdivision of the Oligocene difficult. In Cores 398D-21 and 398D-20, middle Eocene foraminifers are still present and the first nannoplankton identifiable with the Oligocene appear in Core 398D-19. There is some indication, however, of a probable early Oligocene hiatus, and the first definite sign of the middle and upper Oligocene appears with the *Globorotalia opima opima* and *Globigerina angulicostata* zones in Cores 398D-15 to 398D-13.

### Miocene

From Cores 398D-12 up to 398D-3, the sedimentary sequence is Miocene. The discontinuous coring and the generally poor preservation of the faunas do not allow a complete zonal subdivision. Furthermore, the high latitudinal location of Site 398 constituted an obstacle to applying the standard zonation of Blow (1969), established on the evolutionary trend of tropical taxa. From Cores 398D-12 to 398D-10, the lowermost Miocene could be represented, but the paleontological record is too poor. The occurrence of *Globoquadrina dehiscens dehiscens* (occurring from the uppermost N.4 according to Blow) in Core 398D-12 does not provide a reliable datum for a precise assignment. The foraminiferal assemblage of Core 398D-9 is attributable to N.6 on the basis of the occurrences of *Globigerinoides quadrilobatus trilobus*, *G. quadrilobatus sacculifer*, and *Globorotalia continuosa* (only from Zone N.6 according to Blow). Core 398D-12 to Core 398D-10 then can be placed between N.4 and N.6.

The occurrence of *Globigerinita dissimilis* s.l. and *Globigerinita unicava* (disappearing in N.6 according to Blow) up to Section 398D-8-4 suggests that the lower part of this interval is still referable to N.6; however, it is not excluded that the above-mentioned taxa may be reworked. From Sample 398D-8-3, 104-106 cm (in which *Praeorbulina* gr. *Globigerinoides sicanus* and transitional forms of *Globorotalia archeomenardii* to *G. praemenardii* first occur) up to Core 398D-7 is undoubtedly attributable to N.8.

A gap including N.7 could be discerned within Core 398D-8 or between Cores 398D-8 and 398D-9. N.9 is present from Sample 398D-6, CC, in which *Orbulina suturalis* first occurs. The N.9/N.10 boundary is tentatively placed in Section 398D-6-4 on the basis of the last occurrence of *Praeorbulina glomerata circularis* and the first appearance of *Globorotalia praemenardii*. The absence of the evolutionary lineage *G. fohsi* s.l., on which N.10/N.11 and N.11/N.12 are defined, does not allow the recognition of the zones of this time interval. On the other hand, the *Globigerinoides quadrilo* group that is so useful for the biostratigraphic resolution in the Miocene is very rare. In Sample 398D-5-2, 124-126 cm, the N.12/N.13 boundary is placed at the first appearance

of *Sphaeroidinellopsis subdehiscens subdehiscens*. The lower part of N.16 is recorded from Core 398D-4 (occurrence of *Globorotalia acostaensis*, *G. continuosa*, transitional forms of *G. continuosa* to *G. acostaensis* and *G. cultrata* s.l.). Then a hiatus including N.14 and N.15 occurs between the top of Core 398D-5 and Sample 398D-4, CC. The lower part of N.17 seems to be present at Core 398D-3, although the data for such a biostratigraphic assumption are not very consistent. More detailed information is presented by Iaccarino and Salvatori (this volume).

### Pliocene

Five of the six Pliocene foraminiferal zones used in the Mediterranean region (Cita, 1973) are represented. Zones M Pl 2 and M Pl 3 *Globorotalia margaritae* occurs in Cores 398D-2, 398B-1 and 398A-2; *Globorotalia puncticulata* of Zone M Pl 4 appears in Cores 398D-2 and 398B-1. Although the latter two cores are from a deeper level in the hole than Core 398D-2, it seems likely that these cores recovered the younger material with *G. puncticulata* at higher levels, since Core 398B-1 was cut from the sea floor to 239 meters and Core 398D-2 was cut from 9.5 to 280.5 meters.

The latter apparently contained sediment with *Globorotalia inflata*, characteristic of the M Pl 6 Zone of the upper Pliocene, and stacked this sediment above that of the M Pl 5 and M Pl 3 zones from deeper in the section.

### Pleistocene

The Pleistocene is represented from Core 398-3 up to Sample 398-1, CC by a rich and well-preserved planktonic assemblage including *Globorotalia truncatulinoides*, *Globigerina calida calida*, *Globorotalia inflata*, *Neoglobobulimina pachyderma*, and *Neoglobobulimina pachyderma borealis* assignable to Zone N.22.

### Cenozoic Calcareous Nannofossils

Calcareous nannofossils were found throughout the Cenozoic sediments recovered at Site 398. A nearly complete Paleogene sequence allows for a fairly detailed biostratigraphic analysis of this interval (Figure 26). Discontinuous coring through the Neogene sequence blurs the biostratigraphic resolution. The calcareous nannofossil zonation used in this report is described in Blechschmidt (this volume). In some cases, due to poor preservation and sedimentary disturbances, it is impossible to differentiate some of the zones. This is particularly true in the Paleogene sediments, where mass gravity processes play a major role in sedimentation at this site.

### Paleocene

The lowermost Paleocene flora encountered in Sample 398D-41-2, 39 cm is representative of the *Markalius inversus* Zone. Much reworking of Cretaceous species is found in this core and also in Core 398D-40, which contains a flora characteristic of the *Cruciplacolithus tenuis* Zone. The *Chiasmolithus danicus* Zone was not differentiated from the *C. tenuis*

Zone in these cores. A few specimens of *Ellipsolithus macellus* in Section 398D-39-4 place this section in the *E. macellus* Zone. The remainder of Core 398D-39 and Sections 398D-38-4 and 398D-38-5 are assigned to the *Fasciculithus tympaniformis* Zone. *F. tympaniformis*, *C. danicus*, and *C. tenuis* are major components of the nannoflora found in these cores. *Heliolithus kleinpellii* is sparse in Sections 398D-38-3 through 398D-38-1, placing these sections in the *H. kleinpellii* Zone. The discoasters are found in Core 398D-37, with the presence of *Discoaster mohleri* and *Discoaster nobilis* placing this core in the *D. mohleri* Zone. *Discoaster multiradiatus* is first encountered in Core 398D-36, which is assigned to the *D. multiradiatus* Zone. *Fasciculithus schaubi* and *Fasciculithus involutus* are also common components of this nannoflora assemblage. The sedimentation rate was quite low in the mid-Paleocene at this site.

### Eocene

The base of the Eocene is encountered in Core 398D-37, which is assigned to the *Marthasterites contortus* Zone. *M. contortus* is rare in assemblages found in this core which are dominated by *D. multiradiatus*, *Chiasmolithus consuetus*, and *Fasciculithus*. Cores 398D-35 through 398D-33 are assigned to the *Discoaster binodosus* Zone. *D. binodosus*, *Discoasteroides diastypus*, and *Cruciplacolithus staurion* are found in them. Some reworking of Paleocene taxa is noted in Cores 398D-35 and 398D-34. *Marthasterites tribrachiatus* is common in Section 398D-33-1 through Core 398D-32, placing them in the *M. tribrachiatus* Zone. Also present are *Sphenolithus radians*, *Chiasmolithus grandis*, and *Discoaster lodoensis*. The *Discoaster lodoensis* and *Discoaster sublodoensis* zones could not be differentiated in Cores 398D-31 through 398D-28. Possibly Core 398D-29 represents the base of the *Discoaster sublodoensis* Zone, based on the lowest occurrence of *Discoaster nonaradiatus*. The base of *Chiphragmalithus alatus* was encountered in Core 398D-27, placing this core in the *C. alatus* Zone. *Discoaster sublodoensis*, *Chiasmolithus solitus*, *Discoaster nonaradiatus*, and *Discoaster barbadiensis* are present in this core. Cores 398D-26 through 398D-23 contain a flora characteristic of the *Discoaster nodifer* Zone, including *Reticulofenestra umbilica*, *Discoaster tani*, *Discoaster nodifer*, and *C. solitus*. Preservation of calcareous nannofossils in the upper Eocene is poor making differentiation of zones difficult. The *Discoaster saipanensis* and *Chiasmolithus oamaruensis* zones could not be differentiated due to the very rare occurrence of *C. oamaruensis* in this interval. Cores 398D-22 through 398D-21 are assigned to the *D. saipanensis*/*C. oamaruensis* zones (undifferentiated). *D. saipanensis*, *Discoaster barbadiensis*, and *R. umbilica* are fairly common in these cores. The uppermost Eocene sediments show very poor preservation of calcareous nannofossils. Cores 398D-20 and Sections 398D-19-2 and 398D-19-3 contain *Isthmolithus recurvus*, *D. barbadiensis*, *D. saipanensis*, and *C. grandis*, characteristic of the *I. recurvus*/*Sphenolithus pseudoradians* zones. *S. pseudoradians* is very rare at

this site. The Eocene/Oligocene boundary is defined by the last occurrence of *D. barbadiensis*.

### Oligocene

The lower Oligocene is represented only in Section 398D-19-1. *R. umbilica* and *Cyclococcolithus formosa* are major components of the nannofloral assemblage in this core. Cores 398D-18 through 398D-16 contain *Sphenolithus predistentus*, *Sphenolithus distentus*, and *Discoaster tani*; these are representative of the *S. predistentus* Zone. Sphenoliths in all samples examined are sparse, but present in sufficient numbers to allow recognition of the mid- and upper Oligocene zones. *Sphenolithus ciperoensis* is first encountered in Core 398D-15 which is assigned to the *S. distentus* Zone. The last *S. distentus* occurs at the top of Core 398D-13. Cores 398D-13 and 398D-14 are assigned to the *S. ciperoensis* Zone. Overcalcified *Discoaster deflandrei* is common in these cores. The Oligocene/Miocene boundary is defined by the highest occurrence of *Sphenolithus ciperoensis*.

### Miocene

Lower Miocene sediments were recovered in Cores 398D-12 through 398D-7. Core 398D-12 contains a nannoflora characteristic of the *Triquetrorhabdulus carinatus* Zone. *Discoaster deflandrei* and *Cyclicargolithus floridanus* dominate the nannoflora in this core. *Discoaster druggi* is present in Cores 398D-9 and 398D-10, placing these cores in the *D. druggi* Zone. A very rare occurrence of *Sphenolithus belemnus* in Sample 398D-10, CC may indicate downslope displacement of sediments in this core. The *S. belemnus* Zone was not found at this site. It is not clear whether this zone was lost in discontinuous coring or is not present. Cores 398D-8 through Section 398D-6-2 are assigned to the *Sphenolithus heteromorphus* Zone. *Helicopontosphaera ampliapertura* was not found in any of the samples examined from this interval, making recognition of the *H. ampliapertura* Zone impossible. The lower part of the *S. heteromorphus* Zone may actually represent the *H. ampliapertura* Zone. *S. heteromorphus*, *D. deflandrei*, and *Discoaster exilis* are common in these cores. No *S. heteromorphus* was found in Section 398D-6-1, which is tentatively placed in the *D. exilis* Zone. *D. kugleri* is present in Core 398D-5, placing this core in the *D. kugleri* Zone. Core 398D-4 is assigned to the *Discoaster calcaris* Zone. *D. calcaris* is not found in sediments examined from this core, but *Discoaster neorectus* (which is correlative with *C. calcaris*) allows this age assignment. Other common taxa present are *Discoaster challengerii*, *Coccolithus miopelagicus*, and *Discoaster variabilis*. *Discoaster quinqueringus* was found in small numbers in Core 398D-3 and one specimen was found in Section 398D-4-1. This interval is assigned to the *D. quinqueringus* Zone.

### Pliocene

Biostratigraphic subdivision of the Pliocene is somewhat difficult at this site due to the sparsity of Ceratoliths, which are generally used in Pliocene zonations.

Section 398D-2-1 is assigned to the *Discoaster surculus* Zone and is apparently displaced due to coring disturbance. The remainder of Core 398D-2 is placed in the *Ceratolithus tricorniculatus* Zone. *C. tricorniculatus* is found very rarely in this core. *Discoaster asymmetricus*, *D. challengerii*, *Reticulofenestra pseudoumbilica*, and *D. variabilis* are found in Cores 398B-1 and 398A-2. These cores are assigned to the *D. asymmetricus* Zone. The base of Core 398A-1 is tentatively assigned to the *R. pseudoumbilica*, based on the presence of *R. pseudoumbilica* and the lack of *C. tricorniculatus*. The upper portion of this core and Core 398A-4 is placed in the *Discoaster surculus* Zone. Common elements in the nannoflora present in this core are *Discoaster surculus*, *Cyclococcolithus leptopora*, and *Pseudoemiliana lacunosa*. The Pliocene/Pleistocene boundary is not particularly well defined at this site. Some reworking of older taxa (Paleogene and Cretaceous) is seen in samples from Cores 398-1 through 398-4. This reworking tends to obscure the boundary. Discoasters are very sparse in Core 398-4, while *Gephyrocapsa caribbeanica* extends into Pliocene sediments at this site. The last occurrence of discoasters is used to define the boundary in this report.

### Pleistocene

Sediments of Pleistocene age were recovered in Cores 398-1 through 398-3. Core 398-3 contains *Pseudoemiliana lacunosa*, *G. caribbeanica*, *C. leptopora*, and *Gephyrocapsa oceanica*, which place this core in the lower Pleistocene *P. lacunosa* Zone. The last occurrence of *P. lacunosa* is found at the top of Core 398-3. *B. oceanica*, *C. leptopora*, *G. caribbeanica*, and Discolithinids are common in the two upper cores of Hole 398. These cores are assigned to the *G. oceanica* Zone. No *Emiliana huxleyi* was found in any of the samples studied.

### Preservation and Paleoenvironment

In general, pelagic sedimentation has progressed without interruption at Site 398 throughout the Cenozoic, with a dominantly pelagic sequence in the Neogene and an increase in terrigenous input during the Paleogene. Calcareous nannofossils were found in nearly all samples examined, but they show marked variations in preservation.

Calcareous nannofossils in the lower Paleocene sediments recovered show poor preservation with only the most resistant taxa being present. The sedimentation rate in this interval is quite low. Nannofossil assemblages indicate a cooling trend across the Cretaceous/Tertiary boundary along with increased dissolution. Apparently, there was an upward migration of the CCD in the mid-Paleocene as evidenced by the lack of calcareous material at the base of Core 398D-38 in an otherwise calcareous sequence. There is a general improvement in preservation of nannofossils in the upper Paleocene with greater diversity and increased numbers of solution-susceptible species. This improvement in preservation continues into the Eocene. Lower and mid-Eocene nannofossil assemblages are fairly diverse and

well preserved. The increase in Discoaster abundance and general diversity provides evidence of a warming trend in the mid-Eocene. During the late Eocene there was apparently an upward migration of the CCD as evidenced by poorer preservation of nannofossils and the lack of solution-susceptible taxa. The presence of *Isthmolithus recurvus*, which is generally found in temperate regions, is indicative of a cooling trend in the late Eocene. Tropical and subtropical forms are rare or absent in this interval. Much siliceous debris is present in all upper Eocene and lower Oligocene samples examined. Preservation of nannofossils is also poor in the lower and mid-Oligocene sediments. The cooling trend noted in the late Eocene appears to have persisted into the Oligocene. The sparsity of Sphenoliths in this Oligocene sequence may be due to poor preservation, but is more probably due to paleoenvironmental restrictions. Sphenoliths are generally less abundant in cooler waters and are moderately resistant to solution. Other floral elements in the Oligocene generally show poor preservation with common solution-resistant placoliths, overcalcified discoasters, and a general lack of solution-susceptible taxa. A slight improvement in preservation is noted in the upper Oligocene, a pattern which persists into the Miocene. Another slight improvement in preservation is noted in the mid-Miocene. Discoaster diversity and abundance is generally lower at this site than is usual in tropical and subtropical Miocene sections. Specifically, high-latitude forms are also absent or rare, indicating that this area has been influenced by temperate or transitional water masses at least since the late Oligocene.

Nannofossils are generally well preserved throughout the remainder of the Cenozoic with a gradual improvement in preservation through the Pliocene into the Pleistocene. Many solution-susceptible taxa (such as *Scyphosphaeras*, *Braarudosphaeras*, and other holococcoliths) are present in upper Pliocene and Pleistocene sediments at this site. The nannofossil assemblage in the Pleistocene sequence indicates fairly warm conditions in this area at that time.

#### Comments on Allochthonous Sedimentation

At several levels in the sequence, pebble conglomerates were encountered. Smear slides taken from pebbles within these conglomerates were examined for calcareous nannofossils to determine the age range of these displaced materials.

In Core 398D-33, which was placed in the lower Eocene *Discoaster binodosus* Zone, a pebble conglomerate containing Eocene and Cretaceous pebbles was found. The oldest pebble found in this conglomerate belongs to the lower Cretaceous *Marthasterites furcatus* Zone (Santonian-Coniacian). Other pebbles examined were undifferentiated as having been deposited during the Late Cretaceous and early Eocene. The range of ages of pebbles present in this conglomerate is approximately 30 m.y.

Another pebble conglomerate which is assigned to the lower Aptian *Chiastozygus litterarius* Zone was found in Core 398D-117. Pebbles in this conglomerate

are, for the most part, early Aptian to Barremian. Although deposition was apparently pelagic, preservation in most samples is poor. The oldest pebble containing an adequate flora for dating is Berriasian-lower Valanginian (*Cretarhabdulus crenulatus* Zone). The approximate range of ages in these pebbles is 15 m.y.

In Core 398D-125, a fairly thick Barremian-upper Hauterivian pebble conglomerate was encountered. Most of the 15 pebble samples are of Barremian-upper Hauterivian, but the oldest pebble dated is Valanginian. *Micrantholithus hochschulzi*, *Micrantholithus obtusus*, and nannoconids are fairly common in these samples. The presence of solution-susceptible *Micrantholithus* could represent a somewhat shallower depositional environment, but preservation is frequently poor in the pebbles examined, possibly due to other diagenetic factors. Most of these pebbles are apparently representative of pelagic sedimentation. Their approximate age range is about 10 m.y.

#### Cenozoic Palynology

Very few palynomorphs were recovered from the entire Cenozoic sequences at Site 398. These consisted of few bisaccate grains (comparable to pine pollen) and fern spores.

#### Mesozoic

##### Mesozoic Foraminifers

Stratigraphic assignments will be detailed in the chapter dealing with chronostratigraphy (Sigal, this volume); only the main results will be given here, concerning ages and boundaries within the Lower and Upper Cretaceous.

#### Early Cretaceous

From Core 398D-130 upward, residual arenaceous associations have been distinguished within the benthic assemblages; they typically belong to the hemipelagic facies below the CCD, while the remaining species, i.e., the calcareous benthic species, typically occur in the redeposited materials.

**Oldest levels and the Hauterivian/Barremian boundary** (from bottom to Sample 398D-133-5, 64-66 cm): These levels have been identified as upper Hauterivian according to Aptychus and some foraminifers, and the lack of planktonics. The boundary has been placed, for convenience, where the latter forms first occur (*Hedbergella tuschepsensis*, *H. sigali*), although it is known that they actually appear during the uppermost Hauterivian. Slope inhabitants and rare neritic species are present.

**Barremian** (from Sample 398D-133-5, 64-66 cm to Core 398D-128, inclusive): According to the foraminiferal association, in the absence of markers, a secondary boundary between lower and upper Barremian sediments has been placed (where *H. aptica* first occurs). Transported benthos comprises slope inhabitants as well as neritic species. The Barremian/Aptian boundary is not satisfactorily assigned between Cores 398D-128 and 398D-127, because one of the generally accepted mark-

ers (*H. similis*) is already found there with Barremian Ammonites; conversely, another species (*Spirillina neocomiana*) seems to continue through the boundary.

**Aptian** (from Core 398D-127 to Core 398D-104, inclusive): An Aptian age and a Bedoulian/Gargasian boundary around Cores 119 and 118 of Hole 398D are established on general associations, mainly on planktonics. Nevertheless, some guide forms are lacking, for instance, *Schackoina cabri* for MCi 19. The lower part of the Bedoulian is not well characterized, and a rather anomalous succession observed here suggests that a short stratigraphic break could exist at the base of this stage. Planktonic association are richer in the upper part of Gargasian; consequently, zonal stratigraphy can be more exactly established: *Trochoidea* zone (MCi 22) from Sample 109-2, 118-120 cm upward. The lower part of this zone is still present in Core 398D-104, according to the coexistence of *Globigerinelloides barri* and *Planomalina cheniourensis*.

Core 398D-104 belongs to the youngest Aptian. The next marker occurs in Core 398D-99 (Ammonites) and gives an early (not the earliest) Albian age. The thickness of deposits between these cores does not seem to correspond to the time increment between these two chronologically well-localized levels, particularly if we take into account the high sedimentation rate at that time. This suggests that a stratigraphic gap occurs there.

Slope as well as neritic forms again occur amongst the transported benthos, while residual arenaceous associations play an increasingly important part, particularly from Core 398D-120 upward. Reworked specimens of Neocomian or Barremian species are frequently observed, especially in the turbiditic or slumped intervals.

The boundary between Aptian and Albian deposits occurs as aforesaid, between Cores 398D-104 (exclusive) and 398D-99 (exclusive). For convenience and because it marks a sharp sedimentological boundary, it has been placed between Cores 398D-104 and 398D-103.

**Albian** (from approximately Cores 398D-103 to 398D-58, inclusive): As mentioned, the base of the stage cannot be precisely located and a gap may truncate it. The first positive data come from Ammonites of Core 398D-99 with an early (not the earliest) Albian age (*Mamillatun* Zone). Many of the Albian cores mainly yield arenaceous residual associations, which are not useable for chronologic zonation.

Consequently, an exact boundary between lower and middle Albian cannot be traced; it occurs somewhere in Cores 398D-93 to 398D-90 according to the Ammonites. During the middle Albian (close to lower limit), the presence of some species (*H. rischi*, *Ticinella primula*) could localize the MCi 24/MCi 25 boundary.

Calcareous foraminifers, mainly the planktonics, become more abundant and diverse from around Core 398D-71 upward; as a consequence, chronostratigraphic limits and zones are more easily localized: middle/upper Albian boundary (or MCi 25/26, i.e., first occurrence of *Biticinella breggiensis*) at Sample 398D-69-2, 89-91 cm; middle part of upper Albian (first *Rotalipora ticinensis*) at Sample 398D-65-1, 135-137 cm (approx-

imately); MCi 26/27 (or last occurrence of *B. breggiensis*) at Sample 398D-60-3, 13-15 cm; upper Albian s. str./Vraconian boundary (first occurrence of *Rotalipora balernaensis* and *Planomalina bustorfi*) at Sample 398D-62-2, 148-150 cm (approximately); and middle part of Vraconian (last occurrence of *R. ticinensis*) at Sample 398D-59-3, 103-105 cm (approximately).

The base of Core 398D-57 corresponds to the first Cenomanian level (first occurrence of *Thalmaninella brotzeni*, *Rotalipora globotruncanoides*, wide specific diversification of *Schackoina*).

### Late Cretaceous

**Cenomanian** (from Core 398D-57, inclusive, to Sample 398D-56-2, 19 cm): The rapid succession of the first occurrence of lower Cenomanian association (Samples 398D-97, CC and 398D-57-5, 60-62 cm) was followed somewhat higher, still in the lower Cenomanian, by the first occurrence of *R. montsalvensis* (Sample 398D-56-2, 105-107 cm). Lastly, the first occurrence of *R. cushmani* group (Sample 398D-56-3, 76-77 cm) is abnormal and suggests that either continuous but condensed sedimentation occurred, or that sedimentation was interrupted. In that sense, it must be emphasized that from Sample 398D-56-5, 118-120 cm upward, the yielded associations are considerably poorer (especially for the planktonics) and specifically less diversified than previously (with the exception of the two short middle Cenomanian detrital intercalations at Samples 398D-56-3, 76-77 cm and 398D-56-3, 45-67 cm); even they are sometimes barren.

**Middle Cenomanian to Santonian possible gap:** Above the sharp boundary observed in Sample 398D-56-2, 19 cm, continuing to Sample 398D-50-6, 15-17 cm where planktonics again occur, only arenaceous, probably residual, assemblages are encountered, with the exception of some scattered Cenomanian calcareous forms. These arenaceous assemblages are rare and specifically homogeneous since their first occurrence in Section 398D-56-2; this suggests that from this section upward, deposits have the same age, which could be early Senonian according to some agglutinated species. As a consequence, a wide gap must be present between Cenomanian (i.e., middle Cenomanian of Section 398D-56-3) and early Senonian; and the scattered Cenomanian species would be reworked.

**Late Senonian** (from Samples 398D-50-6, 15-17 cm to 398D-41-6, 38-40 cm): The coexistence of *Globotruncana stuartiformis* (Sample 398D-50-6, 15-17 cm) and *G. concavata* (Sample 398D-50-2, 16-18 cm) demonstrates that the renewed presence of calcareous planktonic and mostly benthic assemblages in Sample 398D-50-6, 15-17 cm took place approximately at the Santonian/Campanian boundary.

The assemblages are generally abundant and still display solution marks. They are of Campanian, then of Maestrichtian age, and the boundary lies approximately in Core 398D-46. *Mayaroensis* Zone has been identified, with its guide-form, Sections 398D-43-3 and 398D-43-1.

**Latest Senonian levels** (from Samples 398D-43-1, 31-33 cm upward to 398D-41-6, 38-40 cm): Very small *Globigerinids* occur together with Maestrichtian species,

and *Chilogumbelina* first occurs in Sample 398D-41-5, 52-54 cm. This indicates a Maestrichtian/Danian boundary between Sections 398D-41-5 and 398D-41-6.

Maestrichtian specimens are still observed, sometimes richly, as high as Sample 398D-41-2, 33-35 cm. They precede a second Danian level (beginning with Sample 398D-41-1, 132-134 cm) yielding "larger" small *Globigerinids* of the classical *Eugubina* Zone.

### Hiatuses

In summary, hiatuses occur several times: possibly at the Barremian/Aptian boundary, very probably in the topmost Aptian or the lowermost Albian, and certainly above the middle Cenomanian (and probably extending until somewhere into the lower Senonian).

### Mesozoic Calcareous Nannofossils

Mesozoic sediments have been recovered at a number of DSDP sites in the Atlantic Ocean, allowing fairly detailed study of their calcareous nannofossils. The Mesozoic section recovered at Site 398 provides further information about the nannofossil assemblages in a continental margin area of the North Atlantic which has not been previously studied.

The calcareous nannofossil distribution at this site was found to be discontinuous through large portions of the sequence, in part due to sedimentary hiatuses, but more importantly to dissolution of carbonate in much of the section. This is most apparent in the mid-Cretaceous. Also the predominance of redeposited sediments (displaced downslope) further blurs the nannofossil record. Despite these problems, the nannofossil assemblages define a fairly complete biostratigraphic analysis, as well as providing much paleoenvironmental information.

The Cretaceous zonation for calcareous nannofossils used in this report is described in Blechschmidt (this volume). For the most part, an attempt was made to sample sediments representative of the background pelagic sedimentation, but in some portions of the section, sediment displacement and reworking obscure zonal boundaries, so that some zonal assignments may actually reflect maximum ages.

### Early Cretaceous

The lowermost sediments cored at 1740 meters sub-bottom are upper Hauterivian, probably in the *Crucellipsis cuvillieri* Zone. A few *C. cuvillieri* are found in Cores 398D-136 through 398D-138. Preservation in these cores is generally poor, with micritization of nannofossils in limestone layers and dissolution in interbedded sediments.

The Hauterivian/Barremian boundary is not recognizable using calcareous nannofossils. Core 398D-135 is tentatively assigned to the *Calcicalathina oblongata* Zone. *C. oblongata* has its last occurrence at the top of this core. *Nannoconus colomi*, *Zygolithus crux*, and *Parhabdolithus asper* are fairly common components of the floral assemblage present.

Cores 398D-134 through 398D-128 contain relatively sparse nannofossil assemblages typical of the Barremian

stage. Nannoconids are common in these cores, with a predominance of solution-resistant species. In general, preservation through this interval is poor with marked dissolution of nannofossils in most samples. Occasional samples from the more calcareous layers contain solution-susceptible species, such as *Stephanolithon lafittei*. A slight improvement in preservation was noted in Core 398D-128.

Cores 398D-127 through 398D-98 are Aptian with poor preservation of nannofossils through most of this interval. Cores 398D-127 through 398D-109 contain nannofossils characteristic of the *Chiastozygus litterarius* Zone. The lowermost *C. litterarius* was found in Core 398D-123. However, due to poor preservation of nannofossils in most of the samples examined, this endpoint could not be definitely established. The foraminiferal age assignment is probably more reliable in this interval. *N. colomi* which is probably reworked is found in small numbers in Cores 398D-127 through 398D-124. Other common taxa found in these cores are *P. asper*, *Z. crux*, *Zygodiscus diplogrammus*, and *Cretarhabdus crenulatus*. Cores 398D-119 through 398D-111 are mostly barren of calcareous nannofossils, with only a few samples containing nannofossils (Cores 398D-15 through 398D-13). These contain nannofloras similar to those described above. *Lithastrinus floralis* is first encountered in Section 398D-109-2, giving this interval a mid-Aptian appellation. *Parhabdolithus angustus* is first found in Section 398D-108-2, defining the upper Aptian. These boundaries are only approximate because of the extensive dissolution of carbonate. Cores 398D-109 through 398D-98 are assigned to the late Aptian *P. angustus* Zone.

The base of the Albian stage could not be precisely determined with calcareous nannofossils. The lowermost *Prediscosphaera cretacea*, which is used to define this boundary, first occurs in Core 398D-92. Foraminiferal data indicate that this boundary occurs between Cores 398D-97 and 398D-98. The *P. cretacea* Zone is quite thick, encompassing most of the Albian interval. Preservation in the lower part of this interval is poor; many of the cores recovered are barren of nannofossils. Cores 398D-101 through 398D-99 are mostly non-calcareous. Cores 398D-92 and 398D-93 show somewhat better preservation, containing *P. cretacea*, *Z. diplogrammus*, *C. litterarius*, and *Corollithion achylosum*. Cores 398D-91 through 398D-88 and the lower sections of Core 398D-89 are barren. Relatively well preserved assemblages similar to those found in Core 398D-92 are found in Cores 398D-97 through 398D-84 with another interval in Cores 398D-83 through 398D-77.

Cores 398D-76 through 398D-61 contain relatively well preserved Albian nannofloral assemblages with fairly common *P. cretacea*, *Parhabdolithus embergeri*, and *C. litterarius*. Rare *Podorhabdus albianus* is found in some samples. Preservation of nannofossils appears to be facies dependent with barren samples interspersed with well-preserved samples. The base of *Eiffellithus turriseiffeli* is encountered at the base of Core 398D-60.

The late Albian *E. turriseiffeli* Zone is well represented in Cores 398D-60 through 398D-58 and may

extend to Section 398D-57-2. *Lithraphidites alatus* which is used to define the base of the Cenomanian stage, is present in Section 398D-57-1. Unfortunately, this species is solution susceptible, so that one cannot discount the possibility of dissolution when determining this boundary. Preservation of nannofossils through this interval is somewhat better than in lower cores. *E. turriseiffeli*, *C. litterarius*, *Vagalapilla matalosa*, and *P. embergeri* are important components of the nannoflora in these cores.

A few specimens of *Lithraphidites alatus* are found in Core 398D-56, placing it in the *L. alatus* Zone (Cenomanian). A fairly abrupt improvement in preservation occurs in Section 398D-56-3, between 95 and 105 cm. In Section 398D-56-2, there is a transition from green calcareous ooze and black shale to a non-calcareous red clay. This red clay was recovered in Section 398D-56-2 through Core 398D-50.

### Late Cretaceous

In Section 398D-50-6, there is an abrupt lithologic change to a calcareous ooze which contains a Campanian nannoflora. This flora is characteristic of the *Tetralithus aculeus* Zone, containing *Broinsonia parca*, *T. aculeus*, *Micula staurophora*, and *P. cretacea*, which places it in the mid-Campanian. This flora persists through Core 398D-48.

*Tetralithus trifidus* is fairly common in Cores 398D-48 through 398D-46. These cores are assigned to the *T. trifidus* Zone of the late Campanian-early Maestrichtian. *Tetralithus gothicus* and *Tetralithus pyramidus* are also common components of the nannofloral assemblage found in these cores. The Campanian/Maestrichtian boundary is defined by the lowermost occurrence of *Eiffellithus eximius* at the base of Core 398D-46. *E. eximius* is rare in all samples studied from this interval. *T. trifidus* has its last occurrence in Section 398D-46-1.

Cores 398D-45 through 398D-43 are assigned to the *Lithraphidites quadratus* Zone (mid-Maestrichtian). *L. quadratus* is rare in Core 398D-43 and absent in Cores 398D-44 and 398D-45. It is not clear whether the absence of this species is due to environmental restrictions or non-preservation. Other taxa characteristic of this zone, including *Arkhangelskiella cymbiformis*, *Micula staurophora*, *E. turriseiffeli*, and *B. parca* are present in these cores.

A diverse and well-preserved late Maestrichtian flora representative of the *Micula mura* Zone is found in Cores 398D-41 and 398D-42. *A. cymbiformis*, *M. mura*, *M. staurophora*, and *Microrhabdulus decoratus* are dominant in this assemblage. *Nephrolithus frequens* was not found in samples from these cores.

The Cretaceous/Tertiary boundary was penetrated in Core 398D-41 at a sub-bottom depth of approximately 795 meters. It is characterized by a marked lithologic change, as well as floral and faunal changes. Many reworked Cretaceous specimens were found above this boundary, mixed with a characteristic Danian flora (predominantly *Markalius inversus*). No Danian elements were found below Sample 398D-41-2, 39 cm.

### Preservation and Paleoenvironment

Preservation of calcareous nannofossils is dependent on several factors. Among these are the level of the carbonate compensation depth (CCD) in the water column, the sedimentation rate, and the calcium carbonate saturation of interstitial waters in sediments (post-depositional changes). Preservation data for each sample examined is given in Blechschmidt (this volume).

The lowermost Hauterivian and Barremian sediments recovered at Site 398 generally contain poorly preserved nannofossils. However, the species composition (including *Conusphaera mexicana* and *Nannoconus colomi*) indicate a tropical or subtropical marginal sea environment. The poor preservation is probably due to post-depositional changes.

Preservation of nannofossils in the Aptian-Albian interval is very poor with occasional calcareous layers. In general, only the most solution-resistant species are found in sediments from this interval. This probably represents a deep-water environment. There is an improvement in preservation of nannofossils in the upper Albian, probably indicating a deepening of the CCD during this depositional interval. Solution-susceptible species (such as *Lithastrinus floralis*) become more abundant in this interval. Lower Cenomanian sediments show even better preservation, indicating increased deepening of the CCD. The red clay sediments devoid of calcareous material in Sections 398D-56-3 through 398D-50-6 indicate a very high CCD. Biostratigraphic control in this interval is poor, but benthic foraminiferal data indicate a sedimentary hiatus.

Preservation of calcareous nannofossils is much better in the Campanian-Maestrichtian sediments at Site 398, with a slight improvement in the Maestrichtian. A warming trend is noted through this interval, with the tropical *Micula mura* present in Maestrichtian sediments. No *Nephrolithus frequens*, which is indicative of more temperate conditions, are found in samples of Maestrichtian sediments. This warming trend is supported by isotopic analysis of these sediments (Arthur et al., this volume).

The abrupt floral change at the Cretaceous/Tertiary boundary in Sample 398D-41-2, 40 cm, and the marked increase in dissolution above this level indicate an abrupt upward migration of the CCD as well as probable cooling.

### Mesozoic Palynostratigraphy

Palynomorphs of potential chronostratigraphic value occur in the Mesozoic section at Site 398, but are irregularly distributed and rare, thus providing little information for precise age dating. Sporomorphs are usually most abundant in the palyniferous samples, but are represented in large part by species which are long-ranging in the Lower Cretaceous. Dinoflagellates are more valuable, but occur less frequently. Thus, the information presented below is based on the biostratigraphic dating provided by foraminifers (Sigal, this volume) and nannoplankton (Blechschmidt, this volume).

Cores of late Hauterivian age contain a dinoflagellate flora consisting of *Druggidium deflandrei* (Milloud), *Polysphaeridium warrenii* (Habib), *Spiniferites cingulatus* (Wetzel), and *Oligosphaeridium complex* (White), all of which occur in small percentages. The oldest sample studied, Sample 398D-138-2, 90-92 cm, contains *D. rhabdoreticulatum* Habib as well. It also marks the lowest occurrence of the sporomorph *Ephedripites multicostratus* Brenner, which ranges upward through the Albian.

The first specimens of *Clavatipollenites hughesii* Couper were found in Barremian Sample 398D-129-7, 38-41 cm. This species is rare, but increases in frequency up hole. The highest observed occurrence of *D. deflandrei* is in Bedoulian Aptian Sample 398D-123-5, 72-74 cm. This sample also marks the first occurrence of the sporomorph *Clavatipollenites tenellis* Paden-Phillips and Felix.

The first tricolpate angiospermous pollen grains were observed in middle Albian Sample 398D-88-6, 91-93 cm. It is represented by *Tricolpites minutus* (Brenner) which forms less than 1 per cent of the palynomorph assemblage. Tricolpate pollen increase in abundance upwards in the Albian, represented by *T. auritus* (Bolkhovitina) in Sample 398D-85-1, 48-50 cm, and also by *Retitricolpites georgensis* Brenner and *R. sphaeroides* Pierce in Sample 398D-84-5, 55-57 cm. In Core 398D-82, tricolpate species form more than 11 per cent of the total palynomorph assemblage. The first angiosperm pollen of the Normapolles group occurs in middle Cenomanian Sample 398D-56-2, 25-27 cm, and are represented by cf. *Complexiopollis* sp. and *Atlantopollis* sp.

The dinoflagellate *Subtilisphaera perlucida* (Alberti) was found in middle Albian Sample 398D-79-4, 35-37 cm. The dinoflagellate flora increases in diversity upwards from the stratigraphic level of Core 398D-74 (upper-middle Albian) in the more palyniferous samples. The first occurrence of *Deflandrea vestita* (Bridaux) was found in Sample 398D-74-3, 120-122 cm, and ranges through the stratigraphic interval represented by Sample 398D-69-3, 108-110 cm. This is succeeded by an interval where very few palynomorph specimens were recovered. However, in uppermost Albian Sample 398D-59-1, 96-98 cm, the first specimens of *D. echinoidea* Cookson and Eisenack were found. This dinoflagellate species occurs with *D. acuminata* Cookson and Eisenack in the middle Cenomanian in Sample 398D-56-2, 25-27 cm.

Palynomorphs are exceedingly rare in the Upper Cretaceous interval represented by Cores 398D-55 to 398D-41.

#### Mesozoic Palynology

The distribution of palynomorphs in the stratigraphic interval represented by Cores 398D-56 to 398D-138 (Cenomanian-Hauterivian) shows major fluctuations which correspond to the amount of carbonaceous material in the sediments. The highly fossiliferous palynomorph assemblages are composed of abundant land-plant spores and pollen grains (sporomorphs) with only few or no dinoflagellate cysts or acritarchs (marine

microplankton). For example, in the samples from Core 398D-129, a high of 51 species of sporomorphs were counted, of which at least 19 were schizaeaceous spore species. No microplankton were observed. Calculated abundance of specimens in this core reached as high as 83,000 specimens/gram dried weight. Other assemblages are poorly fossiliferous. These contain few specimens, largely of *Classopollis*, bisaccate pollen grains, and microplankton. Microplankton usually occur in higher percentages than sporomorphs in these sediments. Calculation of palynomorph abundance usually give values between 250 and 3000 specimens/gram.

The composition of these assemblages, and their abundance in the sediments, fluctuate in unison with the percentage organic carbon profile (see Site Summary Chart 1 in the rear pocket of this volume). Where organic carbon percentages are high, the assemblages are composed of large numbers of sporomorphs and sporomorph species, as well as abundant palynodebris in the form of (algal?) cellular masses, plant tracheal elements, and cellular plant cuticle. Where the percentages are lower, the assemblages consist of fewer specimens and species (*Classopollis*, bisaccates, microplankton), as well as abundant amorphous carbonaceous particles.

The carbonaceous composition of the more carbonaceous portions of the investigated section is largely terrigenous and is derived from land plants. The lesser carbonaceous intervals may be the result of the much smaller contribution of terrestrial plant materials.

#### SEDIMENTATION RATES AND STRATIGRAPHIC GAPS

Independent curves of accumulative sediment thickness versus time have been constructed based on both the nannofossil stratigraphy and foraminiferal stratigraphy (Figure 27). For the Neogene, the geochronology is taken from the calibrated paleomagnetic time scale of Ryan et al. (1974). For the Paleogene, it is based on the time scale of Berggren and van Couvering (1974). For the Mesozoic, it is based on the time scale of van Hinte (1976). Biostratigraphic age determinations are relatively good in the younger Pliocene and Pleistocene part of the Tertiary and are again reliable in the lowermost Eocene to Paleocene. The resolution is weakest in the lower Miocene to middle Eocene, a period during which the faunas were heavily affected by dissolution overcalcification and periodic reworking.

Rates of sedimentation vary from high (>50 m/m.y.) for the Pliocene, Pleistocene, middle Albian, and late Aptian (uncorrected for compaction effects) to moderately low (<10 m/m.y.) from the Oligocene to the Santonian.

Abrupt changes in accumulation rates are observed in the middle Eocene and lower Miocene. Since the interval of time between these depositional changes was characterized by a strong siliceous component, the variation in sedimentation rate may be partly a response to surface productivity favoring siliceous microfauna over the calcareous organisms, as well as to selective dissolution of carbonate skeletal material.

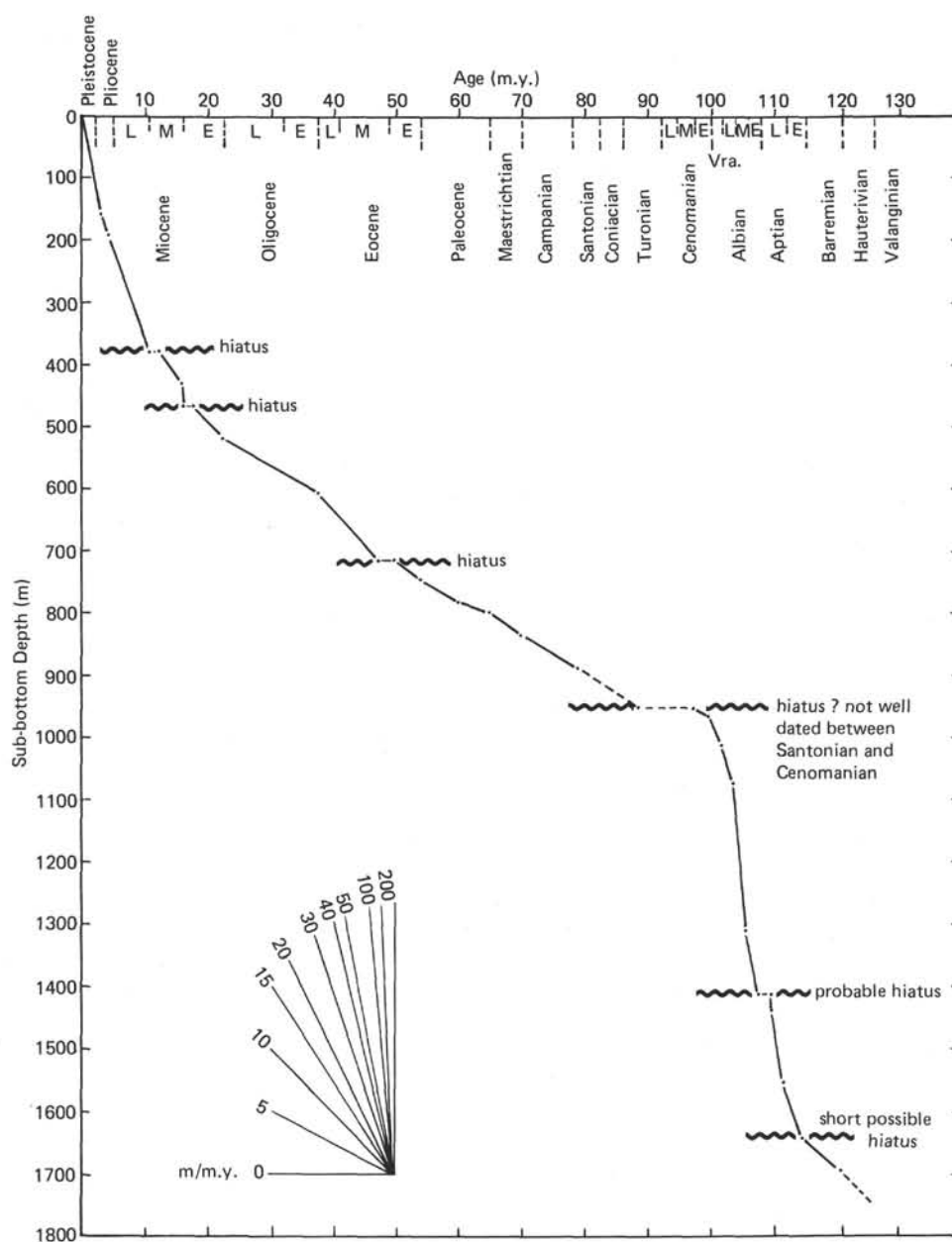


Figure 27. Sedimentation rates and stratigraphic gaps, Site 398. Ages from van Hinte (1976) for the Cretaceous section and from Berggren and van Couvering (1974) for the Tertiary.

Two minor hiatuses are seen at approximately 378 and 470 meters sub-bottom. Because the rates of accumulation are approximately the same above, below, and between these gaps, their tectonic origin is tentatively related to brief episodes of erosion or nondeposition, as contrasted to significant alterations in paleofertility. The supposition of erosion is supported by a strong component of concentrated detrital materials, plus pyrite in Core 398D-6 (which may reflect a residue or lag deposit created by winnowing). The unconformity at 390 meters marks the upper limit of the siliceous deposition and may relate to paleocirculation changes due to isolation

within the Tethys of the Indian Ocean equatorial belt from that of the Atlantic.

A small hiatus in the early Eocene could correspond with the weak extension of the *Edgari* Zone.

In the Cretaceous section, a hiatus extending from middle Cenomanian to probably somewhere in the lower Senonian is well correlated with the end of the dark shales episode. Two other hiatuses may occur: possibly at the Barremian/Aptian boundary and more probably in the uppermost Aptian. The latter is correlated with the presence of a major unconformity on seismic profiles and associated with the initiation of true

sea-floor spreading in the North Atlantic, north of the Newfoundland-Azores-Gibraltar fracture zone.

### PALEOMAGNETISM

Approximately 300 paleomagnetic samples were taken at Site 398 and were investigated both onboard ship and ashore. Although NRM intensities show a considerable total variation, it is possible to divide the section into clearly defined intervals within which the range of intensity values is rather narrow. The transitions from one intensity interval to another generally coincide with lithological changes, particularly color changes. The most marked intensity transition (between 947.1 and 947.5 m) corresponds almost exactly to the boundary between lithologic Units 3 and 4. Samples were subjected to progressive a.f. demagnetization, and the majority reached good stable end-points at fields of between 100 and 300 Oe.

There is some evidence that the stable remanence is carried by both magnetite and hematite, and that the magnetite and hematite magnetizations have very similar directions. Down to a depth of 889 meters (Santonian/Campanian boundary), approximately equal numbers of normal and reversed stable magnetizations are present. Below this depth, virtually all stable magnetizations are normal, presumably representing the long Cretaceous normal interval.

Inclinations of stable magnetizations show some scatter, but when averaged over a dozen samples are consistently shallower (by about 10° to 20°) than would be expected from plate tectonic reconstructions. It is tentatively suggested that this may be due to sediment compaction. (For further details, refer to Morgan, this volume).

### DOWNHOLE TEMPERATURE MEASUREMENTS

A single measurement was made with the downhole temperature recorder at Site 398 (Figure 28). The measurement was made at a sub-bottom depth of 126.5 meters directly following an interstitial *in-situ* pore-water sampling effort. Retrieval of the temperature recorder led to the breaking of the first sandline on the Bowen reel and the termination of the hole.

The minimum temperature measured as the instrument passed through the mudline was approximately 3.3°C. The temperature in the formation was very steady for 20 minutes, leading one to believe that it was a good measurement, i.e., unaffected by leakage into the formation of drilling water.

The "in-bottom" value of approximately 4.6°C gives a gradient of 1.03°C/100 meters. This value is about one-fourth of that which would be expected under a condition of average heat flow. The cause of this low thermal gradient is not understood at present.

Additional temperature measurements were suspended because of concern for further breakages of the sandline which would jeopardize the geological program of Leg 47B.

## CORRELATION OF REFLECTION PROFILES WITH SITE 398 DRILLING RESULTS

### Introduction

Site 398 was located in an area south of Vigo Seamount where a relatively complete and representative sedimentary sequence can be recognized on the seismic reflection profiles located in Figure 29. The acoustic reflectors have sufficient lateral continuity to permit them to be followed with some degree of confidence throughout the general vicinity of Galicia Bank and the Iberian Abyssal Plain (Groupe Galice, this volume). Based on the interpretation of numerous multichannel seismic profiles, four main acoustic units have been identified (Figure 30).

Acoustic Unit 1 can be divided into two parts, the lower part being absent in places in the Galicia Bank area. Acoustic Unit 1A is characterized by a weakly stratified sequence limited at its base by Reflector Green. (The reflectors have been assigned colors to preclude any intention of suggesting correlations to other DSDP drill sites or to other oceanic areas.) Acoustic Unit 1A can be subdivided into an upper, more transparent interval separated from a lower slightly stratified interval which is best revealed on single-channel airgun profiles of the type made by *Glomar Challenger* (Figure 31).

Acoustic Units 1B and 2 show a well-marked series of internal reflectors, some of which exhibit a high acoustic contrast (e.g., Reflector Purple which marks the boundary between Units 1B and 2). The base of Unit 2 corresponds to Reflector Yellow, separating the overlying highly stratified series from the thick acoustically homogeneous interval of acoustic Unit 3. A faint internal reflector can be identified in this unit. Acoustic Unit 3 is limited at its base by the very prominent Reflector Orange, which can be traced throughout the Galicia Bank and Vigo Seamount region. Acoustic Unit 4 lies between Reflector Orange and the acoustic basement (or substratum) and is easily identified on processed profiles (e.g., Figure 30). Discontinuous and hatched reflectors can be correlated with the tectonic and perhaps erosional event associated with Reflector Orange. Acoustic Unit 4 infills hollows in the substratum, and acoustic Unit 3 infills depressions associated with the main tectonic event occurring at the end of the deposition of acoustic Unit 4. Beneath the acoustic basement we can distinguish some reflectors probably associated with the sedimentary nature of the substratum.

Site 398 is close to shot 440 on profile IFP-CNEXO GP-29 and at 17H37 on 13 April 1976 on the *Glomar Challenger*, profile (Figure 31). Two different kinds of seismic profiles are available. The 48-channel migrated section (Figure 30) represented in variable area gives a good estimation of the character of the different units and a good representation of reflectors. On the *Glomar Challenger* profile (Figure 31), obtained with constant

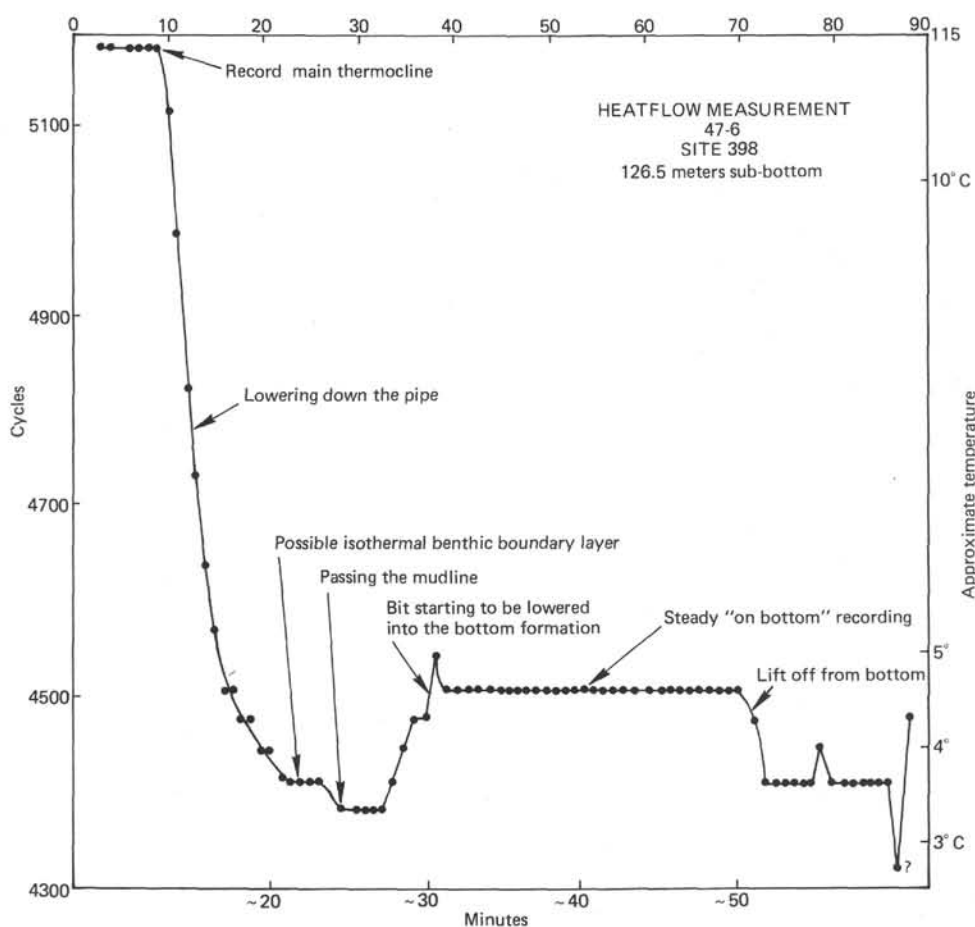


Figure 28. Summary of Site 398 downhole temperature measurements.

gain, the seismic character of acoustic Units 1 and 2 is better defined than on the other type of profile. Consequently, we used both types of profiles to assist in correlation with the drilling results.

#### Method

Two complementary approaches have been taken to correlate reflecting horizons and acoustic units to the drill cores. The first approach is an identification of the main stratigraphical gaps with the angular unconformities on the seismic reflection profile which give a first series of constraints. In this section, we discuss three separate divisions (velocity groups, acoustic units, and lithologic units) and compare two sets of data (calculated interval velocities and averaged measured velocities).

Particular emphasis is given to two horizons (Reflectors Yellow and Orange) where visible angular unconformities demonstrate stratigraphic onlap. Thus, these two horizons require correlation to the drilled section where stratigraphic gaps are present. The other variables (lithologic changes, variations in drilling rate, physical properties changes) then serve as a sort of vernier calibration to provide the best overall correspondence compatible with the observed geological record and physically reasonable velocities.

The second approach is based on the measured compressional wave velocities on drilled samples. Velocity groups were detected from the velocity depth curves (Figure 20) with assistance also from other physical, stratigraphic, and lithological contrasts. Using the mean of all measured velocities within each group, penetration times were calculated for the marked reflectors on the migrated seismic profile GP-19 (Figure 30). Despite the suspected, but unmeasurable discrepancies between velocity measurements on samples and *in-situ* velocities discussed in the "Physical Properties" section (this report), a remarkably close agreement between the two was found, demonstrating the usefulness of velocity measurements on freshly drilled samples and also that the velocity effect of confining pressure on semiconsolidated and consolidated rocks is small.

#### Main Discontinuities in Drilling Rates

The main discontinuities in the physical texture of the sediment are well marked by changes in the drilling rate. Figure 32 depicts drilling time as a function of penetration depth. The curve is a succession of segments of different slopes associated with changes in the nature of the sediments. Sometimes a particularly indurated formation marks a local change in drilling rate. Important changes in the facies units, the mineralogical composi-

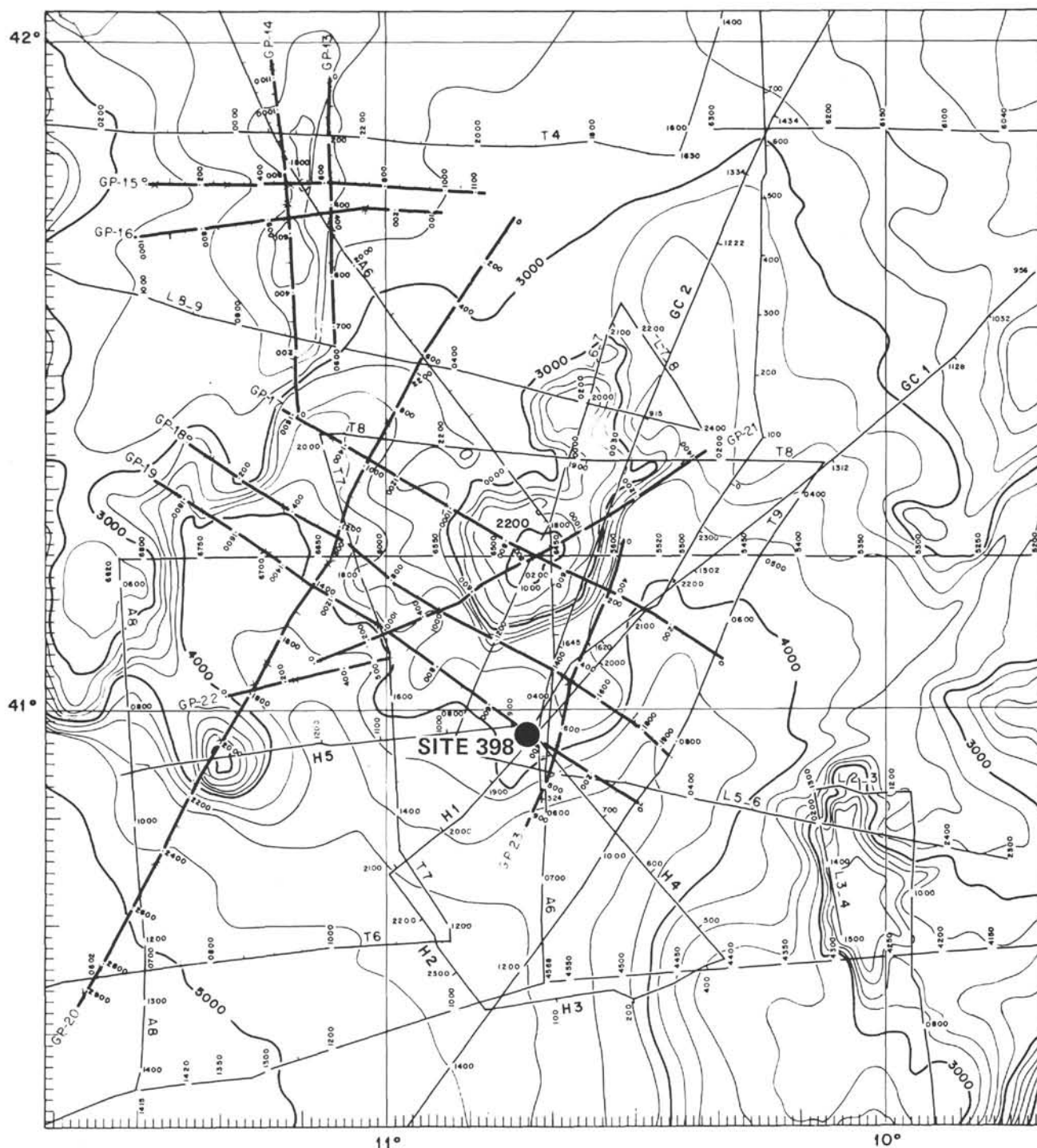


Figure 29. Location of seismic profiles in the area of Site 398.

tion, the velocity and porosity determinations correspond to changes in drilling rates.

#### Identification of Certain Key Reflectors

The correlation of Reflector Orange with the Aptian/Albian boundary is based on a small stratigraphic gap (Sigal, this volume) and a complete change in the lithologic units at this level.

The correlation of the base of acoustic Unit 2 has been based on the fact that Reflector Yellow at 0.98 s is

associated with the upper Cenomanian-Santonian stratigraphic gap found directly above the top of the thick dark shale sequence of acoustic Unit 3. Similarly, acoustic Unit 1 is characterized by an erosional base at 0.415 s and shows some local unconformities, especially immediately to the east of the drill site. The uppermost of two brief and close-spaced stratigraphic gaps of the Miocene (9 and 13 m.y., between 373 and 395 m and between 405 and 415 m) associated with seismic unconformity because of the conspicuous erosional features

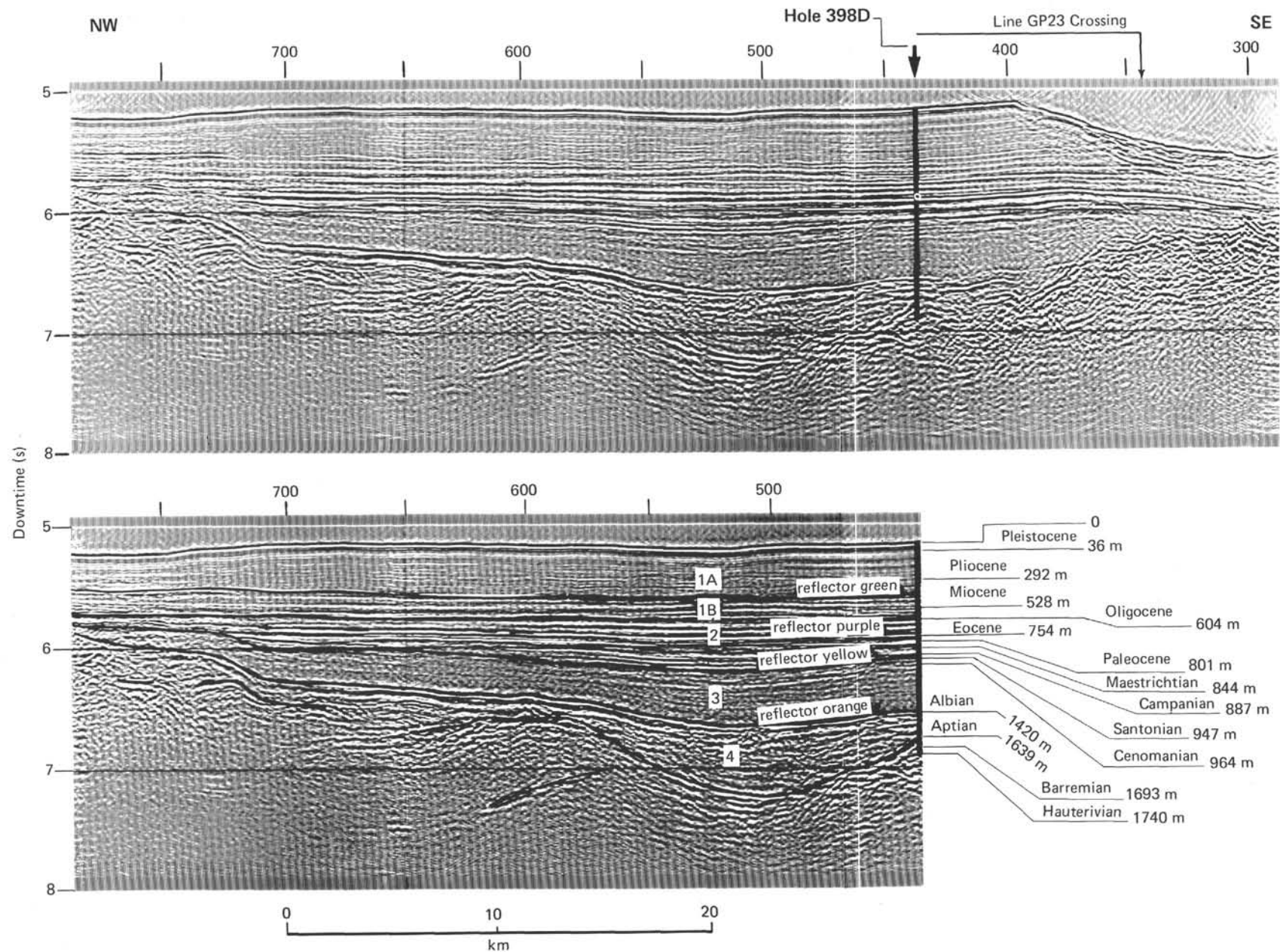


Figure 30. Migrated section of the Flexichoc seismic profile GP 19 (IFP-CNEXO-CEPM) located on Figure 29. Shot numbers at the top of the profile. Shot spacing: 50 meters. Horizontal scale in the lower part. Vertical scale in seconds of double travel time. The main seismic reflectors and acoustic units are shown on the interpreted profile. Limits and depths of geological stages, based on Site 398 results, on the right side.

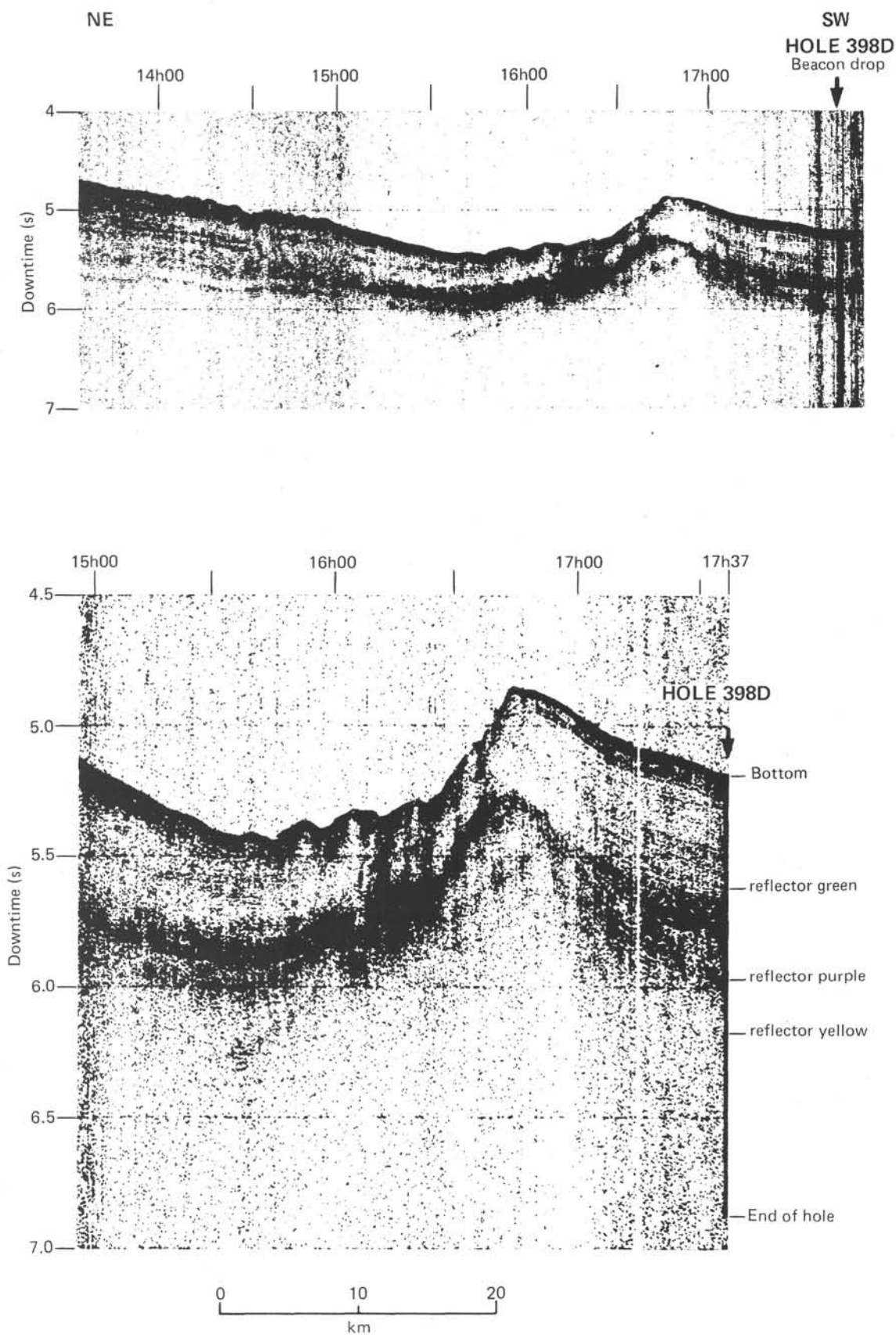


Figure 31. Glomar Challenger seismic profile GC1 located on Figure 29, with the identification of the main seismic reflectors. Note that no reflector can be identified beneath Reflector Yellow.

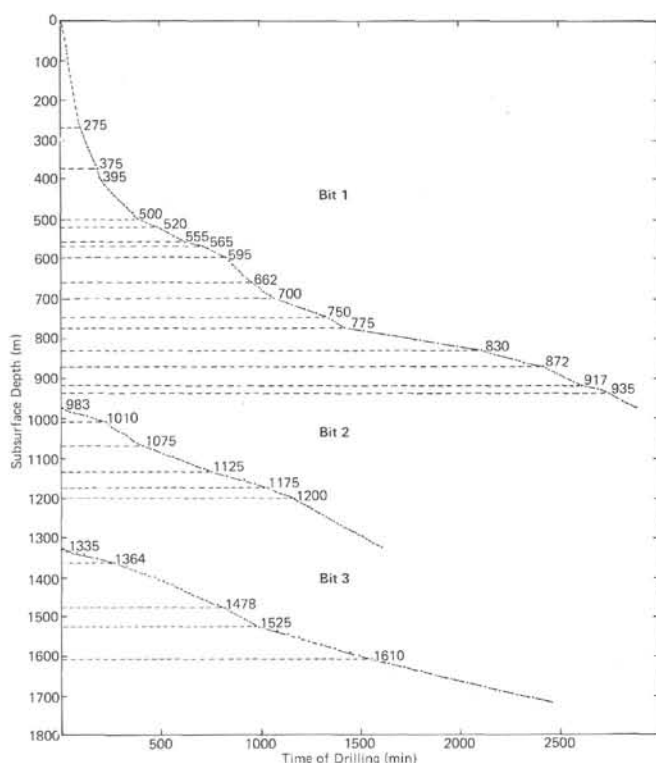


Figure 32. Drilling time versus depth. The main changes in drilling rate are underlined.

and small pinchouts which appear at this level, is related to Reflector Green.

## Identification of Main Acoustic Units

### Nature of Acoustic Unit 1A

Lithologic Sub-units 1A and 1B comprise acoustic Unit 1A. Lithologic Unit 1A is a 326-meter rhythmically bedded marly nannofossil ooze and chalk of Pleistocene to late Miocene age. Unit 1B, from 326 to 424 meters is a marly nannochalk to nannofossil chalk sequence of late Miocene to early Miocene age. The lower limit of Layer 1B is placed between 395 and 424 meters, between the first and the maximum advent of siliceous organisms. At 395 meters, a major change in drilling rate occurs and is correlated with the 1B/1C lithologic boundary. It is considered significant that these first two units, 1A and 1B, which we identified with acoustic Unit 1, have approximately the same thickness on the highs or in the depressions according to whether the sediment is essentially of pelagic or hemipelagic origin. The average velocity adopted for acoustic Unit 1 is 1.82 km/s, which is 10 per cent higher than the measured velocities of 1.65 km/s.

### Nature of Acoustic Units 1B and 2

Acoustic Units 1B and 2 (Figure 33) between Reflectors Green and Yellow are highly stratified and contain some very strong reflectors as Reflector Purple, which marks the limit between acoustic Units 1B and 2 (Figures 30 and 31). These reflectors abut the upper surface of acoustic Unit 3, whose top is not horizontal.

Acoustic Unit 1B cannot be seen everywhere and would not be distinguishable from the underlying Unit 2 but from the existence of a well-marked angular unconformity.

Four main lithological units can be distinguished in acoustic Units 1B and 2. Lithologic Sub-unit 1C (from 424 to 590 m) is a siliceous marly chalk sequence of early Oligocene to early Miocene age; several discontinuities in the drilling rate are associated with several reflectors of the IFP-CNEXO seismic profile (Figure 30). A local change in measured velocities is also noted at 554 meters (Figure 34).

Lithologic Unit 2, from 590 to 774 meters, is a siliceous marly chalk to mudstone sequence of middle Paleocene to early Oligocene age. In this unit three differences in the drilling rate are recognized (Figure 32). The well-marked change at 718 meters is correlated with Reflector Purple (Figure 30) and corresponds to a stratigraphic hiatus. The mean value of measured velocities between Reflectors Green and Purple (378 to 718 m) is 1.92 km/s.

Lithologic Unit 3A, between 774 meters and 839 meters of early Maestrichtian to middle Paleocene age, is constituted by red marly chalk and its upper limit corresponds to the disappearance of siliceous organisms and zeolites. The lower limit of lithologic Unit 3A is well correlated with a change in drilling rate marked by a pyrite bed and corresponds to a seismic reflector at 0.89 s (Figure 34).

Lithological Unit 3B of Santonian to early Maestrichtian age, between 832 and 945 meters, is a red clay unit for which the calculated interval velocity of 2.21 km/s is ~8 per cent higher than the 1.91 km/s mean measured velocity. At the base of this unit, which is correlated with Reflector Yellow, a major stratigraphic hiatus appears between the upper Santonian and middle Cenomanian. Part of this unconformity relates to a sedimentary hiatus visible on seismic profile GP-23. The most complete sequence of acoustical Unit 2 is at shotpoint 510 to the west of the drill site (Figure 30). At Site 398 the lowest reflectors of acoustic Unit 2 have disappeared and correspond to a gap of 0.05 s, i.e., 50 meters of sediments. If we extrapolate the sedimentation rate of the Maestrichtian and Campanian the true base of acoustical Unit 2 should be approximately 50 meters lower. Consequently, by this hypothesis, it seems probable that no really significant hiatus exists near shotpoint 510 and that acoustic Unit 2 is complete. If we extrapolate the sedimentation rate of the Albian to Cenomanian Santonian, a 200-meter-thick series would have been eroded during this period. This possibility is substantiated by the kerogen maturation profile (Pearson and Dow, this volume) which shows a maximum pre-Campanian burial of 320 meters.

### Nature of Acoustic Unit 3

Acoustic Unit 3, between Reflectors Yellow and Orange, is constituted by an isotropic sequence in which we can distinguish some faint semicontinuous reflectors. This acoustic unit infills the hollows limited by the acoustic basement or Reflector Orange and is generally

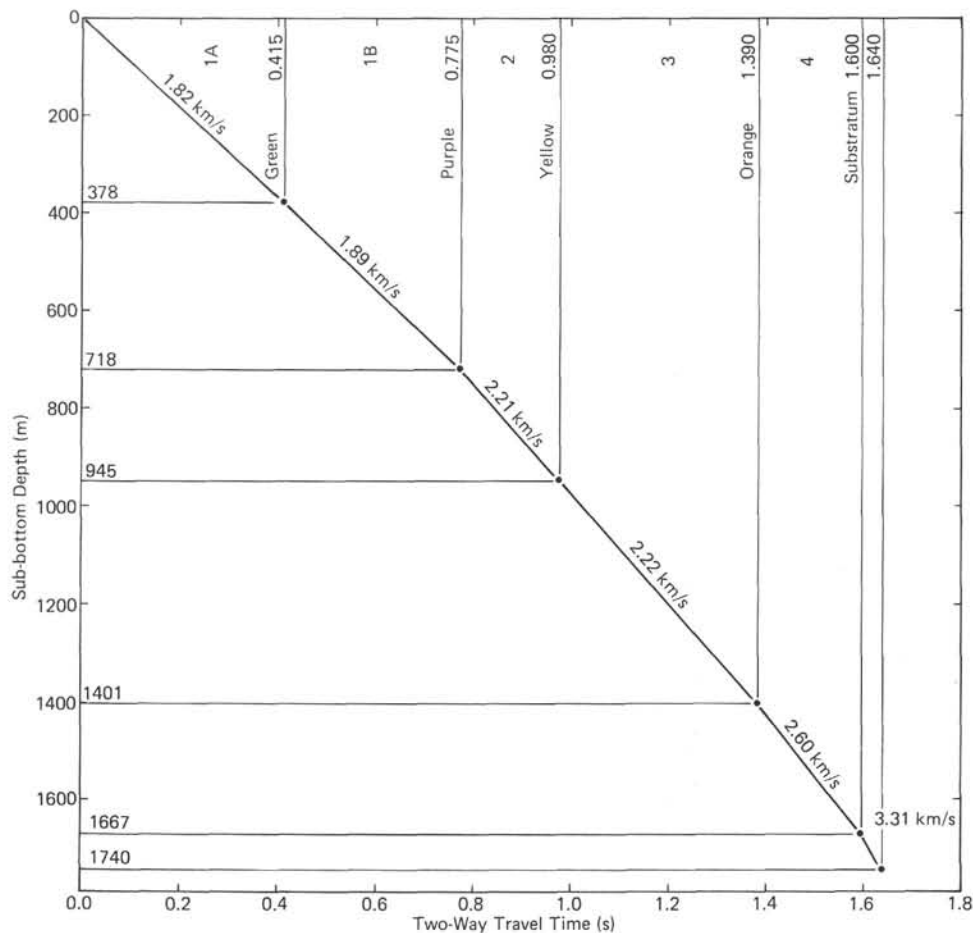


Figure 33. Velocity-depth profile. Main reflectors and acoustic units are identified.

lacking on the plateaus and tops of the fossil topography. When it is bedded, the sequence frequently exhibits very marked slopes. This unit never presents outcrops which can be dredged. In the abyssal plain, acoustic Unit 3 is recognizable as far seaward as magnetic Anomaly 34 (Santonian-Campanian limit in the van Hinte [1976] scale).

Lithologic Units 4A and 4B of latest Aptian to Cenomanian age, between 945 and 1401 meters, are a series of massive black to green-gray mudstones. The calculated interval velocity of 2.22 km/s agrees well with the average measured velocity (Figure 34).

Two slight reflectors of acoustic Unit 3 (Figure 30) are associated with two changes in the drilling rates (Figure 32). Reflector Orange thus corresponds to the transition between dark shales and calcareous mud flows with interbedded turbidites. It is marked by the massive turbidite which ends lithologic Unit 4C. Between lithologic Units 4B and 4C a stratigraphical gap (latest Aptian) can be also related to Reflector Orange.

#### Nature of Acoustic Unit 4

Acoustic Unit 4 between Reflector Orange and the substratum only appears in the deepest depressions created by the formation of half grabens in the basement. The internal reflectivity of Unit 4 is different

from that of Unit 3. Layering is quite conformable with the basement in the deeper parts and is approximately horizontal at the top of Unit 4. Acoustic Unit 4 corresponds to lithologic Unit 4C (1401 to 1667 m) constituted of thin sand-silt-clay graded sequences interbedded with thick slumped beds or debris flows. Since reflectors of acoustic Unit 4 are not horizontal, correlations between these reflectors and changes in drilling rate or in the lithology are not sure. Likewise, as the slope of the acoustic basement is around  $12^\circ$  on profile GP-19 and as Site 398 is located at 400 meters from the seismic profile, the basement depth could be at  $1.60 \pm 0.15$  s.d.t.t. Correlations between acoustic impedance, sonic velocities and lithology (Bouquigny and Willm, this volume) suggest, that basement was penetrated at a depth of 1667 meters and that the last 73 meters of the borehole belong to the basement.

#### Acoustic Basement

The acoustic basement, generally diffractant, is clearly of sedimentary origin on seismic profile GP-19. A strong reflector near a depth of 2 s.d.t.t. is well marked near shotpoint 600 (Figure 30). The last 73 meters of the borehole (1667 to 1740 m) correspond to lithological Unit 5 mainly constituted of a complex sequence of white indurated limestone and marlstone/siltstone.

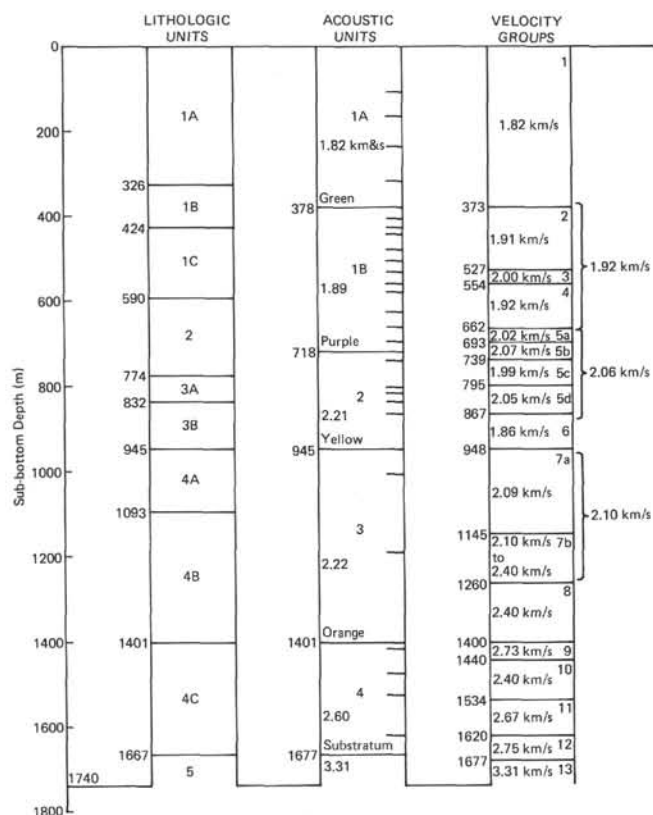


Figure 34. Correspondence between lithologic units, acoustic units, and velocity groups. Main reflectors of the IFP-CNEXO profile GP-19 are shown in the acoustic unit column.

One of the main implications of the borehole data is that, at the site, the last episode of rifting has still affected between early Barremian and latest Aptian the continental margin previously formed. Seismic correlations show that sedimentary deposits are locally affected by tectonic movements during the time of acoustic Unit 4 deposition. Consequently, the so-called late Jurassic-early Cretaceous episode of rifting could end in latest Aptian.

#### Identification of Velocity Groups

The velocity groups determined from the physical properties/depth curves (Figure 20) are briefly discussed here together with their correspondence with seismic reflectors. Figure 34 shows the correspondence between acoustic reflectors, lithologic unit, and velocity groups.

##### Group 1: Sea Bottom to Core D-4 (373 m)

The velocity for this group is a very constant 1.65 km/s (incremented by 10% to 1.82 km/s in the velocity depth profile; Figure 21) and there is little lithologic variation in the gray-blue nannofossil oozes of lithologic and acoustic Units 1A.

The intervals between Cores 3, 4, and 5 were not continuously cored, and there is some question as to exactly where the lower boundary of this velocity group should be drawn. Changes in porosity, grain density, water

content, and an increase in acoustic impedance occur within Core 4, while the beginning of a decrease in  $\text{CaCO}_3$  and also the boundary between measured velocities 1.65 and 1.77 km/s are found between Cores 4 and 5, where a gap in nannoplankton zonation occurs. The division between lithologic Units 1A and 1B, the ooze to chalk transition, however, has been drawn between Cores 3 and 4. A strong paleomagnetic intensity contrast of two orders of magnitude is also observed between Cores 3 and 4. Thus on lithologic and paleomagnetic evidence the boundary should lie between these cores. On porosity and density data and evidence of the existence of microconglomerates, it would be drawn at 373 meters within Core 4. On  $\text{CaCO}_3$  changes and nannoplankton evidence, it would be drawn between Cores 4 and 5, an interval also showing contrasts in core cutting time. Using the adjusted velocity of 1.82 km/s, the lower boundary of this group would occur at 378 meters and coincide with Reflector Green at 0.415 s (2-way travel time). Assuming the boundary to actually lie at 373 meters, this suggests that the 10 per cent increment in velocity added to compensate for the absence of *in-situ* confining pressure is marginally too high and that a velocity of 1.81 km/s is perhaps closer to reality.

Throughout acoustic Unit 1A four other reflectors are observed in particular at 0.12 s (109 m), at 0.185 s (168 m), of which neither horizons were sampled. It is possible that the reflector at 0.12 s may represent the Plio-Pleistocene boundary. The reflector at 0.26 s (237 m) is within Core B1, although it is known that this core sample is not reliably *in-situ* and thus this information will be disregarded. The reflector at 0.35 s (319 m) lies within Core D3 and is perhaps represented by the small (8 per cent) reduction in porosity, increase in wet bulk density, decrease in grain density, and a 10 per cent decrease in  $\text{CaCO}_3$  content. This is also the point at which the sedimentologists placed the contact between ooze and chalk and therefore represents a diagenetic boundary.

Acoustic Unit 1B lies between Reflectors Green and Purple, within it is velocity group 2.

##### Group 2: Core D-4 (373 m) to Section D-13-1 (527 m)

This group has an average measured velocity of 1.77 km/s (incremented by 8 per cent to 1.91 km/s in the velocity/depth profile; Figure 21) and comprises the lower part of lithologic Unit 1B and the upper part of 1C. It also corresponds to the upper part of acoustic Unit 1B.

The grain density is a very constant 2.7 g/cm<sup>3</sup> throughout this group, while the porosity gradually decreases from about 50 per cent at 373 meters to 33 per cent at 527 meters. Conversely the wet bulk density increases from 1.8 in Core D4 to 2.0 g/cm<sup>3</sup> in Core 13.

A very distinct paleomagnetic intensity boundary is also drawn between Sections 13-1 and 13-2 where a decrease in two orders of magnitude in intensity is seen. The boundary occurs at 0.57 s and corresponds with the top of a well-marked reflector.

Within this velocity group five good reflectors are seen which, using the assumed velocity for this group of

1.91 km/s, give the depths listed in Table 4. The reflector at 407 meters lies in the unsampled gap between Cores 5 and 6, between which there exists a porosity decrease of 4 per cent and wet bulk density increases of 0.5 g/cm<sup>3</sup> and CaCO<sub>3</sub> decreases of 15 per cent. The reflector at 0.46 s (421 m) in Core 6 may be related to similar small changes in porosity and density, although it is more likely that it is related to a calcium carbonate contrast of approximately 50 per cent occurring in Section 6-3 within the repeated light grading to dark sequences of silty clays. There is also a stratigraphic gap between 405 and 415 meters.

The reflector at 0.48 seconds (440 m) in Core 7 may perhaps be related to a similar calcium carbonate spike, although unfortunately no intermediate CaCO<sub>3</sub> measurement was made between these two peaks. Core 7 also marks the inflection point at which porosity begins to decrease and density increase sharply, which coincides with the incidence of fine sand layers in all three sections of Core 7.

The reflector at 0.52 s, calculated to lie at 479 meters in Core 9, does not coincide with any particular inflections in the physical properties curve or with any notable characteristic in the lithology of this core,

despite the fact that a minor discordance is observed on the seismic reflection profile at the level of this reflector (Figure 30).

The reflector at 0.545 s (503 m) corresponds to the top of a prominent reflector and coincides with the more frequent occurrence of sandy, siliceous mudstones within the predominantly marly nannofossil chalk in Section 13-1. This change in lithology, surprisingly, does not affect the CaCO<sub>3</sub> level which remains above 50 per cent.

The coincidence of the calculated depth with the paleomagnetic boundary and a lithological change suggests that 8 per cent velocity increment to this velocity group quite accurately compensates for the lack of confining pressure on samples from this level.

#### Group 3: Section D-13-2 (527 m) to Section D-15-5 (554 m)

Core 13 indicates the beginning of the influence of disturbances in the form of minor folds and slumps which continue through the whole of this group, terminating in a large slumped bed in Core 15. An overlap in paleomagnetic intensities in these cores also supports the hypothesis that these sediments are of mixed origins. The CaCO<sub>3</sub> content is >50 per cent, and marginally in

TABLE 4  
Depths and Penetration Times of Seismic Reflectors

Velocity Group	Cores	Vp (measured)	Sub-Bottom Depths (m)	Thickness (m)	2-Way Penetration Depth (s)	Reflector	Computed (m)	Comment (core)
1	1-D4	1.82	0-373	373	0.12	Reflector Green	109	Not sampled
					0.185		168	Not sampled
					0.26		237	Core B1 not reliable
					0.35		319	(3)
					0.415		378	Strat. suggests 373 m
					0.445		407	Not sampled
					0.46		421	(6) strat. hiatus 405 m
					0.48		440	(7) sand layers
					0.52		479	(9)
					0.545		503	
2	D4-13/1	1.91	373-527	154	0.57	Reflector Purple	527	(13) paleomag. boundary
3	13/2-15/5	2.00	527-554	27	0.60		557	(16) lithol. suggests 554 m
4	15/6-27	1.92	554-662	108	0.62		579	Not sampled
	5a	2.02	662-693	31	0.67		624	(23)
		2.02	662-693	31	0.71		662	(27) microbreccia
5b	28-30/1	2.02	662-693	31	0.74		693	(30) microbreccia
	5c	2.07	693-739	46	0.775		718	
		2.06	693-739	46	0.79		739	(34) slumps
5d	30/2-35/2	2.07	739-795	56	0.835		789	(41) 795 m ?
6	35/2-41/1	1.99	739-795	56	0.855		811	
7a	41/2-48/1	2.05	795-867	72	0.875		832	
	7b	2.10	867-948	81	0.92	Reflector Yellow	867	876 m ?
		2.10	867-948	81	0.98		945	(56) 948 m ?
8	48/2-56/2	1.86	867-948	81	1.04		994	(62) 1008 m ?
7a	56/2-75	2.09	948-1145	197	1.22	Reflector Orange	1186	
7b	75-87/1	2.10	1145-1260	125	1.39		1400	1401.5 m lithol./paleo.
8	87/2-103	2.40	1260-1400	140	1.42		1413	
9	103-106	2.73	1400-1440	40	1.47	Substratum	1476	Not sampled
10	107-116	2.40	1440-1534	94	1.51		1524	1534 m strat.
11	117-125	2.67	1534-1620	86	1.58		1620	High CaCO <sub>3</sub>
12	125-131	2.75	1620-1677	57	1.60		1667	
13	132-138	3.31	1677-1740	63	1.64		1740	

excess of that of Group 2, and the acoustic impedance reaches a peak of 5.4. The average velocity is 2.0 km/s giving the reflector at 0.60 s penetration time a depth of 557 meters (Core 16). Inspection of the lithology suggests that 554 meters in Core 15 more appropriately coincides with slumped bedding. Such a minor adjustment is well within the accuracy of the velocity measurements. The lower limit of this group coincides with the reflector at 0.60 s which is not always a strong reflector on the profile. The contrasts observed at Site 398 suggest this should be a strong reflector whereas on profile GP-19 it appears weakly at the extrapolated site location suggesting that the drill site may not be exactly located on the site survey profile.

#### **Group 4: Section D-15-6 (554 m) to Core D-27 (662 m)**

The average velocity for this group is  $1.92 \pm 0.7$  km/s and is less than that of the overlying group. Lithologically it forms part of Unit 1C and in general, this group is characterized by gradually increasing porosity from approximately 30 to 45 per cent, and a corresponding decrease in wet bulk density from approximately 2.0 to 1.85 g/cm<sup>3</sup>. The CaCO<sub>3</sub> content decreases from approximately 20 per cent down to 587 meters and then increases sporadically to around 45 per cent towards the base of this group. The bottom of this group lies at 0.71 s and coincides with 662 meters (Core 27) where a distinct decrease in porosity, increase in density, and increase in velocity occur. This coincides with the several microbreccia horizons in Core 27.

Within this group lie two other marked reflectors at 0.62 s and at 0.67 s, calculated to lie at 579 meters and 624 meters, respectively. At 579 meters a horizon is not sampled, while at 624 meters (Core 23) the physical properties curves show a porosity minimum and a density maximum which are perhaps associated with the reflector. Marked short-period variations in physical properties are seen, however, at 615 meters, a horizon not associated with a reflector at Site 398 on profile GP-19. Geologically this horizon marks the onset of turbidity flows and a lower CaCO<sub>3</sub> level and a lower average velocity which might reasonably be expected to define a reflector. Its non-correlation with a reflecting arrival could either indicate that the velocity/carbonate variation does not constitute a reflector here or again, that Site 398 does not lie directly on profile GP-19.

#### **Group 5: Core D-28 (662 m) to Core D-48 (867 m)**

The velocity group can be subdivided into four sub-groups. Overall it has an average velocity of 2.06 km/s.

##### **Sub-Group 5a: Core D-28 (662 m) to Section D-30-1 (693 m)**

This sub-group has an average velocity of 2.02 km/s and lithologically consists of part of Unit 2. The group contains several thin breccia horizons which diminish in abundance, as does the spread in paleomagnetic intensities, down to Section 30-1. These lithologic variations are reflected in the physical properties curves where higher wet bulk density, lower porosity, and more erratic impedance than in Group 4 occur. The base of this

sub-group occurs at 697 meters coinciding with the reflector at 0.74 s.

##### **Sub-Group 5b: Section D-30-2 (693 m) to Section D-35-2 (793 m)**

This sub-group consists of green, gray to pale brown clays which readily expand upon arrival onboard ship. These clays occur between the microbreccias of Sub-group 5a and the minor slumps observed in Section 33-6 and Cores 34 and 35. The average velocity is  $2.07 \pm 0.14$  km/s.

A discrepancy between GRAPE and gravimetric density and porosity determinations across this unit precludes any accurate observations being made on the density and porosity, although the impedance curve appears more subdued here. Using the average velocity of 2.07 km/s, the reflector at 0.79 s occurs at 739 meters in Core 35, close to the Paleocene/Eocene boundary known from micropaleontology to lie in Section 35-2. It is not impossible that the reflector is coincident with the stratigraphic boundary, although there is no geophysical reason why it should do so. Within this group lies Reflector Purple at 0.775 s. This marks the division between seismic Units 1B and 2. It may seem strange that this reflector seen to mark the boundary between reflectors of different character should lie within a velocity group and not form a boundary to it, although there is essentially no reason why a change in seismic character also needs to be marked as a change in other physical properties.

##### **Sub-Group 5c: Section D-35-2 (739 m) to Section D-41-1 (795 m)**

The average velocity for this sub-group is  $1.99 \pm 0.9$  km/s which lithologically consists of soft red-brown clays of lithologic Unit 3a. The drilling rate was slow in this group with Core 41 taking 150 minutes to cut, compared with 36 minutes for Core 36.

Here again there is some disagreement between GRAPE and gravimetric density and porosity valuations. The GRAPE values show considerably larger variation than the gravimetric data. Both, however, show a possible major inflection at 780 meters (Section 39-1) near the boundary between lithologic Unit 3A—red marly chalk, and Unit 2—siliceous marly chalk mudstone at the Paleocene/Maestrichtian boundary. This corresponds to the reflector at 0.835 s calculated to lie at 789 meters, but which probably corresponds with the stratigraphic boundary at 795 meters, implying that the average velocity for this group is marginally slower than 1.99 km/s.

##### **Sub-Group 5d: Section D-41-2 (795 m) to Section D-48-1 (867 m)**

The average velocity for this sub-group is  $2.05 \pm 0.8$  km/s which falls sharply to just below 1.9 km/s in the underlying velocity group. Between Sections 48-1 and 48-2 there is a decline in velocity, porosity, an increase in density, and a sharp decline in CaCO<sub>3</sub> content. Using the average velocity suggests a correlation with the reflector at 0.92 s, calculated to lie at 876 meters, where it corresponds to a decrease in CaCO<sub>3</sub> level and a zone of nannofossil preservation below 867 meters.

Within this interval are two other marked reflectors at 0.855 s (811 m) and at 0.875 s (832 m). These lie on either side of a velocity maximum reached in Core 43 where the average velocity is 2.18 km/s. The calcium carbonate content varies throughout this core, and there is no lithologic feature to explain these higher velocities.

**Group 6: Section D-48-2 (867 m) to Section D-56-2 (948 m)**

This group lies wholly within lithologic Unit 3B—red-yellow claystones and mudstones. It is characterized by a lower average velocity of  $1.86 \pm 0.08$  km/s. The wet bulk density falls from  $2.1 \text{ g/cm}^3$  at 860 meters to a low of 1.8 at 910 meters (Core 53) and then rises again. The porosity conversely increases from 35 per cent, reaches a peak of 58 per cent at 910 meters, and then decreases once more. The acoustic impedance rises sharply from 3.65 to 4.55 at 945 meters.

The low velocity is a reflection of the very soft nature of these beds, though to what extent this is due to drilling disturbance is not known, since the drilling time is lower for this group than 5c and some of the cores were drilled in as little as 30 minutes. The cause of the physical properties inflections at 910 meters is not obvious from the lithology, although it does correspond with an increase in zeolites.

The age of the strata overlying Core 56 is not clear and it may consist of reworked Santonian. The boundary at Section 56-2 has been precisely defined by foraminiferal studies (Sigal, this volume) as a Santonian/middle Cenomanian unconformity representing a hiatus with probably approximately 200 meters of the section missing between lithologic Units 3B and 4A. The level at 948 meters is located near 0.98 s and corresponds with Reflector Yellow at the base of seismic Unit 2. Within this group is the reflector at 0.92 s corresponding to 876 meters in Core 49 where a velocity decrease and porosity increase is seen and the calcium carbonate content falls to zero.

**Group 7: Section D-56-2 (948 m) to Section D-87-1 (1260 m)**

This group has an average velocity of 2.1 km/s and is divided into three subgroups:

**Sub-Group 7a: Section D-56-2 (948 m) to Core D-75 (1145 m)**

The Core 56 boundary is one of the most marked in Hole 398D for the unconformity there also marks a major change in lithology from soft red clays to the top of a thick sequence of black-green shales. The characteristic reflection profile for the latter constituting seismic Unit 3 is of a semitransparent zone with many discontinuous reflectors.

The average velocity is  $2.09 \pm .09$  km/s, typical wet bulk density  $1.95 \text{ g/cm}^3$ , porosity 45 per cent, water content 22 per cent, and calcium carbonate content 25 per cent. There is a small inflection in the physical properties curves at 1015 meters (Core 63) which may be a manifestation of the conglomerates (drilling breccia ?) at the top of this core and of the fine microconglomerates within Core 63. A similar inflection occurs at 1060 meters and is possibly due to the conglomerates

and microbreccias in Core 68. The reflector at 1.04 s is calculated to lie at 994 meters, but more probably relates to the higher velocity layer in Section 62-5 at 1008 meters.

Much of this core material is highly cleaved and extremely difficult to sample. It is likely that the harder, more massive bands were sampled disproportionately to the average core composition. At Core 76 there occurs a positive inflection in the velocity curve which coincides with the commencement of siderite lenses within the black shales. This is also a possible paleomagnetic intensity boundary where the scatter of intensities is reduced.

**Sub-Group 7b: Core D-75 (1145 m) to Section D-87-1 (1260 m)**

In this group the calcium carbonate level is essentially zero apart from one reading of 20 per cent at 1166 meters. There is an increase in grain density from 41 to 46 per cent, the average water content is 22 per cent, porosity 43 per cent, and wet bulk density between 1.9 and 2.1. There is an inflection in the density and porosity curves at 1186 meters (Core 78) which corresponds with the reflector at 1.22 seconds.

Lithologically the lower boundary of this group has no strongly observable distinguishing characteristics, although it does mark an ammonite-bearing horizon with a remarkably high level of preservation. Core 87 does not coincide with any particular reflector, but marks a level where the average velocity increases from 2.1 to 2.4 km/s.

**Group 8: Section D-87-2 (1260 m) to Core D-103 (1400 m)**

This group has a common lithologic boundary with Unit 4B (black-gray shales with ubiquitous siderite lenses) and the underlying turbidite mudstones of Unit 4C. The average velocity is  $2.4 \pm 0.1$  km/s.

There is again a discrepancy between GRAPE and gravimetric density and porosity analyses, but they indicate a porosity of 30 to 40 per cent and an average density of 2.05 to 2.1. The calcium carbonate content is very low, although this group is typified by a high (up to 3 per cent) organic carbon content. Core 103 coincides with the top of Reflector Orange at 1.39 s (1400 m). Foraminiferal studies indicate a 3- to 4-m.y. hiatus here between Cores 98 and 104, which most probably occurs at the top of the slumped beds in Cores 103 and 104.

**Group 9: Core D-103 (1400 m) to Core D-106 (1440 m)**

According to our interpretation, this group forms part of Reflector Orange with its high (up to 75 per cent) calcium carbonate level, average velocity of  $2.73 \pm 0.4$  km/s (the highest velocity so far at Site 398). Lithologically this group includes fine to coarse conglomerates, sandy layers, and slumped limestone beds which account for the high average velocity. This section of the late Aptian has the only evidence of sufficiently major movements encountered at Site 398 to warrant association with initial rifting and the separation of Iberia and Newfoundland. Thus we know no major tectonic event was felt in the region of Site 398 post-late Aptian, although we do not know what evidence of

earlier tectonic events exists but is beyond our penetration depth.

Both wet bulk density, porosity, and grain density show a very disturbed region across these cores. The major disturbance and the lithologic boundary occurs in Core 104, which coincides with a reflector having a penetration time of 1.42 s and lies at 1413 meters. The end of the major deflection (1440 m) in the curves is marked particularly the end of the high calcium carbonate content, although it does not appear to constitute a reflector on account of the high to low velocity contrast.

#### **Group 10: Core D-107 (1440 m) to Core D-116 (1534 m)**

The density and porosity curves indicate a very varied zone with particularly high disturbance in Core 112, probably caused by the conglomerates in Sections 4 and 5. The calcium carbonate content increases from zero to 25 per cent in this group although the water content remains approximately 20 per cent.

Potentially two reflectors lie within this group, a reflector at 1.47 s which corresponds to a depth of 1476 meters (an unsampled gap between Cores 109 and 111). A reflector at 1.51 s is calculated to occur at 1524 meters within Core 115 (although may actually lie at 1534 meters in Core 117, associated with contrasts in physical properties). Recovery was poor in Cores 115 and 116 (4.5 and 3.92 m, respectively), and the only lithologic character which may be related to the physical properties variations is the inclusion of minor sand layers. These become more numerous in Core 117 and are accompanied by microconglomerate horizons which presumably are responsible for the abrupt velocity increase below Core 116. The average velocity for this group is 2.4 km/s.

#### **Group 11: Core D-117 (1534 m) to Core D-125 (1620 m)**

This group lies with lithologic Unit 4C, which consists of thin turbidite sandstones to mudstones with debris flows. The average velocity is  $2.67 \pm 0.3$  km/s. The wet bulk density and porosity curves again show major variations with the density ranging from 1.92 to 2.43 g/cm<sup>3</sup>.

Major disturbances occur in Cores 117 and 118 due to numerous, often inclined, sand layers and also in Core 119 where calcium-cemented sand layers exhibiting velocities up to 5.17 km/s occur. The high impedance spikes (Figure 24) are due to such sand layers which are not dominant lithology of the core. The base of this group coincides with a reflector at 1.58 s which is associated with a high calcium carbonate peak in Cores 124 and 125. Section 124-4 also shows evidence of Barremian tectonic movements in a well-cemented conglomerate layer giving a velocity of 3.89 km/s.

#### **Group 12: Core D-135 (1620 m) to Core D-131 (1677 m)**

The grain density averages 2.7, wet bulk density 2.2, porosity 30 per cent, and water content 14 per cent with the average velocity being 2.75 km/s. Cores 125 to 128 are interbedded black mudstones, coarse at times, e.g. Sections 128-4 to 128-5.

#### **Group 13: Core D-132 (1677 m) to Core D-138 (1740 m)**

This is the last group penetrated at Site 398. It lies within lithologic Unit 5, consisting of lower Barremian to Hauterivian interbedded limestones and marly mudstones. The average velocity is the highest average in this hole being  $3.31 \pm 0.33$  km/s. There are also considerable density and porosity fluctuations in this group, especially in Cores 133 and 134, which are related to the alternating limestone and mudstone beds. The calcium carbonate level averages approximately 60 per cent, wet bulk density 2.7 g/cm<sup>3</sup>, porosity 22 per cent, and water content 10 per cent. The base of this succession was not reached.

### **SUMMARY AND CONCLUSIONS**

DSDP Site 398 is located on a passive continental margin, south of Galicia Bank, 20 km to the south of Vigo Seamount (Figure 35). Although Galicia Bank is continental, the nature of the crust of the interior basin between Galicia Bank and the Iberian continental margin is not firmly established. The initial creation of the interior basin filled with at least pre-Neocomian sediments may be related to the Permo-Triassic-Liassic and/or Late Jurassic-Early Cretaceous distensive episodes which occurred on land on each side of the North Atlantic (Pautot et al., 1970; AMOCO, 1973; Montadert et al., 1974; Arthaud and Matte, 1975; Ziegler, 1975; Jansa and Wade, 1975; Schlee et al., 1976; van Houten, 1977; Groupe Galice, this volume) and/or with synchronous or posterior N330 strike-slip motions along the northeastern border of the interior basin (Le Pichon et al., 1977; Groupe Galice, this volume). Site 398 is consequently located in the southern part of the interior basin in an area greatly affected by rifting (Groupe Galice, this volume).

#### **Acoustic Stratigraphy**

Site 398 has been drilled about 400 meters laterally off the IFP-CNEXO Flexichoc seismic line GP-19 near shotpoint 440 (Figure 30) in a water depth of 3900 meters. A total penetration of 1740 meters was obtained. Four main acoustic units overlie the acoustic basement.

The acoustic basement is clearly of sedimentary origin on this profile. It is generally diffractive and shows strong reliefs either as broad undulations or as sharp crests corresponding to buried highs. Some of these highs may pierce the sea bottom and crop out as suggested on other seismic profiles. Sharp crests and steeply dipping layers in the basement suggest the presence of tilted fault-blocks. On some profiles, several highs are flat-topped and covered by a thin sedimentary blanket which suggests that they may have been affected by subaerial erosion.

Formation 4, which is a moderately to strongly layered formation, is distinguished from the overlying formation 3 by a strong reflector. Formation 4 lies in troughs between horsts and tilted blocks. Layering is conformable with the structural top of the basement in the lowest part of the fills, and may be nearly flat at the

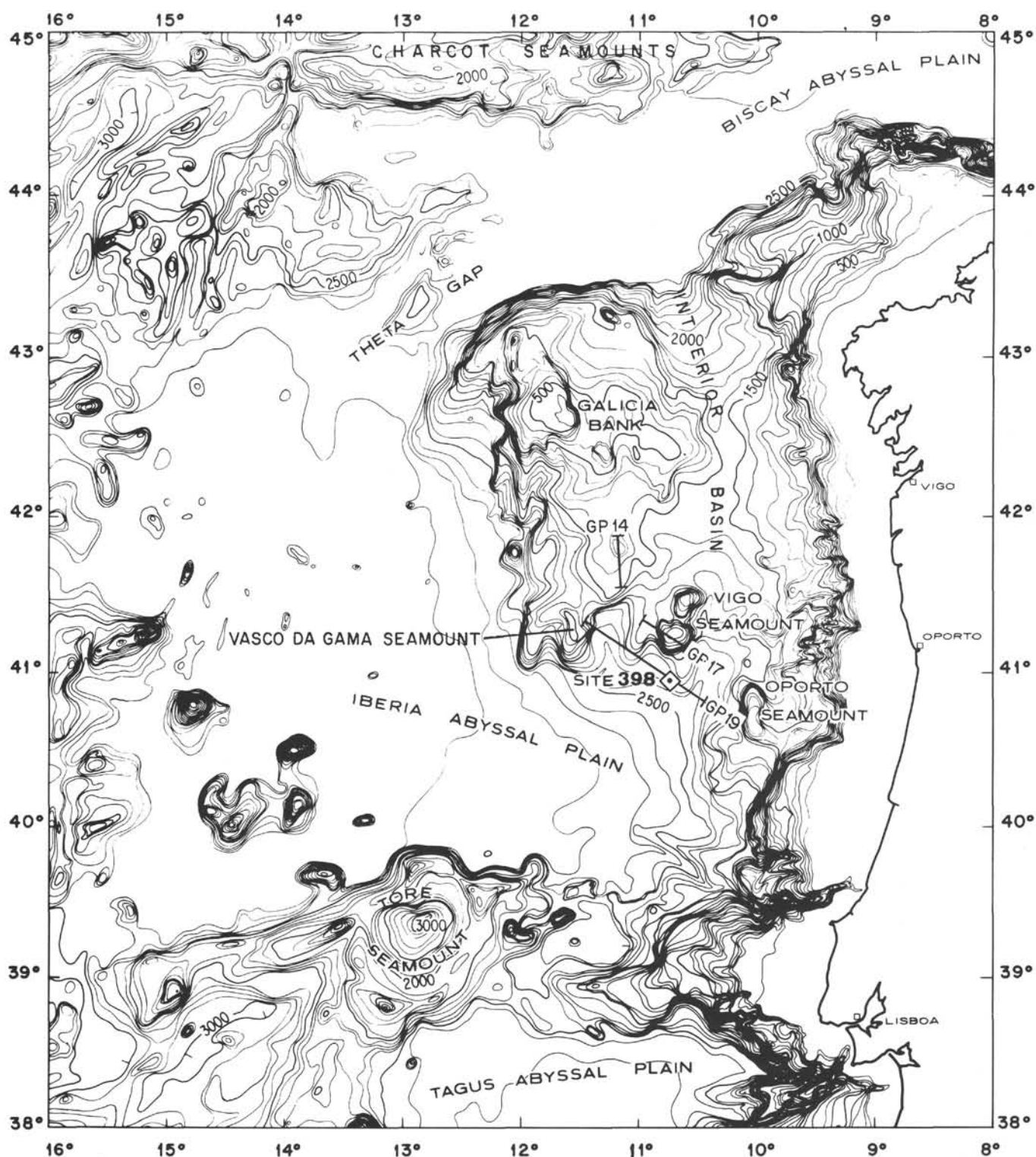


Figure 35. Bathymetric map of the Galicia Bank area (Laughton et al., 1975) in corrected fathoms and position of Site 398.

top of the formation, indicating that sedimentation occurred during tilting motion of basement blocks.

Formation 3 is generally transparent or slightly layered and fills in depressions; it differs from formation 4 by less inclined or horizontal bedding. Formation 3 may be absent on the tops of structural highs.

Formation 2 seems to have been deposited, in many cases, on almost flat topography. It is a layered sequence with several good reflectors. Bedding is generally conformable with the lower boundary.

Formation 1 is acoustically transparent or slightly and regularly layered.

## Stratigraphy From Piston Cores, Dredge Samples, and Hole 398D Cores

The above acoustic formations can be related to the lithologic column of Site 398 and to the stratigraphy obtained from core and dredge samples (Dupeuble et al., 1976 and Groupe Galice; de Graciansky and Chenet; Sigal; Maldonado; all, this volume).

On a basis of correspondence between lithologic and acoustic units, stratigraphic and seismic hiatuses, physical properties, mineralogical composition of sediments, and acoustic impedance, we believe that the bottom-most 73 meters were recovered from the sequence beneath the acoustic basement. They consist of marlstone, siltstone, and white indurated limestone of late Hauterivian to early Barremian age. The limestones were deposited under pelagic conditions, and the marlstone and siltstone layers could have been emplaced by low density turbidity currents in a tranquil environment. The limestones were deposited in water shallower than the CCD but at depths probably reaching 2 km at the site location.

Acoustic formation 4, of late Barremian to late Aptian age, consists of sand-silt-clay graded sequences interbedded with thick (1 to 10 m) slumped beds or debris flows. These sequences are the product of redeposition of previous deposits on submarine slopes, on a subsiding sea floor. A stratigraphic break exists in the uppermost Aptian and corresponds both to a sharp lithological change and to a major reflector between formations 4 and 3.

Acoustic formation 3, of early Albian to middle Cenomanian age, is composed of lower to middle Albian laminated dark shales, mostly of continental provenance at its base, followed by middle to upper Albian interbedded dark shales and marlstones, in turn overlain by upper Albian to middle Cenomanian, mostly redeposited, marlstone and chalk of pelagic origin. The widespread hiatus from Cenomanian to lower Senonian separates acoustic formations 3 and 2.

Acoustic formation 2, of Senonian to late Eocene age, consists of two main lithological units, a reddish to yellowish brown marly nannofossil chalk, calcareous mudstone, claystone, and siliceous mudstone in the lower part overlain by siliceous marly nannofossil chalk and mudstone interbedded with turbiditic sand-silt-marl sequences.

Acoustic formation 1, of Oligocene to Recent age, is essentially composed of marly nannofossil ooze, nannofossil ooze, marly nannofossil chalk, and nannofossil chalk with rhythmic bedding.

## The Early Evolution of the North Atlantic: Triassic/Liassic or Older Tensional Episode

The first epoch of rifting of continents in the North Atlantic is still debated, but is probably linked to several tensional phases occurring between Permian to late Lias in the continental Eurasian-American framework (e.g., Arthaud and Matte, 1975; Groupe Galice, this volume), and to the early history of the Mesogean realm

(Aubouin, 1977). As a general rule, the rifting episode is evidenced by thick evaporitic series linked to fast subsidence of continental blocks. On Grand Banks, Jurassic and older formations are preserved in structural basins bounded by basement block-faulting; salt diapirs are present (Daily Oil Bulletin, 1973). In Aquitaine, the Triassic-Liassic sedimentation is characteristic of a subsident basin filled up with thick detrital and evaporitic deposits (Winnock, 1971; Dardel and Rosset, 1971; Winnock et al., 1973). In initial reconstructions (Laughton, 1972; Le Pichon et al., 1971), the Aquitaine Basin could be extended westward through a system of grabens and basins related to the Labrador-Biscay Fault. In the interior basin between Galicia Bank and Iberia, the deepest sedimentary layers may be of Jurassic or older age (Groupe Galice, this volume). Although the thick sedimentary series (with no evidence of salt diapirism detected in seismic profiles) does not necessarily support the contention that this area was affected by a Triassic-Liassic episode of rifting, in the small basins of the continental slope, as between the Porto Seamount and the Portuguese shelf (Montadert et al., 1974; Wilson, 1975; Groupe Galice, this volume), certain sequences are affected by salt diapirism. There is, thus, supportive evidence for the hypothesis that the initial Eurasian-American continent was affected, at least locally, by intense extension and faulting and by an episode of rifting giving rise to subsiding basins filled with Triassic-Liassic evaporites and/or clastic sediments. The westernmost extension of these basins is located east of the eastern limit of the quiet magnetic zone (Figure 36), but cannot be easily traced because of the sedimentary cover which is especially thick in the Iberian Abyssal Plain, south of Galicia Bank. It is difficult to precisely determine the amount of oceanic crust, if any, that was created during this early tensional episode.

## Late Jurassic-Early Cretaceous Tensional Episode

South of Grand Banks, on the western Nova Scotian shelf, a Berriasian/Valanginian hiatus lies within a series of shallow marine deposits (Gradstein et al., 1975). On Grand Banks a major angular unconformity exists at the base of the Cretaceous section. Beneath this unconformity, Jurassic and older formations are preserved in structural basins bounded by basement block-faulted structures (Daily Oil Bulletin, 1973). Coeval tensional episodes have been recognized in the Alpine-Mesogean domain (e.g., Aubouin, 1977).

In the Galicia Bank and Vigo areas, a major tectonic event occurred in the late Jurassic/Early Cretaceous and is apparently the cause of the main morphologic trends of the continental margin (Groupe Galice, this volume). Faulted blocks subsided and rotated along faults of Panamian (or listric) type. Indeed, rotating faults of this type existed both on the Iberian and American margins during this episode (Montadert, Roberts, et al., 1977). Because the lowest 73 meters at Site 398 (drilled into a half-graben structure) seem to have been deposited above the CCD (at a maximum depth of 2000 m), it is

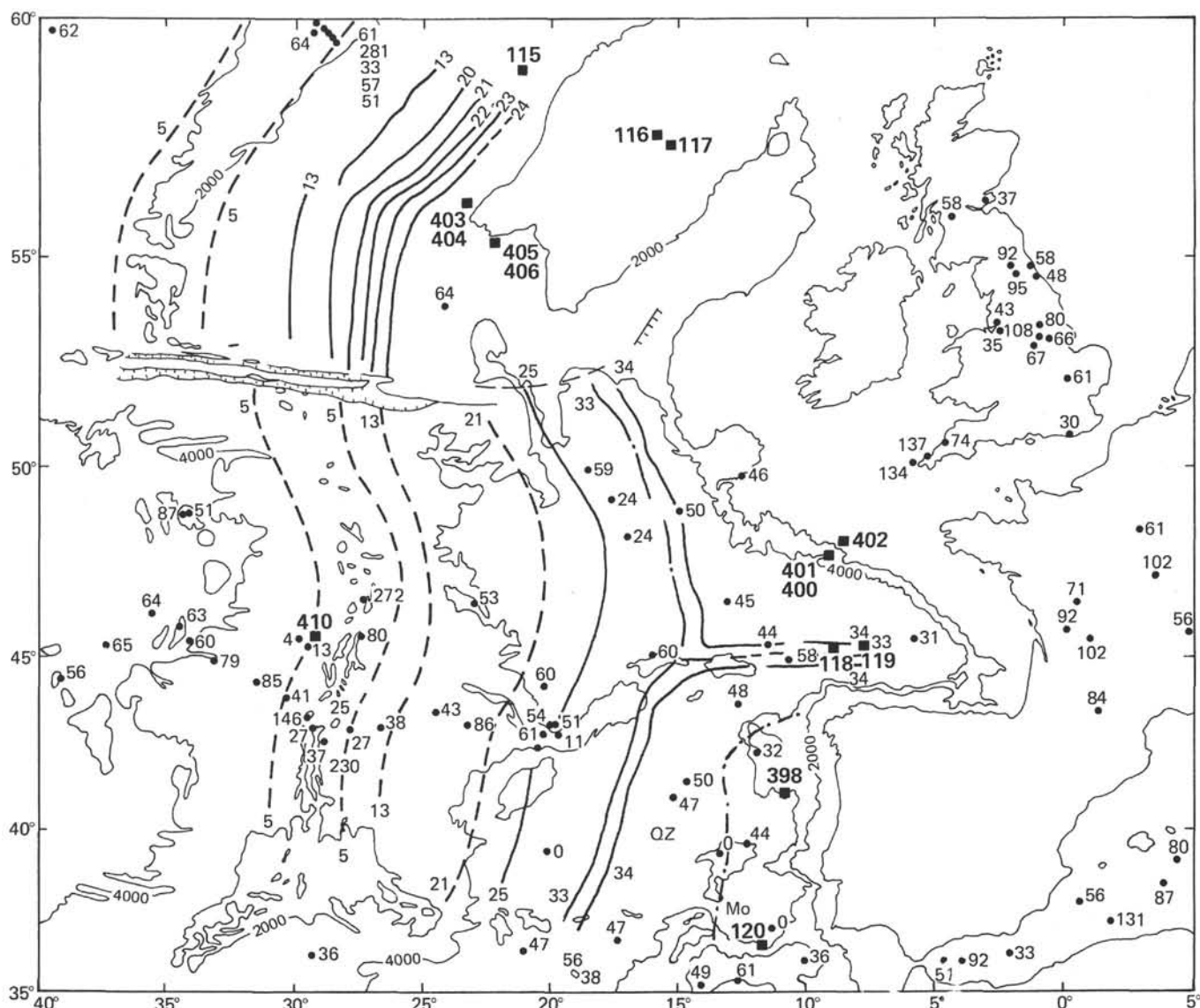


Figure 36. Magnetic lineations in the northeast Atlantic. See text for data sources. Numbered full squares locate DSDP sites.

not possible to distinguish to which of the two tensional episodes the vertical motion can be attributed. Fan-shaped sedimentary features observed in acoustic Formation 4 (Figure 30) show that sedimentation occurred during tilting motion of basement rocks. Borehole data allow only dating of the end of the Upper Jurassic-Late Cretaceous episode as latest Aptian.

The Cretaceous magnetic quiet zone is bounded towards the east by the *J* or *MO* anomaly (Figure 36). East of this limit, the *M* sequence is not observed, but a flat magnetic domain exists which may be related either to a subsided continental area or to the Jurassic magnetic quiet zone. If these assumptions are correct, this would mean that either the Permian to Lias tensional episode has affected a large area between North America and the Iberian Peninsula, with oceanization of continental crust, or, more probably, that an early limited opening occurred during Jurassic time after the Permo-Lias tensional episode. In both hypotheses,

because the *M* sequence appears to be absent, creation of typical oceanic crust between North America and the Iberian Peninsula did not occur before the late Aptian.

### *J*-Anomaly

This marks the beginning of true sea-floor spreading in the northern Atlantic when the paleoenvironmental history of the Tethyan Ocean became independent of the Atlantic evolution. While compressive phases induced the first Alpine deformation, the Atlantic opening occurred.

A first approximate configuration of the landmasses is given in Figure 37. The position of the Iberian Peninsula relative to North America is based on a well-documented definition of the eastern limit of the Cretaceous quiet magnetic zone seaward of the Iberian Peninsula, and on some limited reconnaissance of the *J*-anomaly using available magnetic profiles located east

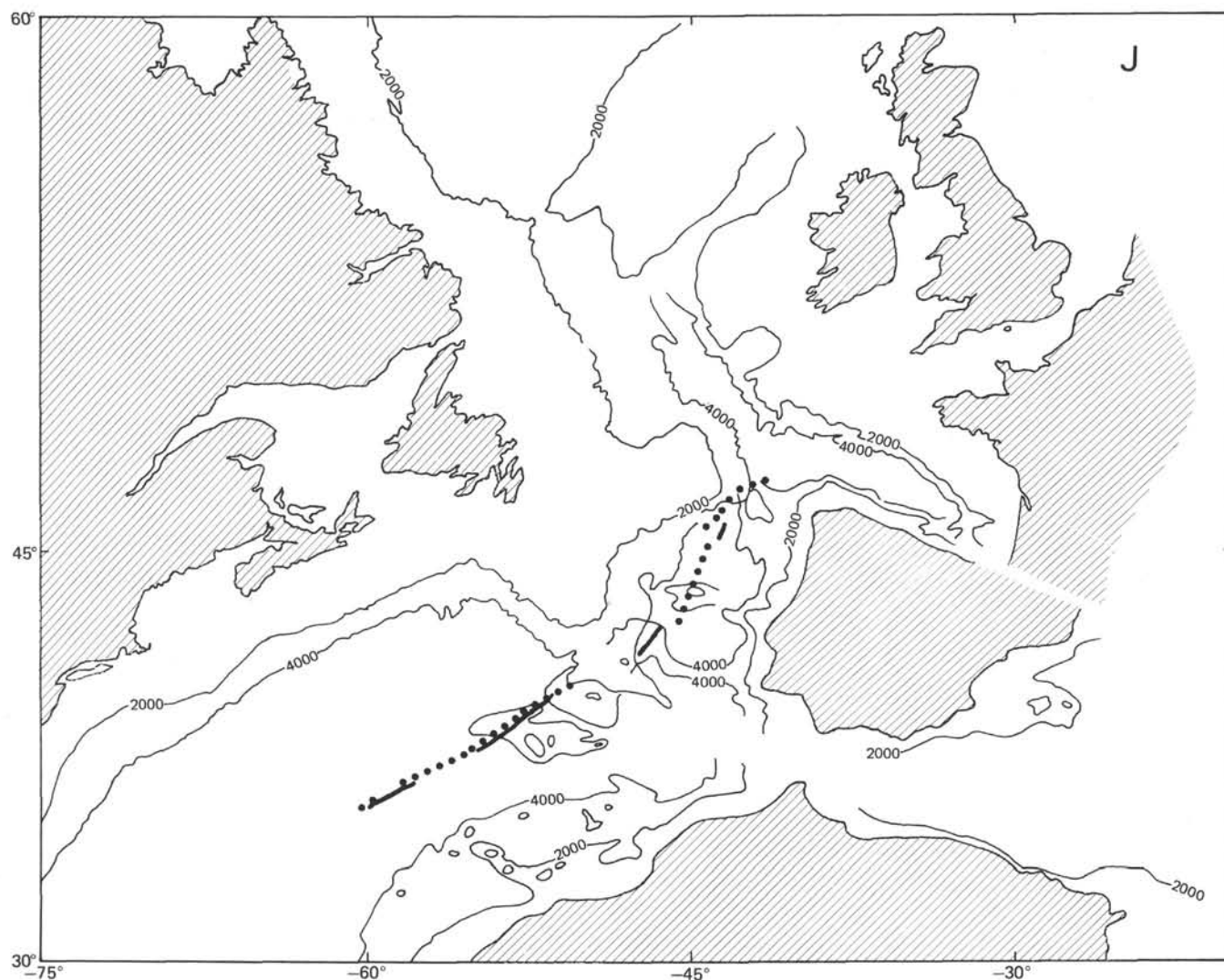


Figure 37. Tentative reconstruction of the positions of the continents at the time of anomaly J (latest Aptian). Bathymetric contours in meters. America is kept fixed. J-anomaly in dotted line on the eastern side and inconspicuous line on the western side of the North Atlantic.

of Grand Banks (Pitman and Talwani, 1972). Positions of Europe and Rockall are those of the initial fit of Le Pichon et al. (1977); data that might give better relative positions of the continents at the time of anomaly J are not available. The fit would be improved by a better definition of the shape of *MO* anomalies on each side of the North Atlantic and by including fracture zone constraints; these have not been considered in Figure 37.

By definition, the *J*-anomaly is associated with topographic features (Pitman and Talwani, 1972) such as the Tore-Madeira Rise on the eastern side of the North Atlantic and the "*J*-Anomaly Ridge" south of Grand Banks and the Newfoundland fracture zone. Ballard et al. (1976) have proposed that these *J*-anomaly twin features were associated with an Azores-like hot spot. Whatever their invoked mode of formation, they would have modified both the tectonic evolution of the nearby continental margins and the style of sedimentation. The change from the Aptian graded sequences,

emplaced by turbidity currents, to the Albian dark shales might thus be explained, as well as the presence of the main seismic discontinuity between acoustic Formations 4 and 3 (Figure 30). The dark shales were deposited on the Armorican margin during middle Aptian time (Montadert, Roberts, et al., 1976) perhaps because the connection between the Iberian Abyssal Plain and the Bay of Biscay was not established north and south of the Flemish Cap-Galicia Bank structural feature at the time of anomaly J.

Since late Aptian, the western continental margin of the Iberian Peninsula subsided because of cooling of the lithosphere as it moved away from the spreading ridge.

#### **Anomaly 34: A Step in the Opening of the North Atlantic**

The trend and length of anomaly 34 on both sides of the North Atlantic have been defined by numerous data. Between the Charlie-Gibbs fracture zone and the

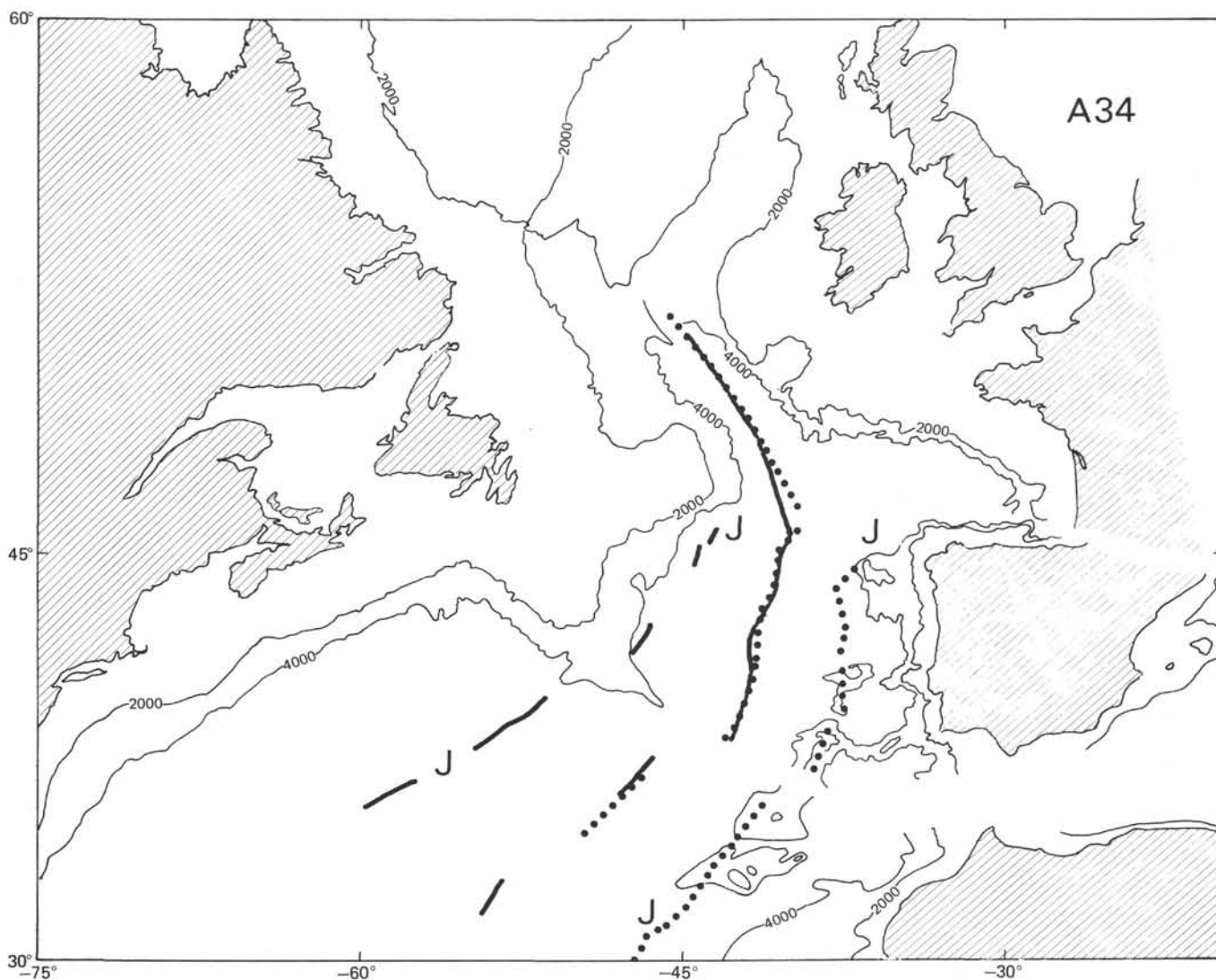


Figure 38. Reconstruction of the position of continents at the time of anomaly 34 (late Santonian). Bathymetric contours in meters. America is kept fixed. Magnetic anomalies J and A 34 in dotted line on the eastern side and in continuous line on the western side of the North Atlantic. Using conventions of Le Pichon et al., (1973), parameters of rotation are: Europe/North America:  $63^{\circ}\text{N}$ ,  $149.3^{\circ}\text{E}$ – $19.0^{\circ}$ ; Iberian Peninsula/North America:  $82.8^{\circ}\text{N}$ ,  $121.3^{\circ}\text{E}$ – $22.6^{\circ}$ .

Azores-Gibraltar line, it is impossible, using the constraints of these two fracture zones, to match the corresponding plate boundaries at the time of anomaly 34 (late Santonian in the van Hinte scale [1976]). Le Pichon and Sibuet (1971) have examined the kinematics of the Eocene episode of compression between the Iberian and European plates and have shown that the boundary between the two plates extended west of the Pyrenées, along the Spanish marginal trench, to end west of King's Trough at a triple junction. Consequently, the positions of anomaly 34 on each side of this plate boundary have been shifted after their creation (Figure 38). Segments of anomaly 34 located north and south of the Charcot and Biscay seamounts, have been unambiguously matched with anomaly 34 on the American side,

using the trend constraints of the Charlie-Gibbs fracture zone and the Azores-Gibraltar line. One of the main kinematic implications is that at the time of anomaly 34, the Bay of Biscay was not completely created, which is supported by the fact that anomalies 34 and 33 might be present in the central part of the Bay of Biscay (Williams, 1975).

In late Santonian, the open sea was well developed south of the Charlie-Gibbs fracture zone ( $53^{\circ}\text{N}$ ). The abrupt appearance of primary minerals formed in upstream soils (illite, chlorite, sandy silicate, kaolinite) in upper Santonian to lower Maestrichtian sediments, is probably due to the supply inherited from high latitudes and transported by the just established north-south oceanic circulation (Chamley et al., this volume). This

oceanic circulation could have been instituted at the time of the early opening of the Labrador Sea (Le Pichon et al., 1971), i.e., at the time of anomaly 34.

The results of Leg 47B integrated with a tentative reconstruction of the positions of the continents at the time of anomalies 34 (upper Santonian) and MO (upper Aptian), and related to the early history of the opening of the North Atlantic, show that the last subsidence and tilting of blocks associated with the Late Jurassic/Early Cretaceous tensional episode are dated as latest Aptian at Site 398. The beginning of true sea-floor spreading in the northern Atlantic is dated as latest Aptian, and the connection of the North Atlantic Ocean with the Labrador Sea was established by Santonian time.

### ACKNOWLEDGMENTS

The shipboard scientific party thanks particularly the Deep-Sea Drilling Project for systematic on board and shorelab analysis; G. S. Odin (University of Paris, France) for his contribution on zeolite analysis; P. C. de Graciansky (Ecole des Mines, Paris, France) for his valuable contribution in the interpretation of the Mesozoic sequence; C. Latouche, N. Maillet (University of Bordeaux, France), and F. Sommer (Compagnie Française des Pétroles, Bordeaux, France) for providing systematic X-ray mineralogy analysis.

### REFERENCES

- Allen, P., 1972. Wealden detrital tourmaline: implications for northwestern Europe, *J. Geol. Soc.*, v. 128, p. 273-294.
- Alvarez, W. Arthur, M. A., Fischer, A. G., Lowrie, W., Napoleone, G., Premoli Silva, I., and Roggenthen, W. M., 1977. Upper Cretaceous-Paleocene magnetic stratigraphy at Gubbio, Italy. V. Type section for the Late Cretaceous-Paleocene geomagnetic reversal time scale, *Geol. Soc. Am. Bull.*, v. 88, p. 383-389.
- AMOCO, 1973. Regional geology of the Grand Banks offshore exploration staffs, *Canadian Soc. Petrol. Geol. Bull., Contrib. Petrol. Geol.* 21, v. 4, p. 479-503.
- Arthaud, F. and Matte, P., 1975. Late Hercynian wrench faults in southern Europe and northern Africa: geometry and nature of deformation, *Tectonophysics*, v. 25, p. 139-171.
- Arthur, M. A. and Fischer, A. G., 1977. Upper Cretaceous-Paleocene magnetic stratigraphy at Gubbio, Italy: I. Lithostratigraphy and sedimentology, *Geol. Soc. Am. Bull.*, v. 88, p. 367-389.
- Aubouin, J., 1977. Téthys, Atlantique et Pacifique: regard tectonique, *Bull. Soc. Géol. France*, v. 4, p. 170-179.
- Ballard, J. A., Vogt, P. R., and Egloff, J., 1976. The magnetic "J-Anomaly" and associated structures in the North Atlantic, *EOS Trans.*, v. 57, p. 264.
- Berger, W. H., 1970. Biogenous deep-sea sediments: fractionation by deep-sea circulation, *Geol. Soc. Am. Bull.*, v. 81, p. 1385-1402.
- Berger, W. and Johnson, T. C., 1976. Deep-sea carbonates: dissolution and mass wasting on the Ontong-Java Plateau, *Science*, v. 192, p. 863-878.
- Berggren, W. A. and van Couvering, R., 1974. *Geological Newsletter*, v. 1976, p. 322.
- Black, M., Hill, M. M., Laughton, A. S., and Matthews, D. H., 1964. Three non-magnetic seamounts off the Iberian coast, *J. Geol. Soc. London*, v. 120, p. 477-489.
- Blow, W., 1969. Late middle Eocene to Recent planktonic foraminiferal biostratigraphy, *Internat. Conf. Plankt. Microfossils, First, Proc.*, v. 1, p. 199-219.
- Bouma, A. H. and Hollister, C. D., 1973. Deep ocean basin sedimentation, *SEPM Pacific Sect. Short Course. Turbidites and deep-water sedimentation*, p. 79-118.
- Brown, G., 1961. *The X-ray Identification and Crystal Structure of Clay Minerals*: London (Mineral Soc.).
- Bullard, E. C., Everett, J. E., and Smith, A. G., 1965. The fit of the continents around the Atlantic. In Symposium on continental drift, *Phil. Trans. Roy. Soc. London*, v. 258, p. 41-51.
- Cande, S. C. and Kristoffersen, Y., 1977. Late Cretaceous magnetic anomalies in the North Atlantic, *Earth Planet. Sci. Lett.*, v. 35, p. 215-224.
- Cita, M. B., 1973. Pliocene biostratigraphy and chronostratigraphy. In Ryan, W. B. F., Hsü, K. J., et al., *Initial Reports of the Deep Sea Drilling Project*, v. 13: Washington (U.S. Government Printing Office), p. 1045-1065.
- Daily Oil Bulletin, 1973 (April 23). *Regional geology of the Grand Banks*, p. 1-5.
- Dardel, R. A. and Rosset, R., 1971. Histoire géologique et structurale du Bassin de Parentis et de son prolongement en mer. In *Histoire Structurale du Golfe de Gascogne*: Paris (Technip), v. 2, p. 1-28.
- Dean, W. E., Gardner, J. V., Jansa, L. F., Čepek, P., and Seibold, E., 1978. Cyclic sedimentation along the continental margin of northwest Africa. In Lancelot, Y., Seibold, E., et al., *Initial Reports of the Deep Sea Drilling Project*, v. 41: Washington (U.S. Government Printing Office), p. 965-989.
- de Charpal, O., Montadert, L., and Roberts, D., 1978. Rifting, subsidence, and crustal attenuation in the N.E. Atlantic continental margins, *Abstracts of the Second Maurice Ewing Symposium, Implications of Deep Sea Drilling Results in the Atlantic Ocean*, p. 24.
- Donovan, D. T., 1961. Cretaceous of East Greenland. In Raasch, G. O. (Ed.), *Geology of the Arctic*: Toronto (University of Toronto Press), v. 1, p. 274-277.
- Drever, J. I., 1971. Magnesium-iron replacements in clay minerals in anoxic marine sediments, *Science*, v. 172, p. 1334-1336.
- Dupeuble, P. A., Réhault, J. P., Auxière, J. L., Dunand, J. P., and Pastouret, L., 1976. Résultats de dragages et essai de stratigraphie des bancs de Galice et des montagnes de Porto et de Vigo (marge occidentale ibérique), *Marine Geol.*, v. 22, p. M 37-M 49.
- Fischer, A. G. and Arthur, M. A., 1977. Secular variations in the pelagic realm. In Cook, H. E. and Enos, P. (Eds.), *Deep water carbonate environments: SEPM Spec. Publ. No. 25*, p. 19-50.
- Gealy, E. L., 1971. Sound velocity, elastic constants, and related properties of marine sediments in the western equatorial Pacific: Leg 7 *Glomar Challenger*. In Winterer, E. L., Riedel, W. R., et al., *Initial Reports of the Deep Sea Drilling Project*, v. 7, Part 2: Washington (U.S. Government Printing Office), p. 1105-1160.
- Gieskes, J. M., 1974. Interstitial water studies, Leg 25. In Simpson, E. S. W., Schlich, R., et al., *Initial Reports of the Deep Sea Drilling Project*, v. 25: Washington (U.S. Government Printing Office), p. 361-364.
- Gradstein, F. M., Williams, G. L., Jenkins, W. A. M., and Ascoli, P., 1975. Mesozoic and Cenozoic stratigraphy of

- the Atlantic continental margin, Eastern Canada. In Yorath, C. J., Parker, E. R., and Glass, D. J. (Eds.), *Canada's Continental Margins and Offshore Petroleum Exploration*: Calgary (Canadian Society of Petroleum Geologists), p. 103-132.
- Hallam, A., 1971. Facies analysis of the Lias of West Central W. Germany and Portugal, *N. Jahrb. Geol. Pal.*, p. 226-265.
- Jansa, L. F. and Wade, J., 1975. Geology of the continental margin off Nova Scotia and Newfoundland: Offshore geology of Eastern Canada, *Geol. Surv. Canada, Paper 74-370*, v. 2, p. 51-105.
- Kinsman, D. S. S., 1975. Rift Valley basins and sedimentary history of trailing continental margins. In Fischer, A. G. and Judson, S. (Eds.), *Petroleum and global tectonics*: Princeton (Princeton University Press), p. 83-126.
- Laughton, A. S., 1971. South Labrador Sea and the evolution of the North Atlantic, *Nature*, v. 232, p. 612-617.
- , 1972. The southern Labrador Sea — A key to the Mesozoic and early Tertiary evolution of the North Atlantic. In Peterson, M. N. A., Edgar, N. T., et al., *Initial Reports of the Deep Sea Drilling Project*, v. 2: Washington (U.S. Government Printing Office), p. 1155-1179.
- Laughton, A. S., Berggren, W. A., et al., 1972. *Initial Reports of the Deep Sea Drilling Project*, v. 12: Washington (U.S. Government Printing Office).
- Le Pichon, X. and Sibuet, J. C., 1971. Western extension of boundary between European and Iberian plates during the Pyrenean orogeny, *Earth Planet. Sci. Lett.*, v. 12, p. 83-88.
- Le Pichon, X., Hyndman, R., and Pautot, G., 1971. Geophysical study of the opening of the Labrador Sea, *J. Geophys. Res.*, v. 76, p. 4724-4743.
- Le Pichon, X., Francheteau, J., and Bonnin, J., 1973. Plate tectonics. In *Developments in geotectonics*: Amsterdam (Elsevier), v. 6, p. 300.
- Le Pichon, X., Sibuet, J. C., and Francheteau, J., 1977. The fit of the continents around the North Atlantic Ocean, *Tectonophysics*, v. 38, p. 169-205.
- Manheim, F. T., 1976. Interstitial waters of marine sediments. In Riley, J. P. and Chester, R. (Eds.), *Chemical oceanography*: London (Academic Press), v. 6, p. 115-187.
- Manheim, F. T. and Sayles, F. L., 1974. Composition and origin of interstitial waters of marine sediments based on deep-sea drill cores. In Goldberg, E. D. (Ed.), *The sea*: New York (John Wiley and Sons), v. 5, p. 527-568.
- Montadert, L., Winnock, E., Delteil, J. R., and Grau, G., 1974. Continental margins of Galicia-Portugal and Bay of Biscay. In Burk, C. A. and Drake, C. L. (Eds.), *The geology of Continental Margins*: New York (Springer-Verlag), p. 323-342.
- Montadert, L., Roberts, D. G., Auffret, G. A., Bock, W. O., Dupeuble, P. A., Hailwood, E. A., Harrison, W., Kagami, H., Lumsden, D. N., Müller, C., Schnitker, D., Thompson, R. W., Thompson, T. L., Timofeev, P. P., 1976. *Glomar Challenger* sails on Leg 48, *Geotimes*, v. 21, p. 19-23.
- Montadert, L., Roberts, D. G., et al., 1977. The nature of the continent-ocean boundary, Biscay and Rockall (abstract). Meeting on the evolution of passive margins in the light of recent deep drilling results, London, October 19-20.
- Oertel, G., 1956. Transgressions in Malm des Portugiesischen Estramadura, *Geol. Rundsch.*, v. 45, p. 304-314.
- Pautot, G., Auzende, J. M., and Le Pichon, X., 1970. Continuous deep-sea salt layer along North Atlantic margins related to early phase of rifting, *Nature*, v. 227, p. 351-354.
- Pitman, W. C. and Talwani, M., 1972. Sea-floor spreading in the North Atlantic, *Geol. Soc. Am. Bull.*, v. 83, p. 619-649.
- Ramirez de Pozo, R., 1971. Biostratigrafia y microfases del Jurassico y Cretacio del Norte de España (regional Cantabaca), *Mem. Inst. Geol. Min. Espana, Madrid*.
- Ruffman, A. and van Hinte, J. E., 1973. Orphan Knoll — a "chip" off the North American "Plate." In Hood, P. J. (Ed.), *Earth science symposium on offshore eastern Canada*: *Geol. Soc. Canada, Paper 71-23*, p. 407-449.
- Ryan, W. B. F., Cita, M. B., Rawson, D., Burkle, L. H., and Saito, T., 1974. A paleomagnetic assignment of Neogene stage boundaries and the development of isochronous datum planes between the Mediterranean, the Pacific and Indian oceans in order to investigate the response of the world ocean to the Mediterranean "salinity crisis," *Riv. Ital. Paleontol.*, v. 80, p. 631-688.
- Savin, S. M., Douglas, R. G., and Stehli, F. G., 1975. Tertiary marine paleotemperatures, *Geol. Soc. Am. Bull.*, v. 86, p. 1499-1510.
- Schlanger, S. O. and Douglas, R. G., 1974. The pelagic ooze-chalk-limestone transition and its implications for marine stratigraphy. In Hsü, K. J., Jenkyns, H. C. (Eds.), *Pelagic sediments: on land and under the sea*: *Spec. Publ. Int. Assoc. Sedimentol.*, v. 1, p. 117-148.
- Sherwin, D. F., 1973. Scotian shelf and Grand Banks. In Grossan, M. (Ed.), *The future petroleum provinces of Canada*: *Canadian Soc. Petrol. Geol.*, p. 519-559.
- Sclater, J. G., Hellinger, S., and Tapscott, C., 1977. The paleobathymetry of the Atlantic Ocean from the Jurassic to the present, *J. Geol.*, v. 85, p. 509-552.
- Schlee, J., Behrendt, J. L., Grow, J. A., Robb, J. M., Mat-tick, R. E., Taylor, P. T., and Lawson, B. J., 1976. Regional geologic framework off northeastern United States, *Am. Assoc. Petrol. Geol. Bull.*, v. 60, p. 926-951.
- Thorez, J., 1975. *Phyllosilicates and clay minerals*: Dison (Lelotte Edit), 582 p.
- Tucholke, B. E., Vogt, P. R., et al., 1979. *Initial Reports of the Deep Sea Drilling Project*, v. 43: Washington (U.S. Government Printing Office).
- van Andel, T. H., 1975. Mesozoic/Cenozoic calcite compensation depth and the global distribution of calcareous sediments, *Earth Planet. Sci. Lett.*, v. 26, p. 187-195.
- van Hinte, J. E., 1976. A Cretaceous time scale, *Am. Assoc. Petrol. Geol. Bull.*, v. 60, p. 498-516.
- van Houten, F. B., 1977. Triassic-Liassic deposits of Morocco and eastern North America, *Am. Assoc. Petrol. Geol. Bull.*, v. 61, p. 79-99.
- van der Linden, W. J. M., 1975. Mesozoic and Cenozoic opening of the Labrador Sea, the North Atlantic and the Bay of Biscay, *Nature*, 253, p. 320-324.
- von Rad, U. and Rösch, H., 1972. Mineralogy and origin of clay minerals, silica and authigenic silicates in Leg 14 sediments. In Hayes, D. E., Pimm, A. C., et al., *Initial Reports of the Deep Sea Drilling Project*, v. 14: Washington (U.S. Government Printing Office), p. 717-751.
- Williams, C. A., 1975. Sea-floor spreading in the Bay of Biscay and its relationship to the North Atlantic, *Earth Planet. Sci. Lett.*, v. 24, p. 440-456.

- Williams, C. A. and McKenzie, D. P., 1971. The evolution of the northeast Atlantic, *Nature*, v. 232, p. 168-173.
- Williams, G. L., 1972. Palynological analysis, AMOCO-10C, A-1, Eider, Grand Banks, Newfoundland, *Geol. Survey Canada Internat. Rept.*, EPGS-PAC, p. 8-72 GLW.
- Wilson, R. C. L., 1975. Atlantic opening and Mesozoic continental margin basins of Iberia, *Earth Planet. Sci. Letters*, v. 25, p. 33-43.
- Winnock, E., 1971. Géologie succincte du Bassin d'Aquitaine (contribution à l'histoire du Golfe de Gascogne). In *Histoire Structurale du Golfe de Gascogne*: Paris (Technip), v. 1, p. 1-30.
- Winnock, E., Fried, E., and Kieken, M., 1973. Les caractéristiques des sillons aquitains, *Bull. Soc. Geol. France*, v. 1, p. 1-76.
- Worsley, T., 1974. The Cretaceous-Tertiary boundary event in the ocean, *SEPM Spec. Publ. No. 20*, p. 94-125.
- Ziegler, W. H., 1975. Outline of geological history of North Sea. In Woodland, A. W. (Ed.), *Petroleum and continental shelf of north-west Europe, 1*, *Geology*: New York (Plenum Press), p. 31-42.

CORE DESCRIPTIONS, SITE 398<sup>1</sup>

SITE 398

SITE 398		HOLE		CORE 1		CORED INTERVAL: 15.5-25.0 m	
TIME-ROCK UNIT	BIOSTRAT ZONE	FOSSIL CHARACTER		SECTION	METERS	GRAPHIC LITHOLOGY	LITHOLOGIC DESCRIPTION
		FORAMS	NANNOS				
PLEISTOCENE	NN 20 N 22	Ae <sup>+</sup> Cg		1	0.5		MARLY NANNO OOZE, 5Y7/2 (yellowish gray) homogeneous, sticky, no obvious structure
				2	1.0		
							SS (5.20, 75) 63% nannos 30% clay mins. 4% forams 1% quartz 1% carb. unspec. 1% pellets tr. mica tr. dolomite tr. sponge spics. tr. pyrite

Explanatory notes in Chapter 1

SITE 398		HOLE		CORE 2		CORED INTERVAL: 25.0-34.5 m	
TIME-ROCK UNIT	BIOSTRAT ZONE	FOSSIL CHARACTER		SECTION	METERS	GRAPHIC LITHOLOGY	LITHOLOGIC DESCRIPTION
		FORAMS	NANNOS				
PLEISTOCENE	NN 20	Ae <sup>+</sup> Cg		1	0.5	VOID	General: soft MARLY NANNO OOZE, lt. ol. gray to white, variable total carbonate, disturbed by drilling, many laminated intervals, occasional dark discolorations due to pyrite and/or organic material
				2	1.0		
							SS: 1-92 [5, 40, 55] 44% clay 20% nannos 20% carb. unspec. 5% quartz 3% mica 3% forams 3% pellets (fecal) 1% volc. glass 1% pyrite tr. feldspar, dolom. tr. spics.
							pyritized burrow filling alternating layers of N-8 and 5Y5/2 w/0.2-5cm laminae, organic (blk) layers w/organic pyrite-filled blebs
							blk. organic specs
							SS: (3-47) [80, 10, 10] 54% qtz 10% nannos 8% feldspar 5% mica 5% glauconite 5% forams 5% carb. unspec. 5% clay 1% dolom. 1% heavy mins. (hypersthene) 1% volc. glass
							quartz sand turb (?) no obvious grading
							occasional faint lamination & dk. organic or pyrite specs
							occasional 5Y5/2 laminae, gradational at top
							lt. ol. gray at top and bottom of interval, grading to 5Y4/2 towards the center, plastic, highly deformed w/smeared N-8, no obvious laminae
							COLORS 1 lt. ol. gray 5Y5/2 2 lt. gray N-8 3 white N-9 4 med. ol. gray 5Y4/2
							GRAIN SIZE 3-18 = 2, 33, 65
							SHIPBOARD 2-21 24 0.4 3-113 67 0.2 3-148 13 0.6
							SHOREBASED 3-76 68 0.2 5-58 8 0.2

<sup>1</sup> Information on core description sheets represents field notes taken aboard ship under time pressure. Some of this information has been refined in accord with postcruise findings, but production schedules prohibit definitive correlation of these sheets with subsequent findings. Thus the reader should be alerted to the occasional ambiguity or discrepancy.

SITE 398 HOLE		CORE 3		CORED INTERVAL: 34.5-44.0 m				
TIME-ROCK UNIT	BIOSTRAT ZONE	FOSSIL CHARACTER				SECTION METERS	GRAPHIC LITHOLOGY	DRILLING DISTURBANCE SERIES

Explanatory notes in Chapter 1

SITE 398 HOLE			CORE 4		CORED INTERVAL: 120.0-126.5 m			
TIME-ROCK UNIT	BIOSTRAT ZONE	FOSSIL CHARACTER			SECTION METERS	GRAPHIC LITHOLOGY	CORRELATION DISTURBANCE SEDIMENTARY LITHOLOGIC SAMPLE	LITHOLOGIC DESCRIPTION
		FORAMS	NANNOS	RADS				
PLIOCENE — PLEISTOCENE	N 19-20 NN 18-19 <i>Pseudomillammina lananensis</i> <i>Planorbina browni</i>	Ag	Ag		1			General Description: NANNO OOZE w/limited MARLY NANNO OOZE and FORAM NANNO OOZE, generally lt. shades of gray w/darker laminae of organic and/or pyrite-rich sediment; core disturbed w/mud balls or clasts of 5Y5/2 (lt.ol.gray); bioturbation limited
		Ag	Ag					
		Ag	Ag		2			Smear (3-102) [5.5,90] 70% nannos 18% clay 5% forams 3% carb.unspec. 2% dolomite 2% pyrite tr. quartz,mica, heavy mins.
		Ag	Ag					
		Ag	Ag		3			Smear (4-56) [15.20,65] 55% nannos 20% clay 15% forams 4% carb.unspec. 2% fecal pellets 1% dolomite 1% quartz 1% mica tr. glauconite, pyrite, diatoms
		Ag	Ag					
		Ag	Ag		4			Smear (4-98) [5.35,60] 40% nannos 32% clay 15% quartz 3% silic.unspec. 2% mica 2% pellets 2% dolomite 2% pyrite 1% heavy mins
		Ag	Ag					
		Ag	Ag		5			GRAIN SIZE 3-73 = 1.34,65
		Ag	Ag					
								</

SITE 398 HOLE A CORE 1 CORED INTERVAL: 172.5-182.0 m																																																																																																																																																																																																																																																																																																																																																																																																																																																																																																																																																																																																																																																																																																																																																																																																																																																																																																																																																																																																																																																																																																																																																																																																																														
TIME-ROCK UNIT	BIOSTRAT ZONE	FOSSIL CHARACTER			SECTION METERS	GRAPHIC LITHOLOGY	DRILLING DISTURBANCE	SEDIMENTARY STRUCTURE	LITHOLOGIC SAMPLE	LITHOLOGIC DESCRIPTION																																																																																																																																																																																																																																																																																																																																																																																																																																																																																																																																																																																																																																																																																																																																																																																																																																																																																																																																																																																																																																																																																																																																																																																																																				
		FORAMS	NANNOS	RADS																																																																																																																																																																																																																																																																																																																																																																																																																																																																																																																																																																																																																																																																																																																																																																																																																																																																																																																																																																																																																																																																																																																																																																																																																										
PLIOCENE	N 19-20	NN 16(7)	<i>Dicouster auroueus</i>	Ag	Ag						General Description: NANNO OOZE, lt. gray, homogeneous, few laminations; numerous black specs of pyrite-rich blebs  SS: (1-11) [0.10, 90] 54% nannos 40% clay 2% qtz. 2% carb.unspec. 2% forams tr.mica, heavy mins., pyrite, dolomite sponge spics.  SS: (1-48) [5.30, 65] 81% nannos 10% clay 5% forams 2% carb.unspec. 1% quartz 1% mica tr. heavy mins., glauconite, sponge spics  SS: (3-68) [3.30, 67] 52% nannos 30% clay 8% quartz 5% carb.unspec. 3% forams 1% feldspar 1% mica tr. mag. apatite, tourmaline tr. glauconite, pyrite, diatoms  SS: (4-21) [1.20, 79] 65% nannos 20% clay 5% quartz 3% forams 3% carb.unspec. 1% pyrite 1% feldspar 1% mica 1% magnetite. 1% zircon tr. glaucon. sponge spics.  GRAIN SIZE 5-78 = 2,26,72  SHIPBOARD 1-64 64 0.2 SHOREBASED 5-89 68 0.1 6-39 73 0.1																																																																																																																																																																																																																																																																																																																																																																																																																																																																																																																																																																																																																																																																																																																																																																																																																																																																																																																																																																																																																																																																																																																																																																																																																			
				Ag	Ag																																																																																																																																																																																																																																																																																																																																																																																																																																																																																																																																																																																																																																																																																																																																																																																																																																																																																																																																																																																																																																																																																																																																																																																																																									</

SITE 398 HOLE B		CORE 1		CORED INTERVAL: 229.5-239.0 m																																							
TIME-ROCK UNIT	BIOSTRAT ZONE	FOSSIL CHARACTER			SECTION METERS	GRAPHIC LITHOLOGY	DRILLING LOG CORRELATION STRUCTURE LITHOLOGY SAMPLE	LITHOLOGIC DESCRIPTION																																			
		FORAMS	NANNOS	RADS																																							
PLIOCENE	NN 12	<i>Ceratolithus tricorniculatus</i>	Cg	Ag	1		50	General Description: NANNO OOZE, 588/1 (blu. white) alternating w/N9(white)w/sharp contacts, thickness of each varying from 5 to 50cm at top of core, increasing to 20 to 100 cm at bottom; slightly bioturbated throughout w/Chondrites and Mycellia, some halo mottles; numerous thin laminae and isolated blebs of 5GY5/2 (grn. yellow) and 5G6/1 enriched in pyrite and organic material																																			
									Cg	Ag	2		60	SS: (57) [4.6, 90] 65% nannos 29% clay 2% forams 2% carb.unspec. 1% dolomite 1% quartz tr. heavy mins. tr. glauconite, pyrite sponge spics.																													
															Cg	Ag	3		100	SS: (59) [4.10, 86] 65% nannos 26% clay 5% pyrite(1/2 pyrite, 1/2 organic??) 2% forams 2% fecal pellets 1% carb.unspec. 1% dolomite tr. qtz., heavy mins. sponge spics.																							
																					Cg	Ag	4		128	SS: (2-60) [5.10, 85] 65% nannos 28% clay 4% forams 1% carb.unspec. 1% pyrite 1% quartz tr. mica, heavy mins..glauconite																	
																											Cg	Ag	5		103	SS: (6-2) [2.10, 88] 75% nannos 17% clay 2% quartz 2% pyrite 2% forams 1% heavy mins. 1% carb.unspec. tr. mica											
																																	Cg	Ag	6		34	GRAIN SIZE 3-36 = 1.33, 66 CaCO <sub>3</sub> % C <sub>org</sub> % SHOREBASED 3-66 74 0.1 6-27 80 0.1					
																																							Cg	Ag	7		CC

Explanatory notes in Chapter 1

SITE 398 HOLE C				CORE 1		CORED INTERVAL: 0.0-79.0 m					
TIME-ROCK UNIT	BIOSTRAT ZONE	FOSSIL CHARACTER			SECTION	METERS	GRAPHIC LITHOLOGY	DRILLING DISTURBANCE	SYMBOLS	LITHOLOGIC SAMPLE	LITHOLOGIC DESCRIPTION
		FORAMS	NANNOS	RADS							
PLEISTOCENE	NN 19-20	C <sub>0</sub>			1	0.5					MARLY NANNO OOZE-Bluish white to light bluish gray 5B7/1-5B9/1 laminated with purplish gray organic streaks Greenish gray 5GY6/1 organic streaks & mottles  SS:(9) [5,22,73] 65% nannos 31% clay 2% forams 1% quartz 1% mica tr.feldspar.volc. glass, carb. un- spec.
					2	1.0					

Explanatory notes in Chapter 1

SITE 398 HOLE D CORE 1 CORED INTERVAL: 0.0-9.5 m									
TIME-ROCK UNIT	BIOSTRAT ZONE	FOSSIL CHARACTER			SECTION METERS	GRAPHIC LITHOLOGY	DRILLING DISTURANCE	STRUCTURE	LITHOLOGIC SAMPLE
		FORAMS	NANNOS	RADS					
					0.5				
					1				
									NO RECOVERY

SITE 398 HOLE D CORE 2 CORED INTERVAL: 271.0-280.5 m										
TIME-ROCK UNIT	BIOSTRAT ZONE	FOSSIL CHARACTER			SECTION METERS	GRAPHIC LITHOLOGY	DRILLING DISTURANCE	SEDIMENTARY LITHOLOGIC SAMPLE	LITHOLOGIC DESCRIPTION	
		FORAMS	NANNOS	RADS						
PLIOCENE <i>Ceratosiſſus ericomytilatus</i>	NN 12 N 19-20					VOID				
		Aa <sup>+</sup>			0.5				0 to 2-40:MARLY NANNO OOZE alternating 5GY8/1(lt.grn. gray) and 5GY6/1(grn.gray) and 5Y5/2(lt.ol.gray)with limited NANNO OOZE,contacts btw units sharp at base of 5Y5/2 but gradational at top and bottom of 5GY6/1 and 8/1;occasional thin laminae associated w/darker MARLY NANNO OOZE (5Y5/2) and dk. grn.laminae(diagenetic?) w/ gray,more organic-rich intervals,burrowed thruout,moderate to intense,some pyritic burrow fillings(Chondrites, Mycellia)w/halo & composite burrows	SS:ave.1-24,1-29, 1-64,1-85,1-23 [5,15,80] 45% clay 37% nannos 4% dolomite 3% forams 3% quartz 2% carb.unspec. 2% heavy mins. 2% mica 2% fecal pellets 2% pyrite tr.sponge,organic matter
		Aa <sup>-</sup>			1.0					
					2					
		Aq <sup>+</sup>								
		Aq <sup>-</sup>								
		Cg <sup>+</sup>								
		Cg <sup>-</sup>								
		Cl <sup>+</sup>								
		Cl <sup>-</sup>								

Explanatory notes in Chapter 1

SITE 398 HOLE D CORE 3 CORED INTERVAL: 318.5-328.0 m									
TIME-ROCK UNIT	BIOSTRAT ZONE	FOSSIL CHARACTER			SECTION METERS	GRAPHIC LITHOLOGY	DRILLING DISTURANCE	STRUCTURE	LITHOLOGIC SAMPLE
		FORAMS	NANNOS	RADS					
LATE MIOCENE <i>Dicoustea onizaria</i>	NN 10 (?) N 17								
<p>General Description: MARLY NANNO OOZE Rhythmic sequence of beds with sharp, but burrowed basal contacts, generally a color &amp; CaCO<sub>3</sub> content gradation from base to top. 5GY8/1 (lt. grn. gray) at base becoming lighter upward to 5B91/1 (lt. bluish white) and N-9 (white) (see SS:2-55) less calcareous (more clay rich) at base (see SS:6-31). Intensely burrowed thruout, common unidentifiable mottles &amp; halo burrows, also <i>zoophycus</i>, chondrites, &amp; numerous composite burrows. Material from base of rhythm burrowed downward into underlying lter. colored chalk usually as much as 10cm. Diagenetic laminae (see SS:3-102) present in assoc. with more organic rich mottles or intervals, usually above. approx. 5mm outward from organic layer. Laminae &lt;1mm thick, generally dk. green</p> <p>SS: 2-55 [1, 20, 79] 65% nannos 23% clay 5% quartz 3% forams 3% carb. unspec. 1% dolomite tr. pyrite, zeolite, mica, organic matter</p> <p>SS: 3-102 [0, 10, 90] 80% pyrite 10% nannos 5% clay 3% quartz 2% carb. unspec. tr. mica</p> <p>SS: 6-31 [3, 15, 82] 58% clay 30% nannos 4% quartz 3% dolomite 2% carb. unspec. 2% heavy mins. tr. mica, glaucon., forams, sponge spics. 1% pellets</p> <p>Colors 1 lt. grn. gray (5GY8/1) 2 white (N9)</p> <p>GRAIN SIZE 3-21 = tr. 29, 71</p> <p>CaCO<sub>3</sub> % C<sub>org</sub> % SHIPBOARD 2-11 65 SHOREBASED 3-20 72 0.1</p>									

Explanatory notes in Chapter 1

SITE 398

SITE 398 HOLE D CORE 6 CORED INTERVAL: 413.5-423.0 m

TIME-ROCK UNIT	BIOSTRAT ZONE	FOSSIL CHARACTER			SECTION	METERS	GRAPHIC LITHOLOGY	DRILLING DISTURBANCE	SEDIMENTARY STRUCTURES	LITHOLOGIC SAMPLE	LITHOLOGIC DESCRIPTION																																																																																																																																																																																																																																																																																																																																																																																																																																																																																																																						
		FORAMS	NANNOS	RADS																																																																																																																																																																																																																																																																																																																																																																																																																																																																																																																													
MIDDLE MIOCENE	NN 6 N 11-12	Rf	Rf	Rf	Rf	Rf	Rf	Rf	Rf	Rf	Rf	Rf	Rf	Rf	Rf	Rf	Rf	Rf	Rf	Rf	Rf	Rf	Rf	Rf	Rf	Rf	Rf	Rf	Rf	Rf	Rf	Rf	Rf	Rf	Rf	Rf	Rf	Rf	Rf	Rf	Rf	Rf	Rf	Rf	Rf	Rf	Rf	Rf	Rf	Rf	Rf	Rf	Rf	Rf	Rf	Rf	Rf	Rf	Rf	Rf	Rf	Rf	Rf	Rf	Rf	Rf	Rf	Rf	Rf	Rf	Rf	Rf	Rf	Rf	Rf	Rf	Rf	Rf	Rf	Rf	Rf	Rf	Rf	Rf	Rf	Rf	Rf	Rf	Rf	Rf	Rf	Rf	Rf	Rf	Rf	Rf	Rf	Rf	Rf	Rf	Rf	Rf	Rf	Rf	Rf	Rf	Rf	Rf	Rf	Rf	Rf	Rf	Rf	Rf	Rf	Rf	Rf	Rf	Rf	Rf	Rf	Rf	Rf	Rf	Rf	Rf	Rf	Rf	Rf	Rf	Rf	Rf	Rf	Rf	Rf	Rf	Rf	Rf	Rf	Rf	Rf	Rf	Rf	Rf	Rf	Rf	Rf	Rf	Rf	Rf	Rf	Rf	Rf	Rf	Rf	Rf	Rf	Rf	Rf	Rf	Rf	Rf	Rf	Rf	Rf	Rf	Rf	Rf	Rf	Rf	Rf	Rf	Rf	Rf	Rf	Rf	Rf	Rf	Rf	Rf	Rf	Rf	Rf	Rf	Rf	Rf	Rf	Rf	Rf	Rf	Rf	Rf	Rf	Rf	Rf	Rf	Rf	Rf	Rf	Rf	Rf	Rf	Rf	Rf	Rf	Rf	Rf	Rf	Rf	Rf	Rf	Rf	Rf	Rf	Rf	Rf	Rf	Rf	Rf	Rf	Rf	Rf	Rf	Rf	Rf	Rf	Rf	Rf	Rf	Rf	Rf	Rf	Rf	Rf	Rf	Rf	Rf	Rf	Rf	Rf	Rf	Rf	Rf	Rf	Rf	Rf	Rf	Rf	Rf	Rf	Rf	Rf	Rf	Rf	Rf	Rf	Rf	Rf	Rf	Rf	Rf	Rf	Rf	Rf	Rf	Rf	Rf	Rf	Rf	Rf	Rf	Rf	Rf	Rf	Rf	Rf	Rf	Rf	Rf	Rf	Rf	Rf	Rf	Rf	Rf	Rf	Rf	Rf	Rf	Rf	Rf	Rf	Rf	Rf	Rf	Rf	Rf	Rf	Rf	Rf	Rf	Rf	Rf	Rf	Rf	Rf	Rf	Rf	Rf	Rf	Rf	Rf	Rf	Rf	Rf	Rf	Rf	Rf	Rf	Rf	Rf	Rf	Rf	Rf	Rf	Rf	Rf	Rf	Rf	Rf	Rf	Rf	Rf	Rf	Rf	Rf	Rf	Rf	Rf	Rf	Rf	Rf	Rf	Rf	Rf	Rf	Rf	Rf	Rf	Rf	Rf	Rf	Rf	Rf	Rf	Rf	Rf	Rf	Rf	Rf	Rf	Rf	Rf	Rf	Rf	Rf	Rf	Rf	Rf	Rf	Rf	Rf	Rf	Rf	Rf	Rf	Rf	Rf	Rf	Rf	Rf	Rf	Rf	Rf	Rf	Rf	Rf	Rf	Rf	Rf	Rf	Rf	Rf	Rf	Rf	Rf	Rf	Rf	Rf	Rf	Rf	Rf	Rf	Rf	Rf	Rf	Rf	Rf	Rf	Rf	Rf	Rf	Rf	Rf	Rf	Rf	Rf	Rf	Rf	Rf	Rf	Rf	Rf	Rf	Rf	Rf	Rf	Rf	Rf	Rf	Rf	Rf	Rf	Rf	Rf	Rf	Rf	Rf	Rf	Rf	Rf	Rf	Rf	Rf	Rf	Rf	Rf	Rf	Rf	Rf	Rf	Rf	Rf	Rf	Rf	Rf	Rf	Rf	Rf	Rf	Rf	Rf	Rf	Rf	Rf	Rf	Rf	Rf	Rf	Rf	Rf	Rf	Rf	Rf	Rf	Rf	Rf	Rf	Rf	Rf	Rf	Rf	Rf	Rf	Rf	Rf	Rf	Rf	Rf	Rf	Rf	Rf	Rf	Rf	Rf	Rf	Rf	Rf	Rf	Rf	Rf	Rf	Rf	Rf	Rf	Rf	Rf	Rf	Rf	Rf	Rf	Rf	Rf

Explanatory notes in Chapter 1


SITE 398 HOLE D CORE 7 CORED INTERVAL: 432.5-442.0 m

TIME-ROCK UNIT	BIOSTRAT ZONE	FOSSIL CHARACTER			SECTION	METERS	GRAPHIC LITHOLOGY	DRILLING DISTURBANCE	SEDIMENTARY STRUCTURES	LITHOLOGIC SAMPLE	LITHOLOGIC DESCRIPTION															
		FORAMS	NANNOS	RADS																						
MIDDLE MIOCENE	NN 7 N 8-10 2	Rf									<p>General Description: Rhythmically bedded sequence similar to Core 6: MARLY NANNO CHALK, greenish gray (5G6/1) to lt. gluish gray (5B7/1) grades upwards to NANNO CHALK, bluish white (5B9/1); silt at base of MARLY NANNO CHALK interval more significant than in Core 6; it is either massive, parallel or cross-laminated, partly indurated, well sorted and possibly graded, occasionally sandy; rhythms average 15 to 30cm in thickness at top of core and increase downwards to 20 to 60cm; intensely bioturbated throughout</p> <p>SS: (1-33) [20.16, 64] 54% clay 20% nannos 20% carb. unspec. 2% forams 2% sponge spics. 2% quartz tr. rads, silico flags, plant debris</p> <p>SS: (1-43) [40.40, 20] 28% carb. unspec. 20% forams 15% clay 10% quartz 5% nannos 5% sponge spics. 3% feldspar 3% volc. glass 5% glauconite 2% heavy mins 2% dolomite 2% rads tr. diatoms</p> <p>SS: (4-107) [30-40-30] 25% clay 23% carb. unspec. 30% forams 5% sponge spics. 5% nannos 1% rads 1% dolomite 1% pyrite 2% glauconite 5% quartz 1% mica 1% heavy mins.</p> <p>GRAIN SIZE 3-58 = 1, 42, 57</p> <table><tr><td></td><td>CaCO<sub>3</sub>%</td><td>C<sub>org</sub>%</td></tr><tr><td>SHIPBOARD</td><td>2-141 69</td><td></td></tr><tr><td></td><td>3-34 37</td><td></td></tr><tr><td>SHOREBASED</td><td>4-58 82</td><td>0.1</td></tr><tr><td></td><td>4-75 50</td><td>0.1</td></tr></table>		CaCO <sub>3</sub> %	C <sub>org</sub> %	SHIPBOARD	2-141 69			3-34 37		SHOREBASED	4-58 82	0.1		4-75 50	0.1
													CaCO <sub>3</sub> %	C <sub>org</sub> %												
												SHIPBOARD	2-141 69													
													3-34 37													
												SHOREBASED	4-58 82	0.1												
													4-75 50	0.1												

SITE 398 HOLE D CORE 8 CORED INTERVAL: 451.5-461.0 m		FOSSIL CHARACTER		SECTION METERS	GRAPHIC LITHOLOGY	LITHOLOGIC DESCRIPTION
TIME-ROCK UNIT	BIOSTRAT ZONE	FORAMS	NANNOS			
EARLY MIOCENE	NN 4-5 <i>Sphenolithus heteromorphus</i>	Cl		0.5		General Description: Rhythmically bedded sequence as in above cores, w/ the addition of siliceous components; SILICEOUS NANNO MUDSTONE, lt. bluish gray (5B7/1) grades upwards to SILICEOUS MARLY NANNO CHALK, lt. bluish white 5B9/1; rhythms average 30cm in thickness; silty laminae often at base of sequence, rarely in lighter layers, massive to laminated, <1cm thick; intensely bioturbated throughout
				1.0		
				1.5		
				2.0		
				2.5		
				3.0		
				3.5		
EARLY MIOCENE	NN 1-2 <i>Trifarina angulosa</i>	Cl		4.0		Sec. 1-110cm to sec. 3-35cm: wavy laminae to flaser structure, no bioturbation; SILICEOUS MARLY NANNO CHALK, lt. olive gray (5Y6/1) alternating w/lt. bluish white (5B9/1) every 4-8cm; siliceous component perhaps most significant in 5Y 6/1 layers
				4.5		
				5.0		
				5.5		
				6.0		
				6.5		
				7.0		
EARLY MIOCENE	NN 1-2 <i>Trifarina angulosa</i>	Cl		7.5		SS: 1-31 [3, 20, 77] 40% nannos 35% clay 10% carb. unspec. 5% rads 5% sponge spics. 2% diatoms 3% forams tr. qtz., mica, tourmaline, magnetite, volc. glass
				8.0		
				8.5		
				9.0		
				9.5		
				10.0		
				10.5		
EARLY MIOCENE	NN 1-2 <i>Trifarina angulosa</i>	Cl		11.0		SS: 5-76 [5, 20, 75] 30% clay 50% nannos 5% carb. unspec. 5% sponge spics. 5% diatoms & rads 3% pellets 2% quartz tr. mica, forams
				11.5		
				12.0		
				12.5		
				13.0		
				13.5		
				14.0		
EARLY MIOCENE	NN 1-2 <i>Trifarina angulosa</i>	Cl		14.5		SS: 2-33 [0, 20, 80] 40% nannos 36% clay 10% carb. unspec. 5% sponge spics. 3% rads 2% diatoms 3% forams 1% quartz tr. mica, heavy mins.
				15.0		
				15.5		
				16.0		
				16.5		
				17.0		
				17.5		
EARLY MIOCENE	NN 1-2 <i>Trifarina angulosa</i>	Cl		18.0		SS: 5-90 [30, 40, 30] 18% quartz 12% clay 20% sponge spics 12% forams 10% rads 10% nannos 10% carb. unspec. 2% feldspar 2% diatoms 2% glauconite 1% dolomite 1% mica tr. volc. glass tr. magnetite, tourmaline
				18.5		
				19.0		
				19.5		
				20.0		
				20.5		
				21.0		
EARLY MIOCENE	NN 1-2 <i>Trifarina angulosa</i>	Cl		21.5		SS: 2-38 [15, 35, 50] 30% nannos 19% clay 15% forams 10% rads 10% sponge spics. 8% carb. unspec. 5% quartz 2% diatoms 1% glauconite tr. tourmaline, magnetite
				22.0		
				22.5		
				23.0		
				23.5		
				24.0		
				24.5		
EARLY MIOCENE	NN 1-2 <i>Trifarina angulosa</i>	Cl		25.0		GRAIN SIZE 3-68 = 1.44, 55
				25.5		
				26.0		
				26.5		
				27.0		
				27.5		
				28.0		
EARLY MIOCENE	NN 1-2 <i>Trifarina angulosa</i>	Cl		28.5		SHIPBOARD 3-70 68 SHOREBASED 1-41 45 0.1 1-60 42 0.1
				29.0		
				29.5		
				30.0		
				30.5		
				31.0		
				31.5		

Explanatory notes in Chapter 1

SITE 398 HOLE D CORE 9 CORED INTERVAL: 470.5-480.0 m		FOSSIL CHARACTER		SECTION METERS	GRAPHIC LITHOLOGY	LITHOLOGIC DESCRIPTION
TIME-ROCK UNIT	BIOSTRAT ZONE	FORAMS	NANNOS			
EARLY MIOCENE	NN 1-2 <i>Trifarina angulosa</i>	Cl		0.5		General Description: Rhythmically bedded sequence similar to Core 8; SILICEOUS NANNO MUDSTONE, greenish gray (5GY6/1 to 5G6/1) grades upwards to SILICEOUS MARLY NANNO CHALK, bluish white to white (5B9/1 to N-9); upwards from the base of each rhythm $\text{CaCO}_3$ content increases and grain size decreases; rhythms average 40cm in thickness, and usually begin at base with current-deposited silts up to 2 cm thick, commonly parallel to cross-laminated with fine sand, and marked by erosional lower contacts; intensely bioturbated thruout with predominance of <i>Zoophycus</i> , w/ lesser <i>Mycella</i> and <i>Helminthoides</i> , burrowing is especially concentrated near base of rhythms, though this may be due to greater visibility because of greatest color contrast near base.
				1.0		
				1.5		
				2.0		
				2.5		
				3.0		
				3.5		
EARLY MIOCENE	NN 1-2 <i>Trifarina angulosa</i>	Cl		4.0		SS: 2-26 [30, 30, 40] 20% nannos 20% sponge spics. 19% clay 10% forams 8% quartz 8% diatoms 5% rads 5% carb. unspec. 2% glauconite 1% dolomite 1% mica 1% heavy mins. (magnetite)
				4.5		
				5.0		
				5.5		
				6.0		
				6.5		
				7.0		
EARLY MIOCENE	NN 1-2 <i>Trifarina angulosa</i>	Cl		7.5		SS: 2-28 [30, 40, 30] 15% nannos 15% quartz 15% sponge spics. 12% clay 8% rads 8% diatoms 8% forams 8% carb. unspec. 3% glauconite 2% feldspar 2% mica 2% (tourmaline magnetite, zircon, pyroxene) 2% dolomite tr. zeolite
				8.0		
				8.5		
				9.0		
				9.5		
				10.0		
				10.5		
EARLY MIOCENE	NN 1-2 <i>Trifarina angulosa</i>	Cl		11.0		SS: 2-37 [3, 17, 80] 50% nannos 31% clay 5% carb. unspec. 3% quartz 3% diatoms 3% rads 3% sponge spics 2% forams tr. mica, heavy mins.
				11.5		
				12.0		
				12.5		
				13.0		
				13.5		
				14.0		
EARLY MIOCENE	NN 1-2 <i>Trifarina angulosa</i>	Cl		14.5		GRAIN SIZE 2-98 = tr, 42, 58
				15.0		
				15.5		
				16.0		
				16.5		
				17.0		
				17.5		
EARLY MIOCENE	NN 1-2 <i>Trifarina angulosa</i>	Cl		18.0		SHIPBOARD 2-94 58 SHOREBASED 2-96 64 0.1
				18.5		
				19.0		
				19.5		
				20.0		
				20.5		
				21.0		

SITE	398	HOLE	D	CORE	10	CORED	INTERVAL:	489.5-499.0 m
TIME-ROCK UNIT	BIOSTRAT ZONE	FOSSIL CHARACTER		SECTION	METERS	GRAPHIC LITHOLOGY	ORIENTED DISTURBANCE SEDIMENTARY STRUCTURE LITHOLOGIC SAMPLE	LITHOLOGIC DESCRIPTION
		FORAMS	NANNOS	RADS				
EARLY MIocene	<i>Buccella frigida</i> <i>abundant</i>	T	C					NANNO CHALK, greenish gray, (5G6/1)
					0.5			
					1			
					1.0			

SITE	398	HOLE	D	CORE	11	CORED INTERVAL:	499.0-508.5 m					
TIME-ROCK UNIT	BIOSTRAT ZONE	FOSSIL CHARACTER				SECTION	METERS	GRAPHIC LITHOLOGY	BRILLIANT DISTURBANCE	SEDIMENTARY STRUCTURE	LITHOLOGIC SAMPLE	LITHOLOGIC DESCRIPTION
		FORAMS	NANNOS	RADS								

Explanatory notes in Chapter 1

SITE	TIME-ROCK UNIT	BIOSTRAT ZONE	HOLE	D	FOSIL CHARACTER	CORE SECTION	METERS	GRAPHIC LITHOLOGY	DRILLING DIFFERENCE	SEDIMENTARY LITHOLOGICAL SAMPLE	LITHOLOGIC DESCRIPTION
					FORAMS NANNOS RADS						
LATE OLGOCENE - EARLY MIOCENE <i>Trochammina inflata</i> - <i>Sphenolithus apiculatus</i>	(OLIGOCENE)	N 2	R <sub>P</sub>				0.5	[Pattern]			General Description: Rhythmically bedded sequence; 1-2mm thick silt-sized interval, pale olive (10Y5/2) usually with erosional lower contact, grades upwards to SILICEOUS MARLY NANNO CHALK, gray to olive gray (5Y5/1 to 5GY6/1); rare white to bluish white (N=9 to 5B7/1) MARLY NANNO CHALK to NANNO CHALK at top of rhythm/bioturbation moderate to intense throughout; rhythms average 12-15cm in thickness.
	NN 1 - NP 25						1.0	[Pattern]			
							2	[Pattern]			Sec. 1, 0-95cm: drilling breccia, white (N=9) NANNO CHALK and greenish gray (5G6/1) MARLY NANNO CHALK
							3	[Pattern] VOID			SS: 2-51, [8, 35, 57] 35% nannos 25% clay 15% sponge spics. 10% quartz 5% carb.unspec. 3% forams 2% rads 1% dolomite 1% feldspar 1% mica 1% heavy mins (magnetite, zir.) 1% glauconite 1% organic matter tr. diatoms
							4	[Pattern] VOID			SS: 2-140, [3, 15, 82] 65% nannos 24% clay 3% carb.unspec. 3% sponge spics. 2% quartz 1% dolomite 1% diatoms 1% rads tr. mica, heavy mins., gluc., forams
							5	[Pattern] VOID			SS: 5-53, [30, 25, 45] 30% nannos 25% quartz 15% clay 15% sponge spics. 5% organic matter 2% mica 2% forams 2% carb.unspec. 1% heavy mins. 1% glauconite 1% pyrite
							6	[Pattern]			Grain Size 3-84 = tr. 49, 51 CaCO <sub>3</sub> % C org %
						7	[Pattern]				
						CC					

SHIPBOARD 2-81 34  
SHOREBASED 3-83 27 0.1

Explanatory notes in Chapter 1

**SITE 398**

SITE	398	HOLE D	CORE	15	CORED INTERVAL:	546.5-556.0 m
TIME-ROCK UNIT	BIOSTRAT ZONE	FOSSIL CHARACTER	SECTION	METERS	GRAPHIC LITHOLOGY	LITHOLOGIC DESCRIPTION
		FORAMS NANNOS RADS			DRILLING DISTANCE DISTANCE TO TOP OF CORE DEPTH OF CORE LITHOLOGIC SAMPLE	
LATE OLIGOCENE		Rp-				
				0.5		General Description: Rhythmically bedded sequence of MARLY NANNO CHALK to NANNO CHALK with silty lower contacts as in Core 14, interrupted by slumped sediments
				1.0		Sec.1-59-147cm: 2 slump units of different lithologies; upper unit is thinly laminated MARLY NANNO CHALK to NANNO CHALK in rhythmical alteration of grn.gray (5GY 6/1) and lt.bl.gray (5B7/1), w/rare Chondrites burrows at top, plus isoclinal, recumbent and monoclinial folds which grade downward to yel. gray (5Y7/2); more nearly flat-lying NANNO CHALK w/occasional laminae of lt.bl.gray (5B7/1); the lower folded unit is contorted granular conglomerate, lt.bl.u.gray to yel.gray (5B7/1 to 5B7/2) w/white granules of hard, sub-rounded calcite and angular quartz.
				2		SS:1-102 [2.10,88] 60% nannos 29% clay 5% carb.unspec. 2% forams 2% quartz 2% sponge spics 1% dolomite tr.glaucanite
				3		SS:2-143 [8.10,232] 44% nannos 40% clay 5% forams 5% carb.unspec. 2% quartz 2% sponge spics 1% mica 1% dolomite tr.heavy mins
				4		Sec.1,147cm to Sec.5,62cm: MARLY NANNO CHALK, colors ranging between lt.grays (5Y7/2), yel.gray (5Y8/1), pale olive (5Y6/3), lt.bl.u.gray (5B7/1) and grn.gray (5G6/1); isoclinal folds, axial cleavage, crenulations in several intervals: Sec.2,40-135cm, Sec.4,38-42cm and Sec.4,50-65cm; remainder is finely laminated (1mm) to flat bedded (3cm); layer of hard calcite granules at 2-145; cut & fill & cross bedding in Sec.3,10-120cm; no bioturbation; microfaulting w/steep & shallow dips, offset of laminae as much as 3mm.
				5		SS:5-142 [25.40,35] 38% clay 20% nannos 10% sponge spics 10% forams 8% carb.unspec. 5% quartz 2% feldspar 2% glauconite 2% rads. 1% dolomite 1% heavy mins. 1% mica tr.diatoms
				6		SS:5-143 [3.20,77] 45% nannos 43% clay 5% carb.unspec. 2% sponge 2% forams 2% quartz 1% dolomite tr.mica tr.heavy mins
				7		
				CC		
						CaCO <sub>3</sub> % C <sub>org</sub> %
					SHIPBOARD	1-22 40
					SHOREBASED	3-98 65
						52 0.1

Explanatory notes in Chapter 1

SITE	398	HOLE D	CORE 16	CORED INTERVAL:	556.0-565.5 m
TIME-ROCK UNIT	BIOSTRAT ZONE	FOSSIL CHARACTER	SECTION	METERS	LITHOLOGIC DESCRIPTION
		FORAMS NANNOS RADS			
LATE Oligocene	NP 25 - 24	<i>Sphenolithus oiparocensis</i> - <i>Sphenolithus dilatatus</i>		0.5 1 1.0	MARLY NANNO CHALK, grn-gray (5G7/1), burrowed, w/lcm of hard SANDY MUDSTONE at base
			2		
			3		

SITE	398	HOLE D	CORE 17	CORED INTERVAL:	565.5-575.0 m
TIME-ROCK UNIT	BIOSTRAT ZONE	FOSSIL CHARACTER	SECTION	METERS	LITHOLOGIC DESCRIPTION
		FORAMS NANNOS RADS			
MIDDLE Oligocene	NP 23	<i>Sphenolithus praedilatatus</i>		0.5 1 1.0	SILICEOUS MARLY NANNO CHALK, yellowish olive (5Y7/2 to 5Y6/2); laminations both parallel and irregular, wavy; part of a fold similar to interval below Sec. 1, 59cm of Core 15D?
			2		SS: (1-10) [7, 13, 80] 50% nannos 24% clay 5% fecal pellets 5% carb.unspec. 2% dolomite 2% quartz 10% sponge spics. 1% mica 1% heavy mins. tr.forams

SITE 398 HOLE D CORE 18 CORED INTERVAL: 575.0-584.5 m

TIME-ROCK UNIT	BIOSTRAT ZONE	FOSSIL CHARACTER			SECTION	METERS	GRAPHIC LITHOLOGY	DRILLING DISTURBANCE STRUCTURE LITHOLOGIC SAMPLE	LITHOLOGIC DESCRIPTION
		FORAMS	NANNOS	RADS					
					1	0.5			NO RECOVERY

Explanatory notes in Chapter 1

SITE 398 HOLE D CORE 19 CORED INTERVAL: 584.5-594.0 m

TIME-ROCK UNIT	BIOSTRAT ZONE	FOSSIL CHARACTER			SECTION	METERS	GRAPHIC LITHOLOGY	DRILLING DISTURBANCE STRUCTURE LITHOLOGIC SAMPLE	LITHOLOGIC DESCRIPTION
		FORAMS	NANNOS	RADS					
LATE EOCENE - EARLY OLILOCENE					1	0.5			<p>General Description: Rhythmically bedded sequence of NANNO CHALK, MARLY NANNO CHALK and CALCAREOUS SANDY MUDSTONE; average rhythm thickness is 15-18cm and within each the following sub-units are recognized: (a) basal CALCAREOUS SANDY MUDSTONE containing 30% or more sand-sized quartz, dusky yel. grn. (5GY 6/2), a sharp upper contact with (b) MARLY NANNO CHALK, usually w/ silt-sized quartz, cl. gray (5GY 4/2), a sharp upper contact with (c) MARLY NANNO CHALK, rarely NANNO CHALK, dusky yel. (5Y6/4), grading upwards to (d) NANNO CHALK to MARLY NANNO CHALK, dusky yel. (5Y 6/4); a transitional greenish interval marks the upward termination of the rhythm and beginning of sub-unit (a); bioturbation throughout entire core.</p> <p>Smear (1-63) [10.25.65] 50% nannos 20% quartz 10% clay 7% sponge spics. 5% pellets 3% dolomite 3% mica 1% heavy mins 1% carb.unspec. tr.glaconite tr.pyrite</p> <p>Smear (1-68) [10.20.70] 50% nannos 17% clay 15% qtz 5% sponge spics. 5% pellets 4% mica 3% dolomite 1% heavy mins.</p> <p>Smear (4-95) [45.25.30] 30% qtz 15% nannos 15% clay 8% carb.unspec. 10% zeolite 5% forams 5% mica 3% feldspar 3% sponge spics. 2% heavy mins 2% diatoms 1% glauconite</p> <p>Smear (1-73) [50.20.30] 45% nannos 25% qtz 10% clay 8% sponge spics. 5% forams 2% mica 2% glauconite 2% pyrite 1% dolomite tr heavy mins.</p>
					2	1.0			
					3				
					4				
					5				
					6				
					7				
					CC				

SITE	398	HOLE	D	CORE	20	CORED INTERVAL:	594.0-603.5 m
TIME-ROCK UNIT	BIOSTRAT ZONE	FOSSIL CHARACTER	SECTION METERS	GRAPHIC LITHOLOGY	DRILLING DISTURBANCE	SEDIMENTARY STRUCTURE	LITHOLOGIC DESCRIPTION
LATE EOCENE - EARLY OLIocene							General description: Rhythmically bedded sequence of MARLY NANNO CHALK and CALCAREOUS SANDY MUDSTONE; average rhythm thickness is 15-18 cm and each consists of the following: CALCAREOUS SANDY MUDSTONE at base, erosional cut-and-fill basal contact common, thinly laminated to massive, ol.gray (5GY 4/2) to dusky yel.grn. (5GY 6/2); grades upwards to MARLY NANNO CHALK, dusky yel.5Y6/4, carbonate content in this sub-unit decreases markedly downcore; bioturbation common throughout entire core, most intense within MARLY NANNO CHALK, w/ zoophycus dominant.
			0.5				Smear (3-133)
			1.0				[30.40.30]
			2				25% carb.unspec.
							20% clay
							20% quartz
							10% zeolites
							10% forams
							5% feldspar
							1% dolomite
							tr.mica
							tr.heavy mins.
			3				
			4				
			5				
			6				GRAIN SIZE
							3-105=tr.42.58
							CaCO <sub>3</sub> % C org.%
							SHIPBOARD 5-19 8
							SHOREBASED 3-104 21 0.1
			7				
			CC				

Explanatory notes in Chapter 1

SITE	398	HOLE	D	CORE	21	CORED INTERVAL:	603.5-613.0 m
TIME-ROCK UNIT	BIOSTRAT ZONE	FOSSIL CHARACTER	SECTION METERS	GRAPHIC LITHOLOGY	DRILLING DISTURBANCE	SEDIMENTARY STRUCTURE	LITHOLOGIC DESCRIPTION
LATE EOCENE							General Description: MARLY NANNO CHALK and RADIO-LARIAN MUDSTONE rhythmically bedded w/ MARLY CHALK; basal MARLY CHALK is predominantly silt-to sand-sized w/more calcareous material than in the overlying sediment and is up to 2cm thick; persistent siliceous component in the finer-grained sediment; color at base of each rhythm is ol.gray (5GY4/2) to dusky yel.grn.(5GY6/2) and grades upwards to dusky yel.(5Y6/4); a darker color (diagenetic Fe reduction) apparently has stained the fine-grained chalk and mudstone 3-8 cm above and below each silt layer; average rhythm is 17-20cm thick.
			0.5				Smear 3-42
			1.0				[20.40.40]
			2				39% clay
							20% rads
							15% quartz
							15% mica
							(chlorite?)
							10% sponge spics.
							1% zeolite
							tr.carb.unspec.
							tr.plant debris
			3				Smear 3-52
							[10.30.60]
							41% clay
							25% nannos
							15% chlorite?
							(mica)
							10% carb.unspec.
							5% quartz
							3% sponge spics.
							1% org.matter
							tr.rads
							tr.fish debris
			4				Smear 3-54
							[50. 30. 20]
							40% carb.unspec.
							19% clay
							20% mics
							10% quartz
							5% nannos
							4% rads
							1% sponge spics.
							1% feldspar
							tr.zeolite
							tr.dolomite
			5				
							GRAIN SIZE
							3-116=tr.37.63
							CaCO <sub>3</sub> % C org.%
							SHIPBOARD 3-46 4
							3-53 24
							SHOREBASED 2-14 27 0.1
							4-38 14 0.1

SITE	398	HOLE	D	CORE	22	CORED INTERVAL:	613.0-622.5 m		
TIME-ROCK UNIT	BIOSTRAT ZONE	FOSSIL CHARACTER		SECTION	METERS	GRAPHIC LITHOLOGY	DRILLING DISTURBANCE	SEDIMENTARY LITHOLOGIC SAMPLE	LITHOLOGIC DESCRIPTION
LATE EOCENE		FORAMS	NANNOS	RADS					
			</						

Explanatory notes in Chapter 1

SITE	398	HOLE	D	CORE	23	CORED INTERVAL:	622.5-632.0 m	
TIME-ROCK UNIT	BIOSTRAT ZONE	FOSSIL CHARACTER	SECTION	METERS	GRAPHIC LITHOLOGY	DRILLING DISTURBANCE	SEDIMENTARY LITHOLOGIC SAMPLE	LITHOLOGIC DESCRIPTION
LATE-MIDDLE EOCENE	NP 16	FORAMS NANNOS RADS	SECTION	METERS	GRAPHIC LITHOLOGY	DRILLING DISTURBANCE	SEDIMENTARY LITHOLOGIC SAMPLE	LITHOLOGIC DESCRIPTION
								General Description: NANNO CHALK and RADIOLARIAN MUDSTONE rhythmically bedded w/ SILICEOUS MARLY CHALK; the latter is silty to sandy, 1mm to 5cm thick, with higher carbonate content than in the finer sediment; color at base of rhythm in coarser sediment is grn.gray 5G6/1 and grades upward to dk.yel.brn. (10YR4/2) to mod.brn.(10YR5/4); grn.gray color begins again several cm below the overlying silt layer, probably due to diagenetic reduction of iron within the silt layer; bioturbation is moderate to intense throughout the core; rare graded bedding; average rhythm thickness 25-28cm.
								Smear 1-34 [12.38.52] 48% clay 18% mica 12% rads 11% quartz 10% sponge spics. 1% diatoms tr.fish remains tr.feldspar tr.heavy mins. tr.dolomite
								Smear 1-53 [12.46.42] 52% nannos 18% clay 12% carb.unspec. 5% sponge spics. 3% rads 8% quartz tr.limonite
								Smear 1-69 [43.35.22] 64% carb.unspec. 15% nannos 8% quartz 3% clay 5% mica (chlorite) 3% forams 2% sponge spics. tr.feldspar,heavy mins.,glauconite pyrite,dolomite, diatoms
								Smear 3-131 [13.31.56] 38% carb.unspec. 33% nannos 13% quartz 10% clay 8% sponge spics. 2% rads 2% forams tr.heavy mins. glau- conite,pyrite,dia- toms
								CaCO <sub>3</sub> % C <sub>org</sub> % SHIPBOARD 2-8 26 2-40 10 SHOREBASED 3-19 35 0.1

SITE 398 HOLE D CORE 24 CORED INTERVAL: 632.0-641.5 m

TIME-ROCK UNIT	BIOSTRAT ZONE	FOSSIL CHARACTER	SECTION METERS	GRAPHIC LITHOLOGY	LITHOLOGIC DESCRIPTION
MIDDLE-LATE EOCENE	NP 16				
			0.5		General Description: SILICEOUS MARLY CHALK and RADIOLARIAN MUDSTONE rhythmically bedded with silty to sandy SILICEOUS MARLY CHALK; coarser sediment at the base of each rhythm is laminated and rarely graded, usually grn. gray 506/1 but w/some calcite granules of white (N-9); the finer overlying sediment is in part unburrowed and laminated, w/occasional cross-cutting laminae, flame structures, smeared out or truncated burrows implying current re-working (contourites?); possibly some syndepositional faults w/offsets less than 3cm within this finer sediment as well, where the color is mod. yel. brown (10YR5/4); average rhythm thickness is 23-26cm.
			1.0		
			2		Smear 1-105 [10.55.35] 35% clay 25% mica (chlorite?) 15% rads 10% sponge spics. 10% quartz 3% plant debris? 1% pyrite 1% zeolite tr carb.unspec.
			3		Smear 1-110 [50.30.20] 15% forams 15% nannos 14% clay 15% mica (chlorite?) 10% carb.unspec. 10% rads 10% sponge spics 10% quartz 1% mica tr. heavy mins. tr. dolomite, zeolite, glauconite, diatoms, plant debris
			4		smeared out, overturned burrows, truncated by laminated marly chalk and mudstone, probably overturned in direction of current flame structure and micro cross-lamination
			5		Smear 1-144 [5.55.40] 30% nannos 32% clay 20% mica (chlorite?) 10% sponge spics. 5% carb.unspec. 2% rads 1% quartz tr. zeolite, diatoms, dolomite, plant debris
			6		GRAIN SIZE 3-125=tr. 35.65 CaCO <sub>3</sub> % C org % SHIPBOARD 3-124 21 SHOREBASED 3-127 15 0.1
			7		
			CC		

Explanatory notes in Chapter 1

SITE 398 HOLE D CORE 25 CORED INTERVAL: 641.5-651.0 m

TIME-ROCK UNIT	BIOSTRAT ZONE	FOSSIL CHARACTER	SECTION METERS	GRAPHIC LITHOLOGY	LITHOLOGIC DESCRIPTION
MIDDLE EOCENE	NP 16				
			0.5		General Description: RADIOLARIAN MUDSTONE and SILICEOUS MARLY NANNO CHALK rhythmically bedded with silty SILICEOUS MARLY CHALK; the coarser sediment at the base of each rhythm is lt. gray (N-6, N-7) to grayish brown (2.5Y5/2, 5YR4/4) and grades upwards to lt. brown-gray (2.5Y6/2) in the finer sediment; average rhythm thickness is 17-20cm; bioturbation throughout core, Zoophycus and composite.
			1.0		Smear (1-73) [3.30.67] 57% clay 10% quartz 10% radiolaria 10% sponge spics. 3% zeolite 3% carb.unspec. 3% nannos 2% dolomite 2% mica tr. heavy mins
			2		Smear (1-83) [10.40.50] 30% nannos 15% sponge spics. 11% clay 10% mica 10% quartz 5% carb.unspec. 5% forams 5% rads 2% feldspar 2% zeolites 2% dolomites 1% diatoms 1% heavy mins. 1% glauconite tr. volc.glass
			3		SHIPBOARD 1-47 10 CaCO <sub>3</sub> % C org %

Explanatory notes in Chapter 1

SITE 398

[illegible]

Explanatory notes in Chapter 1

[illegible]

SITE 398 HOLE D CORE 30 CORED INTERVAL: 689.0-698.5 m		FOSSIL CHARACTER		SECTION	METERS	GRAPHIC LITHOLOGY	DRILLING DISTURBANCE SEDIMENTARY STRUCTURE LITHOLOGIC SAMPLE	LITHOLOGIC DESCRIPTION
TIME-ROCK UNIT	BIOSTRAT ZONE	FORAMS	NANNOS					
MIDDLE Eocene	NP 14-13	<i>Dianocaster lodoensis</i>		1	0.5			General Description: Rhythmic sequence of QUARTZ- OSE MUDSTONE and MARLY NANNO CHALK or CALCAREOUS MUDSTONE; base marked by grn.gray(5G6/1)silt and sand laminae, though coarse material is occasion- ally absent; these laminae are generally <3cm thick, typically only a few mm; graded bedding and micro cross-laminations are common; color grades upwards to brown and pale brown (10YR6/3,5/3) w/ some variegation or mottling of 5G6/1; bioturba- tion is moderate to intense, though some inter- vals are unburrowed, especially at the base of the rhythms; quartz is an important component through- out the core, especially in the coarsest basal intervals; average rhythm thickness is 14-17cm.
					1.0			
				2				
				3				
MIDDLE Eocene	NP 14-13	<i>Dianocaster lodoensis</i>		4				Smear 3-91, [0, 20, 80] 53% clays 15% nannos 10% carb.unspec. 10% zeolites 5% quartz 5% mica 2% dolomite tr.sponge spics tr.heavy mins  Smear 3-96, [40, 30, 30] 35% nannos 30% quartz 28% clay 3% mica 2% heavy mins 2% dolomite 1% carb.unspec. tr.sponge spics  Smear 3-97, [25, 50, 25] 50% quartz 12% clay 12% zeolite 5% feldspar 5% mica 3% carb.unspec. 8% nannos 2% forams 1% tour., magnet. 1% glauconite 1% dolomite  SHIPBOARD 2-86 45
				5				
				6				

Explanatory notes in Chapter 1

SITE 398 HOLE D CORE 31 CORED INTERVAL: 698.5-708.0 m		FOSSIL CHARACTER		SECTION	METERS	GRAPHIC LITHOLOGY	DRILLING DISTURBANCE SEDIMENTARY STRUCTURE LITHOLOGIC SAMPLE	LITHOLOGIC DESCRIPTION
TIME-ROCK UNIT	BIOSTRAT ZONE	FORAMS	NANNOS					
MIDDLE Eocene	NP 14-13	<i>Dianocaster lodoensis</i>		1	0.5			General Description: Rhythmic sequence of QUARTZ- OSE MUDSTONE AND MARLY NANNO CHALK or CALCAREOUS MUDSTONE; base marked by grn.gray(5G6/1)silt and sand laminae, though coarse material is occasion- ally absent; these laminae are generally <3cm thick, typically only a few mm; graded bedding and micro cross-laminations are common; color grades upwards to brown and pale brown (10YR6/3,5/3) w/ some variegation or mottling of 5G6/1; bioturba- tion is moderate to intense, though some inter- vals are unburrowed, especially at the base of the rhythms; quartz is an important component throughout the core, especially in the coarsest basal intervals; average rhythm thickness is 14-17cm.
					1.0			
				2				
				3				
MIDDLE Eocene	NP 14-13	<i>Dianocaster lodoensis</i>		4				Smear 2-76. [30, 35, 35] 35% clay 30% quartz 28% nannos 10% zeolite 2% mica 2% sponge spics 2% Ascidian spics (tunicate) 1% glauconite  Smear 2-76.5. [10, 40, 50] 25% nannos 24% clay 15% quartz 12% zeolite 10% forams 8% carb.unspec. 3% mica 1% feldspar 1% heavy mins. (tour., magnet.. zircon) 1% glauconite 1% dolomite
				5				
				6				

SITE 398 HOLE D CORE 32 CORED INTERVAL: 708.0-717.5 m

TIME-ROCK UNIT	BIOSTRAT ZONE	FOSSIL CHARACTER			SECTION METERS	GRAPHIC LITHOLOGY	DRILLING DISTURBANCE STRUCTURE LITHOLOGIC SAMPLE	LITHOLOGIC DESCRIPTION
		FORAMS	NANNOS	RADS				
EARLY EOCENE	NP 12	<i>Tribuachitius arborescens</i>			0.5			General Description: Rhythmic sequence of silty, sandy NANNO CHALK, MARLY CHALK or MUDSTONE grading upwards to fine grained MARLY NANNO CHALK or CALCAREOUS MUDSTONE; two types of basal silts: (1) white (N9) granules and sand-sized grains of sparry to micritic calcite (shallow water ls?), quartz and forams, and (2) pale grn. (10G5/2) quartz-rich silt, graded, laminated or massive, poorly sorted, generally < 2cm thick, most often 1-4mm; pale green (10G5/2) to grn.-gray (5G6/1, 5G6/6) color usually extends 5-10cm above and below each silty layer, grading into the yel. red (5YR5/6) and red. yel. (5YR6/6) of the fine-grained sediment; bioturbation is rare and faintly visible throughout the core; average rhythm thickness is roughly 45cm.
					1.0			
					2			
					3			
					4			
					5			
					6			
								Smear 1-40. [3, 30, 67] 69% clay 15% quartz 5% mica 5% nannos 3% carb.unspec. 2% heavy mins. 1% dolomite
								Smear 1-45. [5, 20, 75] 30% nannos 30% clay 25% quartz 8% zeolite 2% carb.unspec. 2% feldspar 2% heavy mins. 1% dolomite
								Smear 1-48. [60, 20, 20] 50% quartz 29% clay 10% mica 5% heavy mins. 4% nannos 2% zeolites
								Smear 1-85 [12, 25, 63] 40% nannos 25% clay 20% quartz 5% carb.unspec. 5% mica 2% dolomite 1% heavy mins. 1% pyrite 1% zeolite
								CaCO <sub>3</sub> % C org % SHIPBOARD 3-99 40 SHOREBASED 3-100 43 0.1

Explanatory notes in Chapter 1

SITE 398 HOLE D CORE 33 CORED INTERVAL: 717.5-727.0 m

TIME-ROCK UNIT	BIOSTRAT ZONE	FOSSIL CHARACTER			SECTION METERS	GRAPHIC LITHOLOGY	DRILLING DISTURBANCE STRUCTURE LITHOLOGIC SAMPLE	LITHOLOGIC DESCRIPTION
		FORAMS	NANNOS	RADS				
EARLY EOCENE	NP 11	<i>Dianocaster binodulus</i>			0.5			General Description: Rhythmic sequence of basal sandy or silty MARLY NANNO CHALK grading upwards to fine-grained MARLY NANNO CHALK; color of basal unit is grn.-gray (5G6/1) and grades above and below to lt. blu.-gray (5B7/1), and a sharp change to lt. brn. to v. pale brn. (5YR/6, 10YR7/3) marks the finest-grained unit; lt. blu.-gray color change is obviously diagenetic as it cuts thru burrows; bioturbation often absent in basal gray unit and increases upwards to intense in the brn unit, burrows often oval, 4x4 cm in size; coarse-grained basal unit shows inclined bedding planes as do the several fine laminae of v. lt. brn. to white sand-sized ls. fragments found within the otherwise fine-grained brn. unit; average rhythm thickness is about 40cm.
					1.0			
					2			
					3			
					4			
					5			
					6			
								Sec. 1, 34-40cm: gry. orange (10 YR7/4) soft, "fluffy" MARLY NANO CHALK, w/v. dk. brn. sandy, silty layer at 35cm
								Sec. 1, 51-57cm: grn.-gray (5G6/1) soft "fluffy" SILTY CALC. MUDSTONE
								Sec. 3, 115-116cm: white cse. sand to granule-sized graded ls. fragments
								Smear 1-37, [30, 30, 40] 37% nannos 24% clay 20% quartz 10% mica 3% heavy mins. 3% pellets 2% carb.unspec. 1% pyrite
								Smear 1-55, [30, 30, 40] 50% clay 10% nannos 30% carb.unspec. 5% quartz 2% mica 2% glauconite 1% heavy mins.
								Smear 5-37, [5, 25, 70] 50% nannos 36% clay 5% quartz 30% carb.unspec. 2% mica 2% heavy mins. 1% glauconite 1% pyrite
								Sec. 6, 55-60cm: mud-pebble congl., dk. gray clasts in lt. blu.-gray matrix
								Sec. 6, 72-80cm: ls.-pebble congl.
								GRAIN SIZE 3-79=0, 39, 61
								CaCO <sub>3</sub> % C org % SHIPBOARD 2-25 62 SHOREBASED 3-76 35 0.1

SITE 398 HOLE D CORE 34 CORED INTERVAL: 727.0-736.5 m

TIME-ROCK UNIT	BIOSTRAT ZONE	FOSSIL CHARACTER			SECTION METERS	GRAPHIC LITHOLOGY	DRILLING DISTURBANCE STRUCTURE LITHOLOGIC SAMPLE	LITHOLOGIC DESCRIPTION
		FORAMS	NANNOS	RADS				
LATE PALEOCENE - EARLY EOCENE	NP 10	<i>Marthasterites antitropus</i>			0.5			General Description: Sec.1.0-130cm is three cycles of basal sand, silty MARLY NANNO CHALK, grn. gray (5G6/1) grading upwards to lt. or v. pale brn. (5YR5/6, 10YR7/3) MARLY NANNO CHALK, with a transitional diagenetic discoloration of lt. blu. gray (5B7/1); below 1-130, brown MARLY NANNO CHALK predominates, w/occasional silty laminae containing intact forams, also w/variable bioturbation and color.
					1.0			
					2			
					3			
					4			
					5			
					6			
LATE PALEOCENE - EARLY EOCENE	NP 9	<i>Glauconites multicaulus</i>			7			General Description: Sec.1.0-130cm is three cycles of basal sand, silty MARLY NANNO CHALK, grn. gray (5G6/1) grading upwards to lt. or v. pale brn. (5YR5/6, 10YR7/3) MARLY NANNO CHALK, with a transitional diagenetic discoloration of lt. blu. gray (5B7/1); below 1-130, brown MARLY NANNO CHALK predominates, w/occasional silty laminae containing intact forams, also w/variable bioturbation and color.
					CC			

Explanatory notes in Chapter 1

SITE 398 HOLE D CORE 35 CORED INTERVAL: 736.5-746.0 m

TIME-ROCK UNIT	BIOSTRAT ZONE	FOSSIL CHARACTER			SECTION METERS	GRAPHIC LITHOLOGY	DRILLING DISTURBANCE STRUCTURE LITHOLOGIC SAMPLE	LITHOLOGIC DESCRIPTION
		FORAMS	NANNOS	RADS				
LATE PALEOCENE	NP 9	<i>Glauconites multicaulus</i>			0.5			Sec.1-0 to 80cm: folded MARLY NANNO CHALK, v. pale brn. (10YR 8/4) grading downwards to lt. blu. gray (5B7/1); faint mottles
					1.0			
					2			
					3			
					4			
					5			
					6			
LATE PALEOCENE	NP 9	<i>Glauconites multicaulus</i>			7			General Description: Rhythmically bedded MARLY NANNO CHALK; basal silt to sand laminae (qtz-and/or foram-rich) are grn. gray (5G6/1) and grade above and below to lt. blu. gray (5B7/1) while overlying interval is fine grained and lt. or v. pale brown (5YR5/6, 10YR7/3) bioturbation limited to brown intervals only; laminae occasionally cross-bedded or rippled.
					CC			

SITE 398 HOLE D CORE 36 CORED INTERVAL: 746.0-755.5 m

TIME-ROCK UNIT	BIOSTRAT ZONE	FOSSIL CHARACTER	SECTION METERS	GRAPHIC LITHOLOGY	DRILLING DISTURBANCE	SEDIMENTARY LITHOLOGIC SAMPLE	LITHOLOGIC DESCRIPTION
LATE PALEOCENE	NP 9						General Description: Rhythmically bedded MARLY NANNO CHALK; basal silty to sandy laminae w/ significant qtz. and foram components; grn. gray (5G6/1) grade upwards to fine-grained brown (10YR6/3) sediment; diagenetic discoloration forms transition zone above and below each lamination, lt. blu. gray (5B7/1); average rhythm thickness is 30-33cm; faulting prominent in Secs. 5 and 6.
			0.5				Smear 1-46 [5, 55, 40] 34% clay 30% nannos 12% quartz 8% carb. unspec. 5% zeolite 3% mica 3% feldspar 2% forams 1% heavy mins. (tour. apatite, magnetite) 1% glauconite 1% dolomite
			1.0				qtz-foram sandstone, well cemented
							Smear 1-49, [0, 40, 60] 40% nannos 34% clay 10% carb. unspec. 5% dolomite 5% zeolite 5% quartz 1% glauconite tr. mica, heavy mins.
							pale coloration, intensely mottled
							sand-filled burrow
							reverse fault, w/ 2mm offset 30° off vertical
							laminated MARLY CHALK w/ normal fault, drag apparently in wrong sense; may be post-faulting sag into tensional fracture; 1.5cm slip
							faulted interval, planes dip 45° from vertical, offset indeterminate
							GRAIN SIZE 3-94=2, 33, 65 6-4=tr, 37, 63 CaCO <sub>3</sub> % Corg.% SHIPBOARD 3-93 33 SHOREBASED 3-96 35 0.1

Explanatory notes in Chapter 1

SITE 398 HOLE D CORE 37 CORED INTERVAL: 755.5-765.0 m

TIME-ROCK UNIT	BIOSTRAT ZONE	FOSSIL CHARACTER	SECTION METERS	GRAPHIC LITHOLOGY	DRILLING DISTURBANCE	SEDIMENTARY LITHOLOGIC SAMPLE	LITHOLOGIC DESCRIPTION
LATE PALEOCENE	NP 7						General Description: SILICEOUS NANNO CHALK and SILICEOUS MUDSTONE; rhythmically bedded w/ silty, sandy laminae; rhythms begin at sharp erosional basal contact w/ less than 2cm laminated, poorly sorted siliceous foram sand and silt, salt and pepper color w/ lt. blu. gray (5B7/1); the latter color extends above and below laminae, apparently a diagenetic discoloration; top of each rhythm is pale to v. pale brown (10YR5/3) varying from MARLY NANNO CHALK to SILICEOUS MUDSTONE; average rhythm thickness is 22-25cm; bioturbation rare throughout.
			0.5				Smear 1-40, [3, 47, 50] 45% nannos 18% clay 15% sponge spics. 8% carb. unspec. 5% rads 3% dolomite 2% zeolite 2% forams 1% quartz 1% mica tr. heavy mins.
			1.0				Several zones of faults: Sec. 1, 55cm: 50° dip, 4cm slip trace 2mm wide, possible dewatering trace Sec. 2, 60-100cm: zone of fractures, some offset upto 2 cm, not induced by drilling, lithified, resemble dewatering cracks Sec. 4, 10-40cm: sinuous fault trace, reverse offset, 2cm slip
							Smear 4-54, [0, 10, 90] 65% nannos 26% clay 5% carb. unspec. 3% sponge spics. 1% zeolite tr. quartz, mica, heavy mins.
							Smear 3-79, [20, 50, 30] 35% clay 20% forams 10% nannos 10% carb. unspec. 10% sponge spics. 3% quartz 2% mica 2% zeolite 2% dolomite 1% glauconite 1% feldspar 1% diatoms tr. heavy mins.
							GRAIN SIZE 3-91=3, 34, 63 CaCO <sub>3</sub> % Corg.% SHIPBOARD 1-115 7 SHOREBASED 2-61 52 0.1
							Smear 3-85, [3, 37, 60] 65% clay 15% sponge spics. 5% rads 5% nannos 5% carb. unspec. 1% quartz 1% mica 1% zeolite 1% dolomite 1% diatoms tr. heavy mins.





SITE	398	HOLE	D	CORE	38	CORED INTERVAL:	765.0-774.5 m				
TIME-ROCK UNIT	BIOSTRAT ZONE	FOSSIL CHARACTER		SECTION	METERS	GRAPHIC LITHOLOGY	DRILLING DISTURBANCE	SEDIMENTARY STRUCTURES	LITHOLOGIC SAMPLE	LITHOLOGIC DESCRIPTION	
LATE PALEOCENE	P 3-4	FORAMS NANNOS RADS								General Description: MUDSTONE, often ZEOLITIC, rhythmically bedded w/silty, sandy NANNO CHALK; each rhythm begins w/less than 1cm graded or laminated basal unit, dusky yel.grn.(5GY6/2-5/2), grading above and below to gray.grn.(5GY 7/2-5/2) w/fine-grained mudstone at top.colors brown to mod.brown to pale brown (5YR4/4, 10YR 5/3-7/3); average rhythm thickness is 29-32cm; mudstone intensely bioturbated.	
										Smear 1-36 [0.30, 70] 69% clay 10% zeolite 8% quartz 5% carb.unspec. 5% nannos 2% mica 1% siderite tr. forams tr. mag., tour., zircon	Smear 1-45, [0.40, 60] 69% clay 10% zeolite 8% quartz 3% dolomite 3% mica 2% carb.unspec. 2% nannos 1% feldspar 1% glauconite 1% rads tr.sponge spics. tr.heavy mins.
										Smear 1-52, [0.30, 70] 63% clay 20% nannos 8% quartz 3% carb.unspec. 2% zeolite 2% forams 1% mica 1% dolomite tr.heavy mins.	Smear 2-127, [40, 30, 30] 30% quartz 25% nannos 20% carb.unspec. 10% clay 10% forams 3% zeolite 2% dolomite 2% mica
										GRAIN SIZE 5-79=0, 14, 86 $CaCO_3\%$ C org % SHIPBOARD 2-84 7 SHOREBASED 3-102 18 0.1	

Explanatory notes in Chapter 1

SITE	398	HOLE	D	CORE	39	CORED INTERVAL:	774.5-784.0 m				
TIME-ROCK UNIT	BIOSTRAT ZONE	FOSSIL CHARACTER			SECTION	METERS	GRAPHIC LITHOLOGY	DRILLING DISTURBANCE	SEDIMENTARY STRUCTURES	LITHOLOGIC SAMPLE	LITHOLOGIC DESCRIPTION
EARLY PALEOCENE	P 2-3	NP 3	FORAMS	NANNOS	RADS						General Description:Rhythmically bedded sequence as follows:(1)basal quartz- and foram-rich silt/sand laminae,usually <2cm thick;white to lt.gray (5Y8/1-7/2);bioturbation common;(2)MARLY NANNO CHALK, dusky gray.grn.(5GY5/2 to 10GY5/2),as much as 5 cm above and below laminae; bioturbation common to absent;(3)MARLY NANNO CHALK,variegated mod.yel.brown(10YR5/4) to reddish yellow(5YR4/4); massive,bioturbation intense;reddish yellow color occurs in apparently unburrowed intervals; expands on contact with air or fresh water;distinguishing color of (2) may be diagenetic; average rhythm thickness is 27-30cm
											Smear 1-25, 63% clay 25% nannos 5% dolomite 2% carb.unspec. 2% quartz 1% forams tr.mica,heavy mins.
											Smear 1-75, [100% sand] from laminae-black pyrite,magnetite, tourmaline,quartz placer
											Smear 2-62, [0.20, 80] 49% clay 40% nannos 3% quartz 3% carb.unspec. 2% mica 1% zeolite 1% dolomite 1% forams tr.heavy mins.
											GRAIN SIZE 4-47=tr. 25, 75 $CaCO_3\%$ C org % SHIPBOARD 2-72 46 SHOREBASED 3-58 56 0.5

SITE 398 HOLE D CORE 40 CORED INTERVAL: 784.0-793.5 m									
TIME-ROCK UNIT	BIOSTRAT ZONE	FOSSIL CHARACTER			SECTION METERS	GRAPHIC LITHOLOGY	DRILLING DISTURBANCE	SEDIMENTARY STRUCTURES	LITHOLOGIC DESCRIPTION
		FORAMS	NANNOS	RADS					
EARLY PALEOCENE	<i>Globuligerina engubina</i> ?				0.5				General Description: MARLY NANNO CHALK, rhythmic-ally bedded w/silty, sandy laminae; sequence begins w/basal laminae, predominantly calcareous w/some quartz, white (5Y8/1) to lt. gray (5Y7/2); for several cm above and below laminae the chalk is yellow grn. (5GY6/2), probably a diagenetic stain; elsewhere, the top of each sequence is variegated mod. yel. brown (10YR5/4) to red. yel. (5YR6/6), expanding on contact w/air or water; average rhythm thickness is roughly 70cm; bioturbation intense throughout, w/ <i>Zoophycus</i> dominant; green halos (5GY6/2) around some burrows.
					1				
					1.0				
	<i>Ornatiplicatulus tenuis</i>				2				
					3				
	O.G.				4				
					5				
					6				
					7				
					CC				
Smear 2-85, [0, 20, 80] 60% nannos 25% clay 5% dolomite 3% quartz 2% carb. unspec. 1% mica 1% heavy mins. 1% rads  Smear 2-93, [5, 10, 85] 60% nannos 25% clay 6% carb. unspec. 5% quartz 2% heavy mins. 1% mica 1% dolomite tr. glauconite  Smear 2-97, [45, 30, 25] 30% nannos 25% quartz 20% forams 14% clay 3% mica 3% dolomite 1% glauconite  GRAIN SIZE 3-19=tr. 19.81  coarse-grained calcite granule-rich sandstone  SHIPBOARD 4-91 61 SHOREBASED 3-40 54 0.3									

Explanatory notes in Chapter 1

SITE 398 HOLE D CORE 41 CORED INTERVAL: 793.5-803.0 m									
TIME-ROCK UNIT	BIOSTRAT ZONE	FOSSIL CHARACTER			SECTION METERS	GRAPHIC LITHOLOGY	DRILLING DISTURBANCE	SEDIMENTARY STRUCTURES	LITHOLOGIC DESCRIPTION
		FORAMS	NANNOS	RADS					
EARLY PALEOCENE	NP 1	<i>Morbitella insuavis</i> <i>Globobulimina angulibeta</i>	Ft Cg		0.5				General Description:MARLY NANNO CHALK w/irregularly spaced laminae of silt and sand;laminae are lt.gray(5Y7/2) to white,occasionally quartz-rich, and <1.5cm thick;a few laminae suggest contourite origin;for 1-2cm above and below each laminae the chalk is stained yel.grn.(5GY6/2);remainder of chalk is variegated reddish brown(25YR4/4),mod.yel.brown(10YR5/4),red.yel.(5YR6/6),and is massive w/intense bioturbation.
					1				
MAASTRICHTIAN	<i>Murchia mura</i>				2				Sec.2-44cm:probable Cretaceous -Tertiary boundary;diagenetic gray stain(5Y7/2)5cm above and below a 1cm silt layer;burrowing extends downwards 7cm to a laminated nanno mudstone; burrowing resumes at 80cm of sec.2.
					3				
					4				Smear 1-65 [10, 40, 50] 35% nannos 35% clay 6% forams 10% carb.unspec. 3% dolomite 7% quartz 2% mica 2% heavy mins.  Smear 2-42 [3, 45, 52] 40% quartz 28% clay 15% nannos 5% carb.unspec. 4% dolomite 4% mica 2% zeolite 2% heavy min'
					5				
					6				Smear 2-48, [10, 20, 70] 60% nannos 27% clay 5% carb.unspec. 3% quartz 2% mica 2% dolomite 1% heavy mins
					7				
					CC				Smear 5-46, [3, 10, 87] 75% nannos 20% clay 3% spicula 1% quartz 1% mica
GRAIN SIZE 5-7=0, 34, 66									
SHIPBOARD 1-65 34 SHOREBASED 1-98 36 0.1									

SITE 398 HOLE D CORE 42 CORED INTERVAL: 803.0-812.5 m

TIME-ROCK UNIT	BIOSTRAT ZONE	FOSSIL CHARACTER			SECTION	METERS	GRAPHIC LITHOLOGY	DRILLING DISTURBANCE STRUCTURE LITHOLOGIC SAMPLE	LITHOLOGIC DESCRIPTION
		FORAMS	NANNOS	RADS					
CAMPANIAN-MAASTRICHTIAN (MAASTRICHTIAN)	Nannula mara				1	0.5 1.0			General Description: MARLY NANNO CHALK, rhythmically bedded w/silty, sandy laminae; sequence begins w/1-3mm quartzose lamination within a greenish gray finer-grained interval; this grades upwards into brown to lt.brown chalk; bioturbation increases upwards in each sequence from absent to intense; average sequence is about 45cm thick.  Smear 1-24, [8, 12, 80] 55% nannos 25% clay 5% carb.unspec. 5% pellets 5% quartz 4% mica 3% dolomite 3% carb.unspec. 2% pellets 2% heavy mins. 1% pyrite  Smear 1-51, [8, 15, 77] 55% nannos 26% clay 5% carb.unspec. 60% nannos 20% clay 10% quartz 5% carb.unspec. 2% mica 2% dolomite 1% heavy mins.  CaCO <sub>3</sub> % C <sub>org</sub> % 2-26=0, 27, 73 SHOREBASED 2-28 62 0.0
					2				
					3				

Explanatory notes in Chapter 1


SITE 398 HOLE D CORE 43 CORED INTERVAL: 812.5-822.0 m

TIME-ROCK UNIT	BIOSTRAT ZONE	FOSSIL CHARACTER			SECTION	METERS	GRAPHIC LITHOLOGY	DRILLING DISTURBANCE STRUCTURE LITHOLOGIC SAMPLE	LITHOLOGIC DESCRIPTION
		FORAMS	NANNOS	RADS					
MAASTRICHTIAN <i>Lithothamnium quadratum</i> ?	Cp. Cf.				1	0.5 1.0			General Description: MARLY NANNO CHALK, rhythmically bedded w/silty, sandy laminae; each sequence begins w/a basal quartzose laminae <3mm thick, salt and pepper colors of blues and grays; occasionally coarse laminae are not apparent, and base of sequence is marked by lt.bl.u.gray (587/1) chalk; typically lt.bl.u.gray diagenetic stain extends <5cm above and below each laminae; upwards from each laminae bioturbation increases and color darkens to intensely bioturbated brown to lt.brown (7.5YR5/4, 6/4) chalk; some burrows w/grn. gray halo (587/1, 6/1); average rhythm thickness is about 45cm.  Smear 3-58, [10, 10, 80] 50% nannos 29% clay 10% carb.unspec. 5% quartz 2% dolomite 2% mica 2% heavy mins.  Sec. 2-136 to Sec. 3-100: MARLY NANNO CHALK w/"cloud-like" ragged mottles of brown (7.5 YR5/4) and lt.gray (10YR7/2), each several cm across; no apparent bedding; faint, smaller mottles of unknown origin; truncated laminae, calcite breccia at base; 15cm of parallel laminated, intensely burrowed bl.u.gray and brown chalk above and below this interval.  Smear 3-62, [0, 10, 90] 40% nannos 57% clay 1% quartz 1% dolomite 1% carb.unspec.  Smear 6-33, [6, 10, 84] 50% nannos 30% clay 8% carb.unspec. 5% quartz 3% heavy mins. 2% mica 2% dolomite  GRAIN SIZE 3-72=0.24, 76 6-28=0.19, 81  SHIPBOARD 1-78 52 4-76 63 SHOREBASED 2-91 39 0.1  CaCO <sub>3</sub> % C <sub>org</sub> %
					2				
					3				
					4				
					5				



SITE 398		HOLE D		CORE 46		CORED INTERVAL: 841.0-850.5 m			
TIME-ROCK UNIT	BIOSTRAT ZONE	FOSSIL CHARACTER			SECTION	METERS	GRAPHIC LITHOLOGY	DRILLING DISTURBANCE SEDIMENTARY LITHOLOGIC SAMPLE	LITHOLOGIC DESCRIPTION
		FORAMS	NANNOS	RADS					
CAMPANIAN-MAASTRICHTIAN	<i>Tetralithus trifidus</i>				1	0.5		General Description: MARLY NANNO CHALK to CALCAREOUS MUDSTONE, rhythmically bedded w/silty, sandy laminae; basal quartzose laminae 0-1mm thick, salt and pepper colors; diagenetic stain of lt. blu. gray (5B7/1) extends 1-5cm above and below each laminae, and often occurs with no apparent coarser lamination; color grades into variegated mod. brown (10YR5/4) to yel. brown (5YR4/4), where bioturbation increases to intense, w/some halos of lt. blu. gray (5B7/1); average rhythm thickness (measured between silt laminae) is about 35cm	
					2	1.0			
					3				
					4				
								Smear 2-117 [0, 10, 40] 57% clay 32% nannos 3% quartz 3% mica 1% feldspar 1% dolomite 1% organic mat. tr. heavy mins. 2% carb.unspec.	
								Smear 2-124 [3, 20, 77] 55% clay 25% nannos 9% quartz 5% mica 1% dolomite 1% feldspar 1% organic mat. tr. heavy mins. 3% carb.unspec.	
								GRAIN SIZE 1-37=0.24, 76	
								CaCO <sub>3</sub> % C <sub>org</sub> %	
								SHIPBOARD 2-104 30	
								2-116 35	
								2-121 25	
								SHOREBASED 3-90 33 0.1	

Explanatory notes in Chapter 1

SITE 398		HOLE D		CORE 47		CORED INTERVAL: 850.5-860.0 m			
TIME-ROCK UNIT	BIOSTRAT ZONE	FOSSIL CHARACTER			SECTION	METERS	GRAPHIC LITHOLOGY	CORRELATION DISTANCE TO SEDIMENTARY LITHOLOGIC SAMPLE	LITHOLOGIC DESCRIPTION
		FORAMS	NANNOS	RADS					
L. CAMPANIAN-E. MAASTRICHTIAN	<i>Tetralithus trifidus</i>				1	0.5		82 80 78 76 74 72 70 68 66 64 62 60 58 56 54 52 50 48 46 44 42 40 38 36 34 32 30 28 26 24 22 20 18 16 14 12 10 8 6 4 2 0	<p>General Description: MARLY NANNO CHALK to CALCAREOUS MUDSTONE, rhythmically bedded w/silty, sandy laminae; the basal laminae are both quartzose and calcareous, 0-10mm thick, some fine upwards while others are massive, gray to blue in color; the overlying interval is lt. blu. gray (5B7/1) and grades upwards to variegated mod. brown (10YR5/4) to yel. brown (5YR4/4), bioturbation variable; grayish yellow grn. (5GY6/2) separates this interval from the overlying coarser lamination which begins the next rhythm; average rhythm thickness is 28-30cm.</p>
					2	1.0			
					3				
					4				
					5				
									<p>Smear 1-82, [0, 10, 90] 65% clay 25% nannos 3% mica 2% quartz 2% carb. unspec. 1% dolomite 1% organic mat. tr. heavy mins tr. rads</p> <p>Smear 1-100, [50, 30, 20] 35% quartz 20% nannos 15% carb. unspec. 10% clay 5% mica 5% forams 5% organic mat. 3% heavy mins. 2% glauconite</p> <p>Smear 2-150, [40, 40, 20] 50% carb. unspec. 15% quartz 10% mica 10% nannos 5% clay 4% glauconite 2% dolomite 2% heavy mins. 2% organic mat.</p> <p>GRAIN SIZE 4-47=0, 26, 74</p> <p>CaCO<sub>3</sub> % C<sub>org</sub> %</p> <p>SHIPBOARD 1-77 30 SHOREBASED 3-71 23 0.1</p>

SITE 398 HOLE D CORE 48 CORED INTERVAL: 860.0-869.5 m

TIME-ROCK UNIT	BIOSTRAT ZONE	FOSSIL CHARACTER			SECTION METERS	GRAPHIC LITHOLOGY	DRILLING DISTURBANCE	SEDIMENTARY LITHOLOGIC SAMPLE	LITHOLOGIC DESCRIPTION
		FORAMS	NANNOS	RADS					
CAMPANIAN-MASTRICHTIAN	Bp- Cg- dp- Cg- dp- Cg- dp- Cg- dp- Cg-	Rt- Cg- dp- Cg- dp- Cg- dp- Cg- dp- Cg-	Rt- Cg- dp- Cg- dp- Cg- dp- Cg- dp- Cg-	0.5					General Description:CALCAREOUS MUDSTONE to MARLY NANNO CHALK,rhythmically bedded;basal silt laminae are very rare;base of each rhythm marked by fine-grained interval of lt.bl.u.gray(5B7/1) w/ sharp lower contact;color grades upwards to variegated mod.brown (10YR5/4)to yel.brown (5YR4/4); bioturbation common throughout;average rhythm thickness is 25-28cm.  Smear 4-3, [0, 0, 100] 82% clay 10% nannos 8% iron oxides  Smear 4-51, [0, 20, 80] 55% clay 28% nannos 8% quartz 5% mica 2% dolomite 2% organic mat.  Smear 4-58, [0, 15, 85] 56% clay 35% nannos 5% quartz 3% mica 1% dolomite tr.heavy mins.  GRAIN SIZE 2-73=tr, 22, 78  SHIPBOARD 2-39 22
				1					
				1.0					
				2					
				3					
				4					
				5					
				6					
				7					
				CC					

Explanatory notes in Chapter 1

SITE 398 HOLE D CORE 49 CORED INTERVAL: 869.5-879.0 m

TIME-ROCK UNIT	BIOSTRAT ZONE	FOSSIL CHARACTER	SECTION METERS	GRAPHIC LITHOLOGY	DRILLING DISTURBANCE	SEDIMENTARY LITHOLOGIC SAMPLE	LITHOLOGIC DESCRIPTION
CAMPANIAN-MASTRICHTIAN	Bp- Cg- dp- Cg- dp- Cg- dp-	Rt- Cg- dp- Cg- dp- Cg- dp-	0.5				CALCAREOUS MUDSTONE to MARLY NANNO CHALK; rhythmic bedding identical to core 48D  CaCO <sub>3</sub> % C <sub>org</sub> %  SHOREBASED 1-39 9 0.1
			1				
			1.0				

SITE 398 HOLE D CORE 50 CORED INTERVAL: 879.0-888.5 m									
TIME-ROCK UNIT	BIOSTRAT ZONE	FOSSIL CHARACTER			SECTION METERS	GRAPHIC LITHOLOGY	DRILLING DISTURBANCE	SEDIMENTARY STRUCTURES	LITHOLOGIC DESCRIPTION
		FORAMS	NANNOS	RADS					
CAMPANIAN-MAASTRICHTIAN									
Explanatory notes in Chapter 1									

SITE 398 HOLE D CORE 51 CORED INTERVAL: 888.5-898.0 m									
TIME-ROCK UNIT	BIOSTRAT ZONE	FOSSIL CHARACTER			SECTION METERS	GRAPHIC LITHOLOGY	DRILLING DISTURBANCE	SEDIMENTARY STRUCTURES	LITHOLOGIC DESCRIPTION
		FORAMS	NANNOS	RADS					
Explanatory notes in Chapter 1									

SITE 398 HOLE D CORE 52 CORED INTERVAL: 898.0-907.5 m									
TIME-ROCK UNIT	BIOSTRAT ZONE	FOSSIL CHARACTER			SECTION METERS	GRAPHIC LITHOLOGY	DRILLING DISTURBANCE	SEDIMENTARY STRUCTURES	LITHOLOGIC SAMPLE
		FORAMS	NANNOS	RADS					
					0.5	Sec.1.0-8cm:grn.gray(5G6/1)			
					1	MUDSTONE,dk.red.gray(5YR4/2),homogeneous,unbur-rowed,expands as it dries,w/scattered laminae of cemented quartzose silt(lt.blu.gray,5G7/1); silts also in rare oval fillings w/dk.red. brown halos(2.5YR3/4)			
					1.0				
						"biscuit"deformation throughout			
					2	Smear 1-15 [0, 20, 80] 77% clay 8% quartz 5% mica 3% dolomite 5% oxides 2% feldspar			
					3	Smear 1-92 [0, 55, 45] 45% clay 35% quartz 5% mica 5% chert 3% feldspar 3% dolomite 3% oxides 1% heavy mins.			
					4				
						CaCO <sub>3</sub> % C org %			
						SHIPBOARD 2-135 5			
						SHOREBASED 2-134 2 0.1			

Explanatory notes in Chapter 1

SITE 398 HOLE D CORE 53 CORED INTERVAL: 907.5-917.0 m									
TIME-ROCK UNIT	BIOSTRAT ZONE	FOSSIL CHARACTER			SECTION METERS	GRAPHIC LITHOLOGY	DRILLING DISTURBANCE	SEDIMENTARY STRUCTURES	LITHOLOGIC SAMPLE
		FORAMS	NANNOS	RADS					
					0.5	MUDSTONE,dk.red.gray(5YR4/2),homogeneous,unbur-rowed, expands as it dries;several lt.blu.gray (5G7/1) layers(1-5cm)occasionally w/cemented silty,sandy quartzose laminae;additional lt.blu. gray in oval mottles w/halos of dk.red.brown (2.5YR3/4).			
					1				
					1.0				
						"biscuit" deformation throughout			
					2	Sec.2.85cm:45° normal fault offsets sandy lamination			Smear 2-40 [0,10,90] 89% clay 5% quartz 5% oxides 1% mica tr feldspar tr heavy mins
					3				Smear 2-140 [0,10,90] 90% clay 6% quartz 3% mica 1% feldspar tr heavy mins.
					4	Sec.4.0-50cm:several slight-ly darker brownish gray in-tervals w/mm black blebs			Smear 2-141 [10, 50, 40] 45% quartz 37% clay 5% feldspar 5% mica 3% carb.unspec. 2% glauconite 2% heavy mins 1% dolomite
						O.G.			
					5				
					6				GRAIN SIZE 3-4=0,13,87  CaCO <sub>3</sub> % C org % SHIPBOARD 3-59 3 SHOREBASED 3-58 0 0.1
					7				
					CC				

[illegible][illegible]

Explanatory notes in Chapter 1

SITE 398		HOLE D		CORE 56		CORED INTERVAL: 945.5-955.0 m				
TIME-ROCK UNIT	BIOSTRAT ZONE	FOSSIL CHARACTER				SECTION	METERS	GRAPHIC LITHOLOGY	CORRELATION DISCONTINUANCE SEDIMENTARY LITHOLOGY SAMPLE	LITHOLOGIC DESCRIPTION
		FORAMS	NANNOS	RADS						
EARLY CENOMANIAN <i>Stelliferella turriculifera</i>	B						0.5		42	General Description: top third of core is variegated ZEOLITIC CLAYSTONE, grayish grn., grn. gray and red. brown (10GY5/2, 5GY5/2, 5G6/1, 5YR4/4), structureless except for several silty laminae w/ associated diagenetic discolorations; below 75cm in Sec. 2 dominant lithology is MARLY NANNO-CHALK to CALCAREOUS MUDSTONE, grayish grn. (10GY5/2, 5GY5/2), moderately burrowed, w/ numerous subunits in sections 2 and 3.
	B					1	1.0		14	
	B					2			24	Smear 1-42 [0.50, 50] 54% clay 30% zeolite 10% quartz 5% dolomite 1% mica tr. heavy mins.
	B					3			85	Sediment redistribution indicated in sub-units of Sec 2 & 3: (1) SILTY CLAYSTONE, parallel to wavy laminae, grayish grn. and grn. gray (5GY5/2, 5G6/1). (2) QUARTZOSE SANDSTONE, SILTSTONE, graded, cross-bedded, erosional basal contact, wht. to blu. grn. (N9, 5B9/1.5G 8/1). (3) MUD-CHIP SANDSTONE, graded, w/ thin parallel laminae, grayish grn. to grayish black (10GY5/2, N3)
	B					4			94	Smear 2-94 [40.30, 30] 40% quartz 15% zeolite 12% mica 12% clay 10% carb. unsp. spec. 7% glauconite 3% heavy mins. 1% dolomite
	B					5			97	Several 5cm thick intervals of thinly laminated, unburrowed CLAYSTONE, dk. gray to grayish black (N2, N3) shown as black interval in lithology column
	B					6			73	Smear 2-130 [0.10, 90] 70% clay 10% zeolite 20% org. matter
Ap-Cg						7			111	Smear 6-90 [5.30, 65] 40% clay 35% nannos 10% zeolite 5% quartz 5% carb. unsp. spec. 3% forams 1% mica 1% siderite
	CC								90	GRAIN SIZE 4-19=tr, 39, 71  SHIPBOARD 2-67 <2 SHOREBASED 6-100 35 0.1

SITE 398 HOLE D CORE 57 CORED INTERVAL: 955.0-964.5 m									
TIME-ROCK UNIT	BIOSTRAT ZONE	FOSSIL CHARACTER			SECTION METERS	GRAPHIC LITHOLOGY	DRILLING DISTURBANCE	SEDIMENTARY STRUCTURE	LITHOLOGIC SAMPLE
		FORAMS	NANNOS	RADS					
EARLY CENOMANIAN	<i>Stoffletia turpinea</i> <i>foel</i>								
					0.5				
					1				
					2				
					3				
					4				
						O.G.			
					5				
					6				

Section 1,0-29cm:yel.gray (5Y 6/1)to lt.grn.gray(5GY8/1)	Smear 1-65 [15,20,65]
entire core silty clay size except:	61% clay
sec 1,62,65 cm: SANDY MUDSTONE, dk.grn.to grn.gray (5G4/1-6/1)	10% gypsum
sec 1, 103-105 cm: SILTSTONE infilling a burrow	5% quartz
	5% feldspar
	5% carb.unspec.
	2% mica
	2% forams
	tr.heavy mins.
	zeolite
	10% org.matter
General Description:alternations of MARLY NANNO CHALK and CALCAREOUS MUDSTONE,predominantly w/ gradational contacts;chalk is dk.grn.gray (5GY 4/1) w/occasional layers of ol.grn.(5GY3/2);bioturbation intense at top,decreasing downwards. mottles are grn.black(5G2/1);mudstone is dk. gray to med.dk.gray(N3-4),occasionally med.gray to med.light gray(N5-6);numerous fine white laminae;bioturbation intense.mottles are med.dk. gray;sand size white specks throughout entire core.	
N3-N4 MUDSTONE shown as black interval in lithology column	
	Smear 2-60 [0,40,60]
	40% clay
	30% nannos
	20% zeolites
	3% carb.unspec.
	2% quartz
	2% feldspar
	2% mica
	1% dolomite
	tr.heavy mins.
	Smear 2-106 [0,15,85]
	76% clay
	15% nannos
	3% zeolite
	2% forams
	1% quartz
	1% mica
	1% dolomite
	1% carb.unspec.
	tr. heavy mins.
GRAIN SIZE 3-7=1.19,80	
	CaCO <sub>3</sub> % C <sub>org</sub> %
SHIPBOARD 3-60 31	
4-57 32	
SHOREBASED 3-52 37 0.2	

Explanatory notes in Chapter 1

SITE 398 HOLE D CORE 58 CORED INTERVAL: 964.5-974.0 m									
TIME-ROCK UNIT	BIOSTRAT ZONE	FOSSIL CHARACTER			SECTION METERS	GRAPHIC LITHOLOGY	DRILLING DISTURBANCE	SEDIMENTARY STRUCTURE	LITHOLOGIC SAMPLE
		FORAMS	NANNOS	RADS					
EARLY CENOMANIAN	<i>Stoffletia turpinea</i> <i>foel</i>								
					0.5				
					1				
					2				

MARLY NANNO CHALK,lt.blu.gray(5B7/1)to grn.gray (5G6/1);faintly laminated;bioturbation slight, w/ <i>Chondrites</i> and others	
	CaCO <sub>3</sub> % C <sub>org</sub> %
SHIPBOARD 1-68 32	
SHOREBASED 1-68 31 0.2	
Section 2,65-95cm:CALCAREOUS MUDSTONE, dk.gray to med.dk. gray (N3-N4),well laminated	
	GRAIN SIZE 2-3=2.14,84

Explanatory notes in Chapter 1

SITE	398	HOLE	D	CORE	61	CORED INTERVAL:	993.0-1002.5 m		
TIME-ROCK UNIT	BIOSTRAT ZONE	FOSSIL CHARACTER			SECTION	METERS	GRAPHIC LITHOLOGY	DRILLING SUCCESSION SEDIMENTARY STRUCTURES LITHOLOGIC SAMPLE	LITHOLOGIC DESCRIPTION
		FORAMS	NANNOS	RADS					
LATE ALBIAN	<i>Prodactinella</i>								CALCAREOUS MUDSTONE w/features identical to core 60D.
									Smear 1-105 [0.20,80] 73% clay 15% nannos 2% quartz 2% zeolite 2% dolomite 2% carb.unspec. 1% mica 1% pyrite 1% radiolaria 1% organic mat.
									Smear 1-146 [0.20,80] 70% clay 20% nannos 2% quartz 2% zeolite 2% carb.unspec. 1% feldspar 1% mica 1% dolomite 1% radiolaria tr. organic mat.
	Ag Cl								CaCO <sub>3</sub> % C <sub>org</sub> %
									SHIPBOARD 1-103 26 SHOREBASED 1-104 30
									GRAIN SIZE 2-40=2.29.69

SITE 398 HOLE D CORE 62 CORED INTERVAL: 1002.5-1012.0 m									
TIME-ROCK UNIT	BIOSTRAT ZONE	FOSSIL CHARACTER			SECTION METERS	GRAPHIC LITHOLOGY	DRILLING DISTURBANCE STRUCTURE SAMPLE	LITHOLOGIC DESCRIPTION	
		FORAMS	NANNOS	RADS					
LATE ALBIAN	<i>Prediscopularia arctica</i>				0.5			CALCAREOUS MUDSTONE w/features identical to core 60D	
					1			Smear 1-30 [3.20,77] 70% clay 10% nannos 3% mica 2% zeolite 2% radiolaria 1% quartz,pyrite, dolomite 2% organic mat. tr.heavy mins.	
					2			Smear 1-140 [2.15,83] 79% clay 10% nannos 3% quartz 2% radiolaria vol.glass 1% mica,h.mins, pyrite, dolomite. calc.unsp.	
					3			Smear 2-150 [2.18,80] 59% clay 30% siderite 5% nannos 2% forams, carb.unspec. 1% zeolite,quartz tr. mica, heavy mins	
					4			Smear 7-19 [15.20,65] 70% clay 8% zeolite 5% forams,nannos 2% dolomite, carb. unspec. radiolaria 1% quartz, volc. glass,sponge spics,pyrite	
					5			fault below which all laminae and mottles dip 20°	
					6			zeolitic mudstone,lt.gray (N-7)w/dk.gray(N-2) laminae at top;ol.gray burrows	
					7			White(N-9)sand size specks in wavy laminae	
					CC			SHIPBOARD 4-46 32 SHOREBASED 4-53 39	0.3

Explanatory notes in Chapter 1

SITE 398 HOLE D CORE 63 CORED INTERVAL: 1012.0-1021.5 m									
TIME-ROCK UNIT	BIOSTRAT ZONE	FOSSIL CHARACTER			SECTION METERS	GRAPHIC LITHOLOGY	DRILLING DISTURBANCE STRUCTURE SAMPLE	LITHOLOGIC DESCRIPTION	
		FORAMS	NANNOS	RADS					
ALBIAN	<i>Prediscopularia arctica</i> ?				0.5			drilling breccia:mud clasts and one ls.fragment	
					1			Burrowed dk gray to grayish black (N2,N3 to 5GY 2/1) CALCAREOUS MUDSTONE grading w/ no color change into unburrowed, v.finely laminated MUDSTONE*, w/ occasional sideritic laminae of grn. gray (5GY6/1)	
					2			bedding planes consistently dip 8-10° *identified by black intervals in lithology column	Smear 1-45 [5.30,65] 50% clay 32% calc.nannos 3% dolomite,calc. unsp. quartz 5% forams 2% pyrite 1% mica,zeolite tr heavy mins., sponge spics.
					3				Smear 3-134 [3.20,77] 75% clay 14% nannos 3% forams, carb.unspec. 1% Rad.,sponge spics,zeolite, pyrite,Q.mica
					4				Smear 4-69 [15.20,65] 60% siderite 35% clay 3% pyrite 1% forams,mica
					5				Smear 5-20 [3.20,77] 84% clay(illite sericite chlorite) 3% sponge spics. 2% radiolaria, quartz 3% zeolite 1% mica,dolomite, pyrite 2% org.matter
					6			VOID	GRAIN SIZE 3-57=tr.,29,71 5-70=5,47,48
					7				SHIPBOARD 3-59 23 SHOREBASED 3-66 21
					CC				0.3

SITE	398	HOLE	D	CORE	64	CORED INTERVAL:	1021.5-1031.0 m				
TIME-ROCK UNIT	BIOSTRAT ZONE	FOSSIL CHARACTER			SECTION	METERS	GRAPHIC LITHOLOGY	DRILLING DISTURANCE	SEDIMENTARY STRUCTURES	LITHOLOGIC SAMPLE	LITHOLOGIC DESCRIPTION
		FORAMS	NANNOS	RADS							

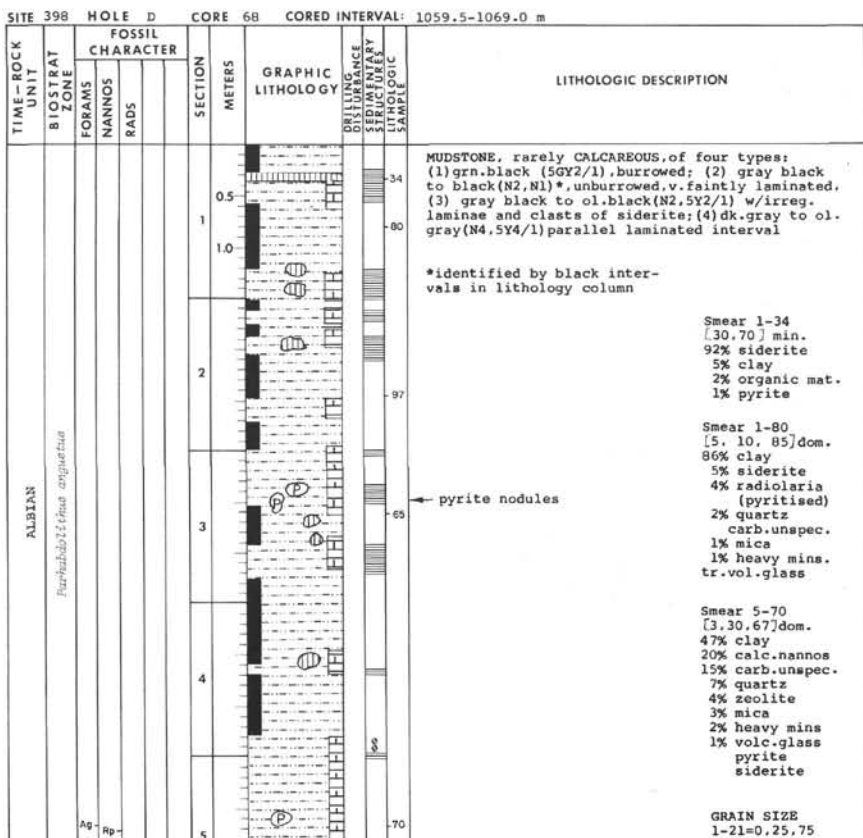
Explanatory notes in Chapter 1

SITE	398	HOLE	D	CORE	65	CORED INTERVAL:	1031.0-1040.5 m
TIME-ROCK UNIT	BIOSTRAT ZONE	FOSSIL CHARACTER		SECTION	METERS	GRAPHIC LITHOLOGY	LITHOLOGIC DESCRIPTION
		FORAMS	NANNOS				

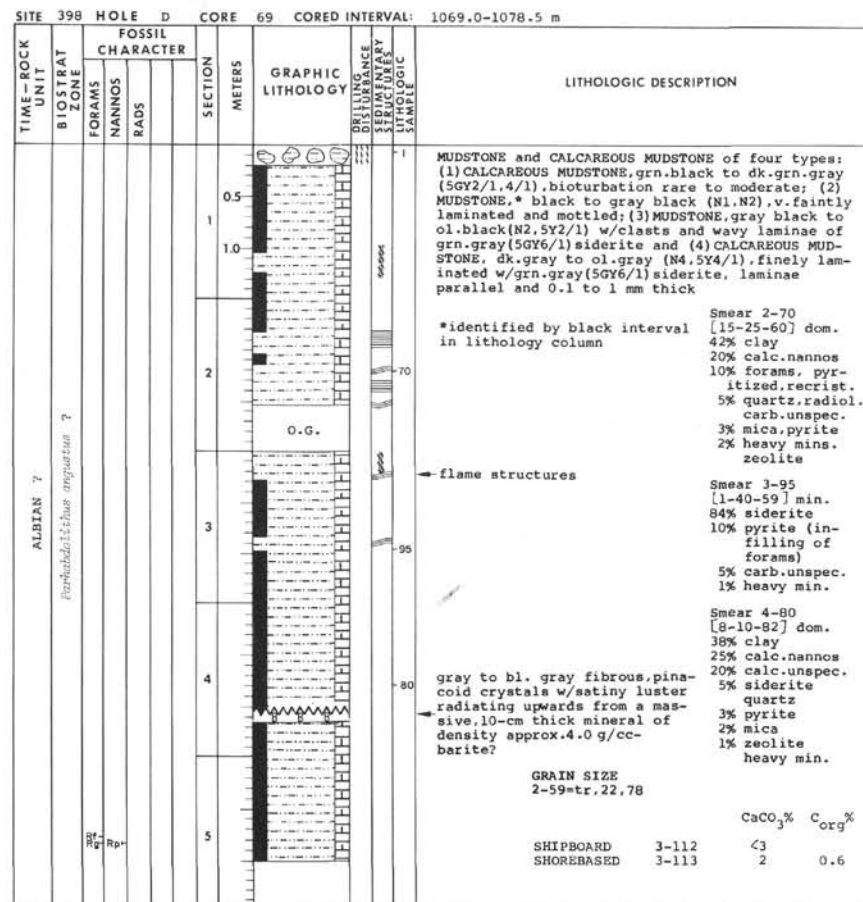
SITE 398		HOLE D	CORE 66	CORED INTERVAL: 1040.5-1050.0 m	
TIME-ROCK UNIT	BIOSTRAT ZONE	FOSSIL CHARACTER	SECTION	METERS	GRAPHIC LITHOLOGY
		FORAMS NANNOS RADS			LITHOLOGIC DESCRIPTION
ALBIAN	<i>Prodiosapherina areolata</i> ?		1	0.5 1.0	pyritized nodule at 18cm of Sec.1  MUDSTONE, rarely CALCAREOUS; dk.gray to grayish black (N2,N3 to 5GY2/1) alternating between faintly burrowed, non-laminated and unburrowed, laminated; sideritic laminae, grn.gray (5GY6/1)
			2		<div> <div>Smear 1-5 [3.47,50] 70% siderite 20% clay 5% calc.nannos 2% forams, zeolite 1% pyrite tr.quartz,heavy mins</div> <div>Smear 1-30 [15,85] 90% clay 2% siderite, zeolite pyrite 1% quartz,mica tr.heavy mins. 1% organic mat.</div> <div>CaCO<sub>3</sub>% 3</div> <div>C<sub>org</sub>% 0.5</div> </div>
SHIPBOARD 1-77					
SHOREBASED 1-74					

Explanatory notes in Chapter 1

SITE 398		HOLE D	CORE 67	CORED INTERVAL: 1050.0-1059.5 m	
TIME-ROCK UNIT	BIOSTRAT ZONE	FOSSIL CHARACTER	SECTION	METERS	GRAPHIC LITHOLOGY
		FORAMS NANNOS RADS			LITHOLOGIC DESCRIPTION
ALBIAN	<i>Prodiosapherina areolata</i> ?		1	0.5 1.0	MUDSTONE, rarely CALCAREOUS; burrowed and irregularly bedded intervals of grn.gray-black (5G 3/1) grading into homogeneous to faintly laminated intervals of dark gray*(N3), occasionally w/sideritic laminae of grn.gray (5GY6/1).
			2		<div> <div>*identified by black intervals in lithology column</div> <div>Smear 1-24 70% siderite 24% clay 3% mica 2% pyrite 1% forams</div> <div>Smear 1-76 [8.25,67] 63% clay 12% carb.unspec. 10% quartz 4% pyrite 3% radiolaria 2% siderite mica 1% zeolite,volc. glass nannos</div> <div>Smear 3-37 [3.15,82] 86% clay 5% organic mat. 3% siderite 2% pyrite 1% quartz,mica, zeolite,nannos radiolaria- pyritised</div> <div>CaCO<sub>3</sub>% 29</div> <div>C<sub>org</sub>% 0.5</div> </div>
SHIPBOARD 2-113					
SHOREBASED 2-116					



Explanatory notes in Chapter 3



SITE 398 HOLE D CORE 70 CORED INTERVAL: 1078.5-1088.0 m

TIME-ROCK UNIT	BIOSTRAT ZONE	FOSSIL CHARACTER	SECTION	METERS	GRAPHIC LITHOLOGY	DRILLING DISTURBANCE	SEDIMENTARY STRUCTURES	LITHOLOGIC SAMPLE	LITHOLOGIC DESCRIPTION
				0.5					
				1					
				1.0					
				2					
				3					
				4					

MUDSTONE and CALCAREOUS MUDSTONE of three types:  
 (1) CALCAREOUS MUDSTONE, grn.black to dk.grn. gray (5GY2/1 to 4/1), bioturbation moderate; (2) MUDSTONE, black to gray.black (N1 to N2), massive to v.faintly laminated and mottled; (3) MUDSTONE, gray black to ol.black (N2 to 5Y 2/1), w/clasts and wavy laminae of grn.gray siderite (5GY6/1)

\*identified by black intervals in lithology column

Smear 2-104  
 [0.15,85]  
 45% clay  
 30% siderite  
 20% nannos  
 5% carb.unspec.  
 tr.heavy mins., pyrite

Smear 2-60  
 [7, 15,78]  
 62% clay  
 15% nannos  
 7% quartz  
 3% carb.unspec.  
 4% siderite  
 3% mica  
 3% pyrite  
 1% heavy mins  
 1% zeolite  
 1% volc.glass

CaCO<sub>3</sub>% C<sub>org</sub>%

SHIPBOARD 1-108 10  
 2-66 13  
 SHOREBASED 1-109 12 0.4 GRAIN SIZE 3-33=tr.,18,82

Explanatory notes in Chapter 1

SITE 398 HOLE D CORE 71 CORED INTERVAL: 1088.0-1097.5 m

TIME-ROCK UNIT	BIOSTRAT ZONE	FOSSIL CHARACTER	SECTION	METERS	GRAPHIC LITHOLOGY	DRILLING DISTURBANCE	SEDIMENTARY STRUCTURES	LITHOLOGIC SAMPLE	LITHOLOGIC DESCRIPTION
				0.5					
				1					
				1.0					
				2					
				3					
				4					
				5					
				6					
				7					
				CC					

General Description: Minor CALCAREOUS MUDSTONE, grn.black to dk.grn.gray (5GY2/1 to 4/1), bioturbation moderate; major portion of core is MUDSTONE of three types: (1) black to gray black (N1 to N2), massive to v.faintly laminated and mottled; (2) gray, black to ol.black (N2, 5Y2/1) w/clasts and wavy laminae of grn.gray siderite (5GY6/1); (3) dk.gray to ol.gray (N4 to 5Y4/1), finely laminated w/grn.gray siderite (5GY6/1), laminae parallel and 0.1 to 1.0 mm thick.

very fine white wavy laminae, much whiter than any others Smear 1-86 [0.25,75]  
 63% clay  
 20% nannos  
 5% zeolite  
 5% siderite  
 3% mica  
 2% carb.unspec.  
 1% quartz  
 1% heavy mins

lens-shaped greenish gray (5GY6/1) to yellowish gray (5Y 8/1) laminae of siderite (?) in sections 2 and 3, Smear 1-105 [10,30,60]  
 56% clay  
 20% nanno  
 5% quartz  
 5% carb.unspec.  
 3% zeolite  
 3% mica  
 3% siderite  
 2% heavy mins.  
 2% radiol.  
 1% volc.glass

several more siderite(?) lens-shaped laminae, often with internal structures (inclusions, claystone wisps) Smear 4-44 [10,40,50]  
 65% clay  
 8% quartz  
 6% radiol.  
 5% zeolite  
 5% carb.unspec.  
 4% siderite  
 3% nannos  
 3% gypsum  
 1% heavy mins

the laminated intervals are best preserved, the remainder of the core is fractured, brecciated

two very light gray (N8) distinct laminae, salt & pepper coloration; firm, clay-sized, distinctly different from siderite

these fine laminae appear to constitute "packages" of laminae; individuals amount to >20/cm, "packages" are 1 every 2cm, with very faintly laminated dark intervening sediment; most are parallel, few are wavy, some are convoluted wisps; some are probably load casts; 2mm clasts are often found at the top of "packages" of laminae

\*identified by black interval in lithology column

GRAIN SIZE 1-100=0,40,60

SHIPBOARD 1-108 23  
 4-69 5  
 SHOREBASED 1-97 23 0.2  
 4-70 3 0.5

SITE 398

SITE 398 HOLE D		CORE 72		CORED INTERVAL: 1107.0-1116.5 m	
TIME-ROCK UNIT	BIOSTRAT ZONE	FOSSIL CHARACTER	SECTION METERS	GRAPHIC LITHOLOGY	LITHOLOGIC DESCRIPTION
		FORAMS NANNOS RADS			
ALBIAN ?			0.5 1 1.0		General Description: CALCAREOUS MUDSTONE, grn. black to dk.grn.gray (5GY2/1 to 4/1), bioturbation moderate, often w/gray black (N2) unburrowed intervals 1-2cm thick, marked by either sharp or gradational contacts; MUDSTONE of three types: (1)*black to gray black(N1 to N2), massive to v.faintly laminated and mottled; (2)gray.black to ol.black(N2 to 5Y2/1) w/clasts and wavy laminae of grn.gray (5GY6/1) siderite; (3)dk.gray to ol.gray(N4 to 5Y4/1), finely laminated w/siderite, grn.gray (5GY6/1), laminae parallel and <1mm thick.
			2		Numerous white specks scattered along bedding surfaces Smear 3-50 [0.20,80] 76% clay 10% nanno 5% siderite 1% forams 1% carb.unspec. 1% zeolite 1% pyrite 1% mica 1% quartz 2% organ.mat. tr.heavy mins. 1% feldspar
			3		*identified by black interval in lithology column
			4		one triangular fragment of siderite, apparently comparable to lens-shaped laminae, but porous (round, sand-sized vugs) w/a large portion of center weathered out(?) approx. 1cm
			5		laminae are approx. 20/cm. in groups of about 10, groups approx. 1cm apart; offset by small normal faults.
			6		GRAIN SIZE 3-68=tr, 29, 71
			7		SHIPBOARD 2-54 14 SHOREBASED 2-55 13 0.4
			CC		

Explanatory notes in Chapter 1

SITE 398 HOLE D		CORE 73		CORED INTERVAL: 1116.5-1126.0 m	
TIME-ROCK UNIT	BIOSTRAT ZONE	FOSSIL CHARACTER	SECTION METERS	GRAPHIC LITHOLOGY	LITHOLOGIC DESCRIPTION
		FORAMS NANNOS RADS			
ALBIAN			0.5 1 1.0		General Description: minor CALCAREOUS MUDSTONE to MARLY NANNO CHALK, grn. black grading to grn. gray (5GY2/1 to 6/1) towards center of unit, bioturbation intense; major portion of core is MUDSTONE of three types: (1)*black to gray black (N1 to N2), faintly mottled and laminated; (2) gray black to ol.black(N2 to 5Y2/1) w/clasts and wavy laminae of grn.gray(5GY6/1) siderite; (3)dk. gray to ol.gray(N4 to 5Y4/1) w/fine parallel laminae of siderite, grn.gray(5GY6/1).
			2		*identified by black interval in lithology column
			3		darkest mudstone is by no means "homogeneous", v.faint mottles and laminae visible throughout; in addition, partings parallel to bedding reveal flattened worm traces grn.gray(5GY6/1) which are nearly 100% pyrite; occasional shell fragments, some apparently hinged molluscs, 1x3 mm within this darkest claystone as well, and noted by * in litho.sample column.
			4		Smear 3-8 [3.17,80] 51% clay 35% nannos 5% siderite 3% carb.unspec. 3% forams 1% quartz 1% mica 1% pyrite tr.zeolite tr heavy mins.
			5		Smear 3-120 [0.20,80] 81% clay 4% organic mat. 3% pyrite 3% zeolite 2% mica 2% carb.unspec. 2% nannos 1% quartz 1% siderite 1% radiolaria
			6		Smear 3-142 [5.10,85] 64% clay 10% gypsum 2% quartz 2% mica 2% pyrite
			7		Smear 4-100 [0.50,50] 70% siderite 17% clay 8% carb.unspec. 2% pyrite 2% nannos 1% mica tr.heavy mins.
			CC		GRAIN SIZE 3-96=0.33, 67
					SHIPBOARD 3-37 20 SHOREBASED 3-38 19 0.2

SITE 398		HOLE D		CORE 74		CORED INTERVAL: 1126.0-1135.5 m	
TIME-ROCK UNIT	BIOSTRAT ZONE	FOSSIL CHARACTER		SECTION METERS	GRAPHIC LITHOLOGY	LITHOLOGIC DESCRIPTION	
		FORAMS	NANNOS				
ALBIAN	<i>Parahoplites argutus</i> ?	Rg		0.5		CALCAREOUS MUDSTONE, yel.ol.grn. (5GY4/2), intensely burrowed, occasionally faintly, irregularly laminated; and MUDSTONE of three types: (1) dk.gray* (N3), homogeneous to faintly laminated, (2) dk.gray to gray (N3 to 5Y6/1) w/wavy laminae of siderite, grn.gray (5GY6/1), and (3) dk.gray (N3) w/parallel laminae of siderite	
				1.0		*noted by black interval in lithology column	
				2.0		occasional lenses, inclusions of siderite within darkest mudstone intervals	
				3.0			
				4.0			
				5.0			
				6.0			
				CC			

*noted by black interval in lithology column		Smear 1-100 [10,40,50] 60% siderite 10% quartz clay
occasional lenses, inclusions of siderite within darkest mudstone intervals		5% carb.unspec. 3% forams 2% feldspar, mica pyrite, zeolite, org.matter 1% heavy min glauconite
		SMEAR 3-60 [0,30,70] 63% clay 18% nannos 10% siderite 2% mica, carbons 1% quartz, pyrite forams, radiol., organic mat.
		SMEAR 4-70 [0,15,85] 82% clay 5% organic mat 4% pyrite 3% mica 2% carb.unspec. organic opal. 1% quartz, zeolite, siderite, nannos radiol.
		SMEAR 5-149 [0,50,50] 50% siderite 30% clay 10% nannos 5% organic mat. 2% micas, pyrite 1% quartz
GRAIN SIZE 3-69=tr, 50, 50		
SHIPBOARD	3-62	19
SHOREBASED	4-86	12
		0.4
		CaCO <sub>3</sub> %
		C <sub>org</sub> %

Explanatory notes in Chapter 1

SITE 398		HOLE D		CORE 75		CORED INTERVAL: 1135.5-1145.0 m			
TIME-ROCK UNIT	BIOSTRAT ZONE	FOSSIL CHARACTER		SECTION METERS	GRAPHIC LITHOLOGY	DRILLING DISTURBANCE	SEDIMENTARY LITHOLOGIC SAMPLE	LITHOLOGIC DESCRIPTION	
		FORAMS	NANNOS						
ALBIAN	APTIAN ?	Rg		0.5				one siderite lens at top of core	Smear 1-39 [3,30,67] dom.
				1.0					
				2.0					
				3.0					
				4.0					
				5.0					
				6.0					
								CC	
				CC					



SITE 398		HOLE D		CORE 78		CORED INTERVAL: 1173.5-1183.0 m	
TIME-ROCK UNIT	BIOSTRAT ZONE	FOSSIL CHARACTER			SECTION METERS	GRAPHIC LITHOLOGY	LITHOLOGIC DESCRIPTION
		FORAMS	NANNOS	RADS			
APTIAN ?	Rg				0.5		General Description: entire core is dk gray (N3) MUDSTONE, occasionally SLIGHTLY CALCAREOUS; much of core is homogeneous, yet very, very faint mottles and laminae are visible, but the latter are so fine that they impart no detectable color change, and are presumed to be rich in siderite
					1		
					1.0		numerous shell fragments marked by *
					2		
					2		SMEAR 2-80 [0.30,70] 74% clay 8% quartz 5% carb.unspec. 3% mica, nannos, pyrite 2% heavy min 1% forams, zeolite tr. radiolaria
					3		truncated, inclined bedding; slump structures?
					4		numerous siderite lenses, often irregular and vuggy
CC	Rg B				5		GRAIN SIZE 4-64=tr, 28.72
					6		
CC					7		SHIPBOARD 2-94 5 SHOREBASED 2-95 3 0.6
					CC		

Explanatory notes in Chapter 1

SITE 398		HOLE D		CORE 79		CORED INTERVAL: 1183.0-1192.5 m	
TIME-ROCK UNIT	BIOSTRAT ZONE	FOSSIL CHARACTER			SECTION METERS	GRAPHIC LITHOLOGY	LITHOLOGIC DESCRIPTION
		FORAMS	NANNOS	RADS			
APTIAN ?	Rg				0.5		uppermost 70cm of core is disturbed and folded-cave-in?
					1		entire core is dk gray (N3) MUDSTONE, homogeneous except for scattered v faint mottles and laminae, numerous grn. gray (5Y6/1) siderite lenses and clasts (some w/ apparent inclusions-aggregates?) and occasional shell fragments. (Inoceramus?) some very well preserved along bedding planes, and marked by *
					2		
					3		SMEAR 3-136 [0.25,75] 71% clay 5% quartz carb.unsp. 4% siderite, mica 3% heavy mins. 2% nannos tr. pyrite, zeolite
					4		
					5		GRAIN SIZE 3-10=tr, 50, 50
					6		
Rg B					7		SHIPBOARD 1-5 7 SHOREBASED 1-4 1 0.6
					CC		

Explanatory notes in Chapter 1SITE 398

SITE 398 HOLE D CORE 82 CORED INTERVAL: 1211.5-1221.0 m

TIME-ROCK UNIT	BIOSTRAT ZONE	FOSSIL CHARACTER			SECTION	METERS	GRAPHIC LITHOLOGY	DRILLING DISTURBANCE	SEDIMENTARY STRUCTURE	LITHOLOGIC DESCRIPTION
		FORAMS	NANNOS	RADS						
APTIAN										
						0.5				numerous gray to ol. gray specks, medium sand size, laminated; concentrations of siderite? of nannofossils?
						1.0				
						2.0				General Description: minor CALCAREOUS MUDSTONE, yel.ol.grn.(5GY4/2), intensely burrowed; and MUDSTONE*, dk.gray (N3) faintly laminated, w/ numerous lenses of grn.gray (5Y6/1)siderite
						3.0				Smear 1-92 [0.20,80] 85% clay 3% mica,pyrite 3% organic mat. 2% nannos 1% quartz,calc. unspec., siderite, forams, Radiolaria, sponge spics.
						4.0				*identified by black interval in lithology column  Smear 1-50 [5.30,65] 61% clay 10% calc.unspec., nannos 3% quartz, siderite, forams 2% feldspar,mica 2% organic mat. 1% hea.mins.pyrite, Radiol.,sponge spics.
						5.0				fine black mottling within siderite lens-Chondrites mottling?  Smear 4-125 [0.15,85] 90% clay 2% mica,pyrite 2% organic mat. 1% quartz, siderite, carb.unspec. Radiolaria tr.heavy mins.
						6.0				GRAIN SIZE 3-149=0,29,71  SHIPBOARD 3-104 CaCO <sub>3</sub> % <2 SHOREBASED 5-122 C <sub>org</sub> % 2 1.2
						7.0				
						CC				

Explanatory notes in Chapter 1

SITE 398 HOLE D CORE 83 CORED INTERVAL: 1221.0-1230.5 m

TIME-ROCK UNIT	BIOSTRAT ZONE	FOSSIL CHARACTER			SECTION	METERS	GRAPHIC LITHOLOGY	DRILLING DISTURBANCE	SEDIMENTARY STRUCTURE	LITHOLOGIC DESCRIPTION
		FORAMS	NANNOS	RADS						
APTIAN						0.5				10 cm of MUDSTONE, dk.gray (N3)

SITE 398 HOLE D CORE 84 CORED INTERVAL: 1230.5-1240.0 m									
TIME-ROCK UNIT	BIOSTRAT ZONE	FOSSIL CHARACTER			SECTION METERS	GRAPHIC LITHOLOGY	DRILLING DISTURBANCE	LITHOLOGIC SAMPLE	LITHOLOGIC DESCRIPTION
		FORAMS	NANNOS	RADS			STRUCTURE		
APTIAN					1	0.5 1.0			General Description: minor MUDSTONE TO CALCAREOUS MUDSTONE, gray-ol. grn. (5GY3/2), burrowed; dominant MUDSTONE*, gray-black (N2) to dk. gray (N3), mostly homogeneous, the lighter intervals w/ both wavy laminae of gray (5GY6/1) and parallel laminae of grn. gray (5GY6/1), presumably rich in siderite; numerous nodules, irregular lenses of siderite throughout the massive intervals, also grn. gray
					2				*identified by black interval in lithology column  several shell fragments, noted by *
					3				Smear 3-75 [40,60] 82% clay 5% organic mat. 3% pyrite, mica 2% zeolite. Radiolaria 1% siderite, quartz. heavy min.
					4				Smear 6-46 [2,18,80] 88% clay 2% volc. glass, organic mat., pyrite, mica. 1% quartz, zeolite, siderite, Radiolaria tr. heavy min.
					5				← siderite within a pelecypod shell  Several gypsum-bearing claystones; located at: Sec 3, 55-60cm Sec 5, 21-23cm Sec 5, 32-34cm Sec 6, 70-72cm
					6				GRAIN SIZE 6-130=0.38,62
					7				SHIPBOARD 5-120 <2 SHOREBASED 7-36 0 0.5
					CC				

Explanatory notes in Chapter 1

SITE 398 HOLE D CORE 85 CORED INTERVAL: 1240.0-1249.5 m									
TIME-ROCK UNIT	BIOSTRAT ZONE	FOSSIL CHARACTER			SECTION METERS	GRAPHIC LITHOLOGY	DRILLING DISTURBANCE	LITHOLOGIC SAMPLE	LITHOLOGIC DESCRIPTION
		FORAMS	NANNOS	RADS			STRUCTURE		
APTIAN					1	0.5 1.0			minor MUDSTONE TO CALCAREOUS MUDSTONE, gray-ol. grn. (5GY3/2), burrowed; dominant MUDSTONE*, gray, black (N2) to dk. gray (N3), homogeneous except for a few siderite-rich parallel laminae and scattered, irregular lenses of siderite, all grn. gray (5GY6/1)
					2				*identified by black interval in lithology column  SMEAR 2-26 [0,40,60] 76% clay 10% organic mat. 6% pyrite 2% mica, nannos 1% quartz, Radiol.
					3				SMEAR 2-133 [0,20,80] 74% clay 18% nanno (Nannocomus) 2% carb. unsp., quartz 1% mica, pyrite, siderite, forams tr. Heavy min.
					4				GRAIN SIZE 2-84=tr,32,68  SHIPBOARD 2-80 5 SHOREBASED 4-74 1 0.3

SITE 398 HOLE D CORE 86 CORED INTERVAL: 1249.5-1259.0 m

TIME-ROCK UNIT	BIOSTRAT ZONE	FOSSIL CHARACTER	SECTION	METERS	GRAPHIC LITHOLOGY	LITHOLOGIC DESCRIPTION
				0.5		uppermost 6cm of core is cave-in breccia
				1		SMEAR 2-5 [0.30,70] 70% clay 18% nannos 2% mica, pyrite, carb.unspec. 2% organic mat. 1% quartz. forams, Radiolaria tr. heavy mins.
				1.0		possibly an upward fining distal turbidite
				2		minor MUDSTONE to CALCAREOUS MUDSTONE, gray.ol. grn. (5GY3/2), burrowed; dominant MUDSTONE*, gray black (N2) to dk.gray (N3) homogeneous except for an interval of siderite-rich parallel laminae in sections 3 and 4, plus numerous irregular lenses of siderite, all grn.gray (5GY6/1)
						*identified by black interval in lithology column
				3		SMEAR 2-36 [0.50,50] 43% clay 40% siderite 12% nannos 2% carb.unspec. 1% foram.quartz mica tr. heavy mins.
				4	O.G.	SMEAR 2-101 [0.20,80] 75% clay 10% nannos 3% mica,pyrite, zeolite 3% organic mat. 2% Radiolaria 1% siderite calc.unspec
				5		GRAIN SIZE 3-133=tr.35,65
						CaCO <sub>3</sub> % C <sub>org</sub> %
						SHIPBOARD 2-36 <2
						SHOREBASED 5-97 1 0.5

Explanatory notes in Chapter 1

SITE 398 HOLE D CORE 87 CORED INTERVAL: 1259.0-1268.5 m

TIME-ROCK UNIT	BIOSTRAT ZONE	FOSSIL CHARACTER	SECTION	METERS	GRAPHIC LITHOLOGY	LITHOLOGIC DESCRIPTION
				0.5		possibly a distal turbidite
				1		minor MUDSTONE to CALCAREOUS MUDSTONE, gray.ol. grn. (5GY3/2), often burrowed; dominant MUDSTONE*, gray black (N2) to dk.gray (N3), homogeneous except for several intervals of siderite-rich, parallel laminae and numerous irregular lenses of siderite, all grn.gray (5GY6/1)
				2		*identified by black interval in lithology column
				3		
				4		
				5		possibly a distal turbidite
						GRAIN SIZE 5-81=0,37,63
						CaCO <sub>3</sub> % C <sub>org</sub> %
						SHIPBOARD 1-29 <2
						SHOREBASED 3-130 1 0.7

SITE 398 HOLE D CORE 88 CORED INTERVAL: 1268.5-1278.0 m

TIME-ROCK UNIT	BIOSTRAT ZONE	FOSSIL CHARACTER	SECTION	METERS	GRAPHIC LITHOLOGY	DRILLING DISTURBANCE	STRUCTURE	LITHOLOGIC SAMPLE	LITHOLOGIC DESCRIPTION
		FORAMS NANNOS RADS							
				0.5					siderite and chert(?) caving breccia
				1					siderite lenses in this interval are lt.gray (N7) instead of the usual grn. gray (5GY6/1)
				1.0					Smear 2-86 (2.15,83) 78% clay 7% nannos 4% quartz 4% mica 3% heavy mins. 3% pyrite 1% zeolite
				2					v.fine grained mudstone, ol. gray (5Y4/1), well-lithified w/soft claystone at base
				3					MUDSTONE*.gray black (N2) to dk.gray (N3), homogeneous except for several intervals of siderite-rich parallel laminae and numerous irregular lenses of siderite, all grn.gray (5GY 6/1); one interval of burrowed MUDSTONE to CALCAREOUS MUDSTONE, gray.ol.grn. (5GY3/2) between sections 1 and 2
				4					*identified by black interval in lithology column
				4	O.G.				Smear 2-116 (5.20,75) 79% clay 6% quartz 5% carb.unsp. 3% mica,pyrite 1% nannos, gypsum, heavy min.
				5					Smear 6-58 98% siderite 2% quartz
				6					Shell fragments
				6					GRAIN SIZE 2-89=5.45,50
				7					SHIPBOARD 3-88 6 SHOREBASED 1-117 1 0.5
				CC					

Explanatory notes in Chapter 1

SITE 398 HOLE D CORE 89 CORED INTERVAL: 1278.0-1287.5 m

TIME-ROCK UNIT	BIOSTRAT ZONE	FOSSIL CHARACTER	SECTION	METERS	GRAPHIC LITHOLOGY	DRILLING DISTURBANCE	STRUCTURE	LITHOLOGIC SAMPLE	LITHOLOGIC DESCRIPTION
		FORAMS NANNOS RADS							
				0.5					MUDSTONE*.gray black (N2) to dk.gray (N3), homogeneous except for several intervals of siderite-rich parallel laminae and numerous irregular lenses of siderite, all grn.gray (5GY 6/1); one interval in section 2 of burrowed MUDSTONE to CALCAREOUS MUDSTONE, gray.ol.grn. (5GY3/2)
				1					*identified by black interval in lithology column
				1.0					Shell fragments noted by *
				2					siderite layer(?) w/Chronodrites-like burrows
				3					
				4					medium gray (N5) mudstone laminated w/lt.gray (N7)
				5					GRAIN SIZE 5-17=2.31,67
				6					SHIPBOARD 4-92 <2 SHOREBASED 5-89 6 2.3
				7					
				CC					

SITE		HOLE		CORE		CORDED INTERVAL: 1287.5-1297.0 m	
TIME-ROCK UNIT	BIOSTRAT ZONE	FOSSIL CHARACTER			SECTION METERS	GRAPHIC LITHOLOGY	LITHOLOGIC DESCRIPTION
		FORAMS	NANNOS	RADS		ORILLING DISTURBANCE SEDIMENTARY LITHOLOGICAL SAMPLE	
					0.5		MUDSTONE*, gray black (N2) to dk.gray (N3), homogeneous except for several intervals of siderite-rich parallel laminae and numerous irregular lenses of siderite.all grn.gray (5GY 6/1);one interval in section 2 of burrowed MUDSTONE to CALCAREOUS MUDSTONE,gray.ol.grn. (5GY3/2)
					1		
					1.0		
					2		*identified by black interval in lithology column
							← shell fragment
					3		
							← medium gray (N5) mudstone w/siderite laminae
					4		
							← siderite layer.laminated and w/chondrites-like burrows
					5	O.G.	
					6		
					7		
					CC		

GRAIN SIZE  
3-20=1.44,55

CaCO<sub>3</sub>% C<sub>org</sub>%

SHIPBOARD 2-104 <2  
SHOREBASED 4-23 1 0.9

SITE	398	HOLE	D	CORE	91	CORED INTERVAL:	1297.0-1306.5 m	
TIME-ROCK UNIT	BIOSTRAT ZONE	FOSSIL CHARACTER			SECTION METERS	GRAPHIC LITHOLOGY	DISTURANCE SEDIMENTARY LITHOLOGIC SAMPLE	LITHOLOGIC DESCRIPTION
		FORAMS	NANNOS	RADS				
					1			MUDSTONE*, gray black (N2) to dk.gray (N3) homogeneous except for several intervals of siderite-rich parallel laminae and numerous irregular lenses of siderite,all grn.gray (5GY 6/1) and thin (<5cm) layers of med.gray (N5) claystone;bottom 70cm of core is interval of olive black (5Y2/1) MUDSTONE, w/laminae of lt.ol.gray (5Y6/1) like above,but much more indurated;this basal unit does not expand as it dries as does the other unit.
					2			*identified by black interval in lithology column Smear 2-16 Siderite  Shell fragments noted by *  med.gray claystone Smear 3-91 [0.10,90] 73% clay 5% carb.unspec. 4% siderite quartz 3% org.mat. 3% nannos 2% mica 1% heavy min. zeolite
					3			ol. gray claystone Smear 4-130 [0.10,90] 70% clay 10% quartz 4% mica 3% heavy min 2% pyrite 2% org.mat. 1% radiolaria
					4			GRAIN SIZE 3-94 = 1.22,77  SHIPBOARD 4-102 <2 SHOREBASED 1-44 1 0.9

SITE 398		HOLE D		CORE 92		CORED INTERVAL: 1306.5-1316.0 m	
TIME-ROCK UNIT	BIOSTRAT ZONE	FOSSIL CHARACTER	SECTION METERS	GRAPHIC LITHOLOGY	DRILLING DISTURBANCE	SEDIMENTARY STRUCTURE	LITHOLOGIC DESCRIPTION
			0.5	*			top 55cm of core is well-indurated, non-expanding CLAYSTONE, ol. black (5Y2/1) w/ v. fine parallel gray black (N2) laminae inclined at 5°
			1.0				predominantly MUDSTONE*, gray black (N2) to dk. gray (N3), homogeneous except for numerous intervals of siderite-rich parallel laminae and numerous irregular lenses of siderite, all grn. gray (5GY6/1); minor amount of burrowed MUDSTONE to CALCAREOUS MUDSTONE, gray. ol. grn. (5GY3/2) in sec. 2
			2.0				unusual occurrence of siderite lens within burrowed interval
			3.0				faint ol. gray at center of burrowed interval, w/ siderite dominant in smear slide
			4.0				several med. gray (N5) CLAYSTONE intervals, ~3cm thick, w/ sharp basal contact, grading upwards to ol. black (5Y2/1)
			5.0				*identified by black interval in lithology column
			6.0				Shell fragments noted by *
			7.0				
			CC				
							CaCO <sub>3</sub> % C <sub>org</sub> %
							SHIPBOARD 3-82 <2
							SHOREBASED 2-150 15 0.4

Explanatory notes in Chapter 1

SITE 398		HOLE D		CORE 93		CORED INTERVAL: 1316.0-1325.5 m	
TIME-ROCK UNIT	BIOSTRAT ZONE	FOSSIL CHARACTER	SECTION METERS	GRAPHIC LITHOLOGY	DRILLING DISTURBANCE	SEDIMENTARY STRUCTURE	LITHOLOGIC DESCRIPTION
			0.5				core is entirely MUDSTONE*, gray black (N2) to dk. gray (N3), homogeneous except for numerous intervals of siderite-rich parallel laminae and numerous irregular lenses of siderite, all grn. gray (5GY6/1); below sec. 2, laminae may show signs of current winnowing
			1.0				*identified by black interval in lithology column
			2.0				Smear 1-68 [2.25, 75] 83% clay 5% org. mat. 3% pyrite 2% quartz, mica radiolaria 1% volc. glass, zeolite
			3.0				Smear 3-77 [50.30, 20] 70% siderite 22% clay 3% org. mat. 1% quartz, mica volc. glass pyrite, zeolite tr. radiolaria (pyritized)
			4.0				Smear 6-82 [25.50, 25] 70% siderite 25% clay 3% org. 1% volc. glass pyrite
			5.0				
			6.0				GRAIN SIZE 1-23=tr, 38, 62
			7.0				CaCO <sub>3</sub> C <sub>org</sub> %
			CC				SHIPBOARD 2-48 3
							SHOREBASED 5-89 1 0.9

SITE 398		HOLE D		CORE 94		CORED INTERVAL: 1325.5-1327.5 m	
TIME-ROCK UNIT	BIOSTRAT ZONE	FOSSIL CHARACTER		SECTION	METERS	GRAPHIC LITHOLOGY	LITHOLOGIC DESCRIPTION
		FORAMS	NANNOS				
BARREMIAN-APTIAN				1	0.5		MUDSTONE, gray black (N2) to dk. gray (N3), homogeneous except for numerous intervals of siderite-rich parallel laminae and several irregular lenses of siderite, all grn. gray (5GY6/1).
				1	1.0		
BARREMIAN-APTIAN				2			<p>Smear 1-42 [0.15, 85] Smear 2-42 [0.0, 100]</p> <p>86% clay 99% siderite</p> <p>6% quartz 1% nannos</p> <p>2% mica</p> <p>2% nannos</p> <p>2% org. mat.</p> <p>1% heavy mins.</p> <p>1% siderite</p> <p>CaCO<sub>3</sub>% C<sub>org</sub>%</p> <p>SHIPBOARD 1-40 9</p> <p>SHOREBASED 1-109 1 1.0</p>

Explanatory notes in Chapter 1

SITE 398		HOLE D		CORE 95		CORED INTERVAL: 1327.5-1335.0 m	
TIME-ROCK UNIT	BIOSTRAT ZONE	FOSSIL CHARACTER		SECTION	METERS	GRAPHIC LITHOLOGY	LITHOLOGIC DESCRIPTION
		FORAMS	NANNOS				
BARREMIAN-APTIAN				1	0.5		<p>dominant MUDSTONE*, gray black (N2) to dk. gray (N3) homogeneous except for occasional intervals of siderite-rich parallel laminae and abundant irregular lenses of siderite all grn. gray (5GY6/1); and occasional shell fragments; minor CLAYSTONE, med. gray (N5).</p> <p>*identified by black interval in lithology column</p> <p>Shell fragments noted by *</p>
				1	1.0		
BARREMIAN-APTIAN				2			<p>← 30° syndepositional (?) fault</p> <p>Smear 4-90 [0.20, 80]</p> <p>85% clay</p> <p>4% quartz</p> <p>4% org. mat.</p> <p>2% carb. unspec.</p> <p>1% nannos, pyrite, mica</p>
				2			
BARREMIAN-APTIAN				3			<p>O.G.</p> <p>Smear 6-85 [4.20, 76]</p> <p>80% clay</p> <p>6% quartz</p> <p>3% nannos</p> <p>3% org. mat.</p> <p>2% mica, heavy mins., carb. unspec.</p> <p>1% pyrite</p> <p>tr. volc. glass</p>
				3			
BARREMIAN-APTIAN				4			<p>← siderite lens attached to underlying ammonite shell</p> <p>GRAIN SIZE</p> <p>2-77=tr, 41, 59</p> <p>CaCO<sub>3</sub> C<sub>org</sub>%</p>
				4			
BARREMIAN-APTIAN				5			<p>SHIPBOARD 6-30 &lt;2</p> <p>SHOREBASED 1-22 1 0.8</p>
				5			
BARREMIAN-APTIAN				6			
				6			
BARREMIAN-APTIAN				7			
				7			

SITE 398 HOLE D CORE 96 CORED INTERVAL: 1335.0-1344.5 m

TIME-ROCK UNIT	BIOSTRAT ZONE	FOSSIL CHARACTER	SECTION METERS	GRAPHIC LITHOLOGY	DRILLING DISTURBANCE	SEDIMENTARY STRUCTURE	LITHOLOGIC SAMPLE	LITHOLOGIC DESCRIPTION
BARREMIAN-APTIAN								
			0.5					dominant MUDSTONE*, gray black (N2) to dk.gray (N3), homogeneous except for several intervals of siderite-rich parallel laminae and abundant irregular lenses of siderite, all grn.gray (5GY 6/1), and occasional shell fragments; minor CLAYSTONE, med. gray (N5)
			1.0					*identified by black interval in lithology column Smear 1-68 [0.60,40] 55% carb.unspec. 20% siderite 20% clay 5% pyrite
			2.0					Shell fragments noted by *
			3.0					siderite nodule w/v.smooth-walled, straight hole-through center; boring? weathering? Smear 1-73 [0.40,60] 67% clay 10% carb.unspec. 5% org.mat. 3% nannos pyrite 2% quartz, mica, volc.glass zeolite 1% heavy mins., siderite, forams, radiolaria
			4.0					several hard, rounded clasts of dk.ol.gray w/soft matrix of v.dk.gray; shell fragments, siderite breccia in calcite cement? Smear 3-104 [0.80,20] 74% carb.unspec. 20% clay 2% volc.glass, zeolite, siderite
			5.0					GRAIN SIZE 3-69=tr.32,68 SHIPBOARD 1-6 9 SHOREBASED 2-137 7 1.9
			6.0					CaCO <sub>3</sub> % C <sub>org</sub> %
			7.0					
			CC					

Explanatory notes in Chapter 1

SITE 398 HOLE D CORE 97 CORED INTERVAL: 1344.5-1354.0 m

TIME-ROCK UNIT	BIOSTRAT ZONE	FOSSIL CHARACTER	SECTION METERS	GRAPHIC LITHOLOGY	DRILLING DISTURBANCE	SEDIMENTARY STRUCTURE	LITHOLOGIC SAMPLE	LITHOLOGIC DESCRIPTION
			0.5					clast of pinkish white porous limestone, w/coral fragments, shell casts, oolites Smear 1-60 [3.30,67] 50% pyrite 50% org.mat.
			1.0					lens containing ooids v.dk.gray (N2) coal-like fragment; hard, pitted, smooth Smear 2-62 [3.30,67] 68% clay 10% carb.unspec. 5% quartz 3% mica, zeolite 3% org.mat. nannos 2% radiolaria, heavy mins. 1% siderite
			2.0					flattened mud chips, possibly graded, salt & pepper gray colors
			3.0	O.G.				dominant MUDSTONE*, gray black (N2) to dk.gray (N3), w/occasional intervals of siderite-rich parallel laminae and numerous irregular lenses, vuggy nodules of siderite, all grn.gray (5GY6/1); several intervals of allochthonous material within dark unit; minor CLAYSTONE med. gray (N5) *identified by black interval in lithology column Smear 2-116 [20.50,30] 52% carb.unspec. 27% clay 5% nannos 3% quartz, zeolite 3% org.mat. 2% mica, pyrite 1% heavy mins., siderite, radiolaria
			4.0					poorly-sorted gravel to cobble-sized conglomerate, clasts possibly imbricated, composed of limestone in sandy/silty dk gray (N2) matrix of low carbonate content; a few pelecypod fragments
			5.0					coal-like fragment like above Shell fragments noted by * Smear 2-34 [2.20,78] 86% clay 3% mica, pyrite 3% org.mat. 2% radiolaria 1% quartz, siderite, heavy mins.
			6.0					
			7.0					GRAIN SIZE 4-26=1.36,63 SHIPBOARD 5-46 3 SHOREBASED 5-55 13 2.0
			CC					CaCO <sub>3</sub> % C <sub>org</sub> %

SITE 398 HOLE D CORE 98 CORED INTERVAL: 1354.0-1363.5 m

TIME-ROCK UNIT	BIOSTRAT ZONE	FOSSIL CHARACTER	SECTION	METERS	GRAPHIC LITHOLOGY	DRILLING DISTURBANCE	SEDIMENTARY STRUCTURE	LITHOLOGIC DESCRIPTION
			1	0.5				washed, brecciated
				1.0				MUDSTONE, gray black (N2) to dk.gray (N3) w/rare siderite-rich parallel laminae and numerous irregular, vuggy nodules of siderite, all grn.gray (5GY6/1)
			2					<div> <div>Smear 1-98 [8.42,50] 62% clay 10% carb.unspec. 5% quartz, radiolaria 5% org.mat. 3% mica, pyrite 2% heavy mins. 1% feldspar, sponge spic., volc.glass</div> <div>Smear 1-104 [0.5,95] 79% clay 5% org.mat. 3% mica, radiolaria, pyrite 2% volc. glass, zeolite 1% quartz, siderite, heavy mins.</div> </div>
			3					<div> <div>SHIPBOARD 1-80 &lt;2</div> <div>SHOREBASED 2-24 4 0.9</div> </div>

Explanatory notes in Chapter 1

SITE 398 HOLE D CORE 99 CORED INTERVAL: 1363.5-1373.0 m

TIME-ROCK UNIT	BIOSTRAT ZONE	FOSSIL CHARACTER	SECTION	METERS	GRAPHIC LITHOLOGY	DRILLING DISTURBANCE	SEDIMENTARY STRUCTURE	LITHOLOGIC DESCRIPTION
			1	0.5				dominant MUDSTONE*, gray, black (N2) to dk.gray (N3) w/occasional siderite-rich parallel laminae and numerous irregular, vuggy nodules of siderite, commonly 1/4 to 2cm in longest dimension, all grn.gray (5GY6/1); minor CLAYSTONE to MUDSTONE med.gray (N5) to med.dk.gray (N4), massive to finely laminated, perhaps w/graded bedding in thickest beds.
			2					<div> <div>*identified by black interval in lithology column</div> <div>Shell fragments noted by *</div> <div>Smear 2-37 [3.60,67] 64% clay 8% carb.unspec. nannos 5% org.mat. 3% mica, pyrite, zeolite 2% quartz, radiolaria 1% heavy mins.</div> </div>
			3					<div> <div>Smear 2-67 [3.30,67] 74% clay 5% radiolaria 5% org.mat. 4% pyrite 3% quartz, mica 2% gypsum, zeolite 1% siderite, heavy mins.</div> </div>
			4		O.G.			<div> <div>Smear 3-85 [5.40,55] 66% clay 5% quartz, carb.unspec., nannos 5% org.mat. 3% mica, radiolaria 2% pyrite, zeolite 1% siderite, forams, gypsum, heavy mins.</div> </div>
			5					<div> <div>GRAIN SIZE 5-37=3,39,58</div> </div>
			6					<div> <div>SHIPBOARD 2-64 &lt;2</div> <div>SHOREBASED 5-112 1 0.7</div> </div>
			7					
			CC					

SITE 398		HOLE D		CORE 100		CORE INTERVAL: 1373.0-1382.5 m			
TIME-ROCK UNIT	BIOSTRAT ZONE	FOSSIL CHARACTER			SECTION	METERS	GRAPHIC LITHOLOGY	ORILLING DISTURBANCE SEDIMENTARY LITHOLOGIC SAMPLE	LITHOLOGIC DESCRIPTION
		FORAMS	NANNOS	RADS					
									dominant MUDSTONE*, gray, black (N2) to dk. gray (N3), w/occasional siderite-rich parallel laminae and numerous irregular, vuggy nodules of siderite, all grn. gray (5GY6/1); minor CLAYSTONE, med. gray (N5).
					0.5				
					1				numerous concentrations of sand-sized siderite fragments, occasionally graded within med. gray claystone, winnowed lag deposit? turbidite?
					2				Smear 1-114 [0.3, 97] 76% siderite 20% clay 3% zeolite 1% volc. glass
									* identified by black interval in lithology column
									Shell fragments noted by *
					3				Smear 2-104 [8, 30, 62] 70% clay 12% radiolaria 8% carb. unspec. 5% quartz 3% zeolite, org. mat. 2% pyrite, mica
					4				
					5				
					6				
					7				
					CC				
									GRAIN SIZE 2-104=26, 28, 46
									SHIPBOARD 2-90 SHOREBASED 5-89
									CaCO <sub>3</sub> % C org % 2 0.9

Explanatory notes in Chapter 1

SITE	398	HOLE	D	CORE	101	CORED INTERVAL:	1382.5-1392.0 m			
TIME-ROCK UNIT	BIOSTRAT ZONE	FOSSIL CHARACTER			SECTION	METERS	GRAPHIC LITHOLOGY	DISCONTINUANCE	SEDIMENTARY LITHOLOGIC SAMPLE	LITHOLOGIC DESCRIPTION
		FORAMS	NANNOS	RADS						
										dominant MUDSTONE*, gray-black (N2) to dk. gray (N3), w/ rare siderite-rich parallel laminae and occasional, irregular, vuggy nodules of siderite, all grn. gray (5GY6/1); minor CLAYSTONE to NANNO CLAYSTONE, med gray (N5), sharp contacts w/ dominant unit, does not expand and splinter as it dries as does the mudstone; plus minor "mud-chip" SILTSTONE/SANDSTONE, perhaps graded, composed of variegated grains of gray, black (N2), dk. gray (N3) to med. dk. gray (N4)
						0.5				
						1.0				
						2				*identified by black interval in lithology column Smear 1-140 [25.30, 45] 54% clay 12% radiolaria (recryst.) 10% carb. unsp. spec. 8% quartz 4% org. mat. 3% mica 2% gypsum(?) heavy mins.. forams. nannos 1% diatoms
						3	O.G.			
						4				Smear 4-10 [0, 12, 88] 63% clay 10% nannos 8% carb. unsp. spec. 5% quartz 4% org. mat. 3% mica radiolaria 2% heavy mins. 1% siderite, forams
						5				Smear 5-107 [7.20, 75] 60% clay 12% nannos 10% carb. unsp. spec. 8% quartz 3% mica org. mat. zeolite heavy mins. 1% gypsum, radiolaria
						6				
						7				GRAIN SIZE 2-2=1, 33, 66
						8				SHIPBOARD 6-77 SHOREBASED 6-50
						CC				CaCO <sub>3</sub> % Corg % 42 1 0.7

SITE 398 HOLE D CORE 102 CORED INTERVAL: 1392.0-1401.5 m

TIME-ROCK UNIT	BIOSTRAT ZONE	FOSSIL CHARACTER	SECTION	METERS	GRAPHIC LITHOLOGY	DRILLING DISTURBANCE	LITHOLOGIC DESCRIPTION
		FORAMS NANNOS RADS					
			1	0.5			dominant MUDSTONE to NANNO MUDSTONE*, gray, black (N2) to dk.gray (N3), w/rare siderite-rich parallel laminae and occasional massive, thin layers of siderite, grn.gray (5GY6/1); minor CLAYSTONE to NANNO CLAYSTONE, med.gray (N5)
			1	1.0			*identified by black interval in lithology column Smear 2-50 [1.15, 84] 63% clay 18% nannos 6% org.mat. 5% quartz 3% mica 1% heavy mins., radiolaria (pyritized) tr. siderite
			2				
			3				Smear 3-117 [0.20, 80] 68% clay 10% nannos 7% org.mat. 5% quartz, carb.unspec. 3% mica 1% heavy min. 1% apatite tr. siderite
			4				Smear 3-118 98% siderite 2% chlorite hard, irregular, slightly vuggy lens, yel.olive.Chondrites -burrowed; looks like all other siderite lenses, but is microcritic calcite
			5				Smear 6-61 [5.15, 80] 56% clay 15% quartz 7% nannos, org.mat. 6% carb.unspec. 5% mica 2% radiolaria 1% zeolite, gypsum(?) brown, granular, vuggy, burrowed siderite layer
			6				parallel-laminated, well indurated fine sand
			7				GRAIN SIZE 3-51=tr, 43, 57 CaCO <sub>3</sub> % Corg%
			CC				SHIPBOARD 1-96 <2 SHOREBASED 1-130 1 0.6

Explanatory notes in Chapter 1

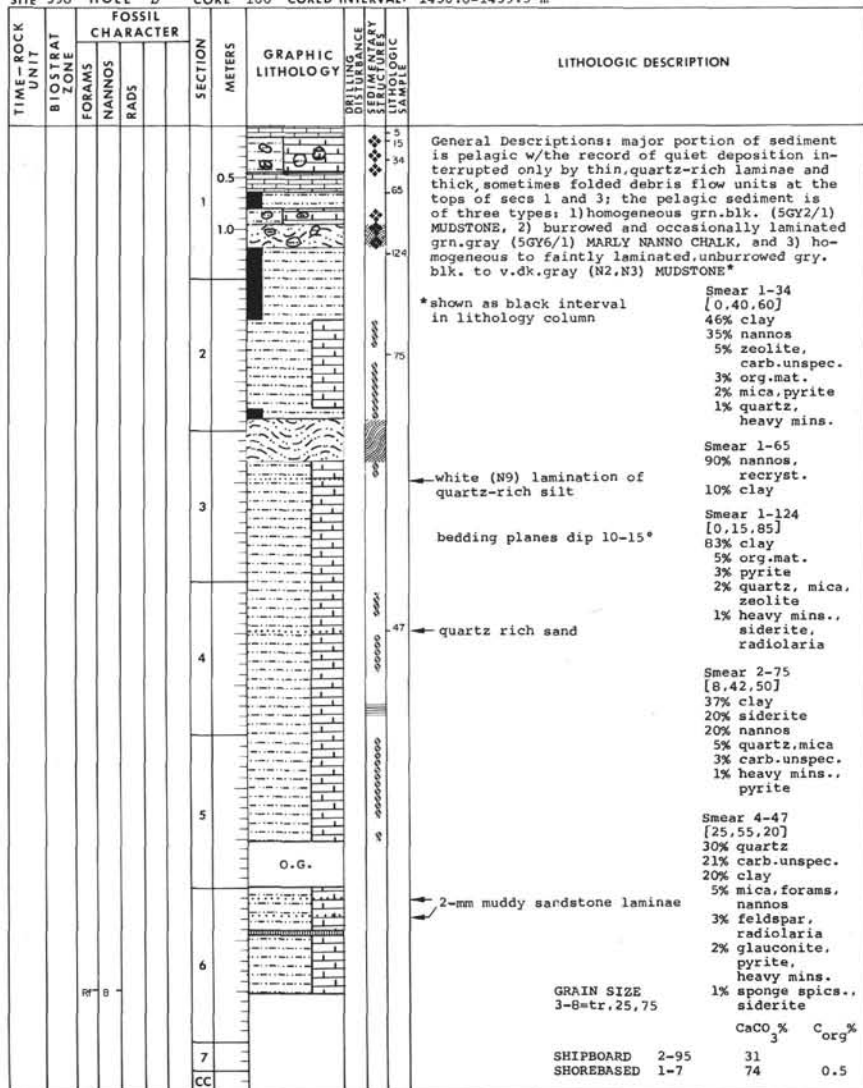
SITE 398 HOLE D CORE 103 CORED INTERVAL: 1401.5-1411.0 m

TIME-ROCK UNIT	BIOSTRAT ZONE	FOSSIL CHARACTER	SECTION	METERS	GRAPHIC LITHOLOGY	DRILLING DISTURBANCE	LITHOLOGIC DESCRIPTION
		FORAMS NANNOS RADS					
			1	0.5			0-30 cm: washed sec 1.41-43 cm: v.lt.gray (N8) extremely hard, v.fine-grained siderite w/dendritic solution infillings, calcite laminae Smear 2-36 [15.28, 57] 52% clay 12% nannos 10% carb.unspec. 8% quartz 6% radiolaria (pyr.) 5% org.mat. 3% mica
			2				sec 2.30-41 cm: graded "mud-chip" sandstone, variegated colors dominant MUDSTONE*, gray black (N2) to dk.gray (N3) w/rare siderite-rich parallel laminae layers, and nodules; other minor units as noted *identified by black interval in lithology column laminae consistently 6" off horizontal Smear 2-41 [35.30, 35] 45% clay 20% carb.unspec. 10% nannos 8% radiolaria 6% quartz 4% mica, org.mat. 3% pyrite
			3				
			4				Smear 6-64 [2.35, 63] 52% clay 18% siderite 18% nannos 5% carb.unspec. 3% quartz
			5				sec 5.40cm - sec 6.120 cm: several intervals of dk.gray (N3) faintly laminated and burrowed SIDERITIC CALC. MUDSTONE in sharp contact w/bl. gray (5B6/1) well-indurated SIDERITIC CALC. MUDSTONE similar to adjacent unit but w/less compaction of mottles, and more siderite-rich and yellowish at center of unit
			6				GRAIN SIZE 5-84=0.35, 65 CaCO <sub>3</sub> % Corg%
			7				SHIPBOARD 3-125 13 0.5 SHOREBASED
			CC				

Explanatory notes in Chapter 1

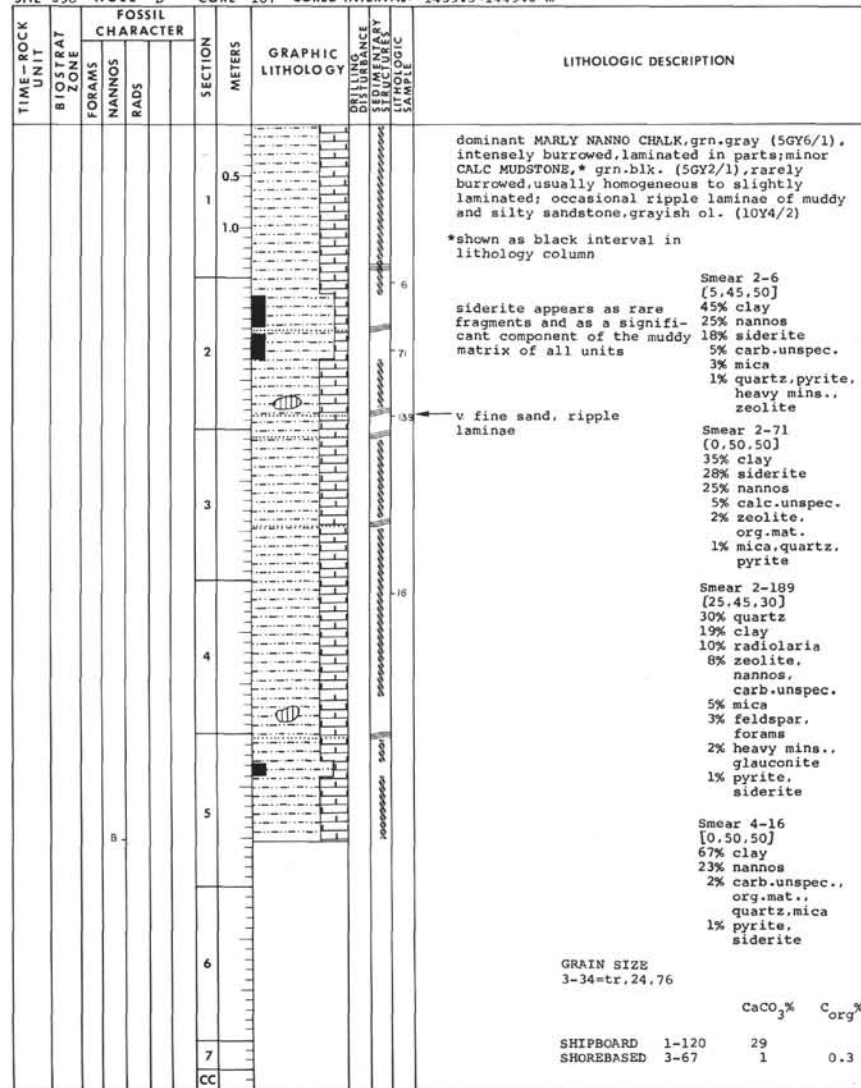
SITE 398

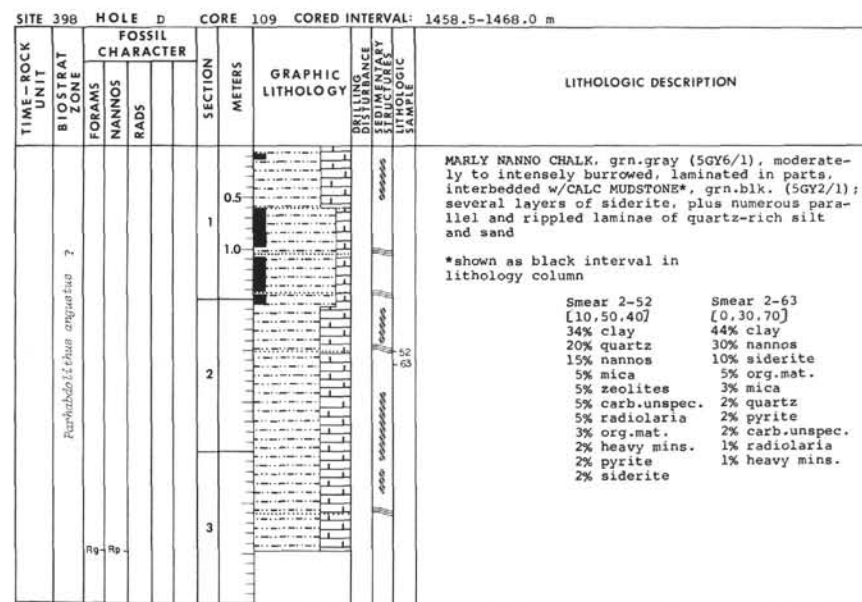
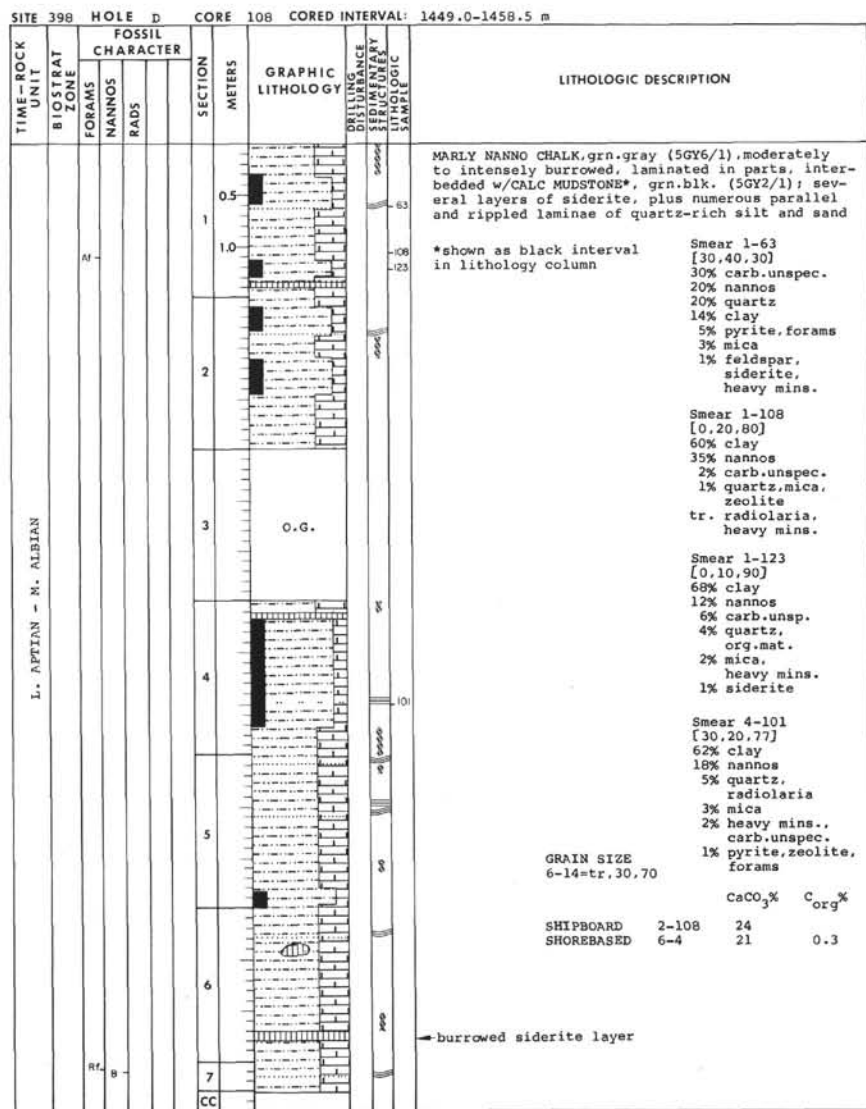
SITE 398 HOLE D CORE 106 CORED INTERVAL: 1430.0-1439.5 m



Explanatory notes in Chapter 1

SITE 398 HOLE D CORE 107 CORED INTERVAL: 1439.5-1449.0 m





SITE 398 HOLE D CORE 110 CORED INTERVAL: 1468.0-1477.5 m

TIME-ROCK UNIT	BIOSTRAT ZONE	FOSSIL CHARACTER	SECTION METERS	GRAPHIC LITHOLOGY	DRILLING DISTURBANCE	STRUCTURE	LITHOLOGIC DESCRIPTION
		FORAMS NANNOS RADS					
			0.5 1.0				Breccia of variegated mudstone, med.to lt. gray (N3-N6)

Explanatory notes in Chapter 1

SITE 398 HOLE D CORE 111 CORED INTERVAL: 1477.5-1487.0 m

TIME-ROCK UNIT	BIOSTRAT ZONE	FOSSIL CHARACTER	SECTION METERS	GRAPHIC LITHOLOGY	DRILLING DISTURBANCE	STRUCTURE	LITHOLOGIC DESCRIPTION
		FORAMS NANNOS RADS					
			0.5 1.0				Dominant MUDSTONE, grn.blk. (5GY2/1) occasionally laminated, moderately mottled w/gray.blk. (N2) burrows (?) that are v. irregular in shape, generally 2x5 mm; erosional surfaces (?) occur at least once every 15 cm, noted by sharp but subtle color changes; minor CALC MUDSTONE, med. lt.-gray (N6), unmottled, always w/a gradational contact w/the overlying dominant unit; in addition sharply defined layers of claystone and laminae of silt/v. fine sand, ol.gray (5Y4/1), ungraded, occur sporadically throughout the core; one siderite fragment is in each of sections 2, 3 and 4.
			2				claystone in section 2 is grn.gray (5GY6/1) and is soft, porous, w/tephra-like texture Smear 1-100 [30.30,40] 20% nannos 17% clay 15% quartz 16% Radiolaria 15% carb.unspec. 4% org.mat. 3% mica 3% pyrite 3% foram 2% heavy mins. 1% zeolite 1% sponge spic.
			3				Smear 2-3 [0.10,90] 87% clay 5% quartz 3% org.mat. 2% carb.unspec. 2% nannos 1% mica
			4				Smear 3-105 [0.10,90] 90% clay 3% quartz 3% org.mat. 2% carb.unspec. 1% mica 1% heavy mins
			5				lighter from here down: dk.grn.gray 5Y4/1 Smear 4-116 [25.30,45] 79% clay 15% quartz 2% mica 2% nannos 1% heavy mins. 1% carb.unspec.
			6				GRAIN SIZE 2-110=0.35,65 CaCO <sub>3</sub> % C <sub>org</sub> %
			7				SHIPBOARD 2-15 <2 3-135 <2 SHOREBASED 3-109 0 0.3

Explanatory notes in Chapter 1

SITE 398

Explanatory notes in Chapter 1

SITE 398		HOLE D		CORE 115		CORED INTERVAL: 1515.5-1525.0 m	
TIME-ROCK UNIT	BIOSTRAT ZONE	FOSSIL CHARACTER			SECTION METERS	GRAPHIC LITHOLOGY	LITHOLOGIC DESCRIPTION
		FORAMS	NANNOS	RADS			
							dominant MUDSTONE, grn.blk. (5GY2/1) to ol.blk. (5Y2/1) to v.dk.gray (N3), intensely mottled w/ gray blk.(N2); minor MUDSTONE to RADIOLARIAN MUDSTONE, ol. gray (5Y4/1), unmottled, often w/ silty, erosional basal contact and upper gradational contact; numerous siderite-rich layers and fragments of siderite
					0.5		Smear 1-2 [15.36,50] 53% clay 15% Radiolaria 8% quartz 5% zeolite 5% carb.unspec. 3% mica 3% gypsum 3% nannos 2% siderite 1% heavy mins. 1% forams 1% pyrite
					1.0		
					2		slumped interval of blk.and ol.gray mudstones plus a 1 cm pebble of gray limestone
					3		interval of graded mud clast sandstone, multicolored (green, gray, white, black)
							Smear 2-138 [0.0,100] 70% siderite 20% carb.unspec. 10% clay
							Smear 3-77 [15,25,60] 52% clay 11% Radiolaria 10% nannos 8% quartz 5% carb.unspec. 3% mica 2% org.mat. 2% feldspar 2% zeolite 1% heavy mins. 1% pyrite 1% siderite 1% forams
					4		Smear 3-60 [3,27,70] 58% clay 18% nannos 5% Radiolaria 3% quartz 3% zeolite 3% carb.unspec. 3% org.mat. 2% mica 2% pyrite 1% heavy mins. 1% siderite 1% forams
							GRAIN SIZE 3-64=7,31,62
							CaCO <sub>3</sub> % Corg%
					5		SHIPBOARD 2-84 <2 SHOREBASED 2-139 27 0.3

SITE 398 HOLE D CORE 116 CORED INTERVAL: 1525.0-1534.5 m									
TIME-ROCK UNIT	BIOSTRAT ZONE	FOSSIL CHARACTER			SECTION METERS	GRAPHIC LITHOLOGY	DRILLING DISTURBANCE	SEDIMENTARY LITHOLOGY	LITHOLOGIC DESCRIPTION
		FORAMS	NANNOS	RADS					
					1	0.5 1.0			<p>← mud flow (?)</p> <p>← debris flow (?)</p> <p>dominant MUDSTONE*, v.dk.gray (N3), homogeneous to faintly laminated; minor RADIOLARIAN MUDSTONE, v. dark gray (7.5YR3/2) w/clasts of white and green limestone; several silty/sandy laminae, yel. gray (5Y 1/2) lt.gray (5Y5/2); several lenses of siderite</p> <p>*shown by black interval in lithology column</p> <p>VOID</p> <p>Smear 1-113 [20,20,60] 55% clay 20% Radiolaria 20% nannos 8% zeolite 5% org.mat. 3% quartz 3% carb.unspec. 2% mica 2% pyrite 1% siderite 1% heavy mins.</p> <p>Smear 2-61 [30,30,40] 37% clay 15% quartz 15% siderite 10% carb.unspec. 5% mica 3% zeolite 3% nannos 3% org.mat. 2% feldspar 2% gypsum 2% forams 2% heavy mins. 1% pyrite</p> <p>CaCO<sub>3</sub>% C<sub>org</sub>%</p> <p>SHIPBOARD 1-69 42 SHOREBASED 3-83 13 0.9</p>
					2				
					3				
					4				

Explanatory notes in Chapter 1

SITE 398 HOLE D CORE 117 CORED INTERVAL: 1534.5-1544.0 m									
TIME-ROCK UNIT	BIOSTRAT ZONE	FOSSIL CHARACTER			SECTION METERS	GRAPHIC LITHOLOGY	DRILLING DISTURBANCE	SEDIMENTARY LITHOLOGY	LITHOLOGIC DESCRIPTION
		FORAMS	NANNOS	RADS					
					1	0.5 1.0			<p>core consists of numerous rhythms of the following sequence: either basal QUARTZOSE SANDSTONE/SILTSTONE, lt.gray (N7) grading upward to MUDSTONE*, dk.gray to gray blk. (N5 to N3); or basal CALC MUDSTONE, gray.ol.grn (3GY3/2), w/ white limestone clasts; overlying both is intensely burrowed MUDSTONE to RAD MUDSTONE, also gray.ol.grn (3GY3/2); average rhythm thickness is 11-14cm; few siderite lenses</p> <p>*shown diagrammatically as black interval in lithology column</p> <p>Smear 2-69 [3,20,77] 76% clay 5% pyrite 5% Radiolaria 5% org.mat. 3% mica 3% zeolite 2% quartz 1% heavy mins.</p> <p>← numerous clasts; mud flow?</p> <p>Smear 2-77 [0,30,70] 49% clay 30% nannos 5% carb.unspec. 5% org.mat. 3% quartz 2% mica 2% siderite 1% heavy mins. 1% zeolite</p> <p>← numerous clasts; mud flow?</p> <p>Smear 2-87 [10,50,40] 41% clay 15% quartz 10% siderite 10% carb.unspec. 8% Radiolaria 3% mica 3% zeolite 3% org.mat. 2% heavy mins. 1% feldspar 1% pyrite 1% forams 1% nannos 1% sponge spic.</p> <p>← 6 cm of fine sand</p> <p>GRAIN SIZE 4-34=0.45,55</p> <p>CaCO<sub>3</sub>% C<sub>org</sub>%</p> <p>SHIPBOARD 3-102 42 SHOREBASED 6-105 21 0.6</p>
					2				
					3				
					4				
					5				
					6				
					7				
					CC				

SITE 398 HOLE D CORE 118 CORED INTERVAL: 1544.0-1553.5 m

TIME-ROCK UNIT	BIOSTRAT ZONE	FOSSIL CHARACTER			SECTION METERS	GRAPHIC LITHOLOGY	DRILLING DISTURBANCE SEDIMENTARY STRUCTURES LITHOLOGIC SAMPLE	LITHOLOGIC DESCRIPTION
		FORAMS	NANNOS	RADS				
					0.5			core consists of numerous rhythms of the following sequence: either basal QUARTZ SANDSTONE/SILTSTONE, lt. gray (N7) grading upward to MUDSTONE*, dk.gray to gray.blk (N5-N3); or basal CALC MUDSTONE, gray ol. grn. (3GY3/2) w/white limestone clasts; overlying both is intensely burrowed MUDSTONE to RAD MUDSTONE, gray.ol.grn. (3GY3/2); average rhythm thickness is 15-18 cm; two slumped intervals are evident
					1			slumped sediment ?
					2			*shown diagrammatically as black interval in lithology column
					3			Smear 1-80 [2.15,83] 84% clay 3% quartz 3% mica 3% pyrite 2% org.mat. 2% siderite 2% nannos 1% carb.unspec.
					4			Smear 1-86 [30.35,35] 41% clay 15% Radiolaria 15% quartz 15% forams 5% siderite 4% pyrite 3% mica 2% heavy mins.
					5			Smear 1-102 [30.35,35] 32% clay 30% carb.unspec. 15% quartz 15% nannos 3% pyrite 3% siderite 2% org.mat.
					6	O.G.		Smear 1-136 [2.20,78] 35% nannos 27% clay 25% carb.unspec. 5% siderite 3% org.mat. 2% quartz 2% pyrite 1% heavy mins.
					7			GRAIN SIZE 4-34=tr,28,72
					CC			SHIPBOARD 2-86 6 SHOREBASED 4-108 0 0.5

Explanatory notes in Chapter 1

SITE 398 HOLE D CORE 119 CORED INTERVAL: 1553.5-1563.0 m

TIME-ROCK UNIT	BIOSTRAT ZONE	FOSSIL CHARACTER			SECTION METERS	GRAPHIC LITHOLOGY	DRILLING DISTURBANCE SEDIMENTARY STRUCTURES LITHOLOGIC SAMPLE	LITHOLOGIC DESCRIPTION
		FORAMS	NANNOS	RADS				
					0.5			core consists of numerous rhythms of the following sequence: either basal QUARTZ SANDSTONE/SILTSTONE, lt.gray (N7) grading upward to laminated MUDSTONE*, dk.gray to gray.blk (N5-N3); or CALC MUDSTONE, gray.ol.grn. (3GY3/2) w/white limestone clasts; overlying both is laminated MUDSTONE to RAD MUDSTONE, gray.ol.grn.(3GY3/2); rhythm thicknesses average 5-10cm.
					1			*shown diagrammatically as black interval in lithology column
					2			Smear 2-68 [2.30,68] 72% clay 18% quartz 3% pyrite 2% mica 2% carb.unspec. 2% org.mat. 1% heavy mins.
					3			Smear 2-71 [30.30,40] 30% carb.unspec. 18% clay 18% Radiolaria 15% quartz 5% pyrite 5% siderite 3% mica 3% org.mat. 2% nannos 1% heavy mins
					4			Smear 3-122 [5.30,65] 60% carb.unspec. 27% clay 8% dolomite 5% quartz
					5			Smear 5-138 [2.25,73] 30% carb.unspec. 30% nannos 18% clay 15% siderite 5% quartz 2% zeolite
					6			GRAIN SIZE 2-10 =1,37,62 5-110 =2,53,45
					7			SHIPBOARD 2-46 42 SHOREBASED 5-145 19 0.2
					CC			CaCO <sub>3</sub> % C <sub>org</sub> %

Explanatory notes in Chapter 1SITE 398

SITE 398		HOLE D		CORE 122		CORED INTERVAL: 1582.0-1591.5 m	
TIME-ROCK UNIT	BIOSTRAT ZONE	FOSSIL CHARACTER			SECTION METERS	GRAPHIC LITHOLOGY	LITHOLOGIC DESCRIPTION
		FORAMS	NANNOS	RADS			
BARREMIAN ?	<i>Microantholithus hochstetleri</i>						
					0.5		
					1.0		

SITE 398 HOLE D CORE 124 CORED INTERVAL: 1601.0-1610.5 m																																																			
TIME-ROCK UNIT	BIOSTRAT ZONE	FOSSIL CHARACTER			SECTION METERS	GRAPHIC LITHOLOGY	DRILLING DISTURBANCE	SEDIMENTARY STRUCTURE	LITHOLOGIC SAMPLE	LITHOLOGIC DESCRIPTION																																									
		FORAMS	NANNOS	RADS																																															
NEOCOMIAN-BARREMIAN	<i>Microantholithus hochheimi</i>									<p>three intervals of unburrowed, laminated, occasionally graded sediment are interrupted by three large grain/mud flow deposits; each of the laminated intervals is composed of several of either of the following sequences: basal CALC SANDSTONE, fine- to coarse-grained, massive, rarely laminated, multicolored, composed of either grains of white micritic limestone or of larger mud chips; or basal MUDSTONE, usually QUARTZOSE and CALCAREOUS, med. dk. gray to lt. gray (N3-N7), parallel and cross laminated; the top of either sequence is MARLY NANNO CHALK, med. dk. gray to med gray (N3-N4), in addition there are three thin (&lt;10 cm) layers of burrowed CALCAREOUS MUDSTONE, within these laminated intervals, alternating grn-gray and black,* presumed to be undisturbed pelagic sediment; the flow deposits grade upward from subangular grain flows to sub-rounded mud flows, the clasts consisting of the following:</p> <ol style="list-style-type: none"><li>1. subrounded oolitic white limestone</li><li>2. deformed white, gray and brown chalks and limestones</li><li>3. black mudstone</li><li>4. rare green chlorite-rich mudstones</li><li>5. burrowed marly limestone</li><li>6. pyrite crystals</li><li>7. graded gray siltstones</li><li>8. mollusc fragments</li></ol> <p>*shown as black interval in lithology column</p> <table><tr><td>Smear 3-66</td><td>Smear 4-67</td></tr><tr><td>[0.40,60]</td><td>[0.35,65]</td></tr><tr><td>60% nannos</td><td>66% clay</td></tr><tr><td>30% clay</td><td>12% nannos</td></tr><tr><td>5% carb.unspec.</td><td>5% org.mat.</td></tr><tr><td>2% org.mat.</td><td>4% pyrite</td></tr><tr><td>1% quartz</td><td>3% quartz</td></tr><tr><td>1% mica</td><td>3% zeolite</td></tr><tr><td>1% pyrite</td><td>3% carb.unspec.</td></tr><tr><td></td><td>2% mica</td></tr><tr><td></td><td>2% radiol.</td></tr></table> <p>Smear 4-145      Smear 5-35</p> <table><tr><td>[0.50,50]</td><td>[0.0,100] pebble</td></tr><tr><td>70% nannos</td><td>65% clay</td></tr><tr><td>27% clay</td><td>32% nannos</td></tr><tr><td>2% carb.unspec.</td><td>3% carb.unspec.</td></tr><tr><td>1% zeolite</td><td></td></tr></table> <p>GRAIN SIZE 4-46=3.45.52</p> <table><tr><td></td><td>CaCO<sub>3</sub>%</td><td>C<sub>org</sub>%</td></tr><tr><td>SHIPBOARD 4-31</td><td>35</td><td></td></tr><tr><td>SHOREBASED 3-43</td><td>68</td><td>0.5</td></tr></table>	Smear 3-66	Smear 4-67	[0.40,60]	[0.35,65]	60% nannos	66% clay	30% clay	12% nannos	5% carb.unspec.	5% org.mat.	2% org.mat.	4% pyrite	1% quartz	3% quartz	1% mica	3% zeolite	1% pyrite	3% carb.unspec.		2% mica		2% radiol.	[0.50,50]	[0.0,100] pebble	70% nannos	65% clay	27% clay	32% nannos	2% carb.unspec.	3% carb.unspec.	1% zeolite			CaCO <sub>3</sub> %	C <sub>org</sub> %	SHIPBOARD 4-31	35		SHOREBASED 3-43	68	0.5
											Smear 3-66	Smear 4-67																																							
											[0.40,60]	[0.35,65]																																							
											60% nannos	66% clay																																							
											30% clay	12% nannos																																							
											5% carb.unspec.	5% org.mat.																																							
											2% org.mat.	4% pyrite																																							
											1% quartz	3% quartz																																							
											1% mica	3% zeolite																																							
											1% pyrite	3% carb.unspec.																																							
												2% mica																																							
											2% radiol.																																								
[0.50,50]	[0.0,100] pebble																																																		
70% nannos	65% clay																																																		
27% clay	32% nannos																																																		
2% carb.unspec.	3% carb.unspec.																																																		
1% zeolite																																																			
	CaCO <sub>3</sub> %	C <sub>org</sub> %																																																	
SHIPBOARD 4-31	35																																																		
SHOREBASED 3-43	68	0.5																																																	
	0.5																																																		
	1																																																		
	1.0																																																		
	2																																																		
	3																																																		
	4																																																		
	5																																																		
	6																																																		
	7																																																		
CC																																																			

Explanatory notes in Chapter 1

SITE 398 HOLE D CORE 125 CORED INTERVAL: 1610.5-1620.0 m									
TIME-ROCK UNIT	BIOSTRAT ZONE	FOSSIL CHARACTER			SECTION METERS	GRAPHIC LITHOLOGY	DRILLING DISTURBANCE	SEDIMENTARY STRUCTURE	LITHOLOGIC SAMPLE
		FORAMS	NANNOS	RADS					
NEOCOMIAN-BAREMIAN	<i>Microantholithus hochheimi</i>								
					0.5				
					1				
					1.0				
					2				
					3				
					4				
					5				
					6				
					7				
		CC							
<p>the upper half of the core is largely mud flow and debris flow deposits; clasts are usually polygenic and pebble-sized; several belemnites observed; limited slumping; matrix is MUDSTONE, med.gray (N5); the lower half is unburrowed, laminated, occasionally graded intervals 1mm to 50cm thick, showing either of the following sequences: basal CALC SANDSTONE, multicolored, fine- to coarse-grained, composed either of grains of limestone or of larger mud chips, or basal MUDSTONE, usually QUARTZOSE and CALCAREOUS, med.dk.gray to lt.gray (N3-N7), laminated; the top of either sequence is MARLY NANNO CHALK*, med.dk.gray to med.gray (N3-N4) w/rare pelecypod fragments; in addition there are several thin (&lt;10cm) layers of MARLY NANNO CHALK, grn.blk. (5GY2/1) throughout the core, presumed to be undisturbed pelagic sediment</p> <p>*shown as black interval in lithology column</p> <p>Smear 5-50 [0.50,50] 45% clay 45% nannos 5% carb.unspec. 2% pyrite 1% quartz 1% mica 1% zeolite</p> <p>Smear 5-57 [30.30,40] 35% nannos 30% carb.unspec. 21% clay 5% org.mat. 4% pyrite 2% glauconite 1% quartz 1% mica 1% zeolite</p> <p>Smear 5-60 [10.50,40] 51% clay 15% org.mat. 10% nannos 5% quartz 5% carb.unspec. 4% pyrite 3% zeolite 3% heavy mins 2% siderite 2% mica</p> <p>GRAIN SIZE 2-56=tr,44,56</p> <p>CaCO<sub>3</sub>% C<sub>org</sub>%</p> <p>SHOREBASED 5-90 17 1.5</p>									

SITE 398		HOLE D		CORE 126		CORED INTERVAL: 1620.0-1629.5 m	
TIME-ROCK UNIT	BIOSTRAT ZONE	FOSSIL CHARACTER		SECTION	METERS	GRAPHIC LITHOLOGY	LITHOLOGIC DESCRIPTION
		FORAMS	NANNOS				
							numerous intervals of predominantly unburrowed, laminated, occasionally graded sediment; each interval varies from 5 to 100 cm thick, averaging 20-25 cm, and at the base each interval is composed of either of the following: CALC SANDSTONE, fine-grained, made up of mud clasts of lt. gray (N7) mudstone, fining upwards to lt. ol. gray (5Y5/2) MUDSTONE; or MUDSTONE usually QUARTZOSE and CALCAREOUS, lt. gray (N7) grading upwards to med. dk. gray (N4), w/parallel and wavy laminae, graded bedding; each interval grades upward to dk. gray (N-3) homogeneous or rarely burrowed CALCAREOUS MUDSTONE*
				1	0.5		
				2	1.0		*shown as black interval in lithology column
							Smear 5-137 [15.55,30] 38% clay 15% carb.unspec. 15% quartz 10% siderite 5% mica 5% nannos 5% org.mat. 2% zeolite 2% pyrite 2% heavy mins 1% feldspar
				3			← pelecypod fragments
							Smear 6-71 [0.60,40] 47% clay 15% org.mat. 10% quartz 10% nannos 5% carb.unspec. 3% mica 3% pyrite 2% feldspar 2% siderite 2% heavy mins. 1% zeolite
				4			
							Smear 6-80 [5.65,30] 40% nannos 29% clay 20% carb.unspec. 3% org.mat. 2% quartz 2% mica 2% siderite 1% pyrite 1% heavy mins.
				5			
				6			
				7			
				CC			
							CaCO <sub>3</sub> % C <sub>org</sub> %
							SHIPBOARD 1-115 60
							SHOREBASED 5-116 15 1.7

Explanatory notes in Chapter 1

SITE 398		HOLE D		CORE 127		CORED INTERVAL: 1629.5-1639.0 m	
TIME-ROCK UNIT	BIOSTRAT ZONE	FOSSIL CHARACTER		SECTION	METERS	GRAPHIC LITHOLOGY	LITHOLOGIC DESCRIPTION
		FORAMS	NANNOS				
							numerous intervals of predominantly unburrowed, laminated, occasionally graded sediment; each interval varies from 5 to 100cm thick, averaging 35-40cm, and at the base each interval is composed of either of the following: CALC SANDSTONE, fine grained, made up of mud chips of lt. gray (N7) mudstone, fining upwards to lt. ol. gray (5Y5/2) MUDSTONE; or MUDSTONE, usually QUARTZOSE and CALCAREOUS lt. gray (N7), grading upwards to med. dk. gray (N4) w/parallel and wavy laminae, graded bedding; each interval grades upward to dk. gray (N3) homogeneous or rarely burrowed CALCAREOUS MUDSTONE*.
				1	0.5		
				2	1.0		*shown as black interval in lithology column
							Smear 3-140 [6,20,74] 30% carb. unspec. 30% nannos 16% clay 4% quartz 4% org.mat. 2% mica 2% pyrite 2% siderite
				3			
							Smear 5-57 [4,30,66] 30% carb.unspec. 29% clay 20% quartz 4% mica 2% pyrite 2% siderite 2% org.mat. 1% heavy mins.
				4			← pelecypod fragments noted by *
							Smear 7-28 [25,30,45] 60% carb.unspec. 16% clay 10% nannos 4% mica 3% quartz 3% pyrite 3% org.mat. 1% heavy mins.
				5			
				6			
				7			
				CC			
							GRAIN SIZE 4-18=1,33,66
							CaCO <sub>3</sub> % C <sub>org</sub> %
							SHIPBOARD 2-43 19
							SHOREBASED 6-75 13 0.5

Explanatory notes in Chapter 3

SITE 398

SITE 398		HOLE 16		CORE 130		CORED INTERVAL 1658.0-1667.5 m	
TIME-ROCK UNIT	BIOSTRAT ZONE	FOSSIL CHARACTER		SECTION	METERS	GRAPHIC LITHOLOGY	LITHOLOGIC DESCRIPTION
		FORAMS	NANNOS	RADS		DRILLING DISTURBANCE SEDIMENTARY LITHOLOGIC SAMPLE	
BAREMTIAN-L. HINUTERIVIAN <i>Lithothamnion bollii</i>					0.5		core consists entirely of intercalations of two sequences 5-100cm thick, averaging 35-40cm, usually distinguished by sharp contacts, one in CALC SANDSTONE, mostly coarse sand size, composed of multicolored mud clases, usually less than 5mm thick; this grades upward to lt. gray (N7) CALC MUDSTONE and higher up to grn. gray (5GY6/1) laminated, unburrowed, pelocypod-bearing CALC MUDSTONE*; the other sequence is CALC QUARTZOSE MUDSTONE, med. lt. gray (N6), w/cross-bedded, parallel and wavy laminae, no apparent grading; the matrix of this last unit is med. gray (N4) and grades upward to grn. gray (5GY6/1) burrowed and faintly laminated MARLY CHALK
					1.0		
					2		
					3		
					4		
					5		
					6		
							</

Explanatory notes in Chapter 1

SITE 398		HOLE D		CORE 131		CORED INTERVAL: 1667.5-1677.0 m			
TIME-ROCK UNIT	BIOSTRAT ZONE	FOSSIL CHARACTER			SECTION	METERS	GRAPHIC LITHOLOGY	DRILLING DISTANCE STRUCTURE STRATIGRAPHY LITHOLOGIC SAMPLE	LITHOLOGIC DESCRIPTION
		FORAMS	NANNOS	RADS					
BAREMTAN-L. HAUTEVIVIAN	<i>Lophospira bellii</i>								
		</							

SITE	398	HOLE D	CORE 132	CORED INTERVAL:
TIME-ROCK UNIT	BIOSTRAT ZONE	FOSSIL CHARACTER	SECTION METERS	LITHOLOGIC DESCRIPTION
BARREMIAN-LAUTERIVIAN <i>Ectophradites bolizii</i>	FORAMS	NANNOS	RADS	
			0.5	two major sediment types: bl.wht. to v.lt.gray (5B8/l-N8) NANNO LIMESTONE, intensely burrowed, abundant pyritized worm tubes and pyrite concretions; and dk.gray to ol. gray (N3-5Y4/l) MARLY NANNO LIMESTONE*, thinly laminated w/no apparent grading; contacts btw these units are gradational; in addition rare QUARTZOSE MUDSTONE, <1cm thick, lt.grn.gray (5G6/l), cross-bedded, parallel or wavy laminated and thin multicolored, graded mud-clast CALC SANDSTONE are both found throughout the core
			1	
			2	*shown as black interval in lithology column Smear 1-78 [2,28,70] 47% clay 40% nannos 5% carb.unspec. 2% pyrite 1% quartz,mica, heavy mins., siderite, forams, org.mat.
			3	Smear 2-30 [20,50,30] 25% carb.unspec. 23% clay 15% quartz 12% nannos 5% mica 5% siderite 3% feldspar 3% org.mat. 3% pyrite 2% zeolite 1% heavy mins 1% glauconite 1% diatoms 1% forams
			4	green diagenetic laminae within limestone Smear 2-35 [0,0,100] 80% nannos (recryst.) 10% carb.unspec. 10% clay
				SHIPBOARD SHOREBASED CaCO <sub>3</sub> % Corg%
				3-90 55 4-59 74 1.7

Explanatory notes in Chapter 1

[illegible]

SITE 398 HOLE D CORE 134 CORED INTERVAL: 1696.0-1705.5 m

TIME-ROCK UNIT	BIOSTRAT ZONE	FOSSIL CHARACTER			SECTION METERS	GRAPHIC LITHOLOGY	DRILLING DISTURBANCE SEMI-QUANTITATIVE LITHOLOGIC SAMPLE	LITHOLOGIC DESCRIPTION
		FORAMS	NANNOS	RADS				
BARREMIAN-L. HAUTERIVIAN	<i>Lithothamnion bollii</i>				0.5			two major sediment types: bl.wht. to v. lt.gray (5B8/1-N8) NANNO LIMESTONE, intensely burrowed, abundant pyritized worm tubes and pyrite concretions, occasional wood fragments; and dk.gray to ol.gray (N3-5Y4/1) MARLY NANNO LIMESTONE*, thinly laminated w/no grading; contacts btw these units are gradational; laminated QUARTZOSE CALC MUDSTONE and mud-clast CALC SANDSTONE rarely found as v.thin layers within the laminated marly limestone
					1			
					2			
					3			
	RF				4			<p>*shown as black interval in lithology column</p> <p>Smear 1-112 [30.30,40] 65% carb. unsp. 12% quartz 8% nannos 6% clay 4% org.mat. 3% siderite 2% mica</p> <p>Smear 2-21 [2.25,73] 35% nannos 26% clay 20% carb.unspec. 7% org.mat. 5% quartz 3% mica 2% heavy mins 2% pyrite</p> <p>Smear 3-54 [15.35,50] 48% carb.unspec. 21% clay 20% nannos 8% quartz 2% org.mat. 1% pyrite</p> <p>CaCO<sub>3</sub>% C org %</p> <p>SHIPBOARD 1-78 43</p> <p>SHOREBASED 3-71 82 1.1</p>

Explanatory notes in Chapter 1

SITE 398 HOLE D CORE 135 CORED INTERVAL: 1705.5-1715.0 m

TIME-ROCK UNIT	BIOSTRAT ZONE	FOSSIL CHARACTER			SECTION METERS	GRAPHIC LITHOLOGY	DRILLING DISTURBANCE SEMI-QUANTITATIVE LITHOLOGIC SAMPLE	LITHOLOGIC DESCRIPTION
		FORAMS	NANNOS	RADS				
BARREMIAN-L. HAUTERIVIAN	<i>Lithothamnion bollii</i>				0.5			two major sediment types: dominant MARLY NANNO LIMESTONE*, dk.gray to ol.gray (N3-5Y4/1), thinly laminated w/no grading; and NANNO LIMESTONE, bl.wht. to wht. (5B8/1-N9), intensely burrowed, w/ pyrite concretions; contacts btw these units are usually gradational; laminated QUARTZOSE CALC MUDSTONE and occasionally graded mud-clast CALC SANDSTONE rarely found as thin layers within the laminated marly limestone
					1			
					2			
					3			
	RF				4			<p>*shown as black interval in lithology column</p> <p>Smear 1-67 [5.20,75] 37% clay 30% nannos 15% carb.unspec. 7% org.mat. 5% quartz 3% mica 2% pyrite 1% heavy mins.</p> <p>Smear 2-52 [0.50,50] 30% carb.unspec. 27% clay 25% nannos 6% mica 5% quartz 4% org.mat. 2% pyrite 1% heavy mins.</p> <p>Smear 3-15 [25.30,45] 95% nannos (recryst.) 5% quartz 14% clay 6% mica 5% org.mat. 4% nannos 1% siderite</p> <p>Smear 4-60 [25.30,45] 45% carb.unspec. 25% quartz 25% quartz 14% clay 6% mica 5% org.mat. 4% nannos 1% siderite</p> <p>CaCO<sub>3</sub>% C org %</p> <p>SHIPBOARD 3-120 74</p> <p>SHOREBASED 3-83 45 0.6</p>

TIME-ROCK UNIT	BIOSTRAT ZONE	FOSSIL CHARACTER	CORE 136	CORED INTERVAL	1715.0-1724.5 m	LITHOLOGIC DESCRIPTION
			SECTION	METERS	GRAPHIC LITHOLOGY	
					DRILLING DISTURBANCE SEDIMENTARY LITHOLOGIC SAMPLE	
BARRENO IN-L-HAUTERIVIAN <i>Lichophydium bolitt</i>				0.5		two major sediment types: dominant MARLY NANNO LIMESTONE*, med. dk. gray (N4), homogeneous except for a few burrowed grn.gray (5G6/l) intervals; and NANNO LIMESTONE, bl. wht. to wht. (5B9/l-N9), intensely burrowed; common mud-clast CALC SANDSTONE, occasionally graded, and rare laminated QUARTZOSE CALC MUDSTONE occur within the marly limestone; rare pyrite concretions
				1.0		
				2		*shown as black interval in lithology column
				3		
				4		

Smear 1-41 [0.20,80]	55% nannos
34% clay	
3% pyrite	
3% carb.unspec.	
2% mica	
1% quartz	
1% siderite	
1% radiolaria	

Smear 1-46 [10.50,40]	Smear 1-53 [0.30,70]
36% clay	48% clay
20% carb.unspec.	40% nannos
15% quartz	5% carb.unspec.
10% nannos	3% siderite
5% mica	2% org. mat.
3% feldspar	1% mica
3% pyrite	1% pyrite
3% siderite	
2% heavy mins.	
2% org.mat.	
1% radiolaria	

CaCO<sub>3</sub>%

SHIPBOARD 2-4 64

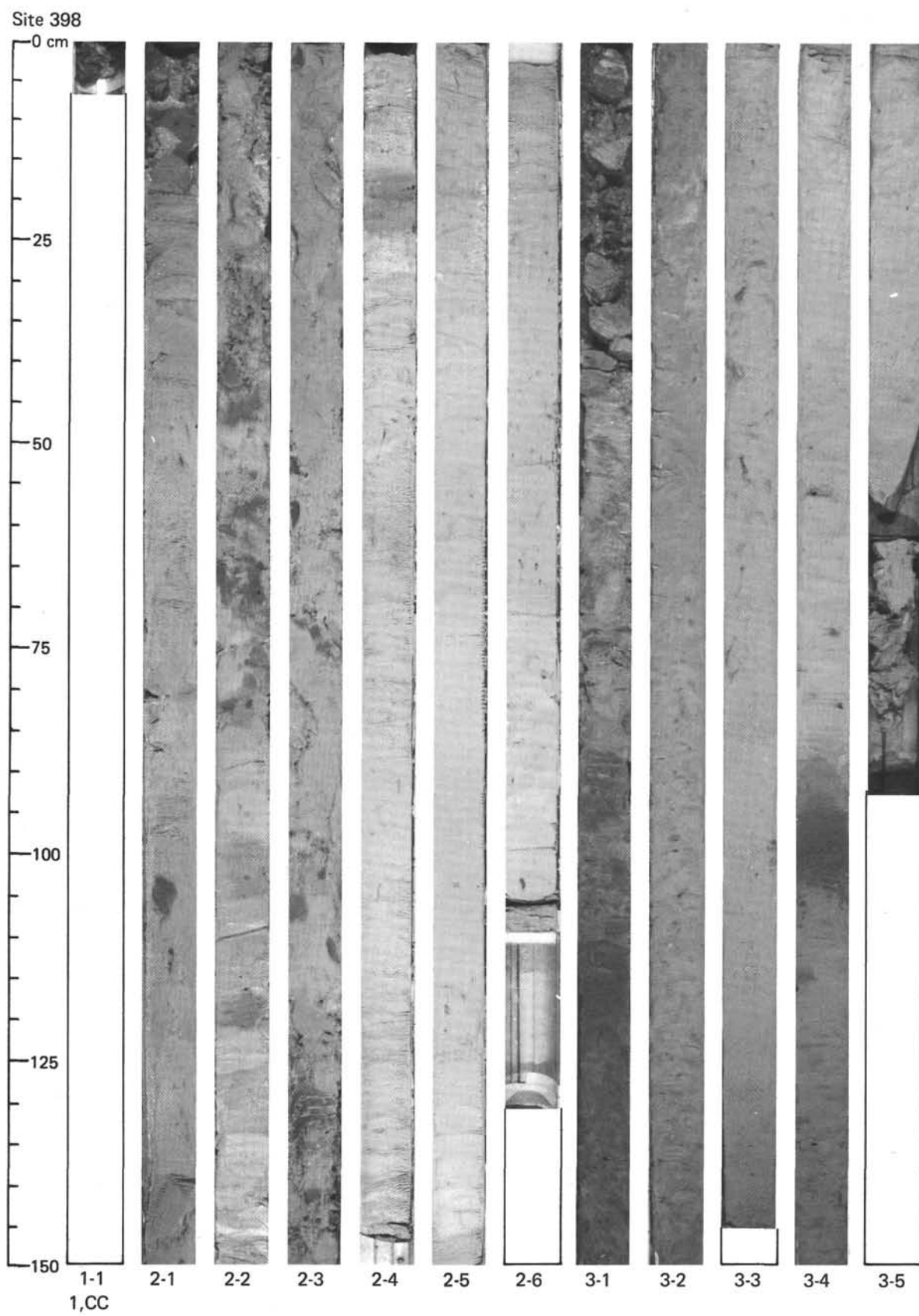
Explanatory notes in Chapter 1

SITE	398	HOLE	D	CORE	137	CORED INTERVAL:	1724.5-1734.0 m		
TIME-ROCK UNIT	BIOSTRAT ZONE	FOSSIL CHARACTER			SECTION METERS	GRAPHIC LITHOLOGY	CORRELATION OF LITHOLOGY	SEDIMENTARY COREY LITHOLOGIC SAMPLE	LITHOLOGIC DESCRIPTION
		FORAMS	NANNOS	RADS					
BARRENIA IN-L. HAUTERIVIAN	Lithothamnium boreale	RF							two major sediment types: dominant MARLY NANNO LESTONE, med. dk. gray* (N4), homogeneous, often grading to burrowed grn.gray (5G6/1) interval at contact w/ NANNO LESTONE, bl.wht. to wht. (5B9/1-N9) which is intensely burrowed; rare mud-clast CALC SANDSTONE, sometimes graded, occurs within the marly limestone
									*shown as black interval in lithology column
		Cg							Smear 1-98 [3,37,60] 51% clay 25% nannos 20% carb.unspec. 1% quartz 1% mica 1% pyrite 1% siderite
									Smear 1-138 [0.0,100] 50% carb.unspec. 40% nannos (recryst.) 10% clay
		RF							Smear 3-106 [0.30,70] 50% clay 30% nannos 5% carb.unspec. 5% org.mat. 3% pyrite 3% mica 1% quartz 1% heavy mins. 1% zeolite 1% siderite
									Smear 3-145 [10,60,30] 35% carb.unspec. 25% quartz 20% clay 5% nannos 4% siderite 3% feldspar 3% mica 2% heavy mins. 2% organic mat. 1% radiolaria
									SHIPBOARD 3-113 33
									SHOREBASED 3-147 47 0.2

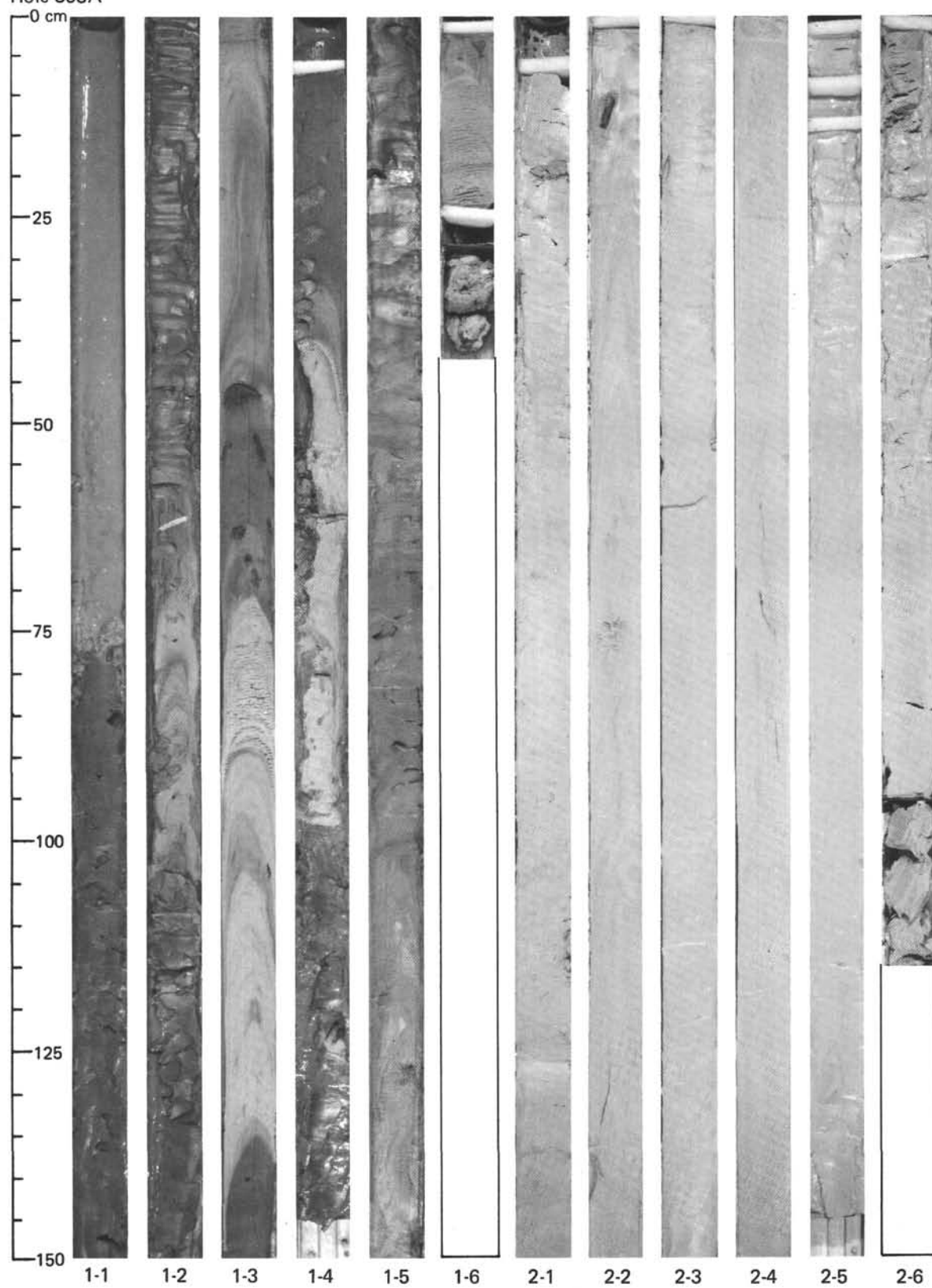
SITE 398 HOLE D CORE 138 CORED INTERVAL: 1734.0-1740.0 m

TIME-ROCK UNIT	BIOSTRAT ZONE	FOSSIL CHARACTER		SECTION	METERS	GRAPHIC LITHOLOGY	DRILLING DISTURBANCE SEDIMENTARY STRUCTURE LITHOLOGIC SAMPLE	LITHOLOGIC DESCRIPTION
		FORAMS	NANNOS	RADS				
BARREMIAN-L. HAUTERIVIAN	<i>Lithothamnion bollii</i>				0.5			two major sediment types: dominant MARLY NANNO LIMESTONE*, med.dk.gray (N4), homogeneous, often grading to burrowed grn.gray (SG6/1) interval at contact w/ NANNO LIMESTONE, bl.wht. to wht. (5B 9/1-N9) which is intensely burrowed, rare mud-clast CALC SANDSTONE, sometimes graded, occurs within the marly limestone
					1			
					1.0			
					2			
					3			
					4			*shown as black interval in lithology column
								←drill cuttings
								CaCO <sub>3</sub> % C <sub>org</sub> %
								SHOREBASED 2-100 89 0.1

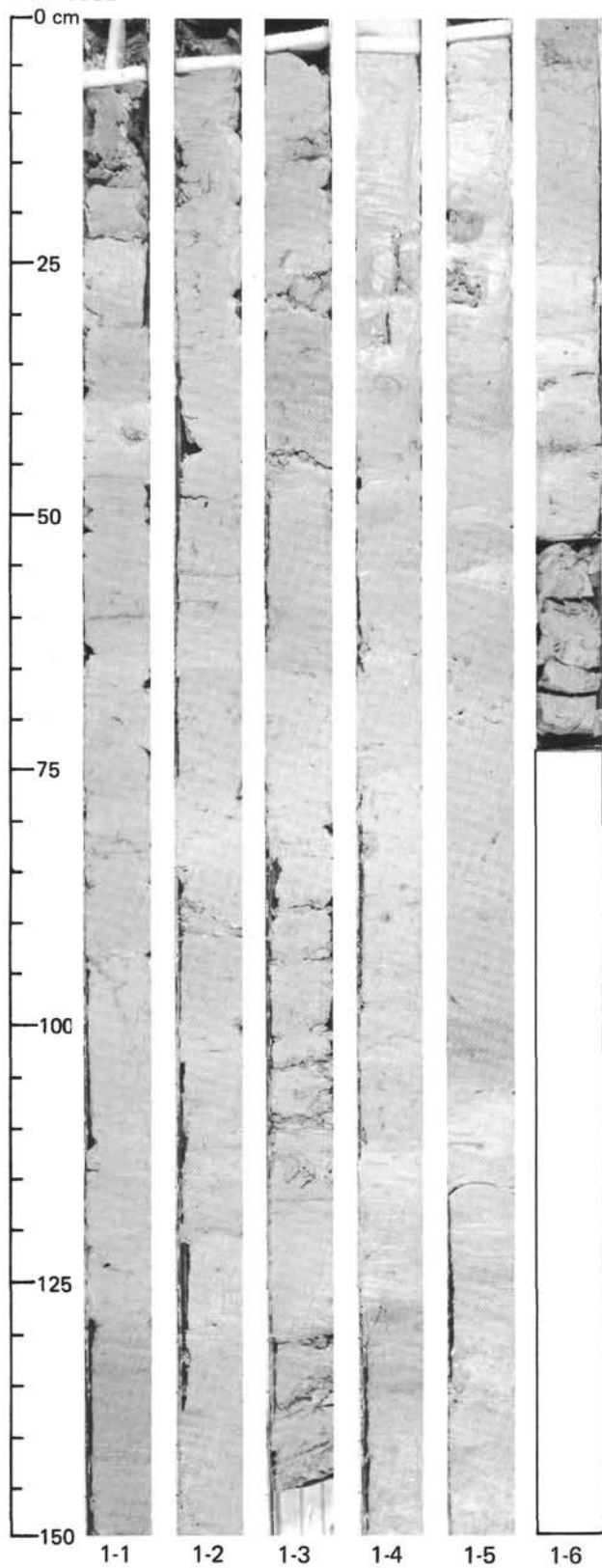
Explanatory notes in Chapter 1



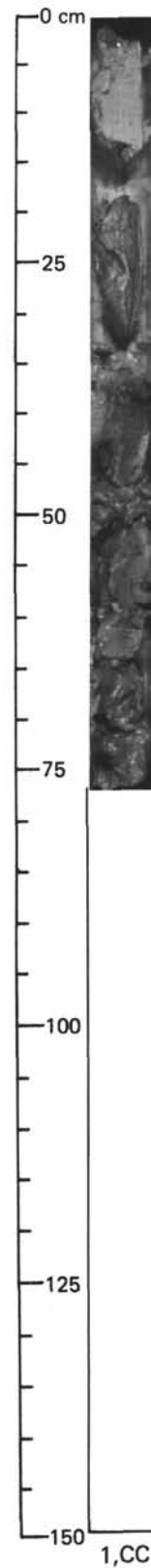
Hole 398A

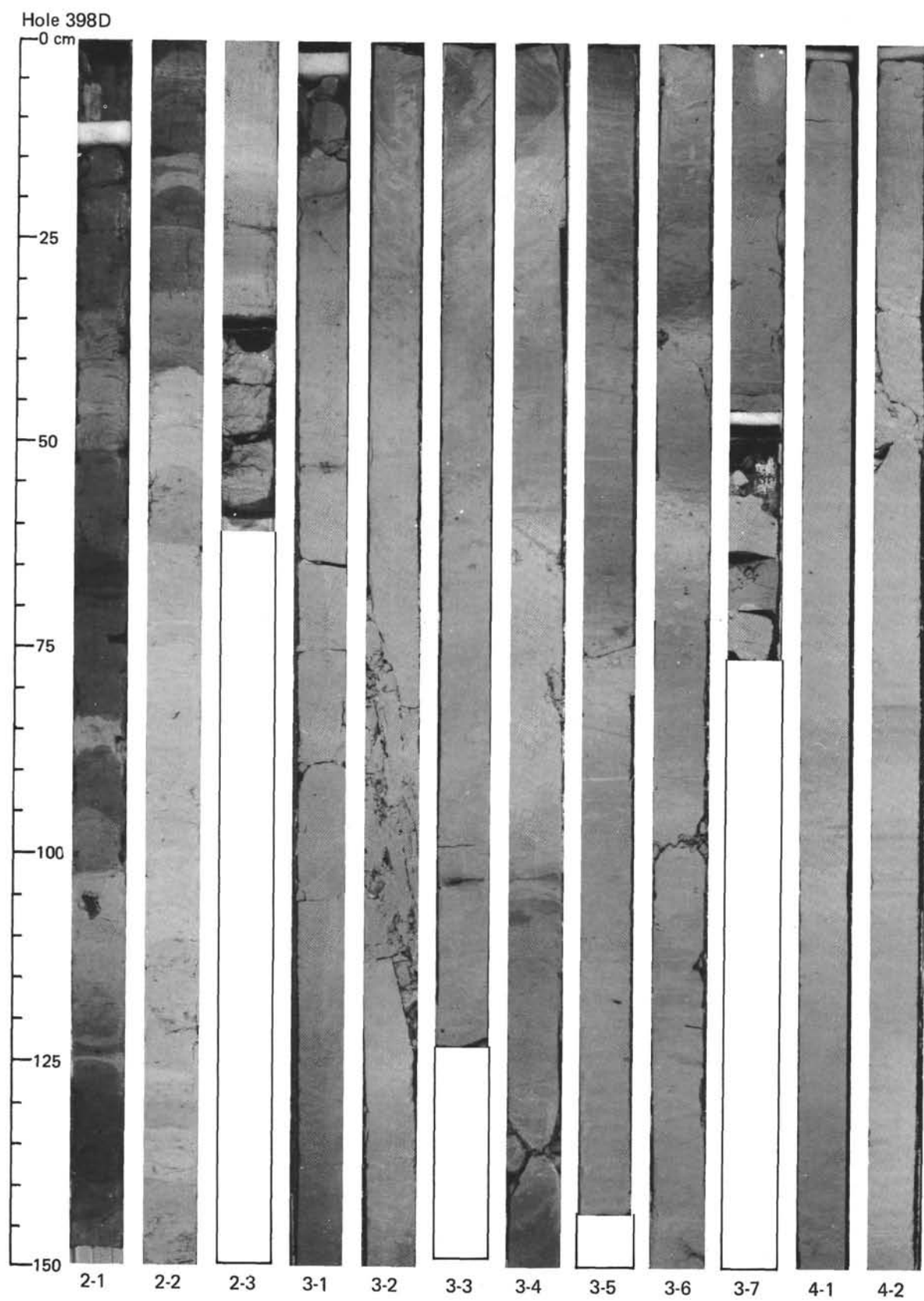


Hole 398B

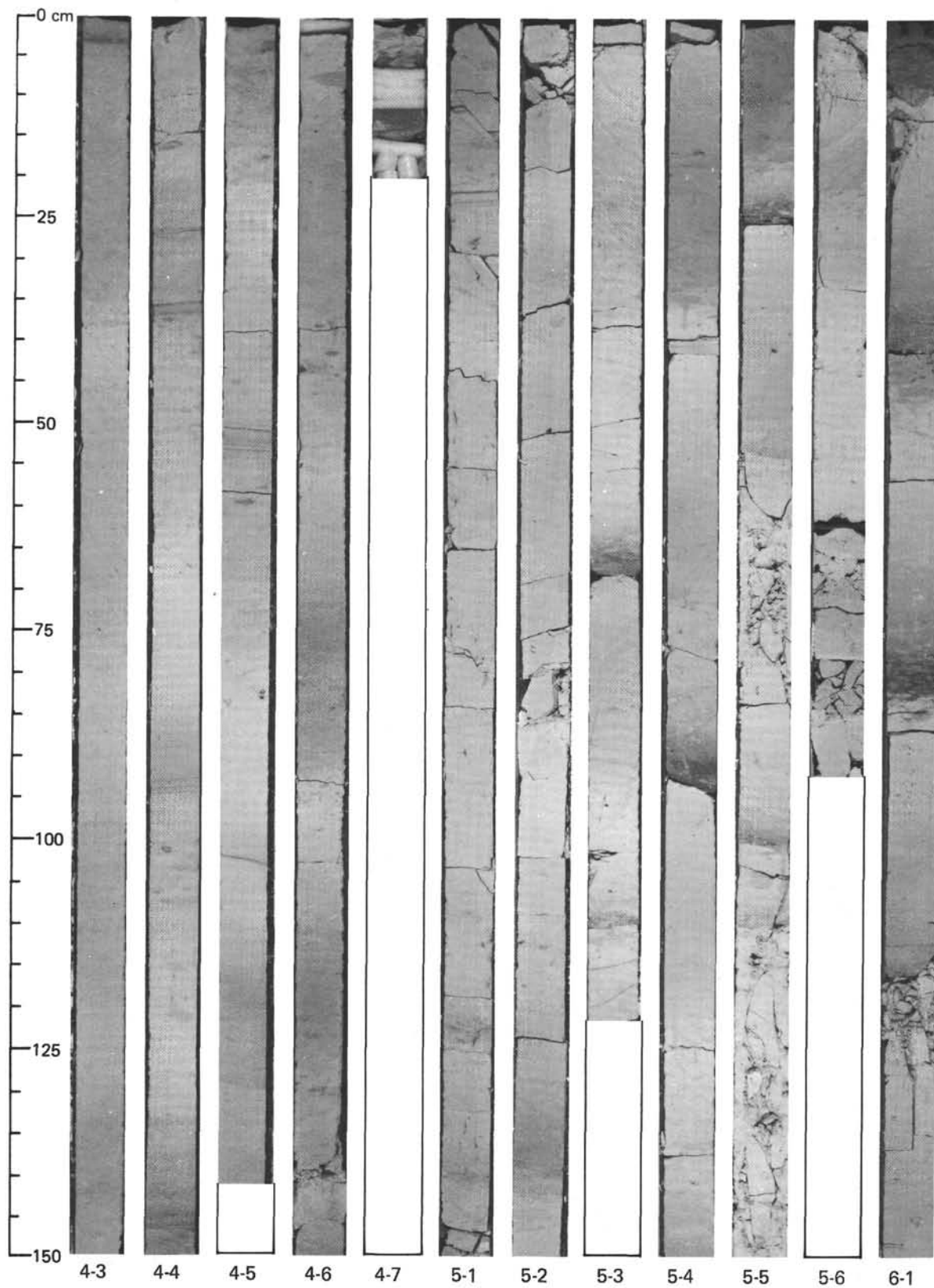


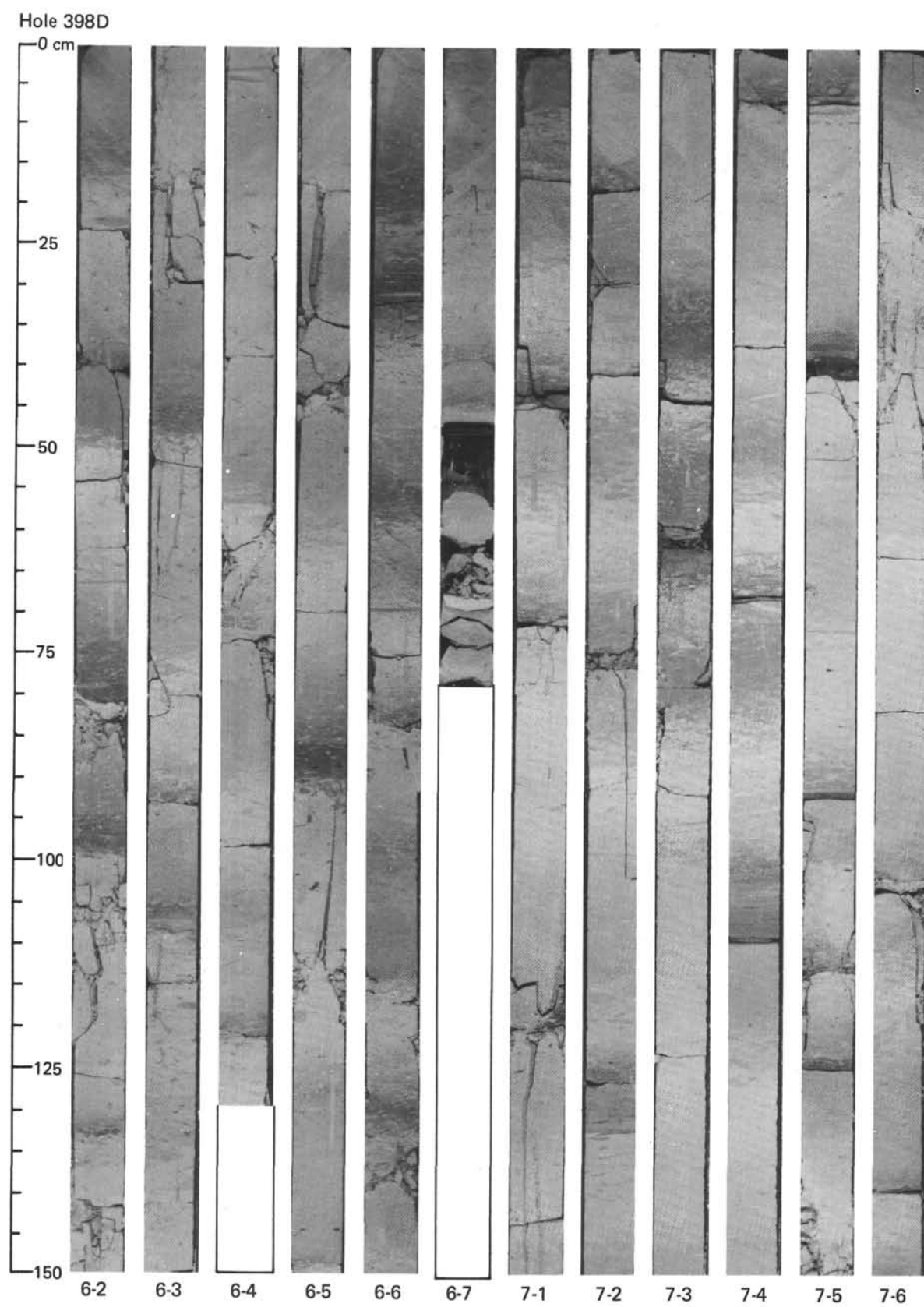
Hole 398C



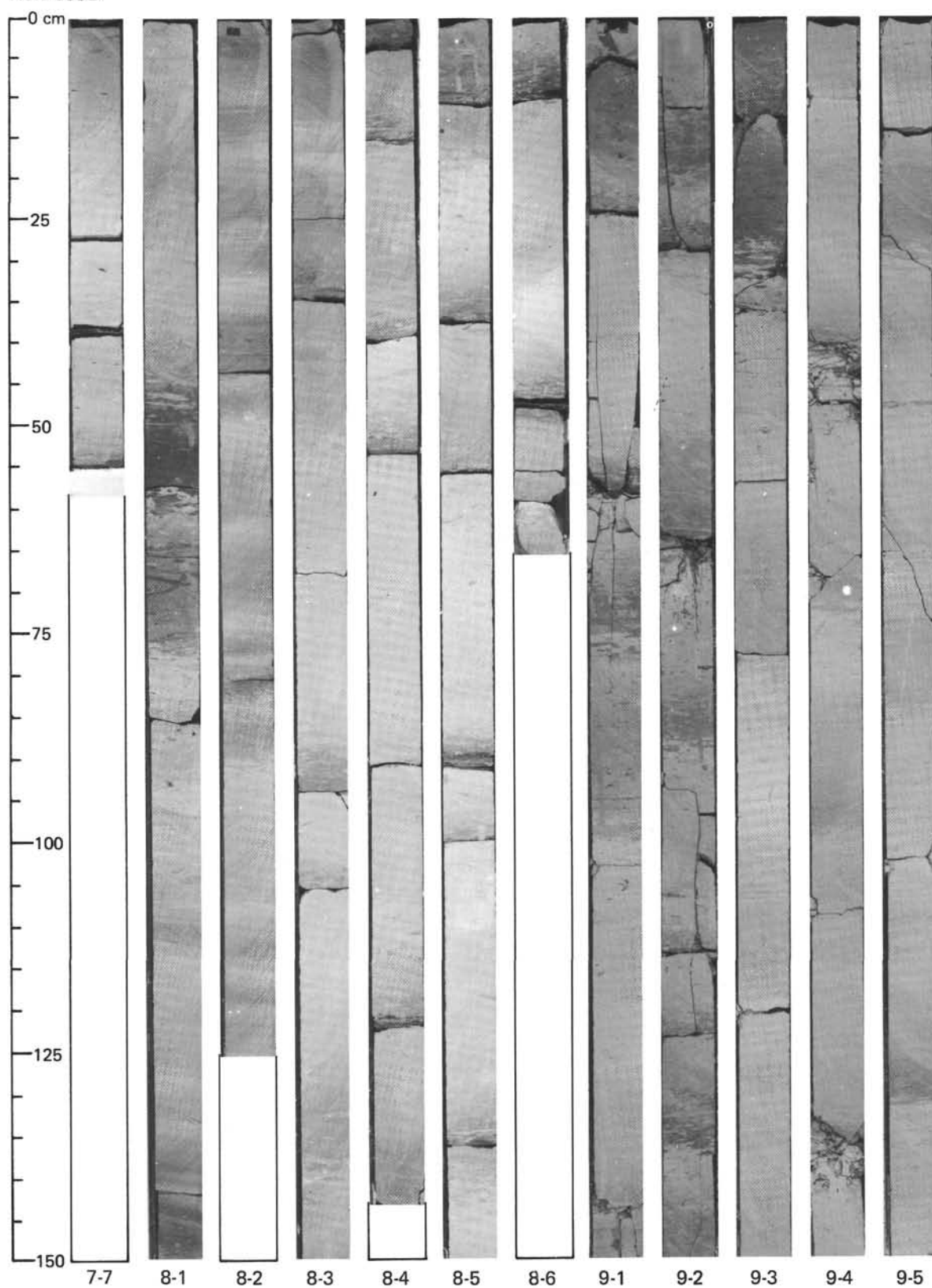


Hole 398D

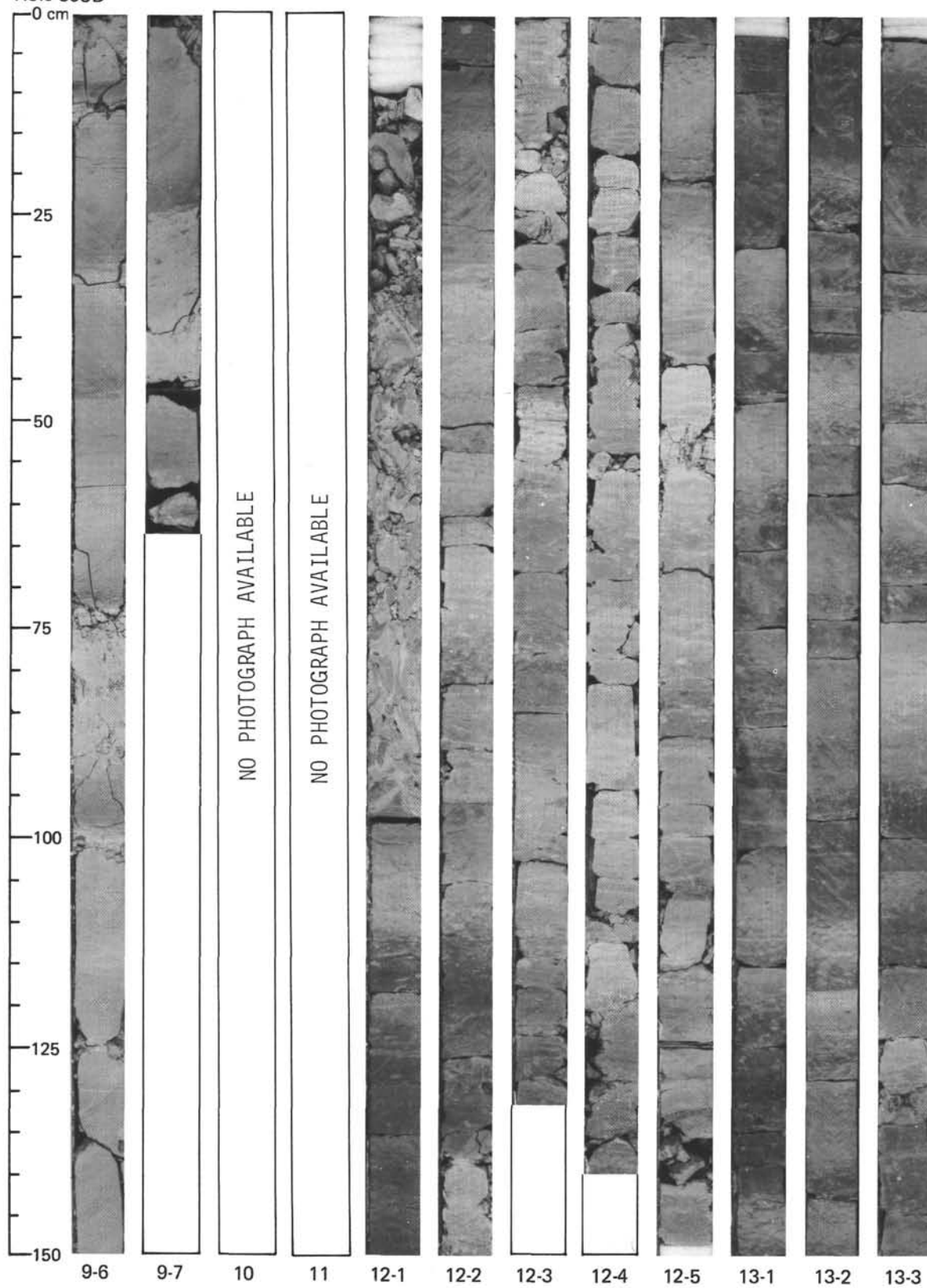


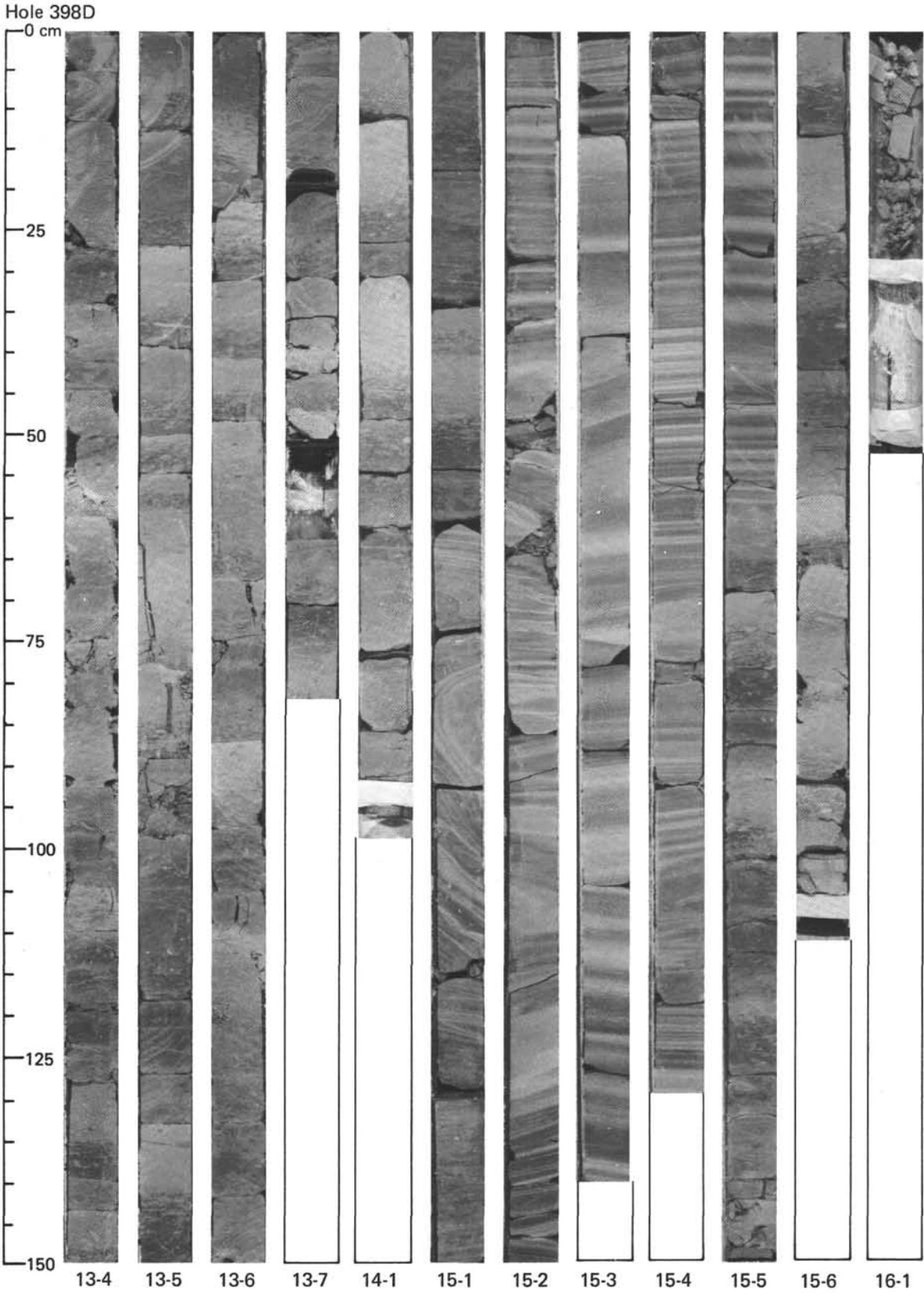


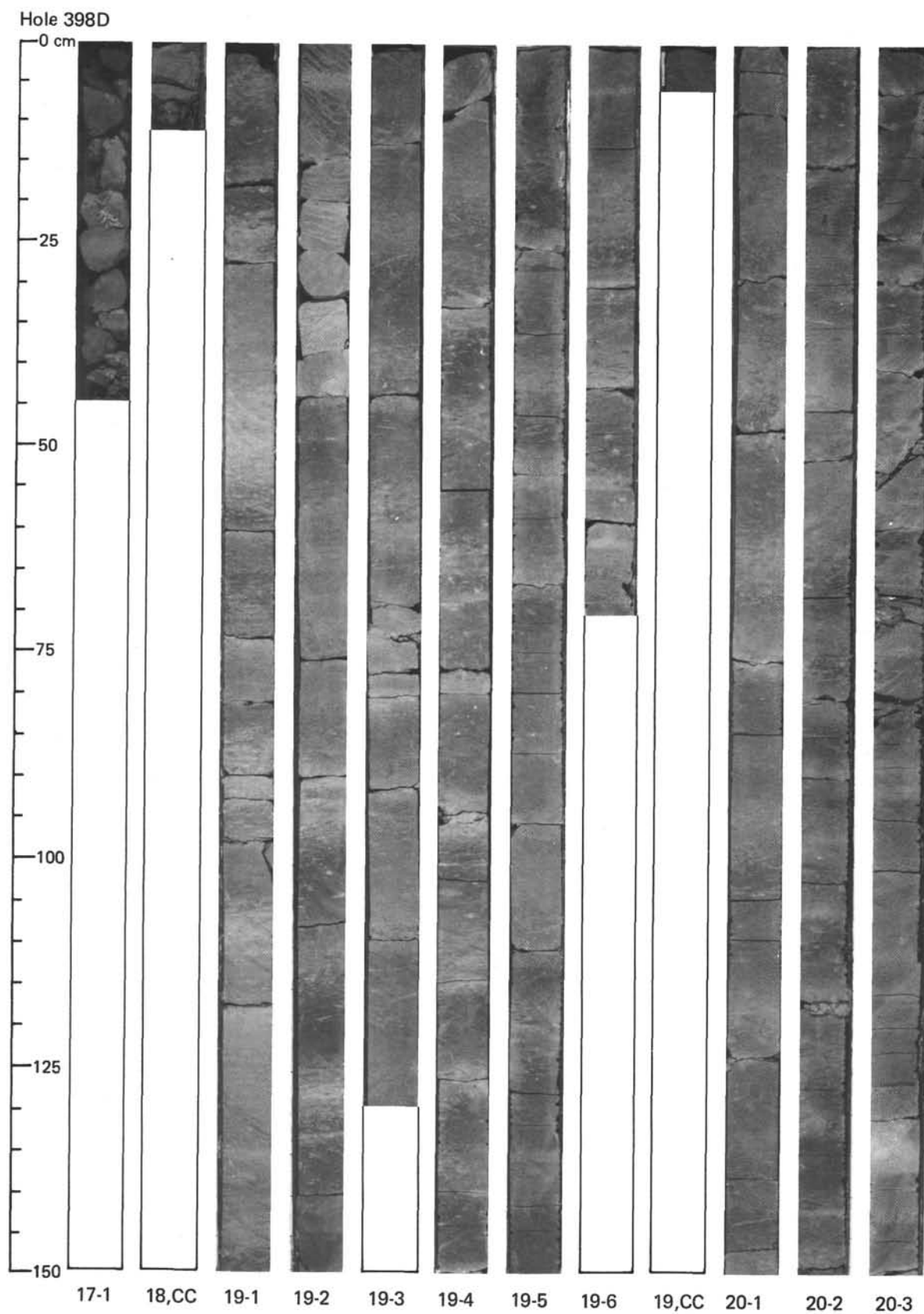
Hole 398D

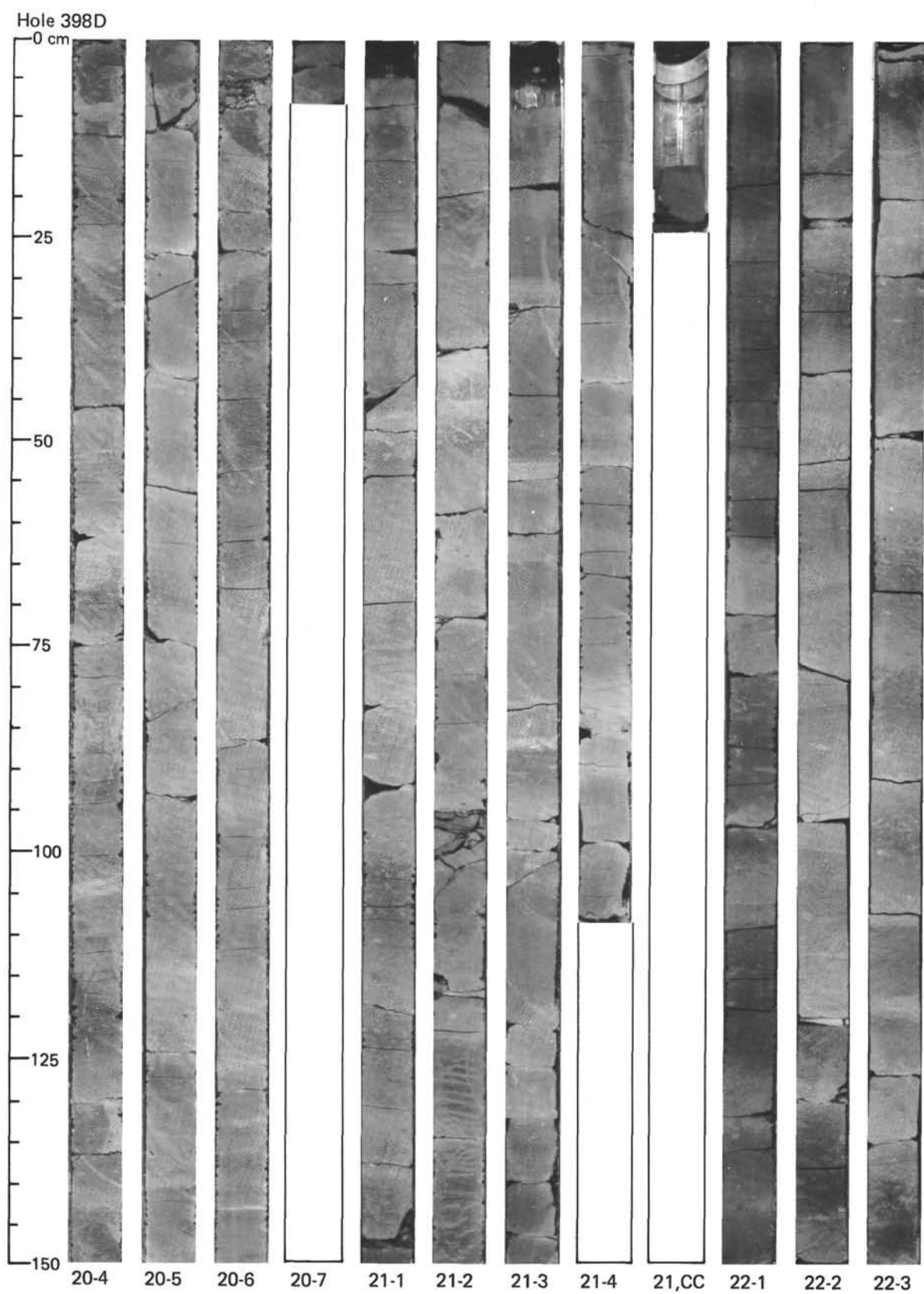


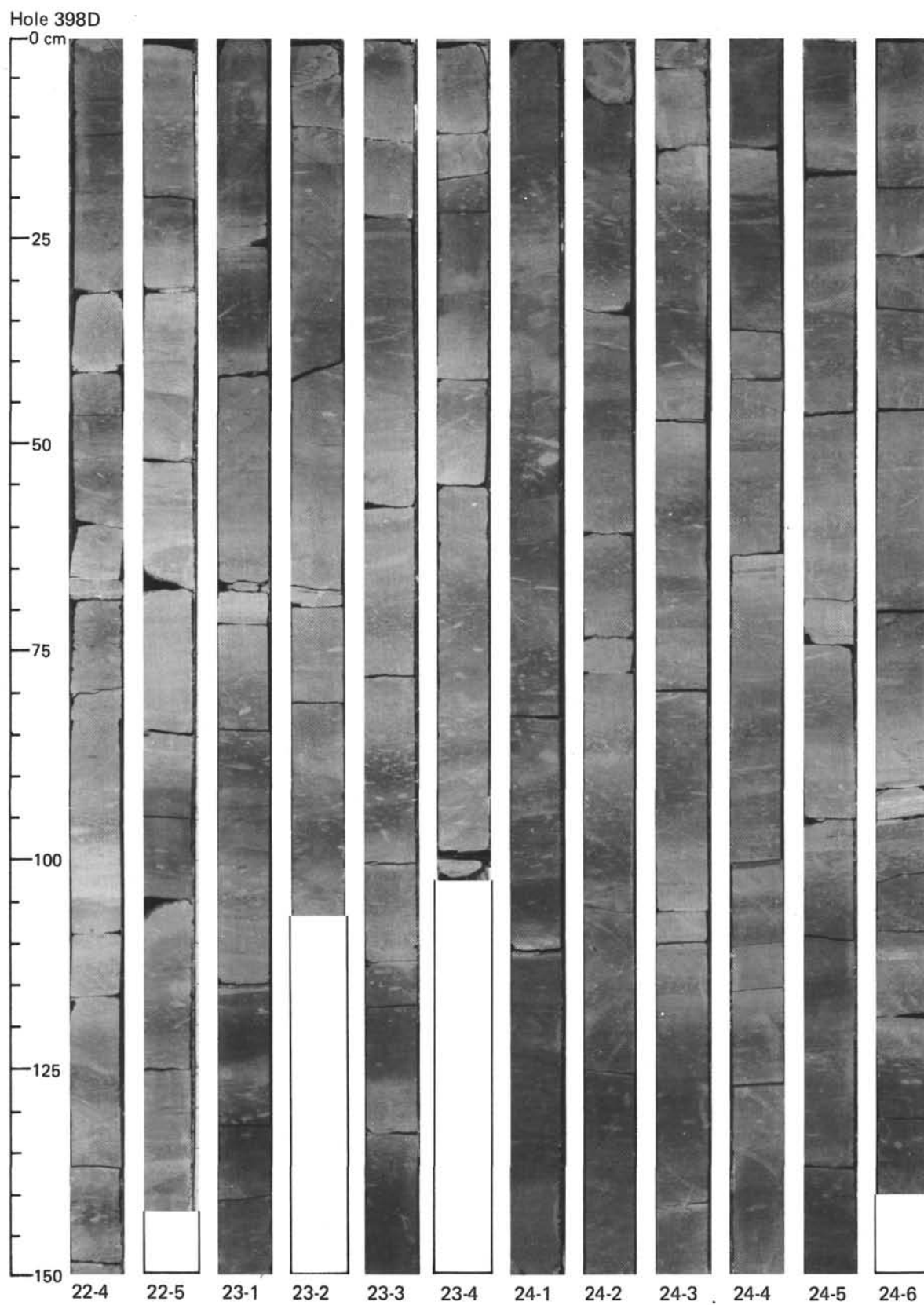
Hole 398D

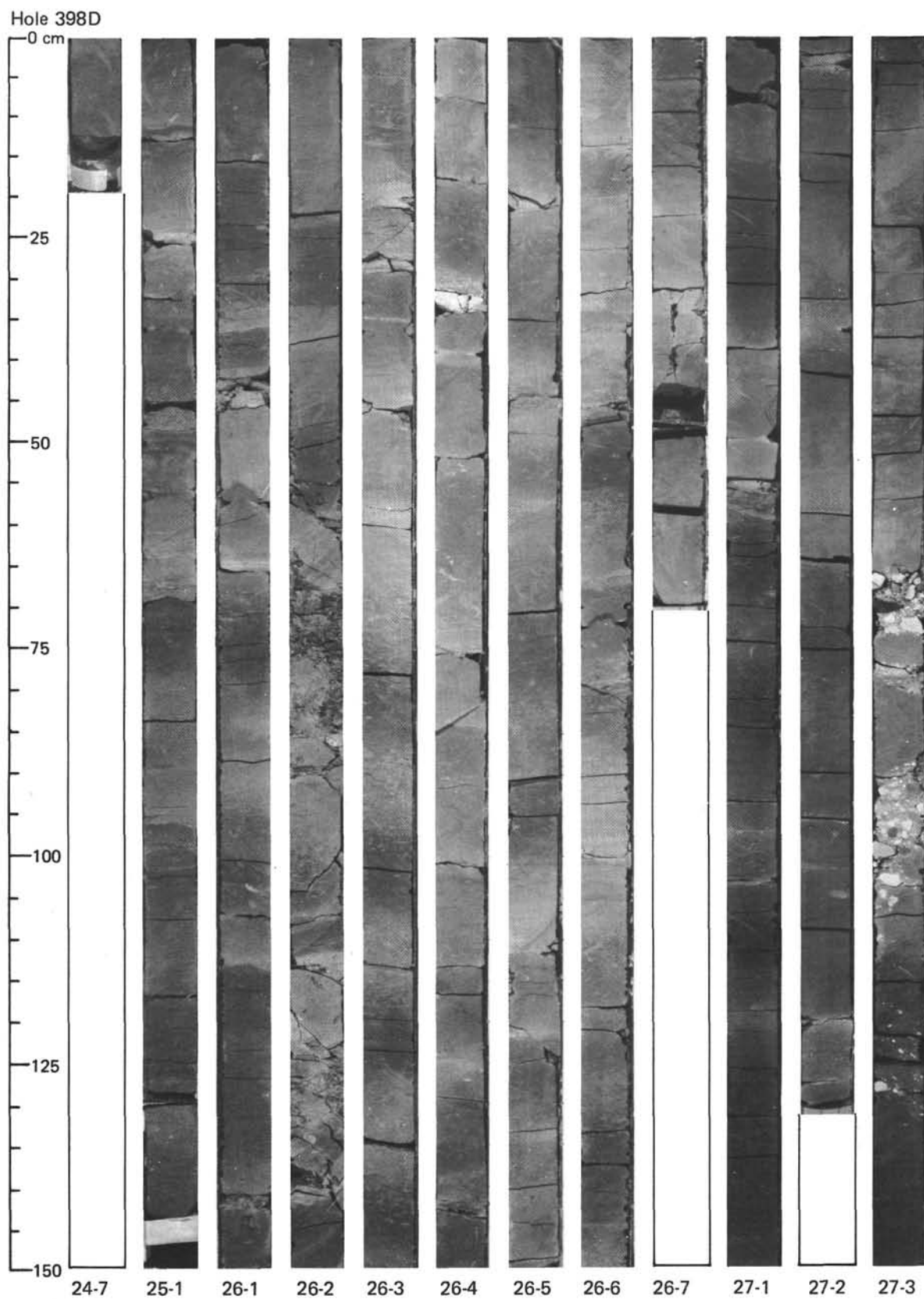




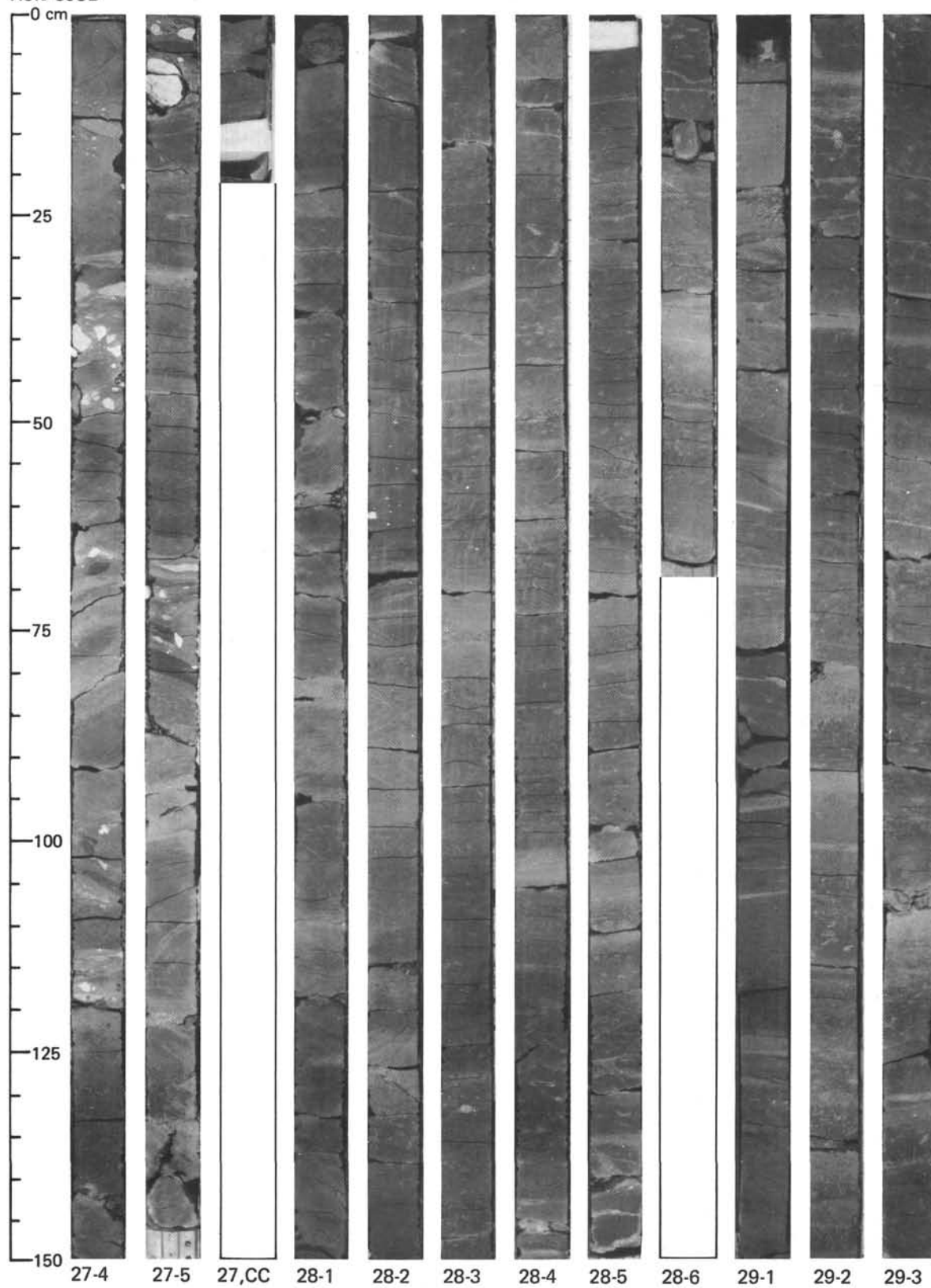




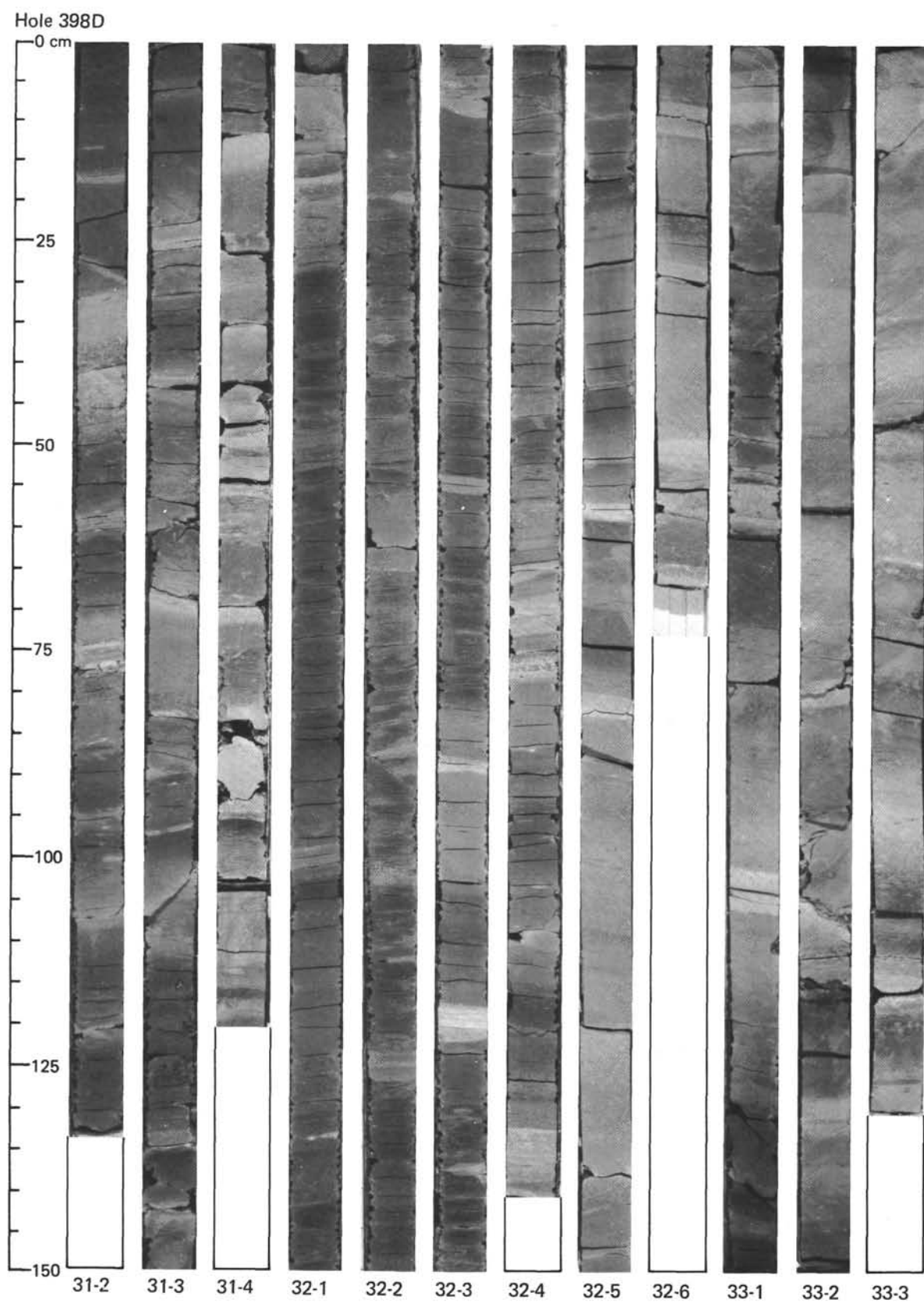


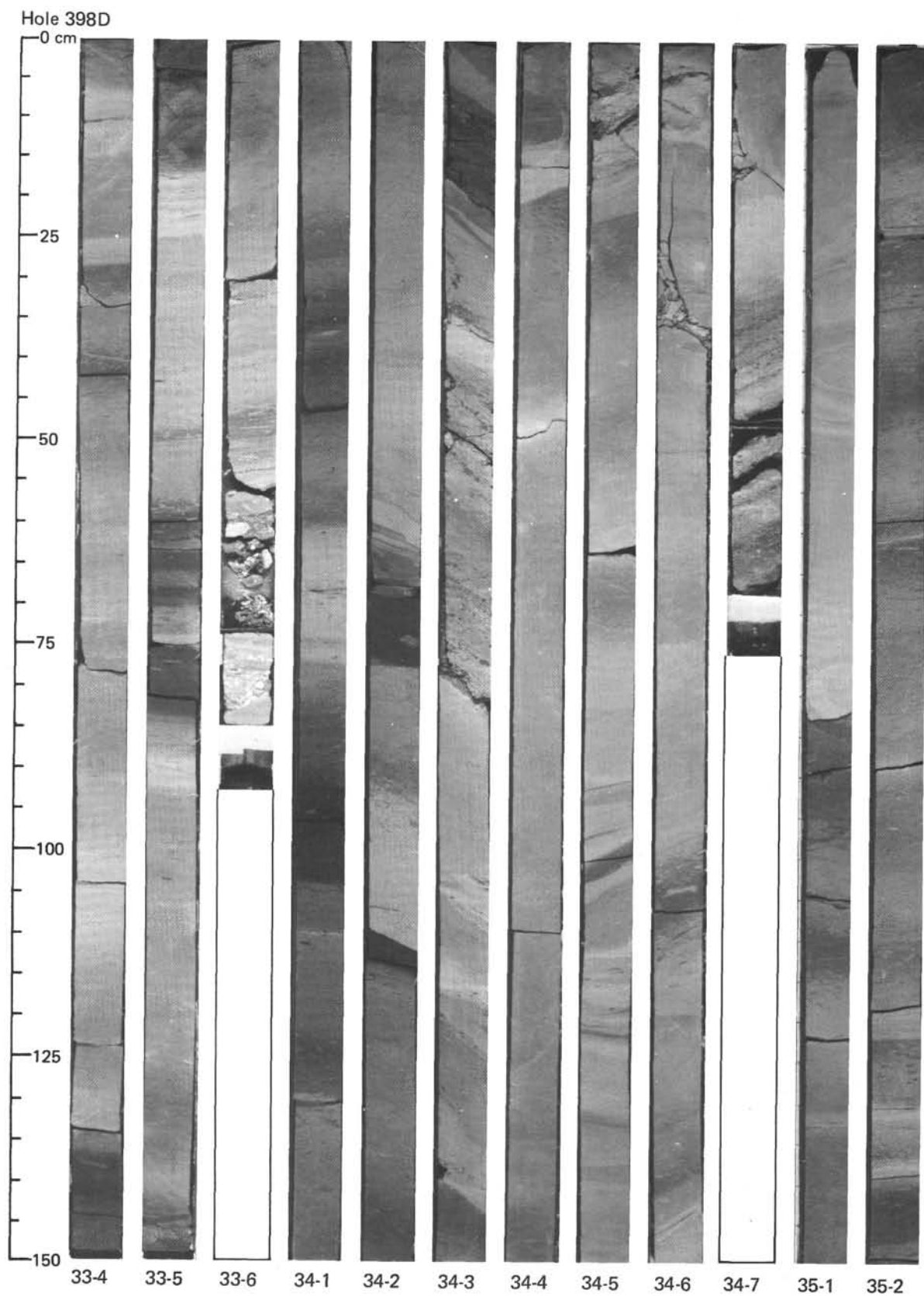


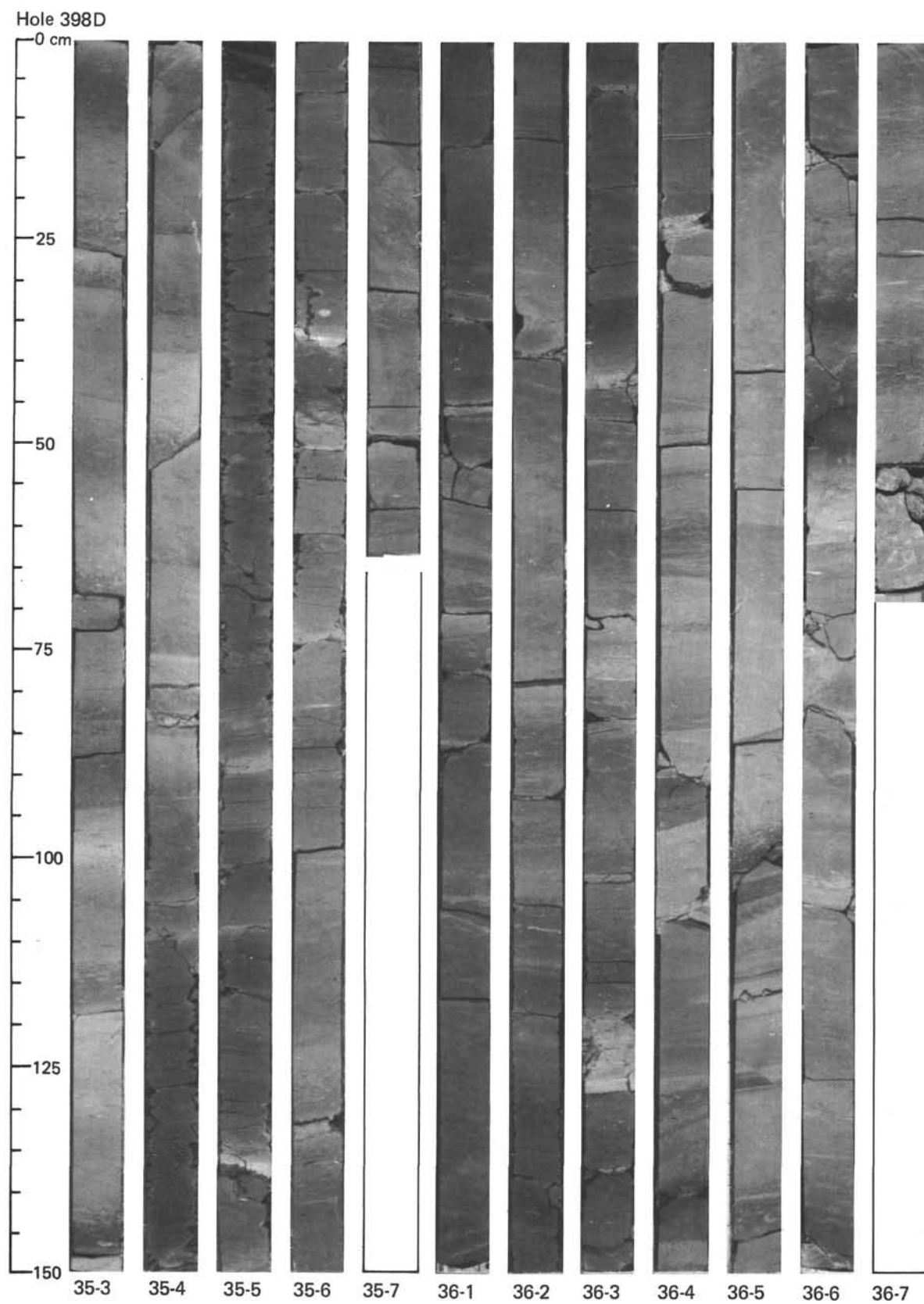
Hole 398D

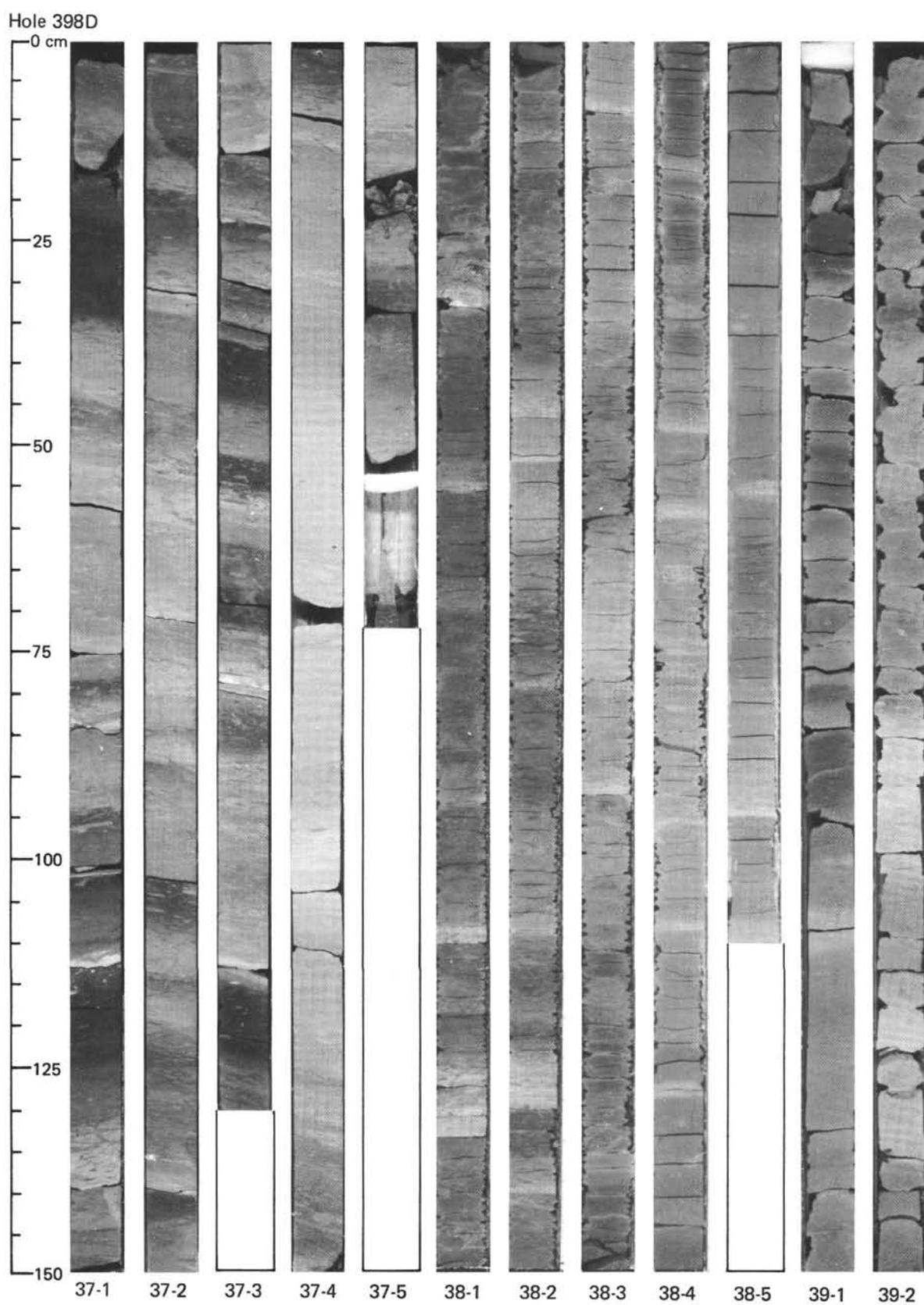




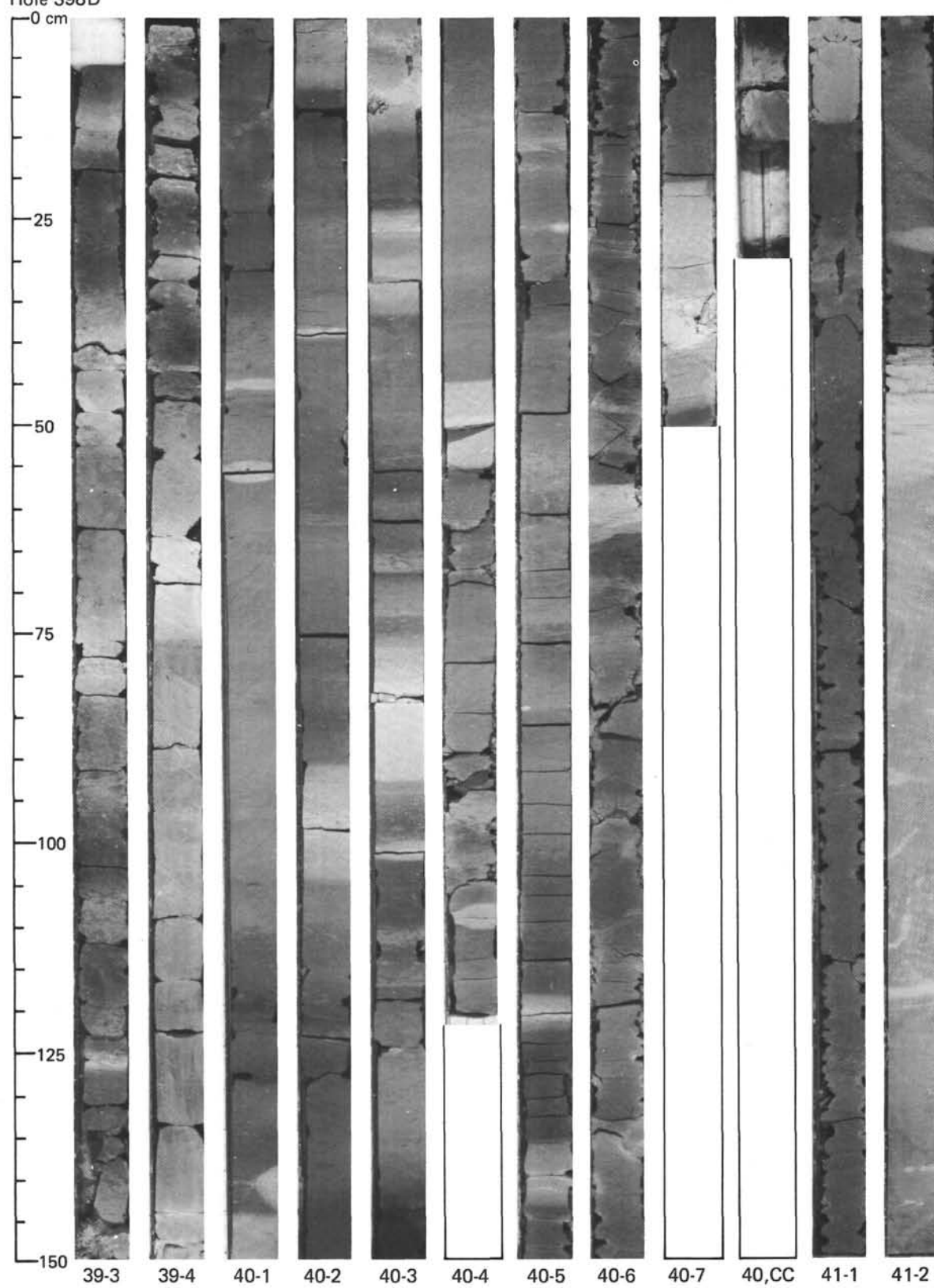


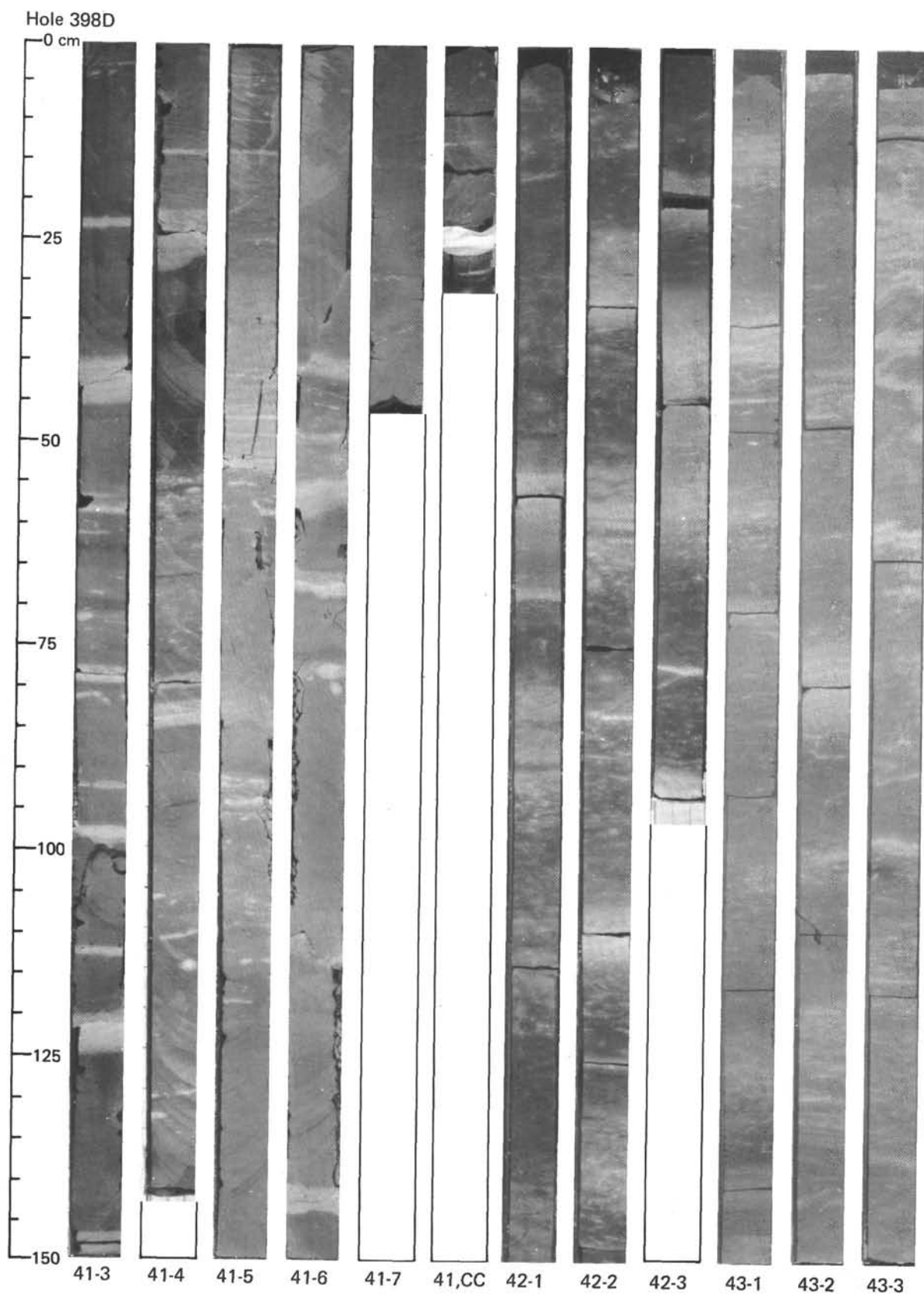


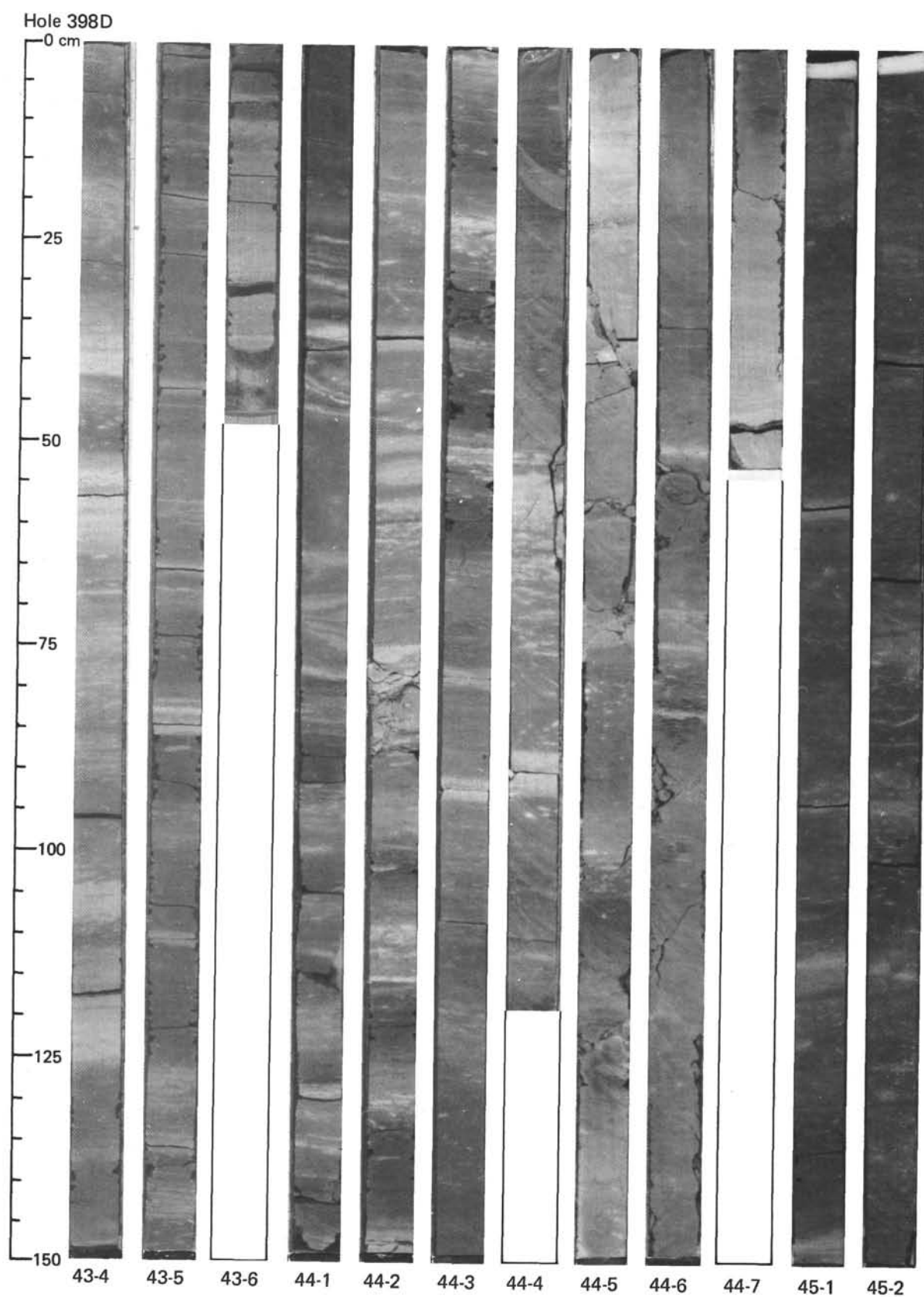


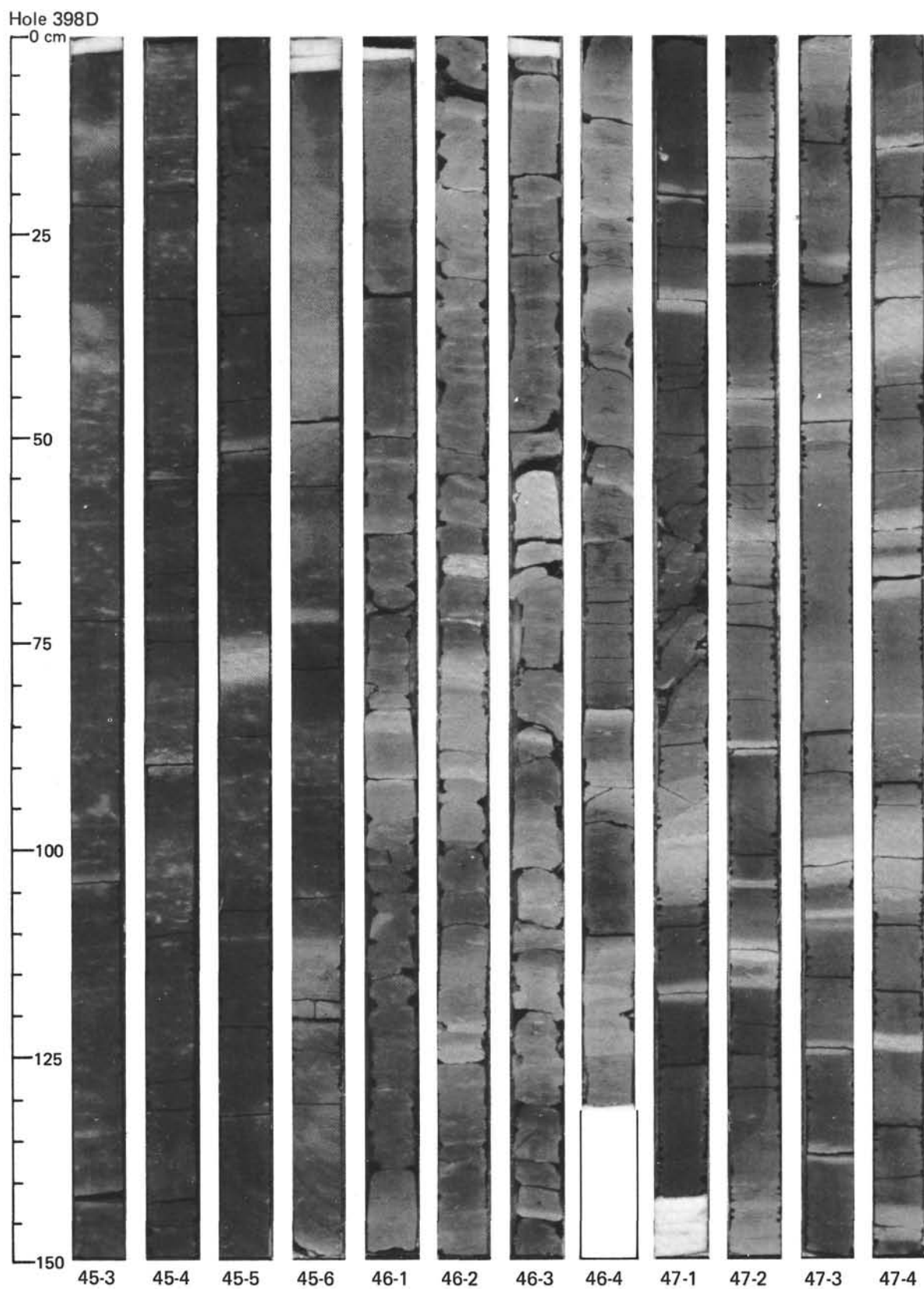


Hole 398D

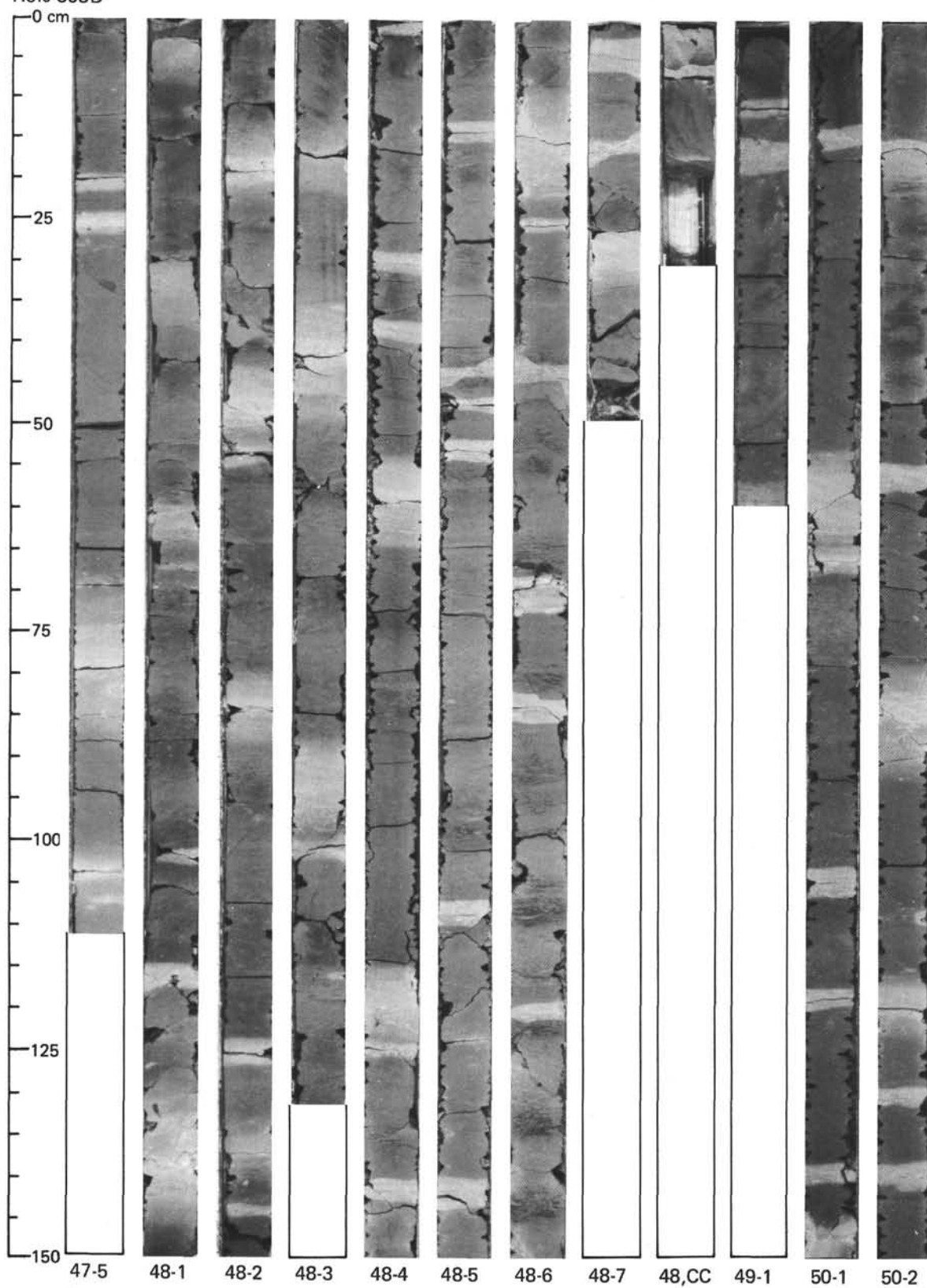


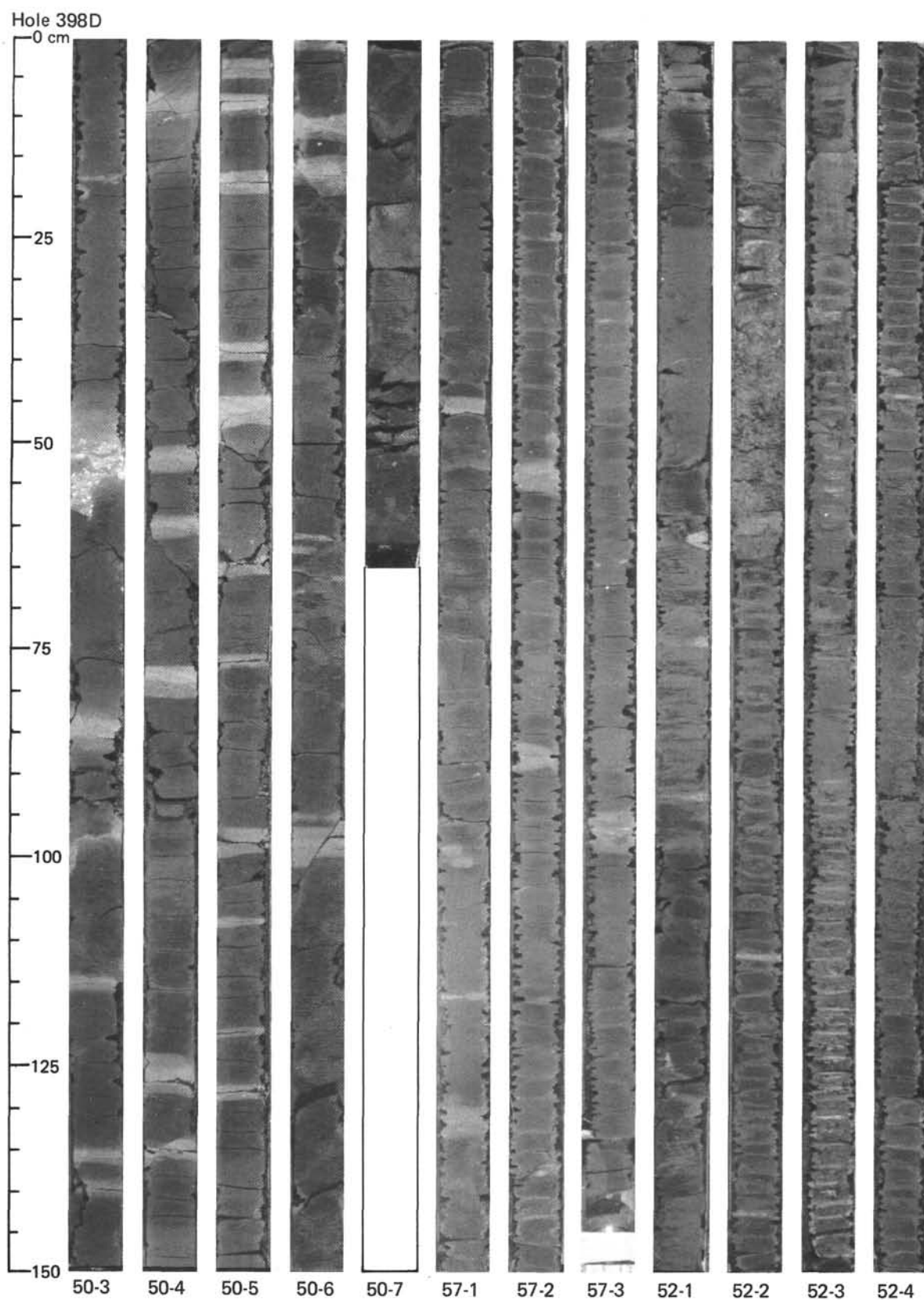


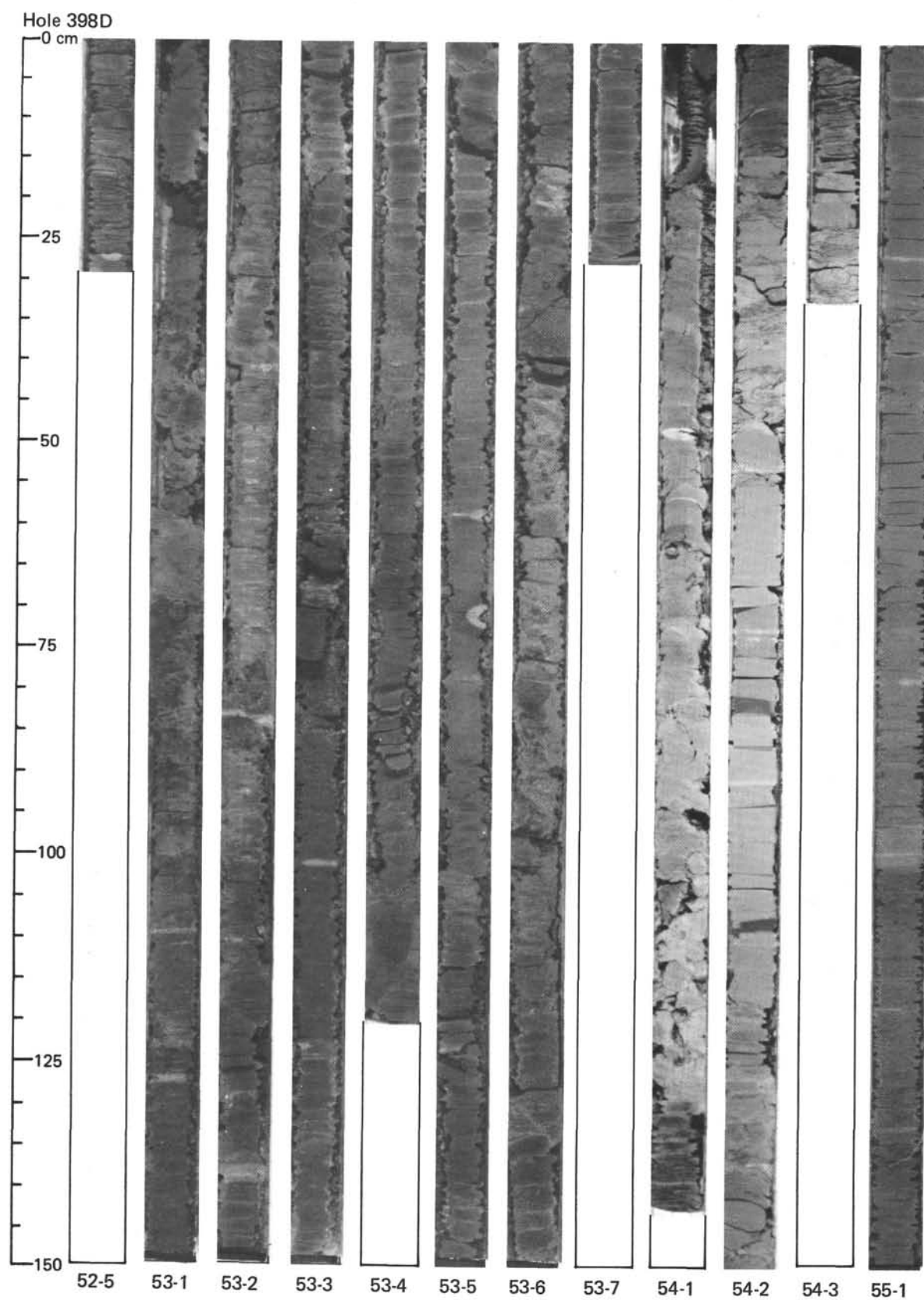


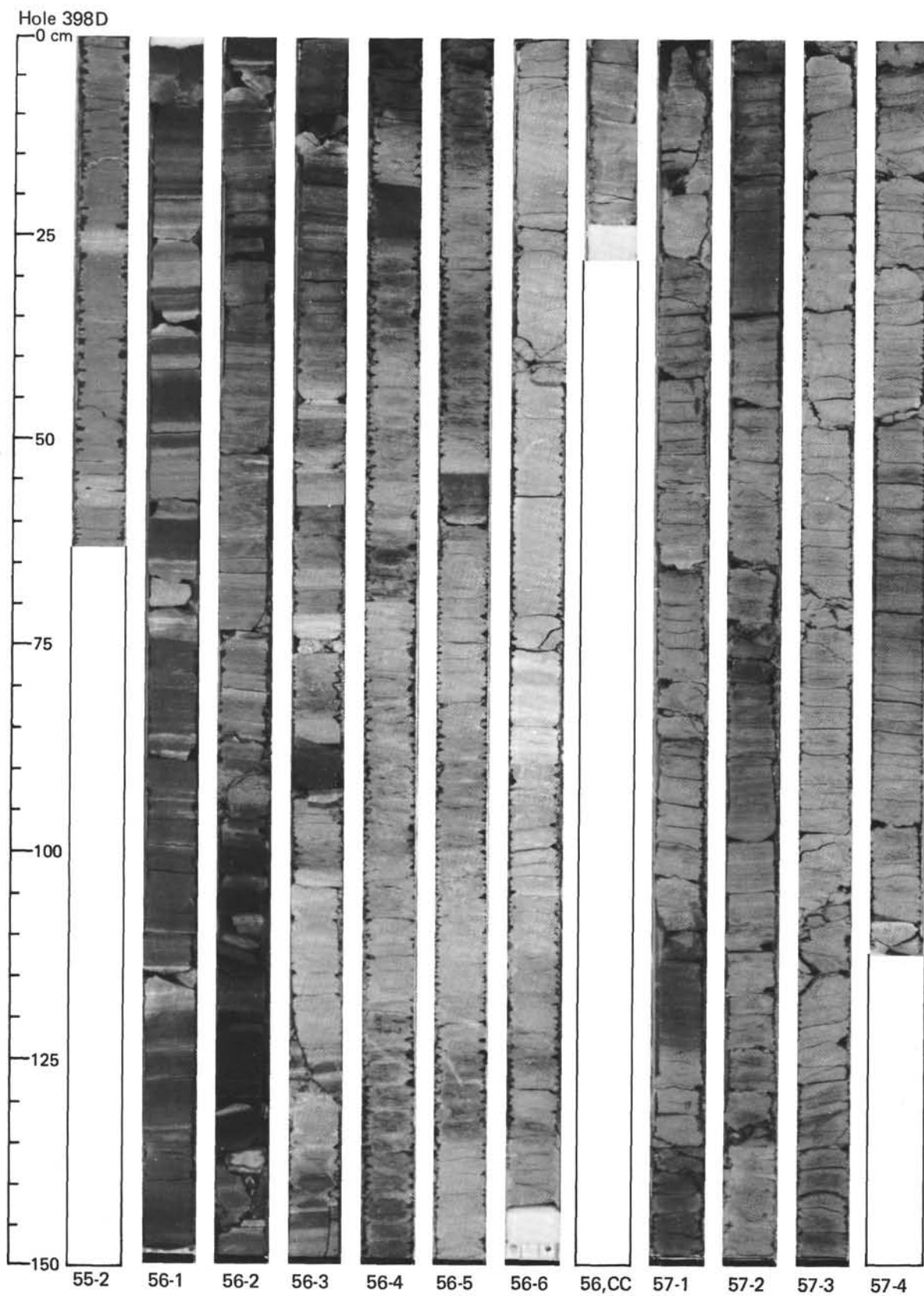


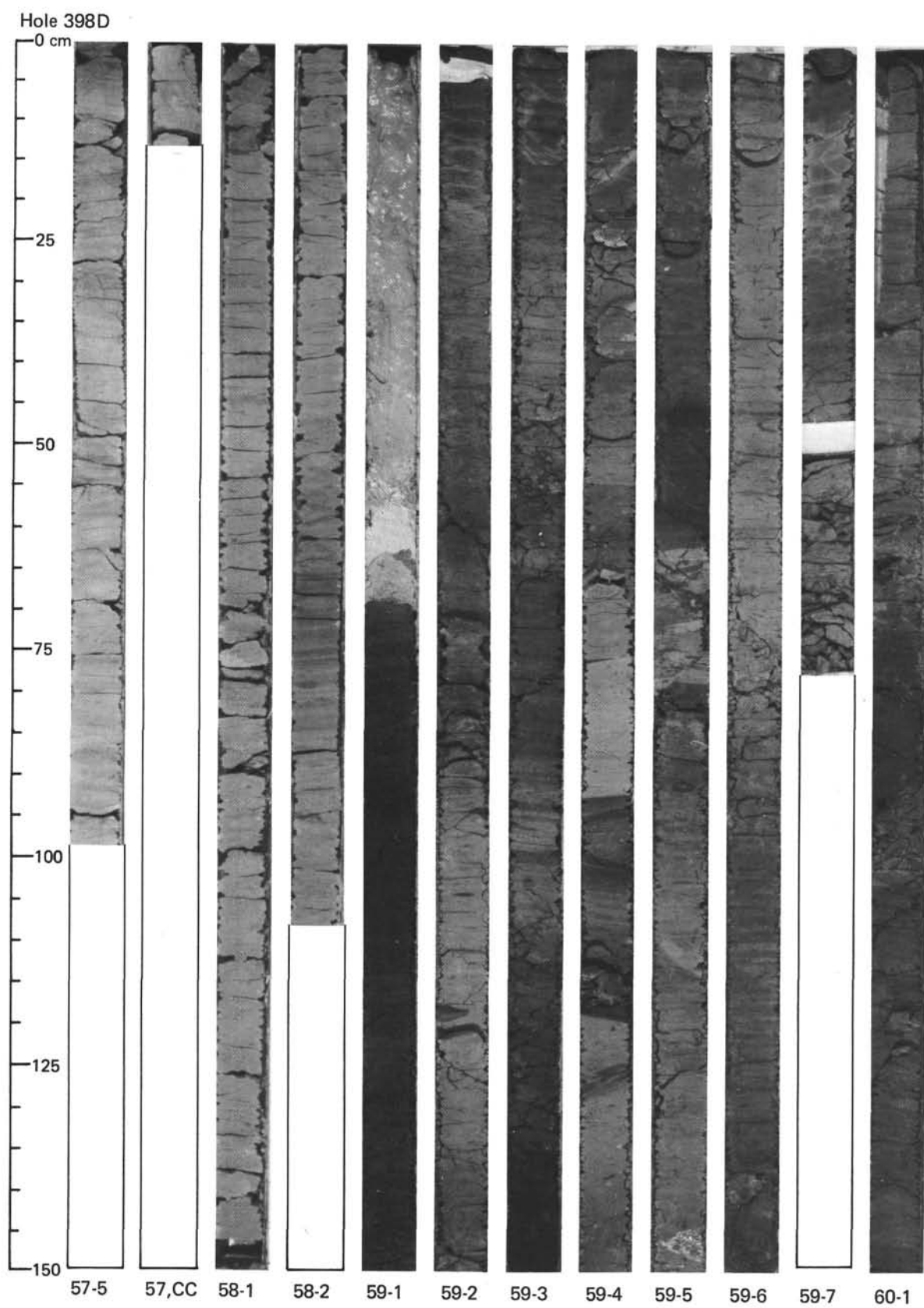
Hole 398D



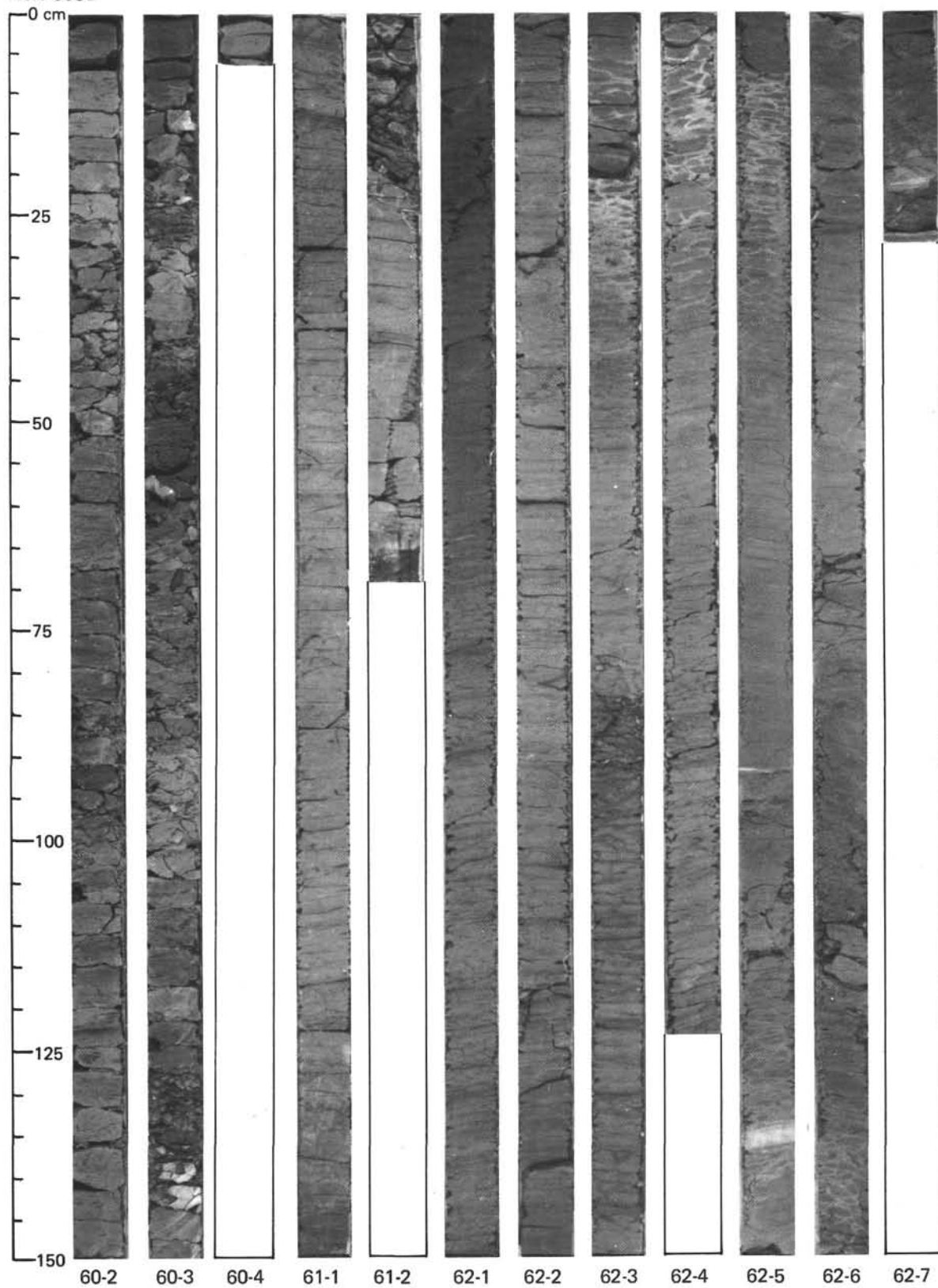


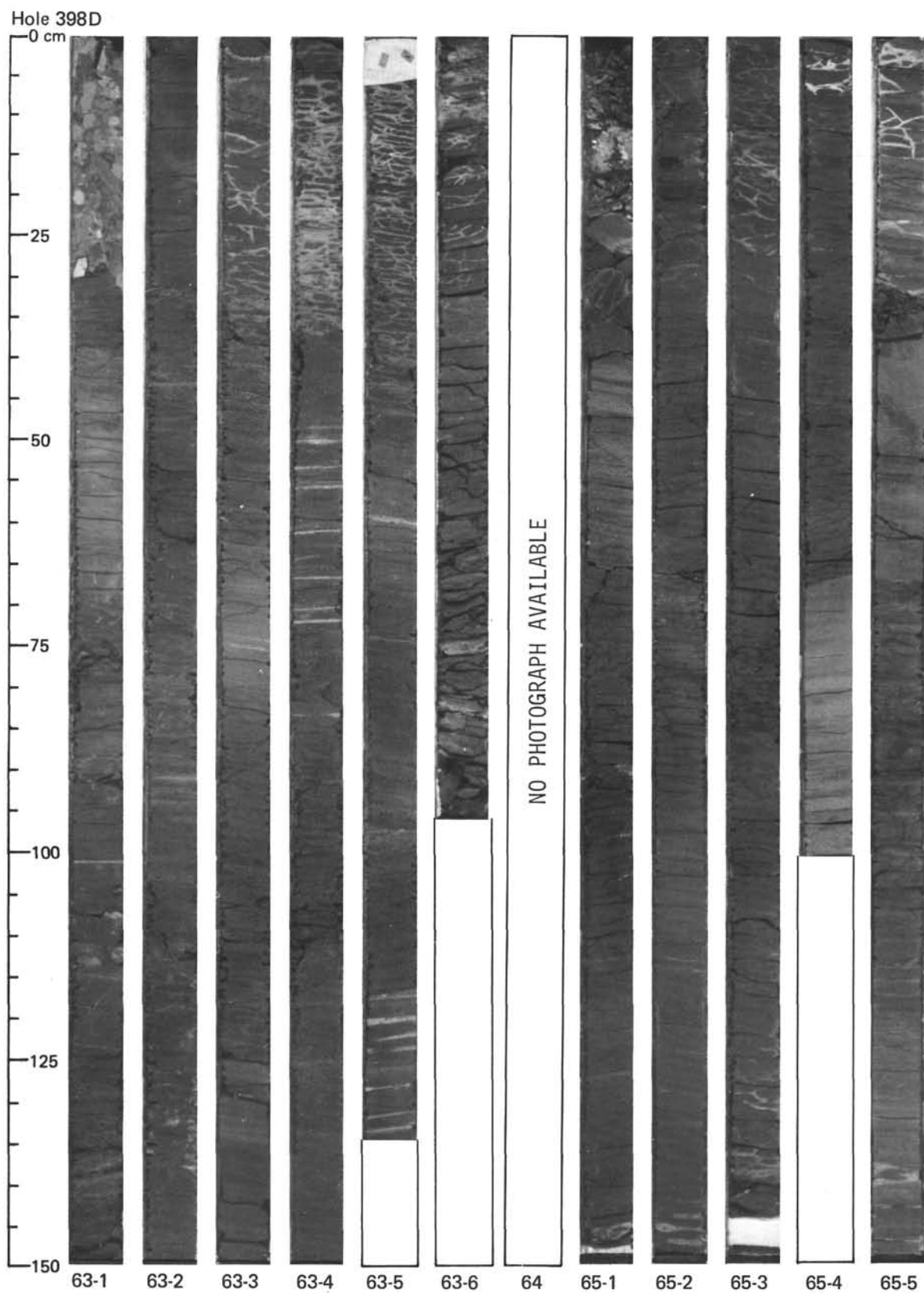


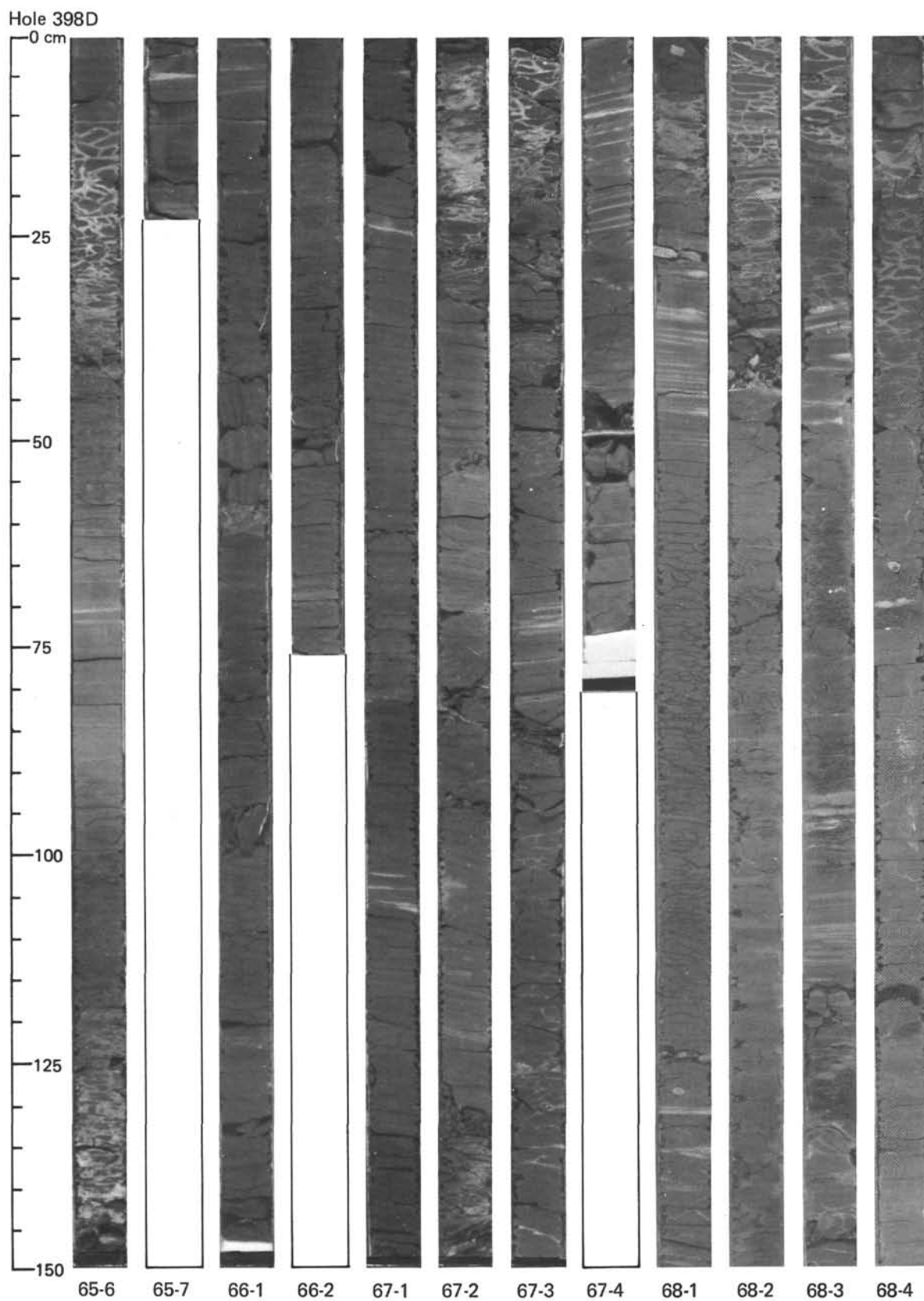


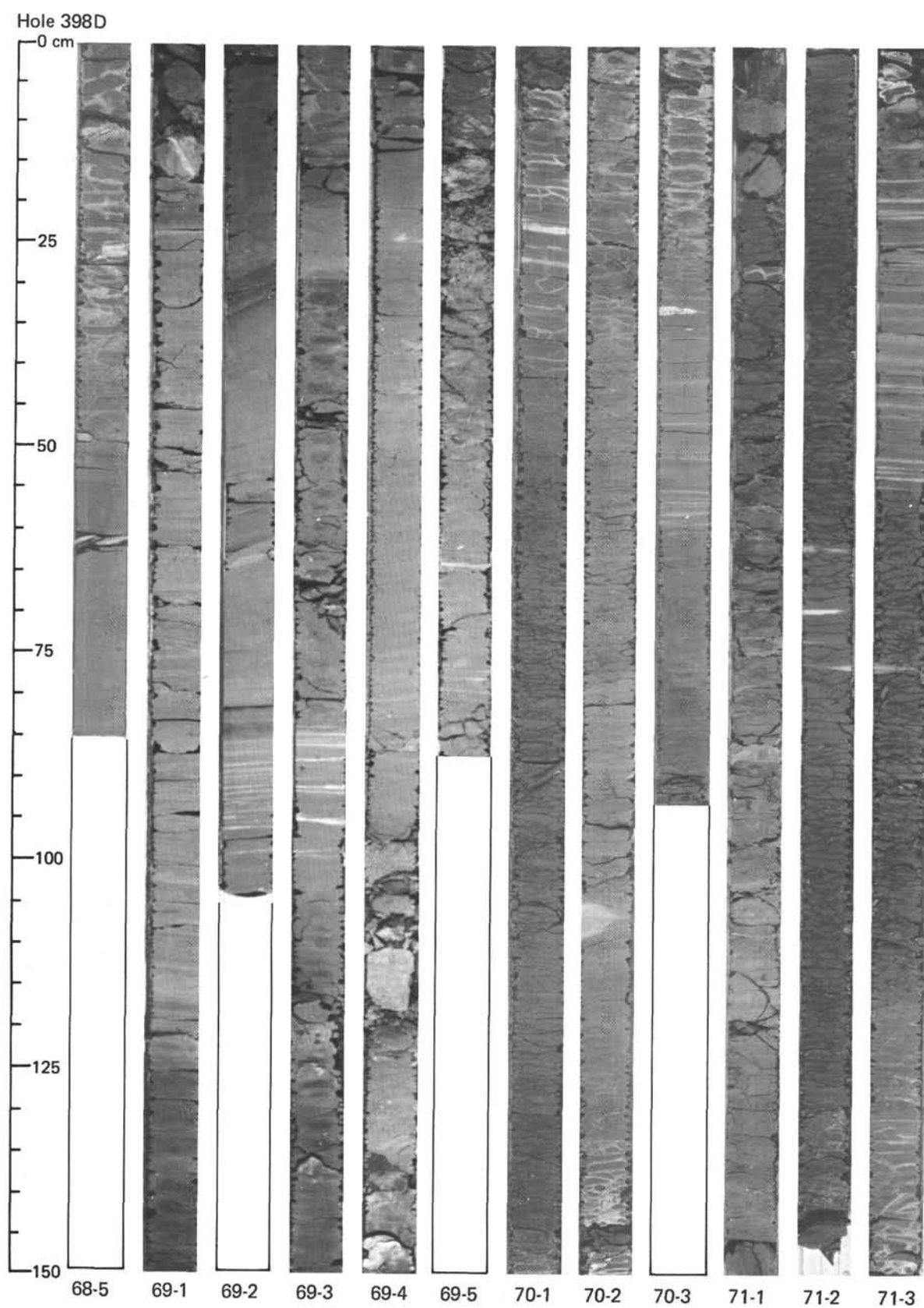


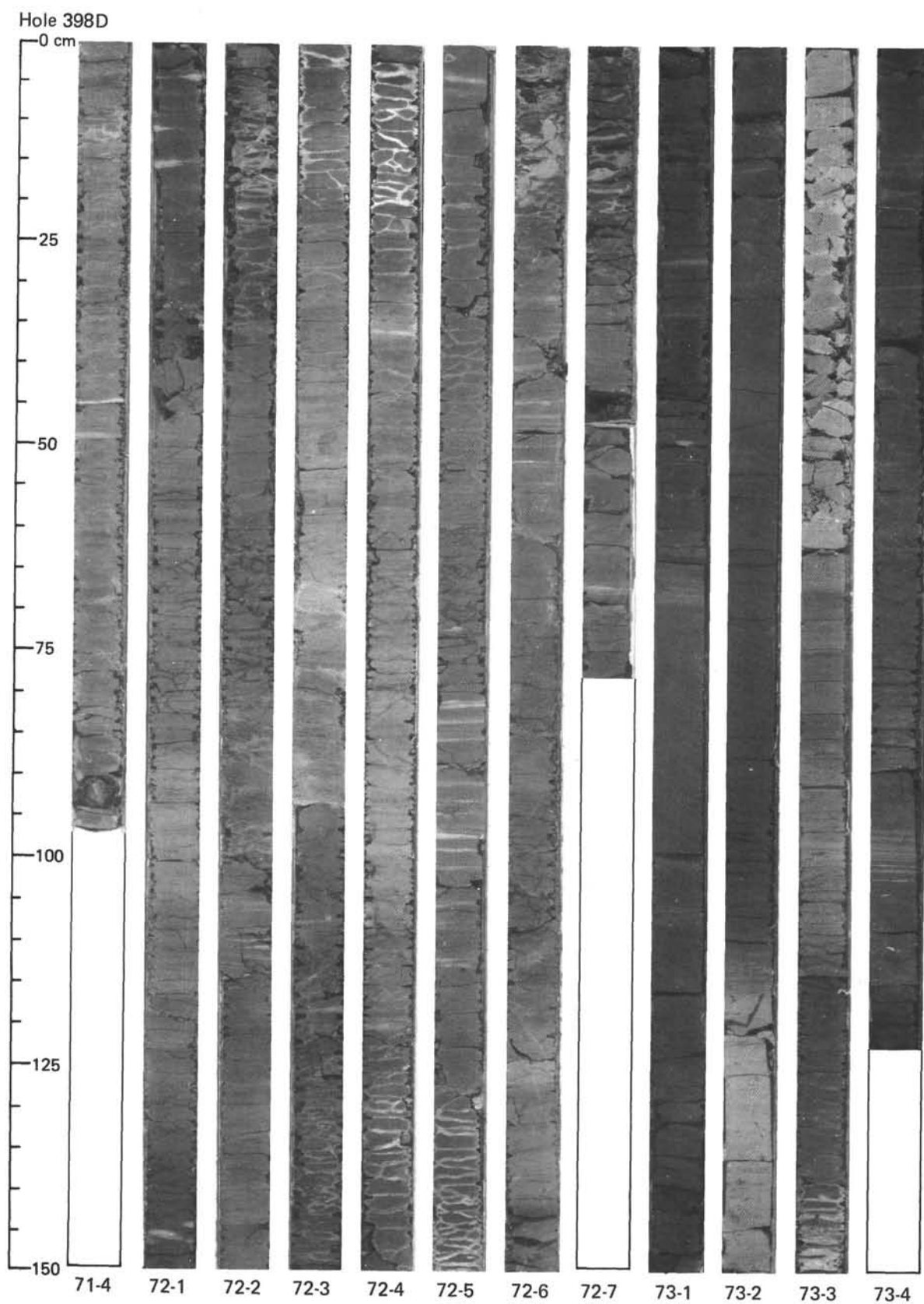
Hole 398D

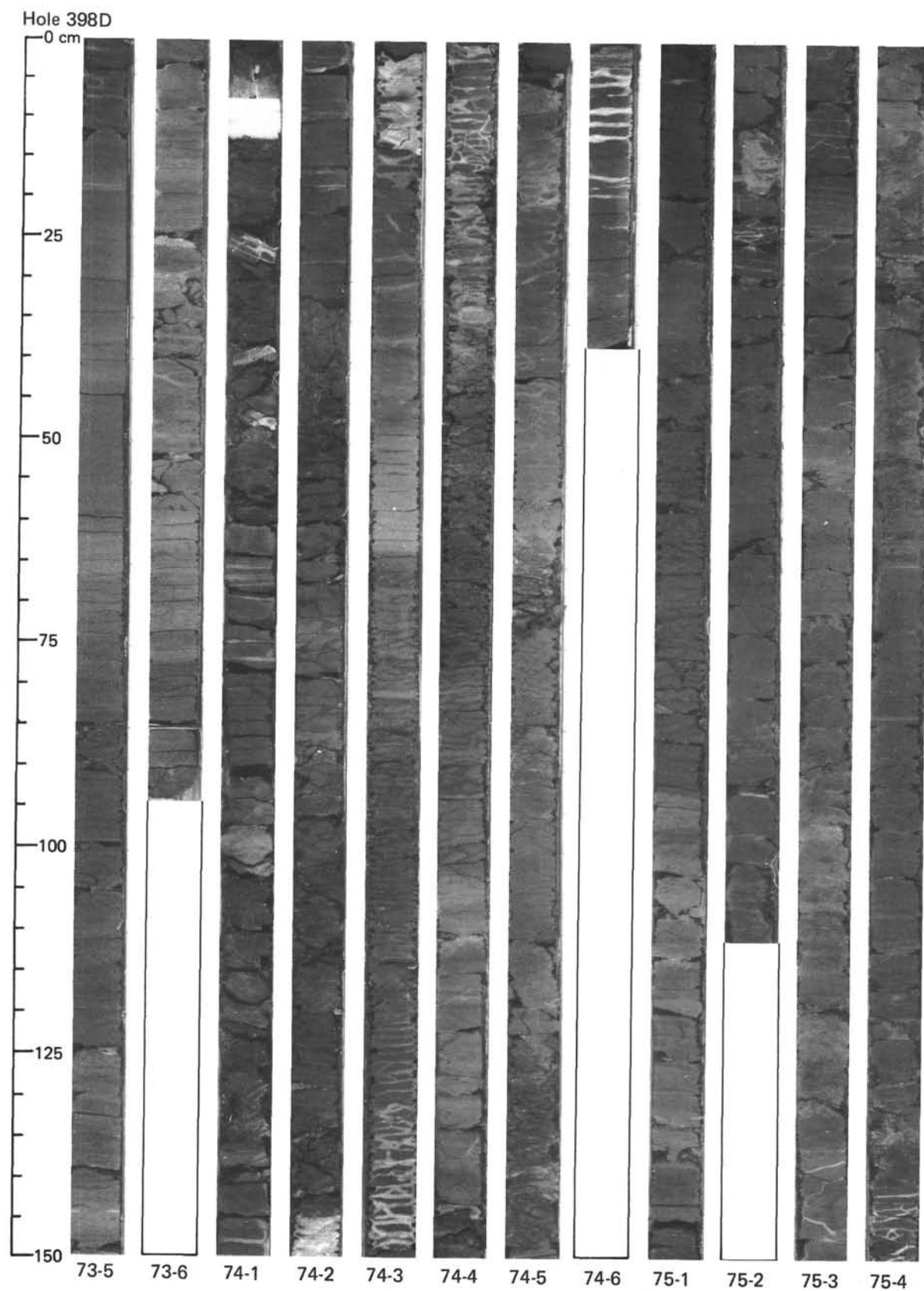


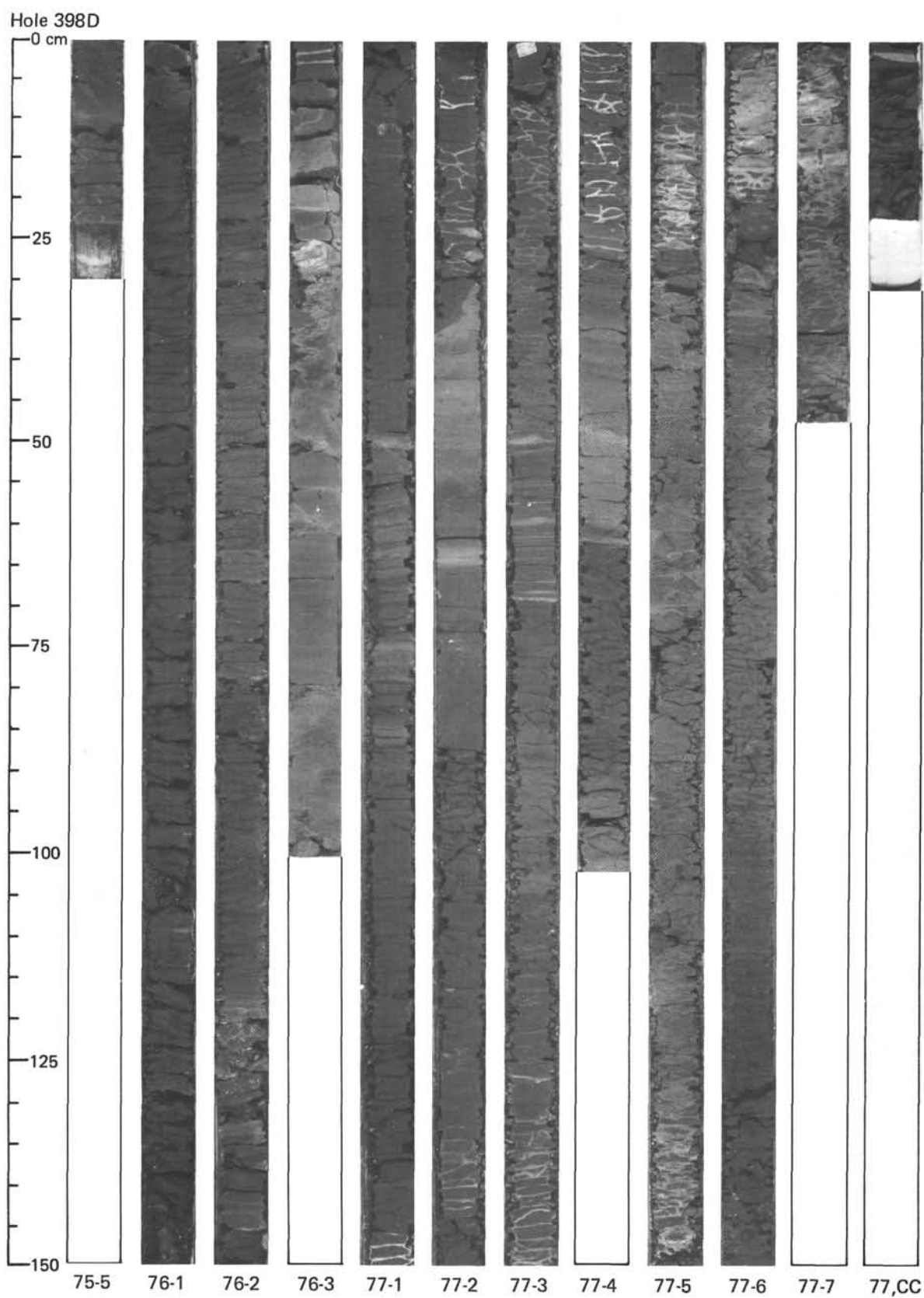


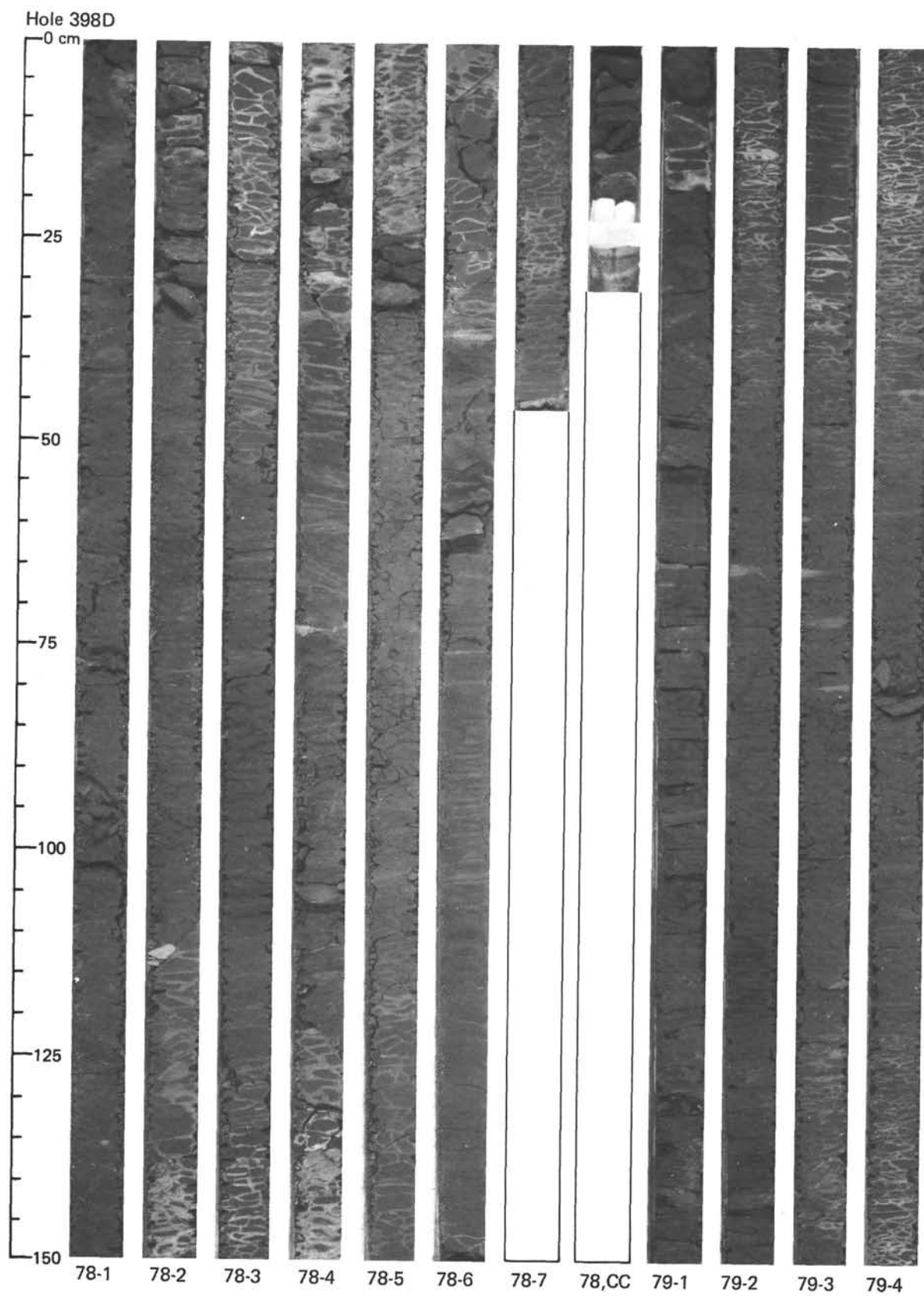


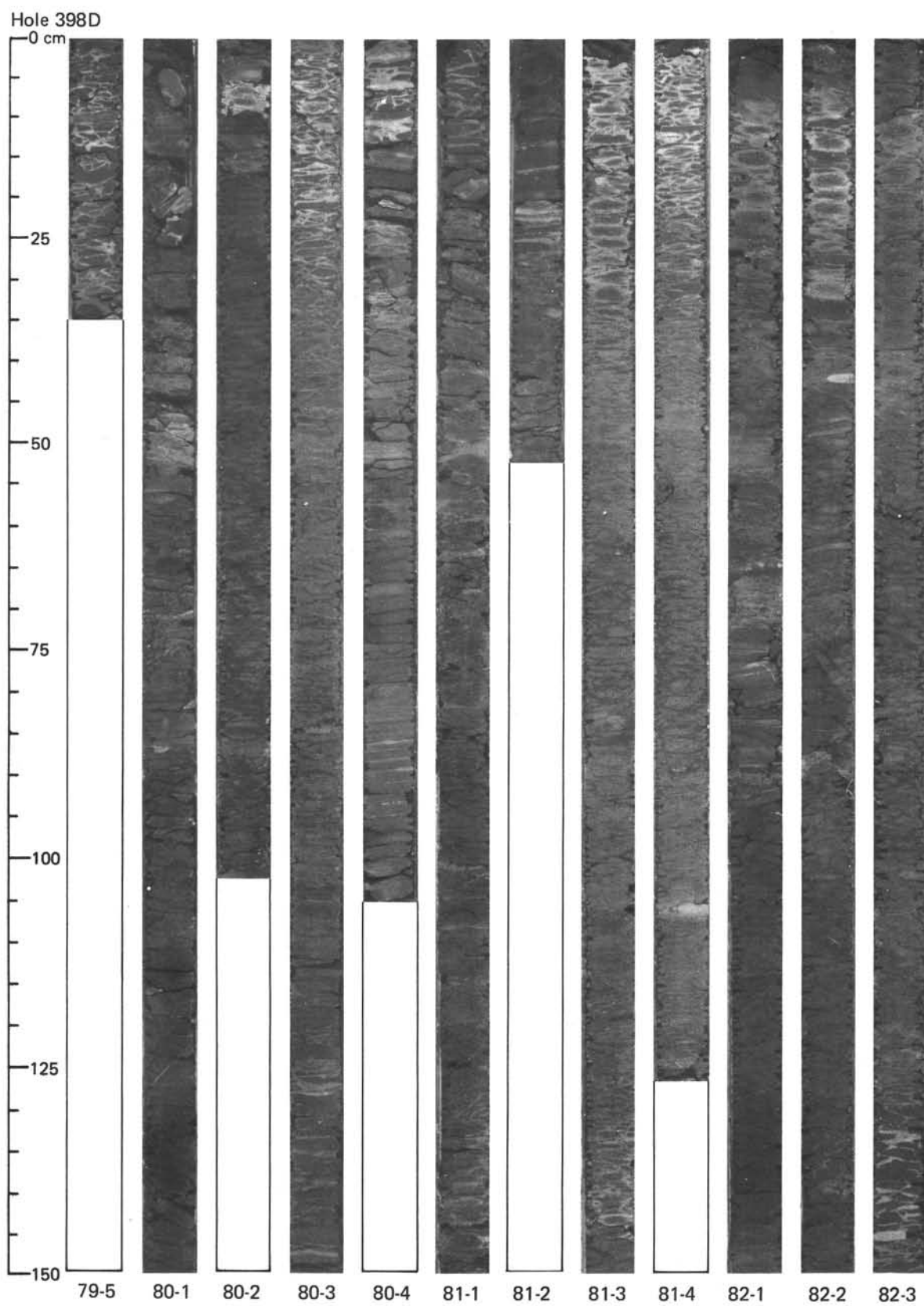




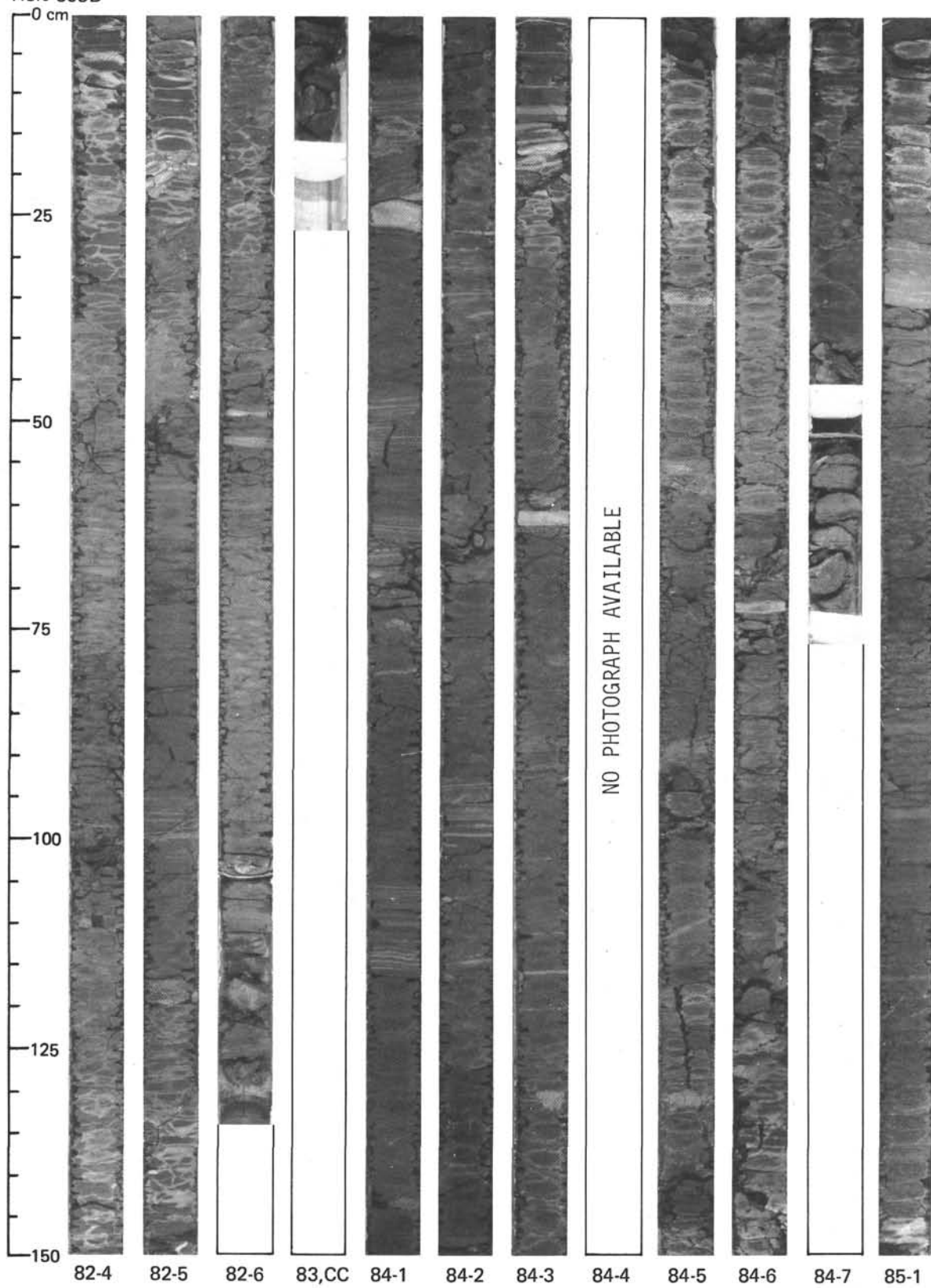


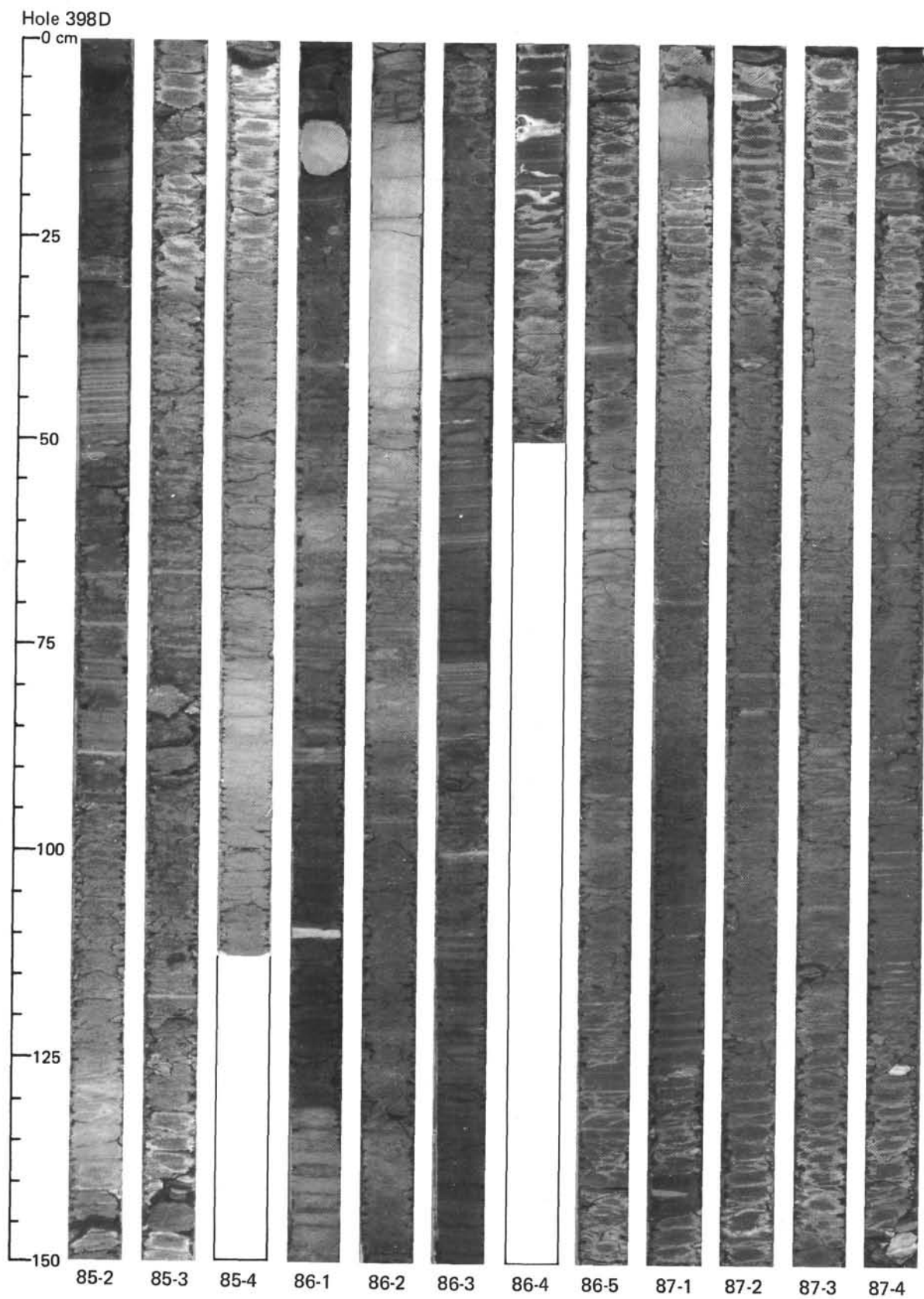


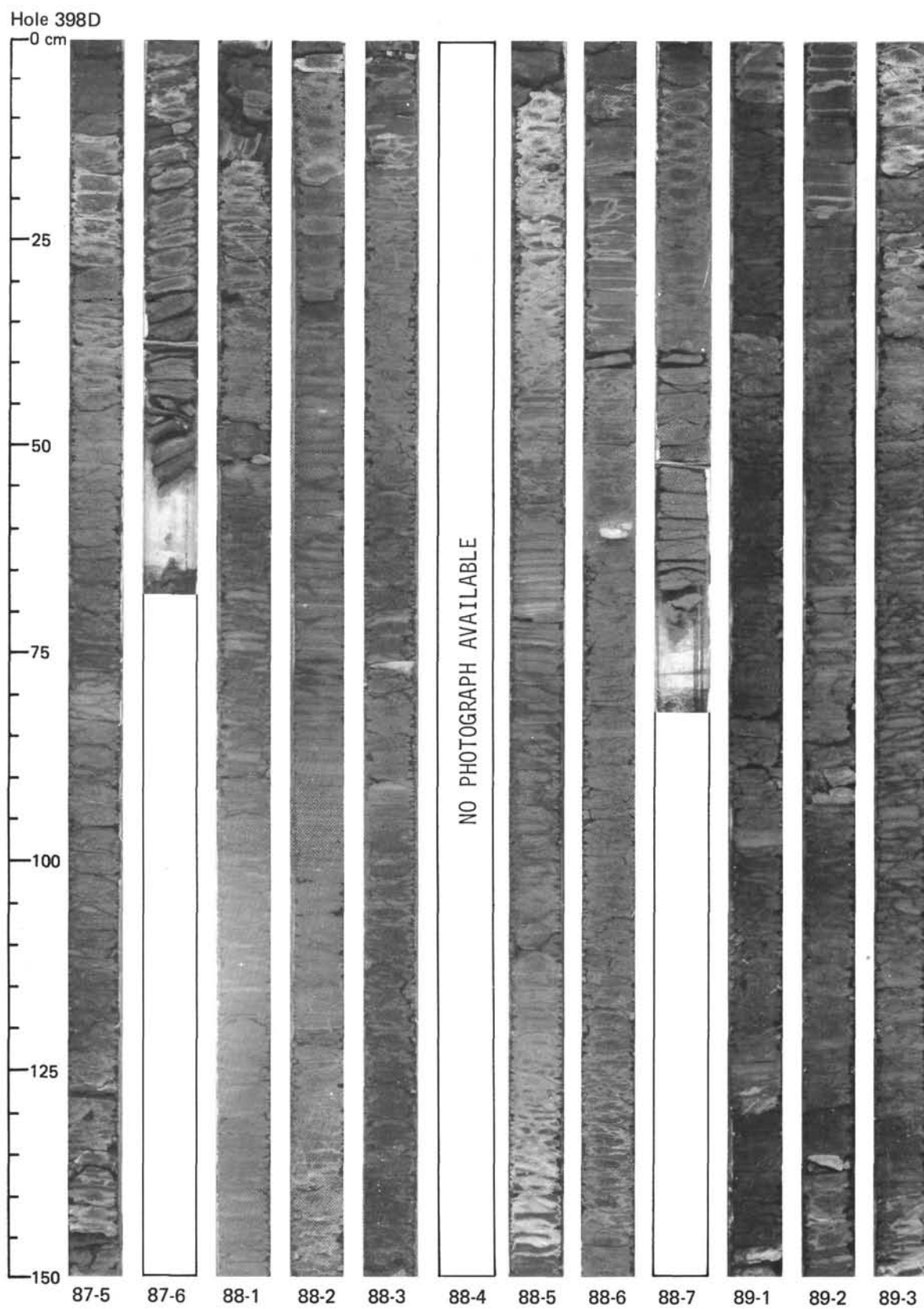


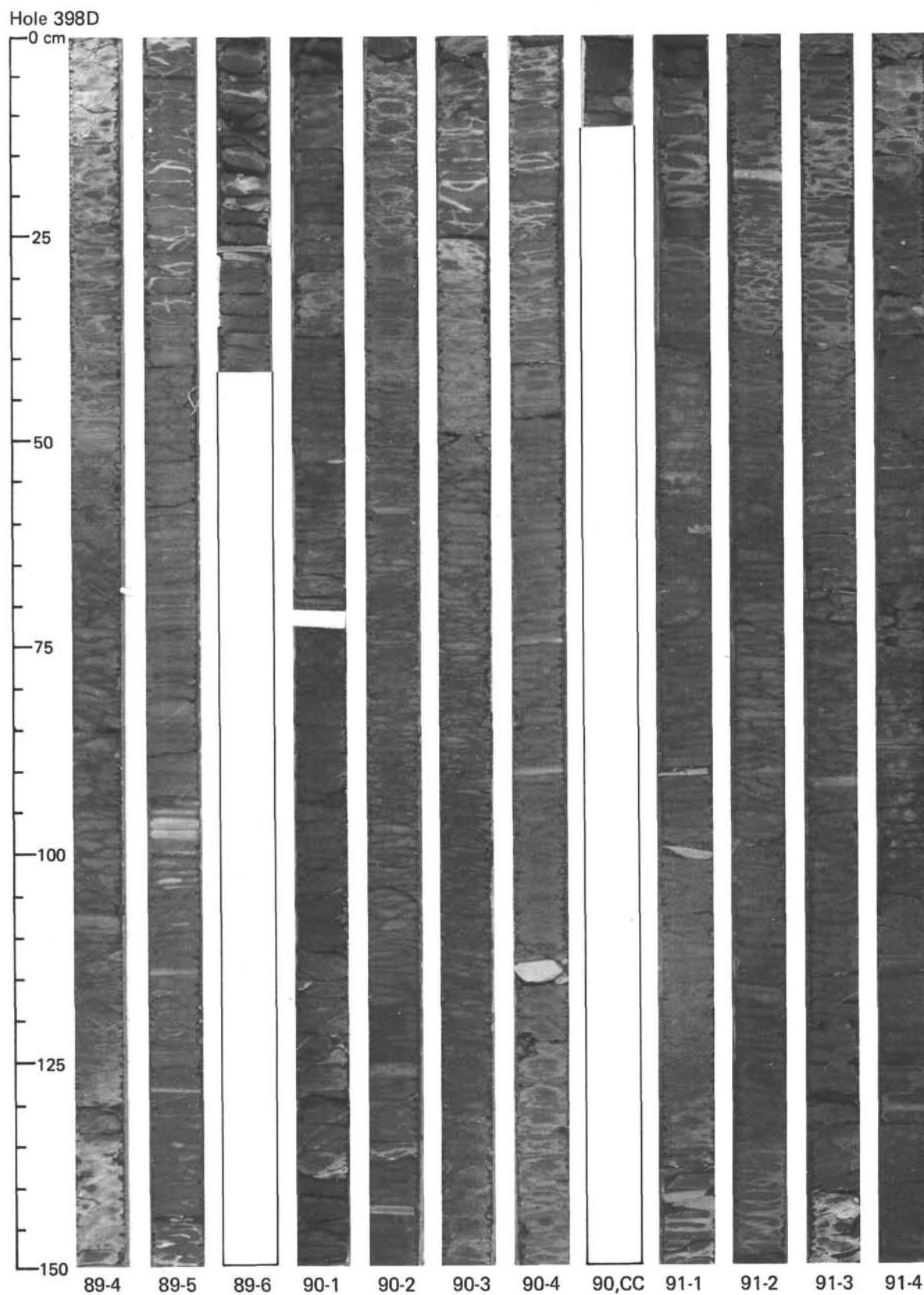


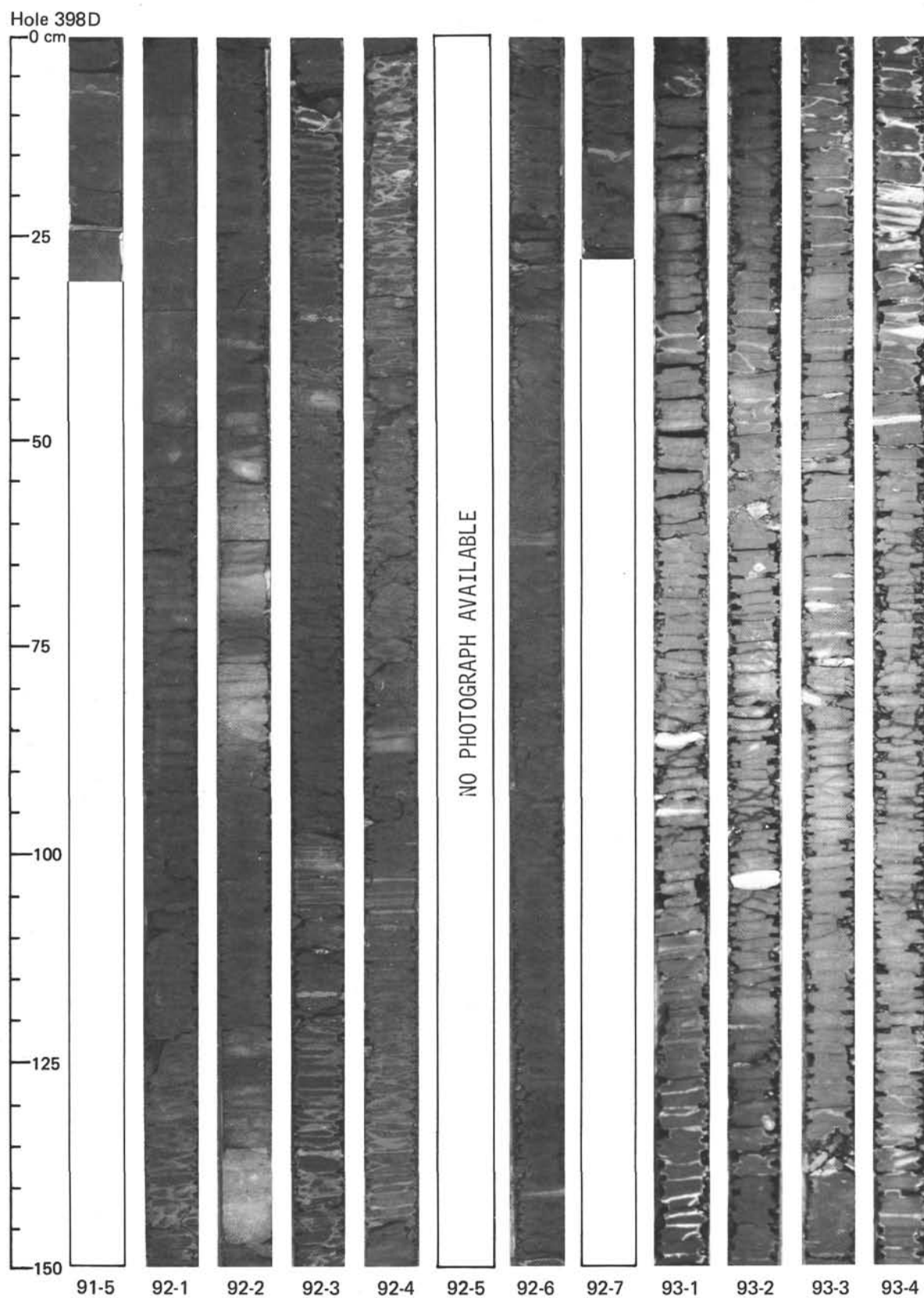
Hole 398D

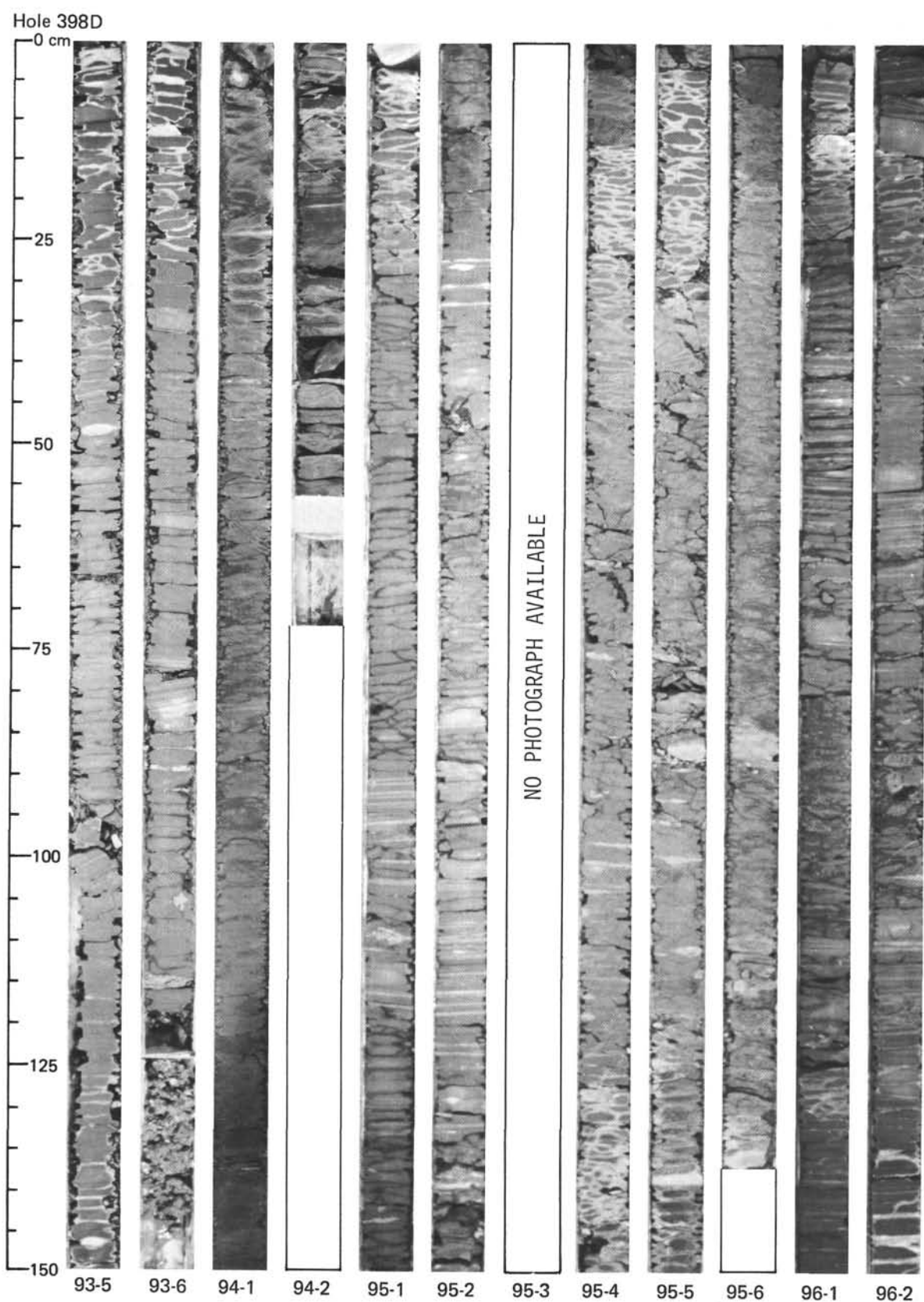




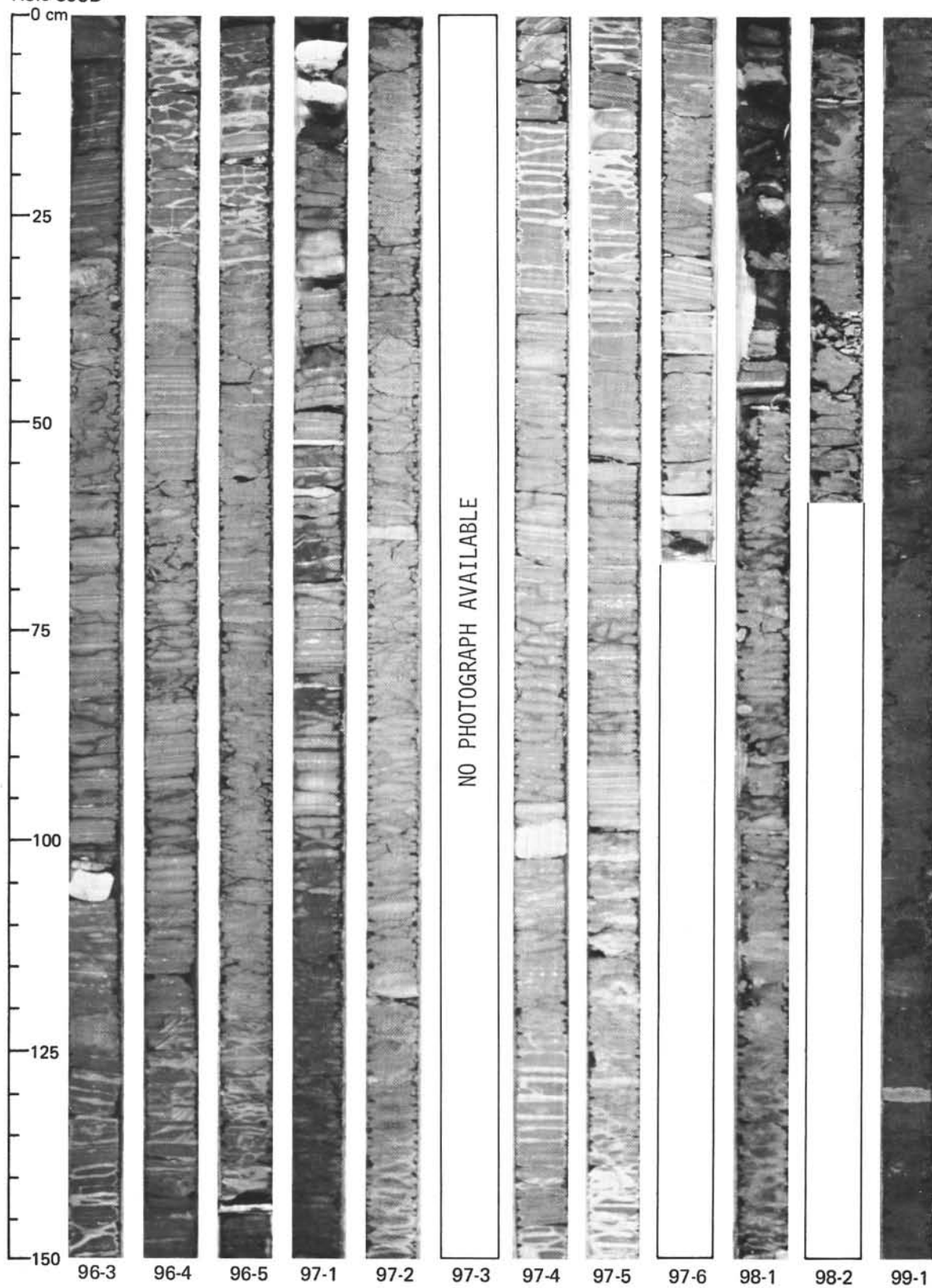


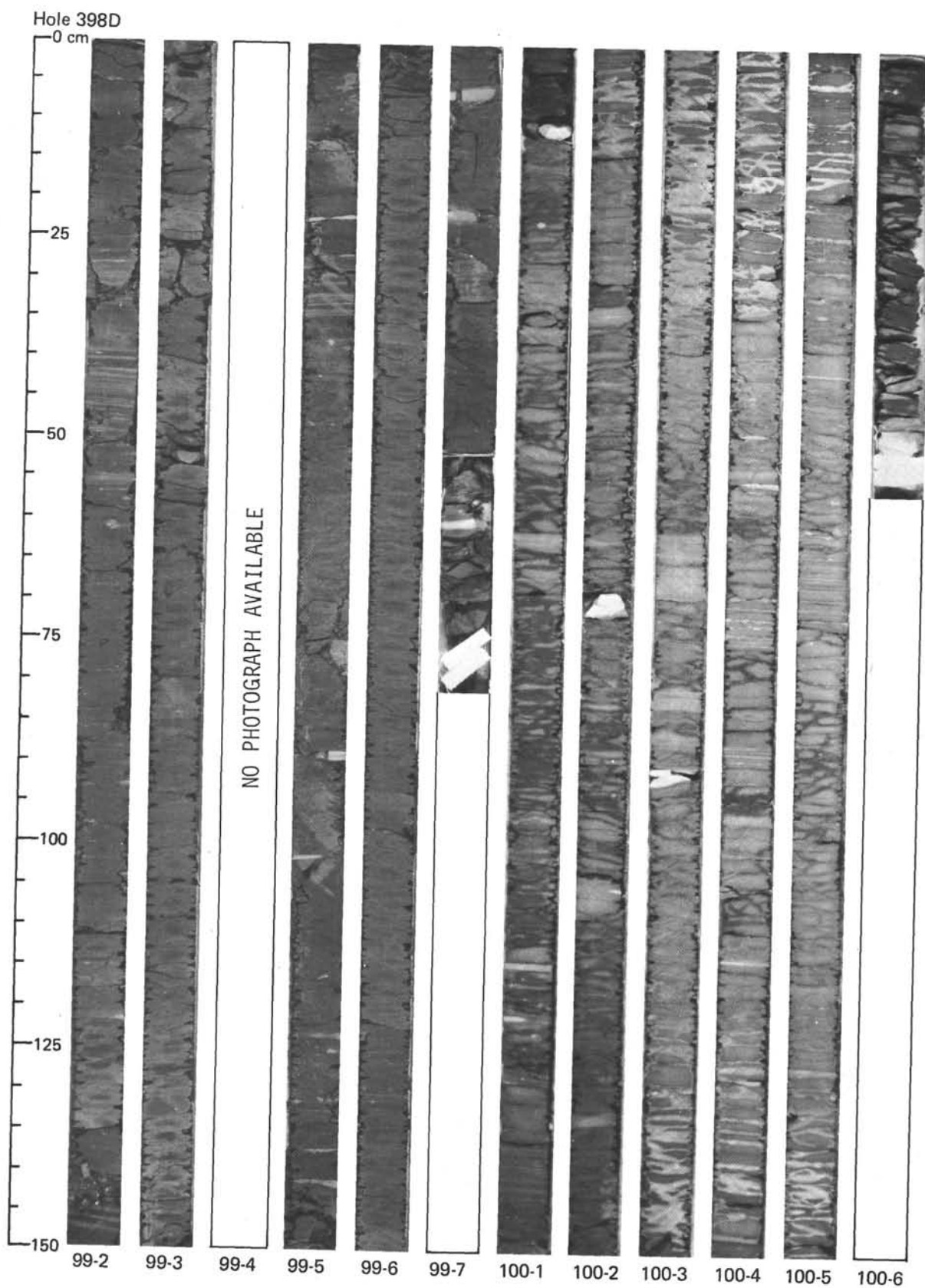


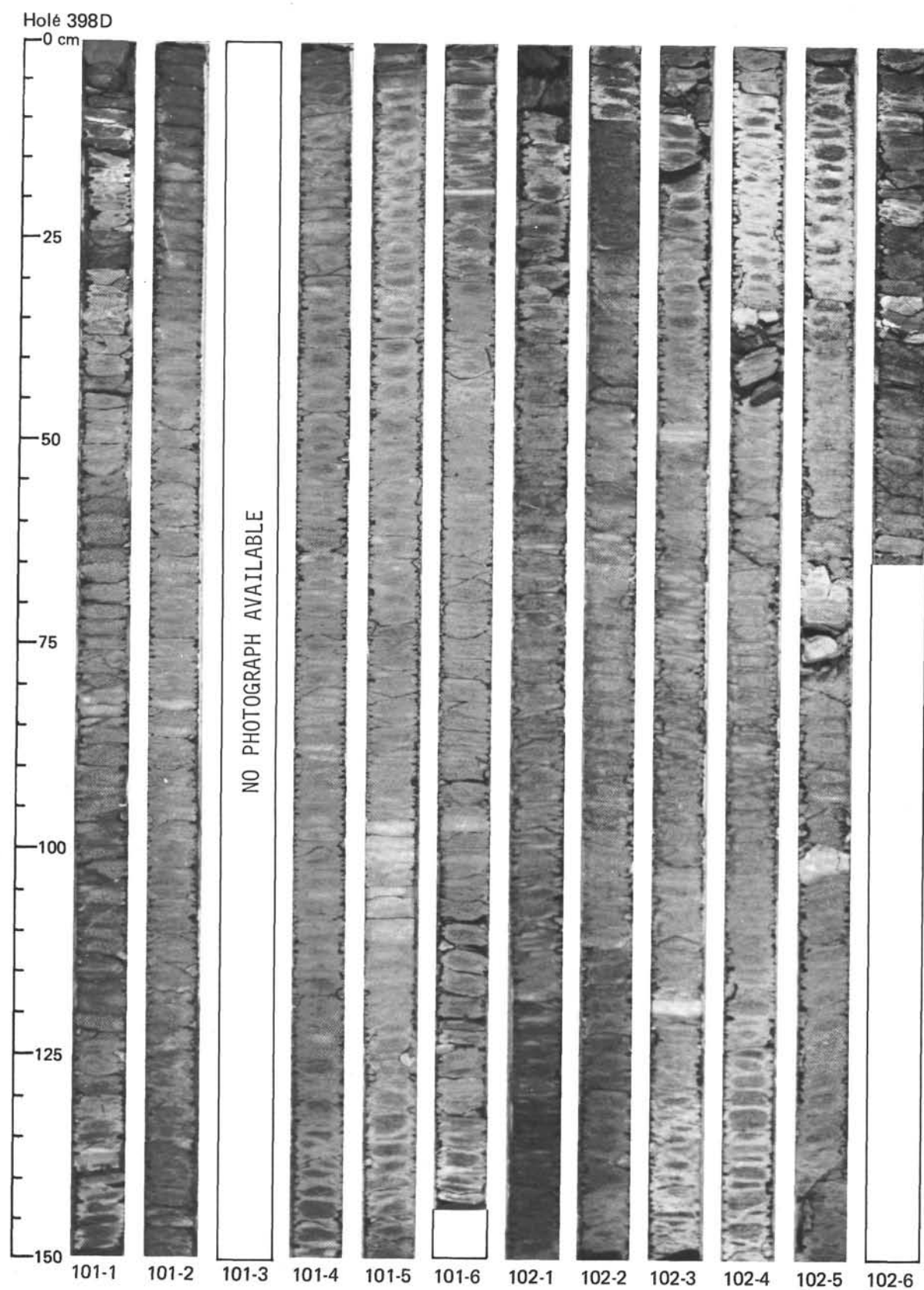


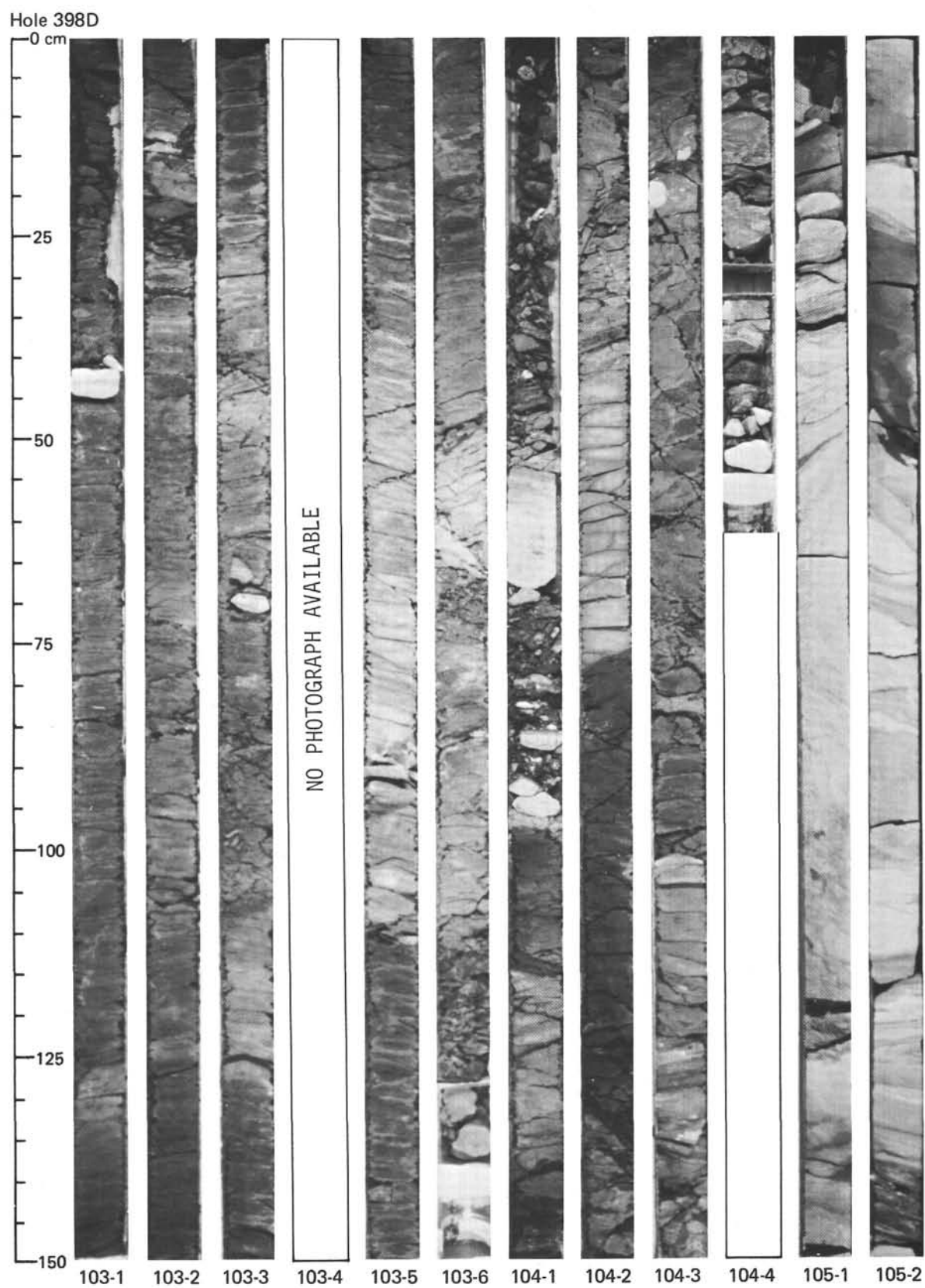


Hole 398D

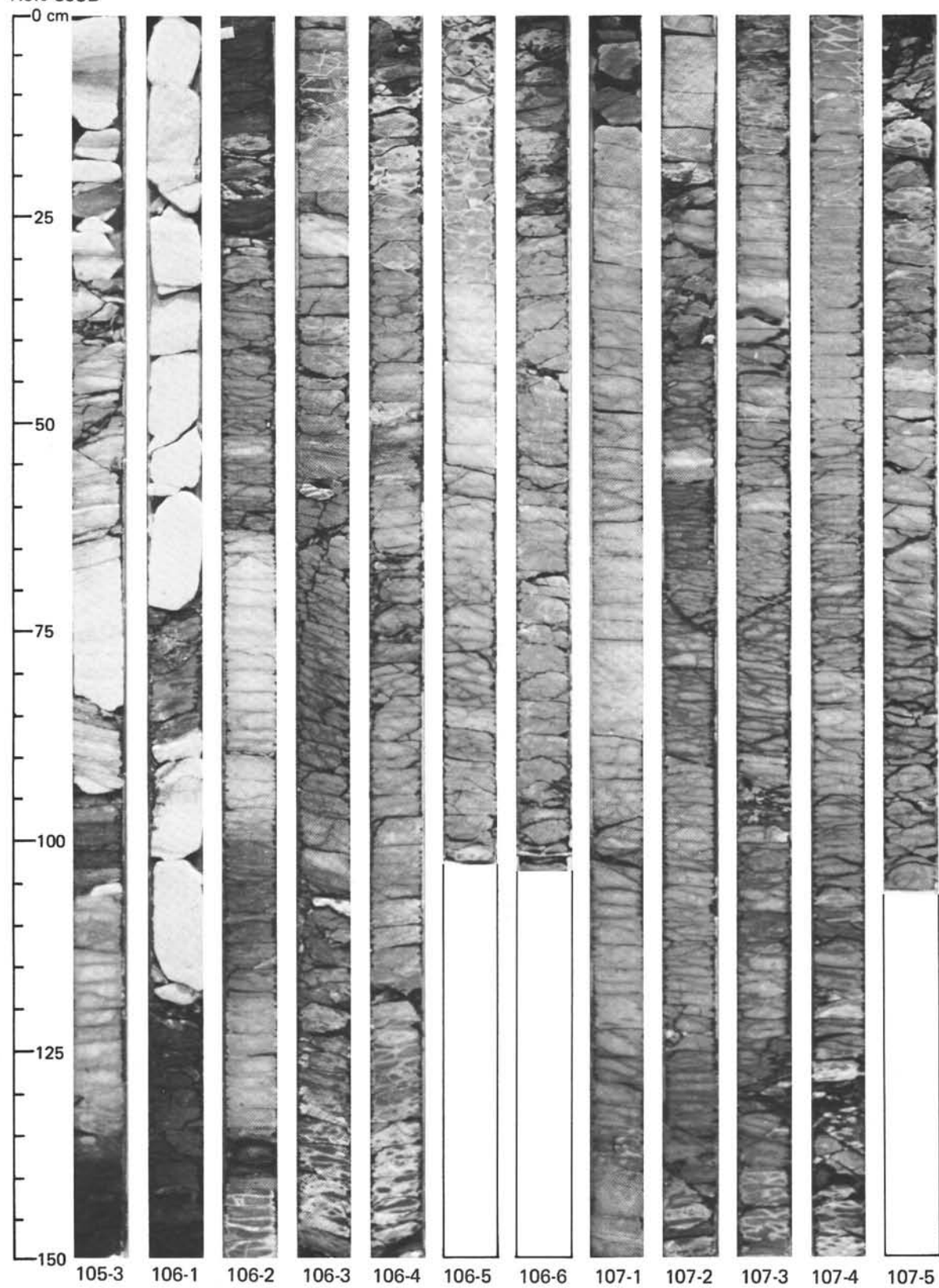


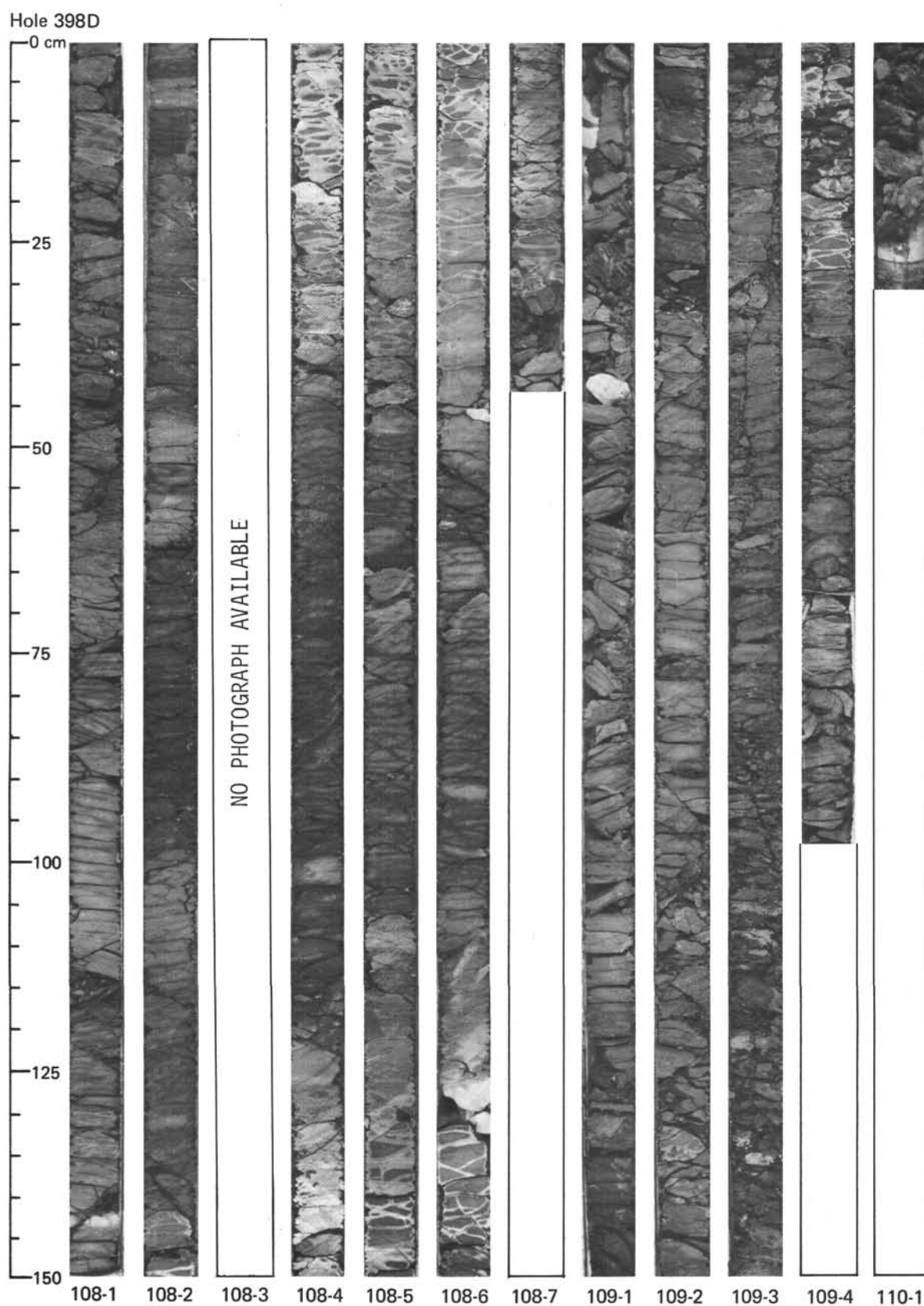


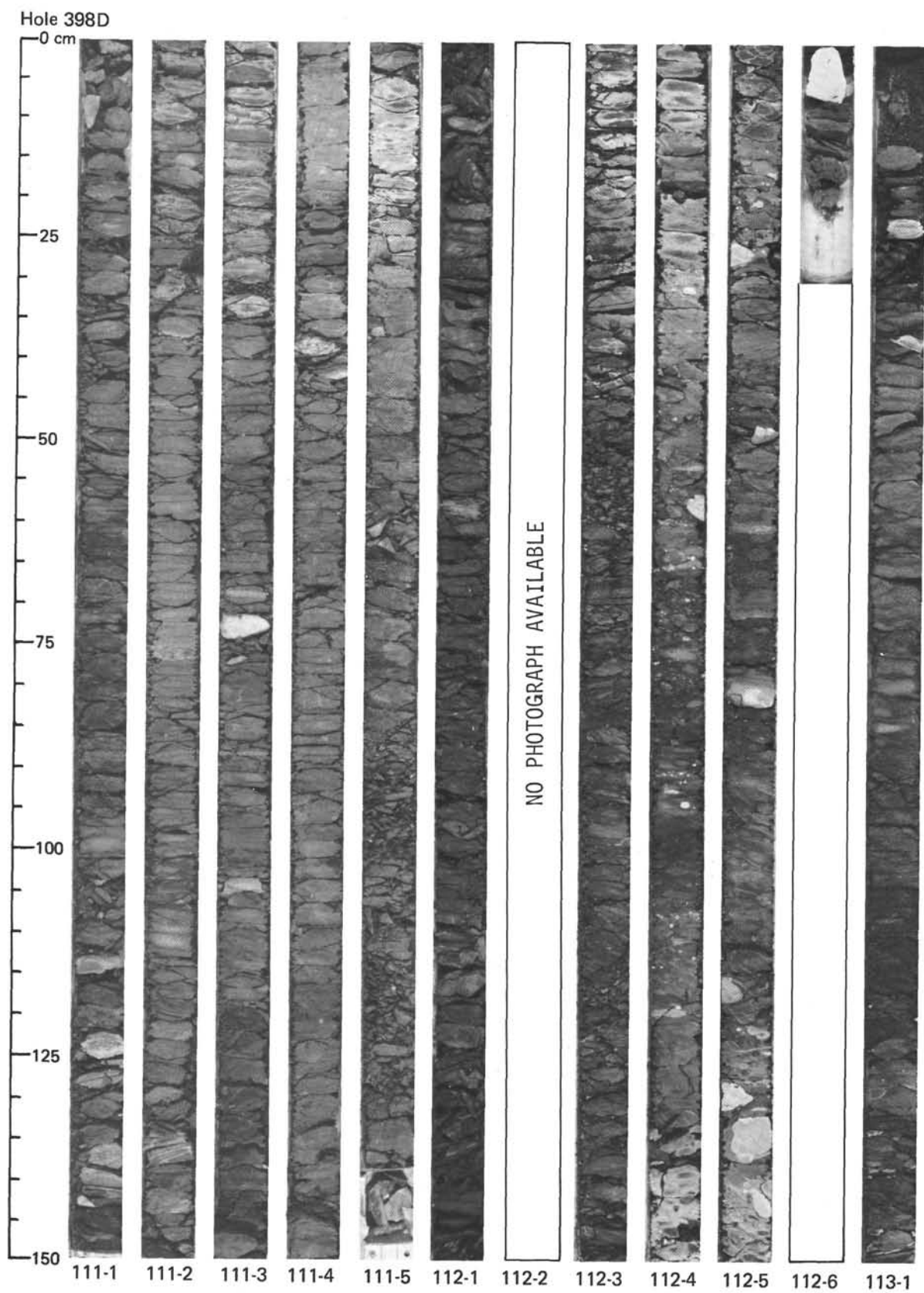


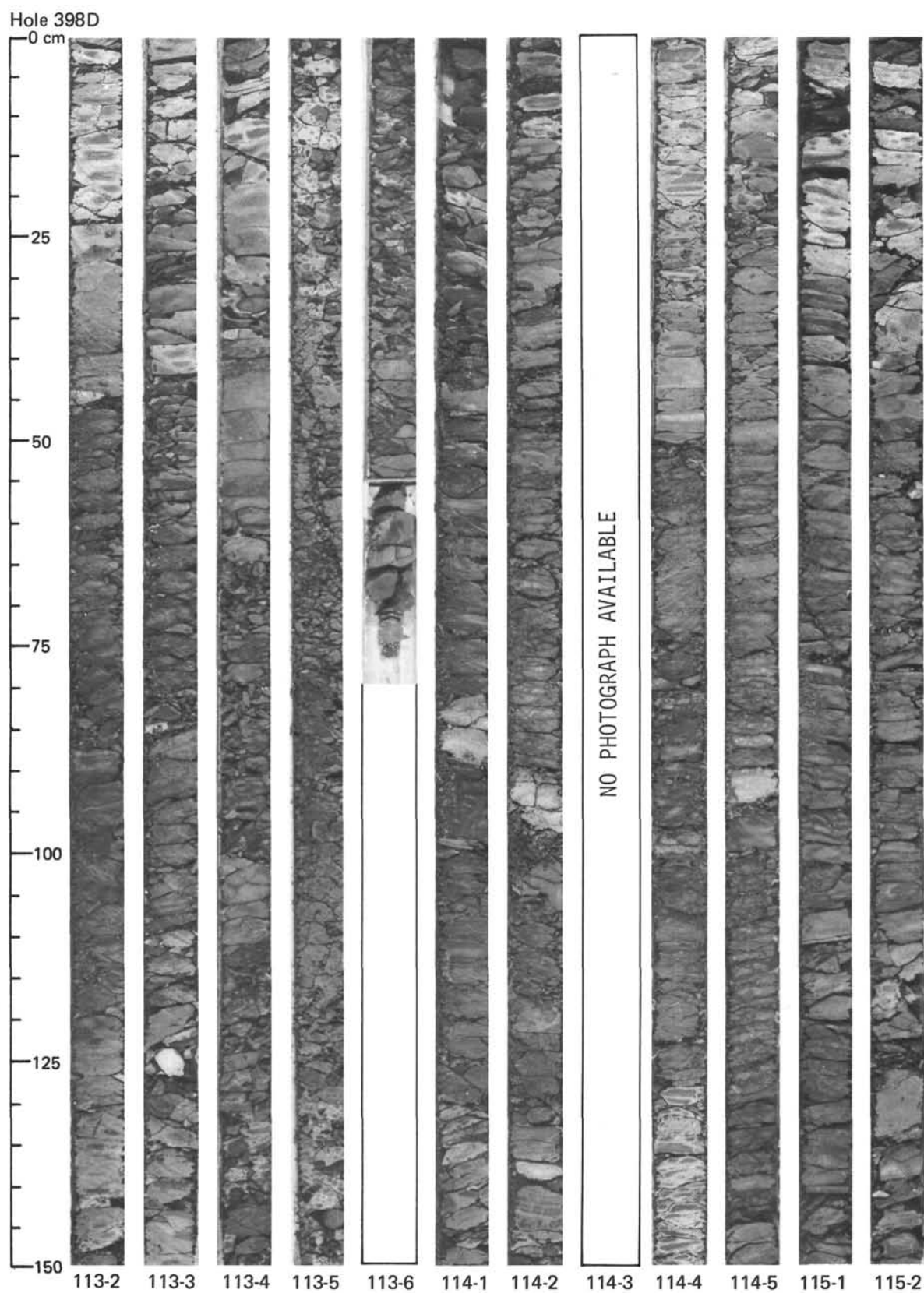


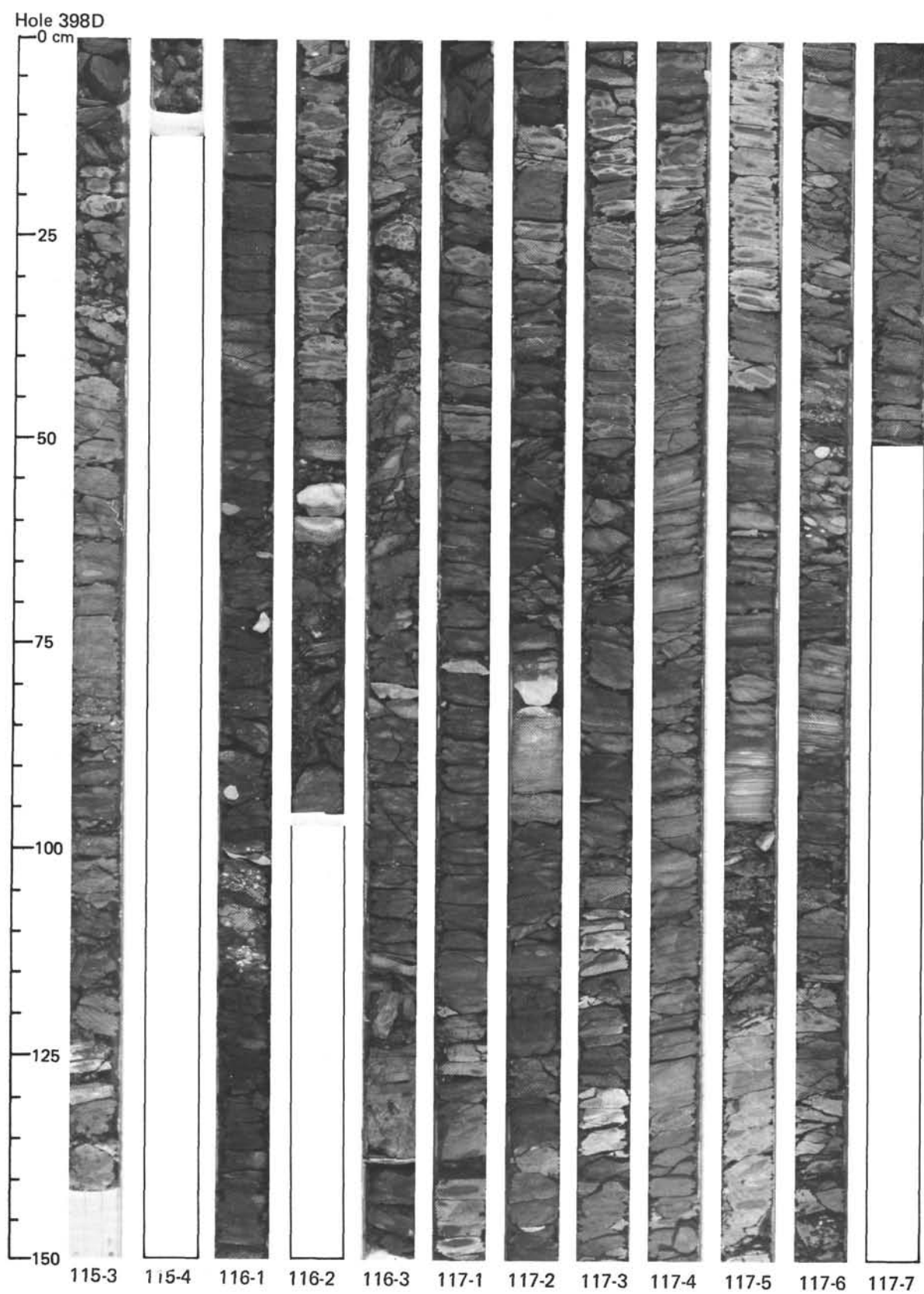
Hole 398D

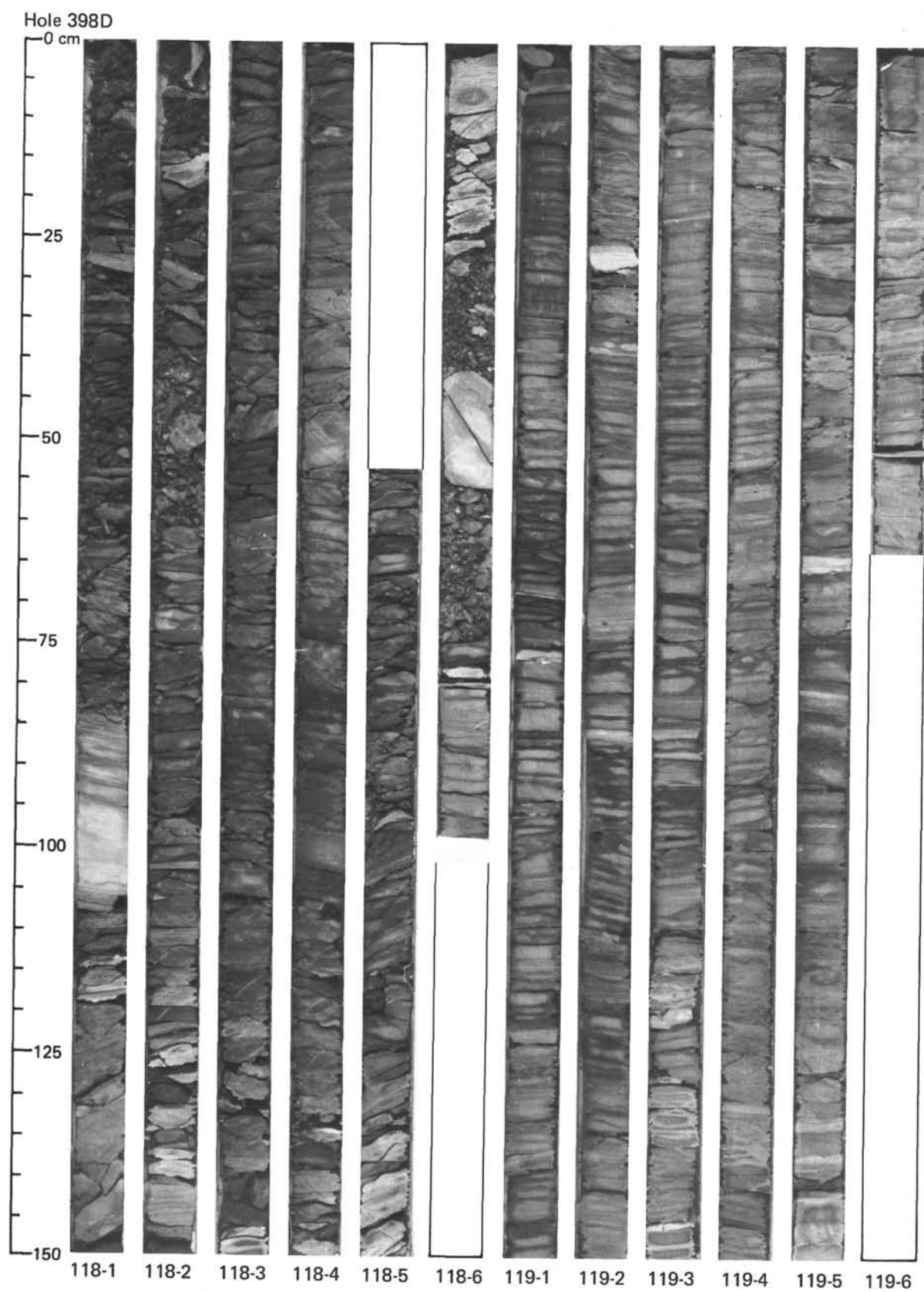




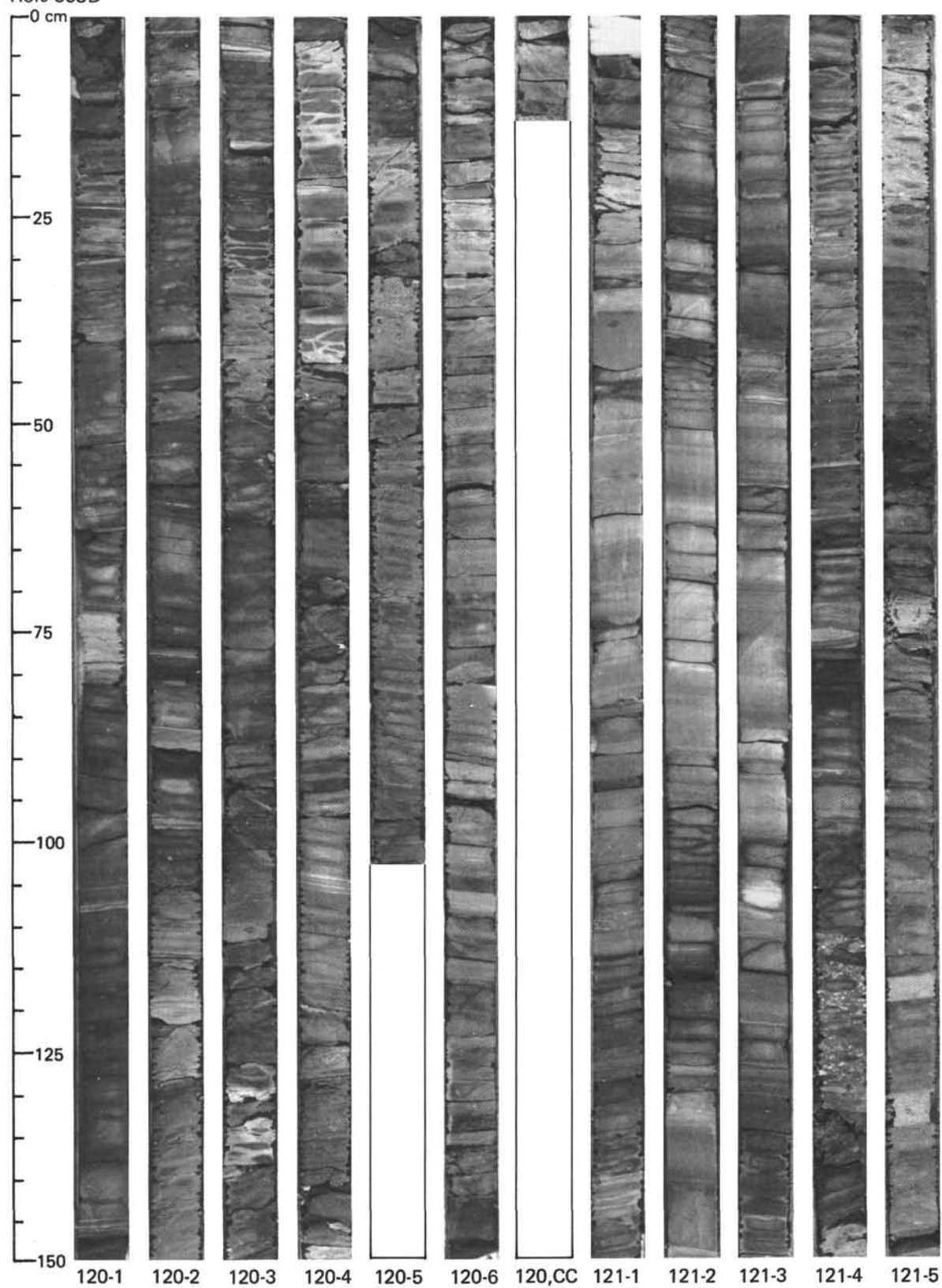


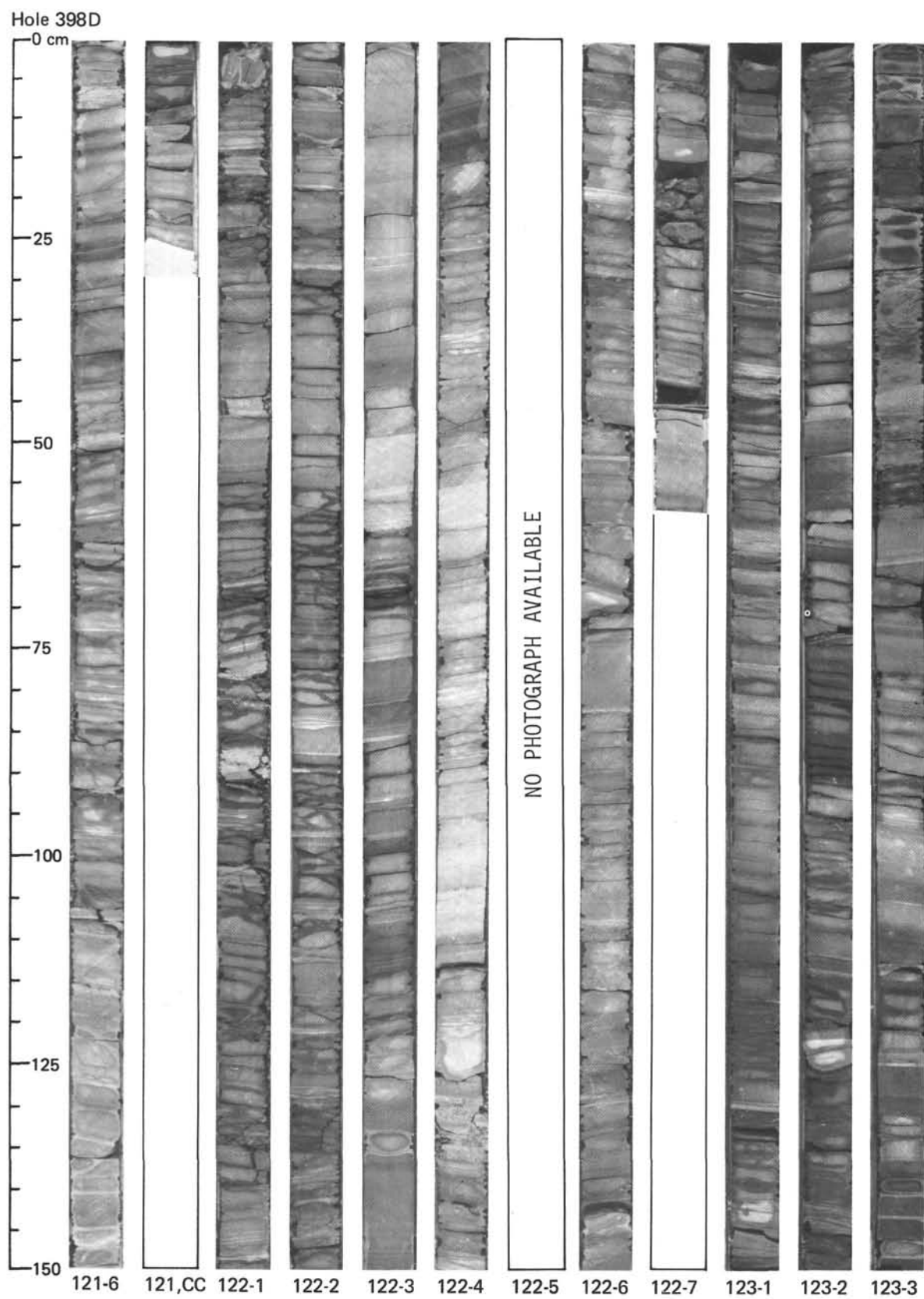




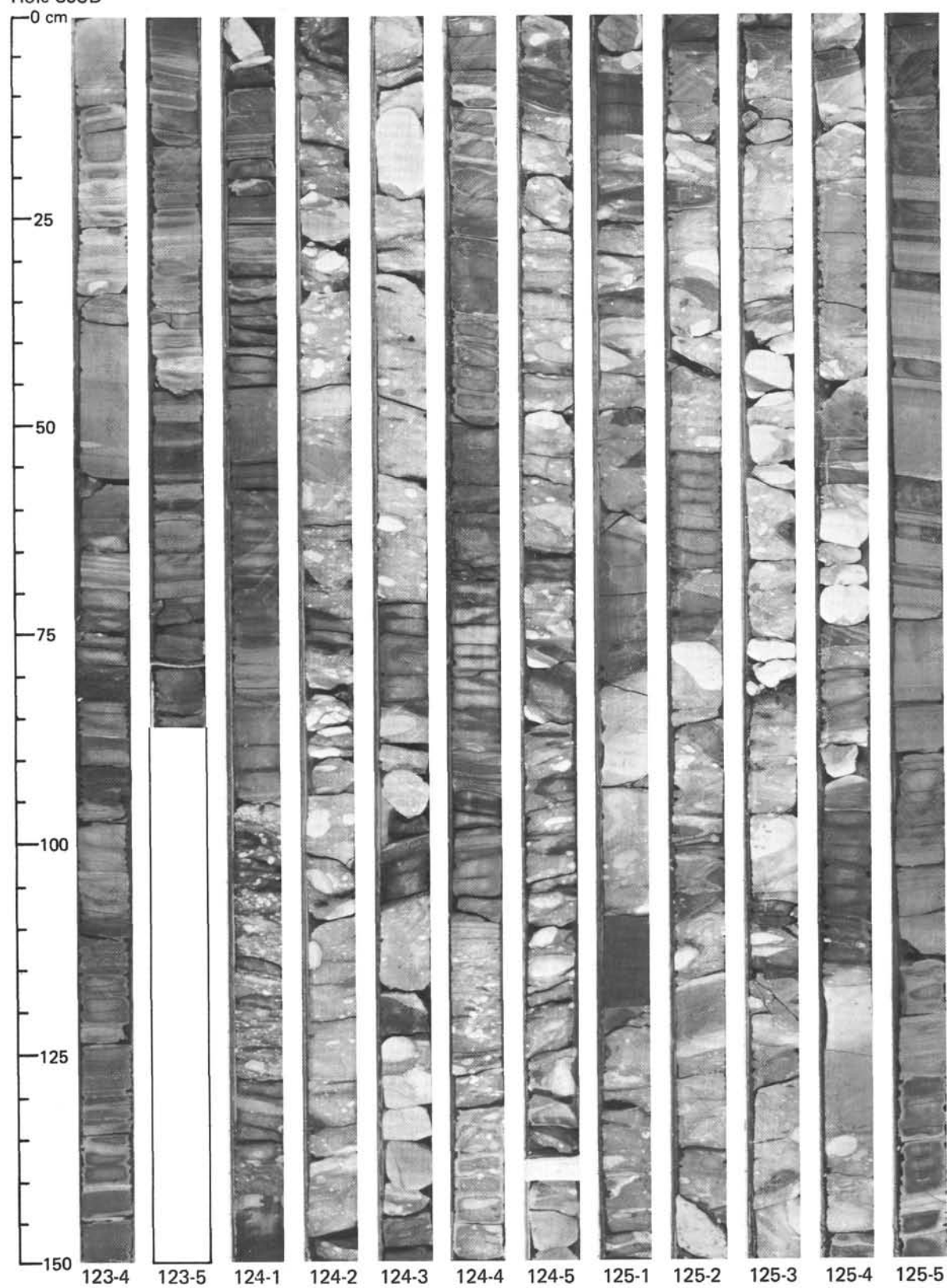


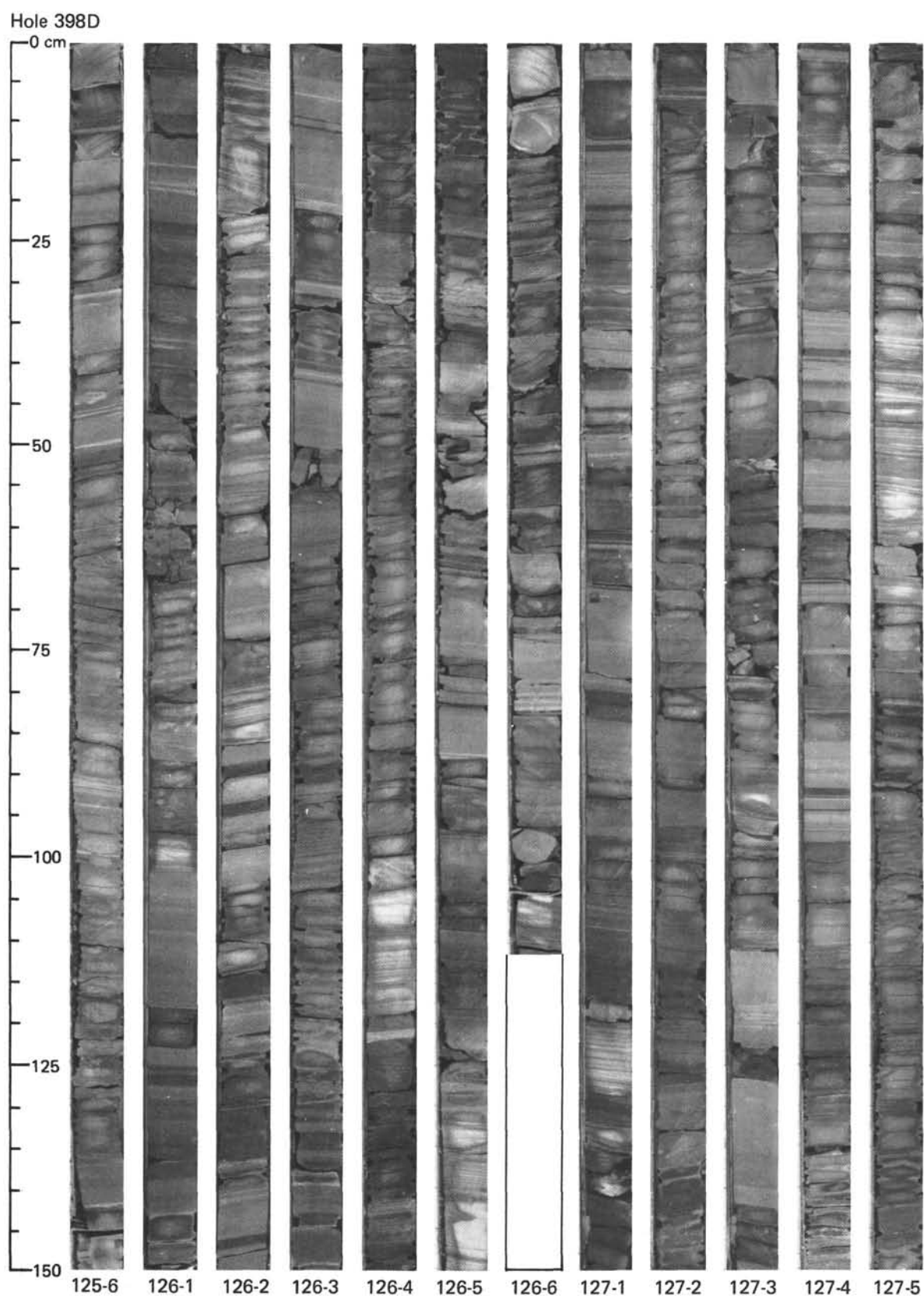
Hole 398D

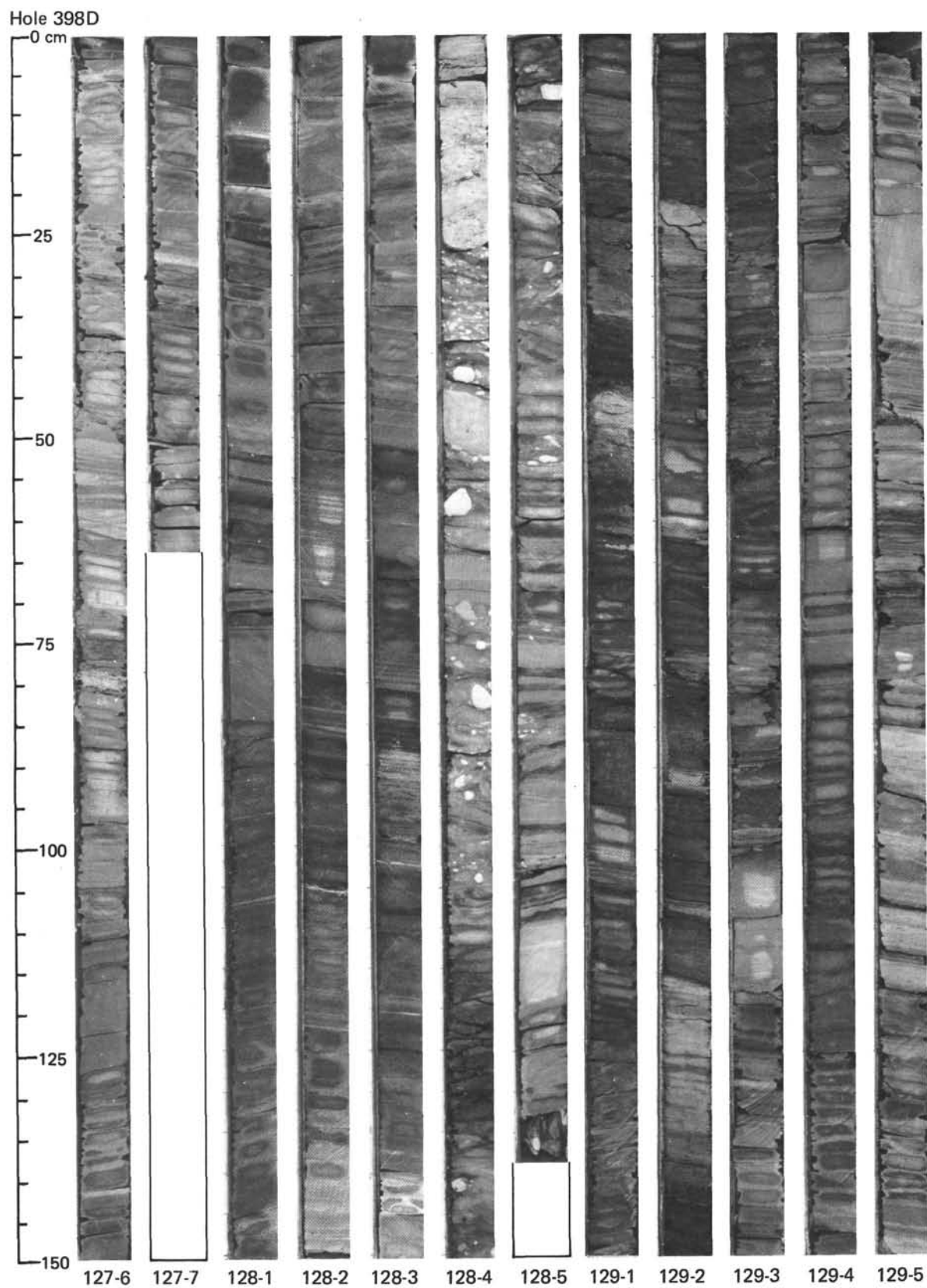


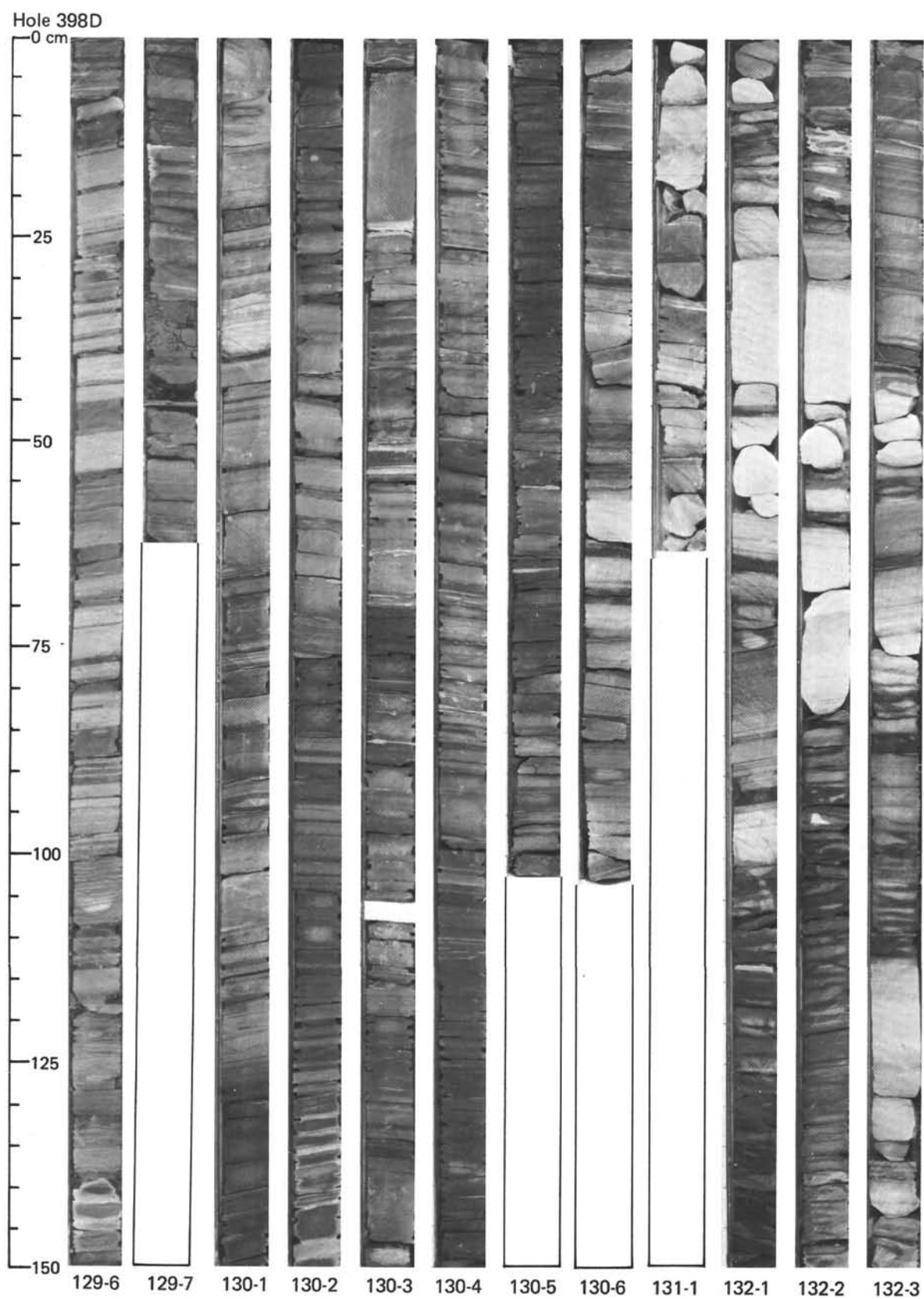


Hole 398D









Hole 398D

